

2011

Drying shrinkage of ternary blends in mortar and concrete

Xuhao Wang
Iowa State University

Follow this and additional works at: <https://lib.dr.iastate.edu/etd>

 Part of the [Civil and Environmental Engineering Commons](#)

Recommended Citation

Wang, Xuhao, "Drying shrinkage of ternary blends in mortar and concrete" (2011). *Graduate Theses and Dissertations*. 10105.
<https://lib.dr.iastate.edu/etd/10105>

This Thesis is brought to you for free and open access by the Iowa State University Capstones, Theses and Dissertations at Iowa State University Digital Repository. It has been accepted for inclusion in Graduate Theses and Dissertations by an authorized administrator of Iowa State University Digital Repository. For more information, please contact digirep@iastate.edu.

Drying shrinkage of ternary blends in mortar and concrete

by

Xuhao Wang

A thesis submitted to the graduate faculty
in partial fulfillment of the requirement for the degree of
MASTER OF SCIENCE

Major: Civil Engineering (Civil Engineering Materials)

Program of Study Committee:

Kejin Wang, Major Professor

Peter C. Taylor

Robert W. Stephenson

Halil Ceylan

Charles T. Jahren

Iowa State Univeristy

Ames, Iowa

2011

Copyright © Xuhao Wang, 2011. All rights reserved

Table of Contents

Acknowledgements	iv
Abstract	v
Chapter 1. Introduction	1
General	1
Objective of thesis	2
Thesis organization	2
References	3
Chapter 2. Literature Review	4
Concrete shrinkage	4
Factors affecting concrete shrinkage	5
Existing prediction models	9
Shrinkage testing methodology	11
Reference	13
List of figures	18
Chapter 3. Short-term Drying Shrinkage of Ternary Blends	23
Abstract	23
Introduction	24
Experimental program	26
Materials	26
Phase I	26
Phase II	27
Results and discussion	27
Ternary mixtures series I: Type I cement, class F fly ash, and slag cement	27
Ternary mixtures series II: Type I cement, class C fly ash, and slag cement	28
Ternary mixtures series III: Type I cement, silica fume, and slag cement	28
Analysis on Ca/Si ratio and alkali content on	29
Discussion	30

Conclusions	32
Acknowledgements	33
References	34
List of figures	36
List of tables	36
Chapter 4. Drying Shrinkage of Ternary Blends for Use in Transportation	
Structure	49
Abstract	49
Introduction	50
Background	52
Experimental program	52
Materials and Mix proportions	52
Test methods	53
Concrete strength and elastic modulus test	53
Free shrinkage test	53
Restrained ring test	53
Methylene blue index test	53
Paste-to-void ratio (by volume)	54
Results and discussion	54
Mechanical properties of concrete	54
Unrestrained shrinkage	54
Unrestrained shrinkage of concrete	55
Unrestrained shrinkage of mortar	54
Restrained shrinkage of concrete	56
Shrinkage cracking potential of concrete	56
Effects of concrete materials on shrinkage and cracking potential	58
Conclusions	59
Acknowledgements	60
References	60
List of figures	63
List of tables	64
Chapter 5. Conclusion	79
Chapter 6. Recommendations for Future Research	82
Appendix. Technical Reports from Additional Research	83

Acknowledgements

I would like to thank my supervisors, Dr. Kejin Wang and Dr. Peter Taylor, who gave me insightful suggestions, invaluable help, and infinite supervision during my study and my future life. Their supports allowed me to become a highly educated concrete researcher and the understanding and encouragement I received from them inspired me to pursue concrete research for my whole life.

Gratitude extended to Concrete Pavement Technology Center (CP Tech Center) at Iowa State, and the research project pooled funded supporters, nine states around America: I appreciate your supports.

I am grateful to my committee members, Dr. Robert W. Stephenson, Dr. Halil Ceylan, and Dr. Charles T. Jahren, who provided precious suggestions and guidance for me.

Portland Cement Concrete lab manager, Bob Steffes, researchers/technicians, Dr. Fatih Bektas, Bryan Zimmerman, Paul Jeremy McIntyre, and officemate, Gilson Lomboy, please accept my sincere appreciations. There was no way that I could successfully finish my work without your wholehearted help and supports.

I am so in debt to my family and all real friends for their endless love, sacrifice, and encouragement: I can say nothing but thanks.

Last but not least, I would like to appreciate my special friend, Xin Shi, who contributed and shared her life with me.

Xuhao Wang

Abstract

The work presented in this thesis involves the study of drying shrinkage behavior of mortars and field concrete mixtures made with ternary cementitious blends. The thesis is composed of two papers resulting from the study: (1) Short-Term Drying Shrinkage of Ternary Blends and (2) Drying Shrinkage of Ternary Blends for Use in Transportation Structure. In the former, statistical response surface analysis was employed to develop shrinkage models to better understand the drying shrinkage behavior of mortar mixes made with ternary blends. In the latter, ternary blend concrete mixtures used for pavement and bridge deck structures in different states were selected. Factors affecting drying shrinkage behavior of these ternary blend concretes were also investigated.

In Paper 1, shrinkage behavior of mortar mixes made with various ternary blends was studied. Ternary blends consisting of different combinations of portland or blended cement, slag cement, fly ash (Class C and F) and/or silica fume were considered: the amounts of slag cement, fly ash and silica fume ranged between 15-35%, 13-30%, and 3-10% by mass of cementitious, respectively. Mortar bars were made with the ternary blends and subjected to a drying condition (i.e., $T = 73 \pm 3$ °F and $RH = 50 \pm 4\%$) after standard curing for 28 days. Free shrinkage of the mortar bars was measured up to 28 days. Based on the test results, a response surface analysis was done to examine the effects of blend proportions on shrinkage behavior of the mortars and a statistical model was developed for predicting the mortar shrinkage behavior. Furthermore, to validate the models, shrinkage strains of an independent group of mortar mixes were measured, and the measured values were compared with the predicted values. The results indicated that among the three supplementary cementitious materials in the ternary blends studied, slag cement showed a dominant effect on mortar shrinkage. The contribution of Class C fly ash to the mortar free shrinkage was slightly less than that of slag cement. Increasing silica fume content slightly increased free shrinkage, while an increase in Class F fly ash content slightly decreased free shrinkage of the mortar. There was a good correlation between the measured shrinkage strain and the strain predicted from the shrinkage model developed from the response surface analysis.

The work discussed in Paper 2 investigated the drying shrinkage behavior of ternary blend concretes that were used in transportation structures. Factors affecting drying shrinkage

behavior of ternary blend concretes were studied. Five concrete mixes, used for either pavement or bridge deck construction, were tested for both restrained and unrestrained shrinkages. The effects of blend materials and mix proportion on the concrete shrinkages were assessed. The results indicated that shrinkage strain rate linearly increased with clay content of fine aggregate, cementitious material content, paste-to-void ratio (by volume), and dosage of water reducer of the concrete mixes.

The study demonstrates that the supplementary cementitious materials (SCMs) can be used to develop a statistical model in order to quantitatively predict drying shrinkage strain. The study gives a better understanding on how SCMs affect mortar and concrete drying shrinkage behavior. Both free and restrained shrinkage methodologies provide efficient analyses on interacted drying shrinkage influence factors. The cracking potential derived from restrained ring shrinkage test can be used to predict drying shrinkage cracking potential of ternary blend concrete mixtures.

Chapter 1

Introduction

General

The present thesis is developed from an on-going research project, *Development of Performance Properties of Ternary Mixes*. The purpose of this research project is to perform a comprehensive study of how supplementary cementitious materials (SCMs), such as fly ash, slag cement, and silica fume, can be used to improve the performance of concrete mixtures. Several different sources of Portland cement and blended cement are used in the experimental program to address the material variability issue. The proposed project is conducted in three phases: Phase I, laboratory study on mortar, which simply served as a filter to identify materials combinations that did not perform adequately; Phase II, laboratory study on concrete, which used the information obtained from Phase I to select a range of materials and dosages to investigate the effects of hot and cold environmental conditions on concrete; Phase III, field demonstration and technical assistance, which will provide on-site technical support for using ternary mixtures and review the specifications based on the performance of field mixtures. The Phase I and II were accomplished already.

Concrete shrinkage is of concern when it relates to structure durability. Excessive shrinkage may cause concrete cracking, even structural failure. Thus, cracking may lead to increased corrosion rate of steel reinforcement in concrete structure. For prestressed concrete structure, the shrinkage induced cracking may not only accelerate the rate of corrosion of steels but also contribute to prestress loss causing failure [1]. Therefore, researchers start to make use of blending of two or three SCMs to optimize durability and cost for the benefit of engineers, owners, contractors and material suppliers. The industrial by-products used as SCMs, such as fly ash and slag cement, have become more efficient admixtures to diminish the shrinkage effects and increase the durability of concrete. This thesis includes a selection of papers encompassing a critical shrinkage mechanism, drying shrinkage, to perform a comprehensive study on mortar and concrete. Statistical analysis software and materials

collected from construction site provided sufficient supports to realize a more practical study on concrete drying shrinkage behavior.

Objective of thesis

The main purpose of this work is to perform a comprehensive study of how SCMs can be used to improve the performance of concrete mixtures through the mortar shrinkage evaluations. In order to accomplish this main purpose, the following objectives are included in this thesis:

- Investigation on determining the effects of different SCMs on drying shrinkage behavior of ternary blends.
- Statistical models development and validity of models verification based on drying shrinkage behavior of mortars produced with ternary blends.
- Evaluation of restrained and unrestrained drying shrinkage behavior for ternary blended concrete mixtures used in transportation structures.
- Cracking risk assessment for ternary blended concrete mixtures used in transportation structures in lab condition compared to field condition.
- Investigation on the influence factors which have different dominances on drying shrinkage behavior of ternary blended concrete mixtures used in transportation structures.

Thesis organization

This thesis is divided into six chapters. Chapter 1 provides a general introduction and thesis objectives.

Chapter 2 gives a brief literature review of the concrete drying shrinkage phenomenon, factors affecting concrete drying shrinkage, and shrinkage testing methodology. The review aims to provide background and general information about concrete shrinkage behaviors.

Chapter 3 and 4 includes selected papers that have been either submitted for publication or ready for submission to peer reviewed journals. The results and conclusions of this thesis are presented in these two chapters.

Chapter 5 summarizes the major findings of the study and chapter 6 provides the recommendations for future research and industrial applications.

Appendix presents the technical reports for five field demonstration transportation structures in New Hampshire, Pennsylvania, Kansas, Michigan, and Iowa.

Reference

[1] Tia M, Liu Y, Brown D. Modulus of elasticity, creep and shrinkage of concrete. Gainesville: Department of Civil & Coastal Engineering, College of Engineering, 2005.

Chapter 2

Literature Review

Concrete shrinkage

Concrete shrinkage types are plastic shrinkage, chemical shrinkage (autogenous shrinkage) and drying shrinkage [1]. Generally, there are two distinct stages: early and later ages. The two stages should be evaluated together as total shrinkage of a concrete. Early age of shrinkage indicates the first day which concrete is setting and starting to harden. Later age, also known as long term, refers to concrete at 24 hours after casting or longer.

Plastic shrinkage occurs at early age from the moisture loss of concrete before, or shortly after, the concrete sets. Chemical shrinkage is also an early age behavior, especially first hour when mixing water with cementitious materials. Carbonation shrinkage is a part of chemical shrinkage which is limited to the surface of the low-permeable concrete and quicker cement reaction may lead to high chemical shrinkage [2]. “The reduction in total solid and liquid volumes is produced by the chemical hydration reaction, which can be considered to be the driving mechanism of autogenous shrinkage [3].” Therefore, the study of autogenous deformations has been affected by experimental assessment of chemical shrinkage. Autogenous shrinkage is “the shrinkage occurring in the absence of moisture exchange due to the hydration reactions taking place inside the cement matrix [4].” Drying shrinkage occurs when the specimen is exposed to the environment and allowed to have volumetric changes. Normally, the entire shrinkage strain is assumed to be from drying shrinkage, and any contribution from autogenous shrinkage is neglected for normal strength concrete (i.e., < 6000 psi at 28 days) [3, 4].

From a microstructural point of view, solids in the hydrated cement paste include four principal solid phases, calcium silica hydrate (40 to 50%); calcium hydroxide (20 to 25%); calcium sulfoaluminate hydrates (15 to 20%) and unhydrated clinker grains [6].

Water can exist in many forms in the hydrated cement paste and they can be classified depending on the degree of ease with which it can be removed from the paste (Figure 1):

The capillary voids that represent the voids not filled by solid hydration products, initially filled with excess unhydrated water. Such voids will retain water by capillary tension. Water in the larger voids (>50 nm) is considered to be “free water” because its removal does not result in volume change. However, water in small capillary voids (5 to 50 nm) may result in large shrinkage strains when water is forced to leave the system [6]. The size and volume of the capillary voids are determined by the initial w/c ratio and the degree of cement hydration. At a constant w/c ratio, increasing the degree of hydration decreases the size and volume of the capillary voids. Subsequent drying then will result in reduced shrinkage strain [6].

Adsorbed water is the water bonded to but not reacted with the surface of hydration products. Water molecules are physically adsorbed onto the surface of solids in hydrate cement by influence of attractive forces such as hydrogen bonding. The removal of adsorbed water will result in shrinkage strains, but such removal will not occur unless the RH of the pore system is low (less than about 40% RH) [31].

Interlayer water is the water held within the calcium silica hydrate (CSH) nano-structure. The water in the interlayer space of CSH voids is held by Van der Waals forces [51]. Because of the extremely small size of the so-called gel pores, removal of interlayer water will only occur under very dry conditions (about 10% RH) [6, 31]. The size and volume of gel pores vary depending on the Ca/Si ratio, type of molecules (non-ionic, anionic or cationic), concentration and pH while they are independent of the initial w/c ratio and degree of hydration [51, 52]. Therefore, increasing the Ca/Si ratio may decrease the size and volume of gel pores and so increase resistance to water removal [54].

The predominant drying shrinkage mechanisms (mainly by water loss) are composed of moisture transport within the porous solid, permeation due to a pressure head, capillary suction due to surface tension and capillary tension, absorption phenomena including fixation and liberation of water molecules due to mass forces [5]. Capillary tension is a well documented drying shrinkage mechanism in drying porous media. Tensile stresses in the

capillary water in the high RH range (up to approximately 50% RH) are subjected to capillary tension. These tensile stresses bring about elastic shrinkage stains [6, 31]. Surface tension is another important mechanism for adsorbed water removal. Due to lack of symmetry of molecules lying on the surface of the material, a resultant force perpendicular to the surface that provokes contraction is referred as surface tension. It is suggested that this mechanism is only valid in the low RH regime (up to 40% of RH) [31]. Another mechanism, movement of interlayer water, is attributed to the layered-structure of the CSH. This phenomenon may migrate the interlayer water out of the CSH sheets when RH drops below 10% [31].

Factors affecting concrete shrinkage

Factors that affect drying shrinkage are usually interrelated although they can be grouped into two main categories – material characteristics and ambient conditions [6]. On one hand, the group contains the characteristic properties of material itself, such as aggregate properties (i.e., size, gradation, content, and elastic properties), the w/c ratio, water content, cementitious material content, cement characteristics, air content, chemical and supplementary cementitious material admixtures. On the other hand, the environmental factors set up the external conditions, such as relative humidity, ambient temperature, and wind velocity [6]. The curing condition influences are falling between the previous two classifications since they are controlled by external conditions which will internally affect the quality of material as well [6, 7].

Because the drying process involves moisture loss from the surface, drying shrinkage mainly depends on the size and configuration of the element [8]. Usually, a larger member dries slower and the thicker specimens have a lower rate of shrinkage. An inverse proportion between shrinkage and the ratio of specimen volume to its drying surface area is obtained from American Concrete Institute (ACI) [4]. Increasing the volume-to-specimen surface area ratio may cause decrease in drying shrinkage. Quantity of aggregate is also a significant factor affecting the potential of shrinkage. Shrinkage is basically related to volume of aggregate content and higher content of aggregate has a lower shrinkage strain at the same w/c ratio [9]. ACI Committee 209 on “*Factors affecting shrinkage and creep of hardened*

concrete” reports that increasing the size of aggregate while decreasing the paste content will decrease the drying shrinkage. The aggregate size changes from 1.4 to 6 inches will result in the aggregate volumetric changes from 0.6 to 0.8 so that the shrinkage reduces at around 50%. This is because the quantity of paste is one of the main parameters affecting the shrinkage potential of a mixture. For a given w/c ratio, decreasing paste content, and so increasing aggregate content leads to reduced shrinkage strain [9]. The methylene blue index (MBI) can be used as an indicator of clay content of fine aggregate in concrete. The higher clay content may absorb more water from the cement system so as to change moisture content in the concrete. The drying shrinkage of concrete increases with the increasing MBI values, especially when MBI value is greater than or equal to 1.45 because clay particles coating aggregate particles will deform significantly with changing moisture content [48]. The elastic properties of the aggregate will also affect concrete shrinkage – the lower the modulus of elasticity of aggregate, the higher the drying shrinkage of the concrete may be [6]. Cement characteristics, such as reduced sulfate content, increasing fineness will reportedly increase drying shrinkage potential.

Relative humidity around concrete can dramatically increase the shrinkage, especially when RH is lower than 10%. It is generally agreed that the interlayer water may migrate out of CSH sheets to reduce the distance between these layers and causing macroscopic shrinkage strain. As long as the air content less than 8%, there is no significant effect on the drying shrinkage strain [10]. Proper, prompt, and sufficient curing period helps to reduce shrinkage [4].

Both supplementary cementitious materials (SCMs) and chemical admixtures can dramatically affect the shrinkage of a mixture. The available literature indicates that for a similar mixture, inclusion of slag cement appears to have marginal effect on increasing shrinkage [36]. A high silica fume content may increase the drying shrinkage in the short term. However, silica fume may not cause an increase in shrinkage with lower replacement dosage over the long term (i.e., 365 days) [11]. Use of slag cement and silica fume in ternary mixes provides the best performance compared to binary mixtures where slag cement and silica fume are used alone [42]. Class F fly ash used in binary mixtures may reduce drying shrinkage with increasing replacement dosages compared to plain portland cement concrete

[43]. Compared to class F fly ash, class C fly ash reportedly causes more shrinkage than control concrete mixtures in most cases, apparently due to low alkali contents and higher Ca/Si ratios [44]. However, both types of fly ash combined with slag cement or silica fume in ternary blends diminish the adverse effects of silica fume or slag cement [42].

Current literature focuses on investigating how binary systems affect drying shrinkage.

- For binary blends of Portland cement and class F fly ash: Gesoğlu et al. replaced PC by FFA at levels of 20%, 40%, and 60% and observed that the free shrinkage was reduced by using FFA and this beneficial effect appeared to be more pronounced with increasing replacement levels [32]. In another study, FFA was used to investigate the drying shrinkage behavior in six mixtures cast with total cementitious contents of 400 and 500 kg/m³. The use of the FFA in 500 kg/m³ cementitious content mixtures resulted in a nominal reduction in shrinkage strain [33].
- For binary blends of Portland cement and slag cement: free shrinkage was reduced by using slag cement in a binary system compared to an ordinary PC mixture. The shrinkage decreased with increased amounts of slag cement [32]. On the other hand, the alkali-activated slag concrete had higher drying shrinkage than plain PC concrete by 1.6 to 2.1 times [34]. In order to assess the influence of slag cement on drying shrinkage behavior, the Slag Cement Association (SCA) performed a critical review based on published shrinkage research. Slag cement was incorporated either as a separately SCM or as a component in blended cement. The authors concluded that given a similar mixture, slag cement appears to have a marginal effect on increasing drying shrinkage [36].
- For binary blends of Portland cement and silica fume: A research project using 5% to 15% mass replacement of PC concluded that SF increased the drying shrinkage [32]. Similar conclusions were reached in another study that the ultimate drying shrinkage of mortar increases with increased of SF content at 28 days, but the long-term drying shrinkage after 365 days was not affected significantly by the addition of SF [11]. One study showed that at early ages, the amount of shrinkage showed an increased sensitivity to changes in water-to-cementitious ratio (w/c ratio) as the SF content was

increased, while high levels of SF (i.e., over 8%) in mixtures may dramatically increase drying shrinkage [36]. However, some conflicting results were found in other studies: the drying shrinkage of SF incorporated concrete was 10 to 22% higher than that of ordinary PC of same w/c ratio and same binder content for short term [37]; on the other hand, SF concrete had lower shrinkage than that of normal portland cement concrete with the same w/c ratio but marginally lower binder content [38]. The lower drying shrinkage of SF concrete could be attributed to its lower w/c ratio used in the study [5].

Some researches into the effects of drying shrinkage with the use of ternary mixtures have been published.

- For ternary blends of Portland cement, slag cement, and silica fume: the adverse effect of the SF was reduced and the shrinkage values compared to control mixture were reduced [32]. Khatri et al. conducted research on shrinkage behavior of the addition of SF to slag cement concrete. It was established that strain due to drying shrinkage was caused by the removal of adsorbed water and the addition of SF to slag cement concrete refined the pore size distribution of the cement paste. The pore refinement could be the cause of reduced loss of water and thus decreased the shrinkage strain [5].
- For ternary blends of Portland cement, slag cement, and class F fly ash: Compared to control mixtures, shrinkage was reduced by using 10% S and 10% FFA, 20% S and 20% FFA, and 30% S and 30% FFA as replacement dosages of PC in ternary blends [32].

A water reducer agent is used to achieve a higher strength at the same workability or to maintain strength at a higher workability. Most researchers have found that drying shrinkage increases when water reducer agent dosage increases regardless of the curing conditions [14, 15, 39, 40]. However, Qi et al. reported the shrinkage of concrete with a higher water reducer content (2.37 percent by weight of cement) was lower than that with lower water reducer content (1.39 percent by weight of cement). The test results also showed that the high water reducer content was effective in inhibiting crack opening and propagation in concrete specimens tested in a restrained condition [41].

A summarized concrete shrinkage influence factors are shown in Table 1.

Existing prediction models

Five existing models have been developed according to large number of concrete tests to predict the concrete shrinkage strain for supplemental cementitious material concrete mixtures. Researchers used the residual value which was equal to predicted value subtract the measured value to indicate if the models had ability to either overestimate or underestimate shrinkage [16]. Five existing prediction models are presented as follows:

1. American Concrete Institute – ACI 209 Code Model [6, 17]

$$\varepsilon_{sh}(t, t_{sh,0}) = \frac{(t - t_{sh,0})}{35 + (t - t_{sh,0})} \varepsilon_{sh \infty} \text{ (moist/cure)}$$

$$\varepsilon_{sh}(t, t_{sh,0}) = \frac{(t - t_{sh,0})}{55 + (t - t_{sh,0})} \varepsilon_{sh \infty} \text{ (stream/cure)}$$

where, $\varepsilon_{sh}(t, t_{sh,0})$ = shrinkage strain (in./in.); t = time (days); $t_{sh,0}$ = time at start of drying (days); $\varepsilon_{sh \infty}$ = ultimate shrinkage strain (in./in.).

2. Gardner/Lockman Model [18]

$$\varepsilon_{sh}(t, t_{sh,0}) = \varepsilon_{sh \infty} (1 - 1.18h^4) \left(\frac{t - t_c}{t - t_c + 97(V/S)^{1/2}} \right) 10^{-6}$$

$$\varepsilon_{sh \infty} = 1000K \left(\frac{4350}{f'_{cm28}} \right)^{1/2} 10^{-6}$$

where, h = humidity; t_c = age drying commenced (days); t = age of concrete (days).

3. Euro-International Concrete Committee – CEB 90 Code Model [6, 17]

$$\varepsilon_{cso} = -1.55\varepsilon_s(f_{cm}) \left(1 - \left(\frac{RH}{100} \right)^3 \right)$$

$$\varepsilon_s(f_{cm}) = \left(160 + 10\beta_{sc} \left(9 - \frac{f_{cm}}{1450} \right) \right) 10^{-6}$$

where, ε_{cso} = drying shrinkage of Portland cement concrete (in./in.); ε_s = drying shrinkage obtained from RH-shrinkage chart; β_{sc} = coefficient depending on type of cement; f_{cm} = average 28-day compressive strength (psi).

4. Bazant B3 Model [19]

$$\varepsilon_{sh}(t, t_{sh,0}) = -\varepsilon_{sh \infty} K_h S(t)$$

$$\varepsilon_{sh \infty} = -\alpha_1 \alpha_2 (26w^{2.1} f_c'^{-0.28} + 270) 10^{-6}$$

$$K_h = 1 - h^3$$

$$S_{(t)} = \tanh \sqrt{\frac{t - t_0}{T_{sh}}}$$

where, α_1 and $\alpha_2 = 1.0$; w = water content of concrete (lb/yd³); K_h = cross-section shape factor; h = relative humidity (%); t = age of concrete (days); t_0 = age of concrete at beginning of shrinkage; $S_{(t)}$ = time function for shrinkage.

5. Sakata Model [20]

$$\varepsilon_{sh}(t, t_{sh,0}) = \varepsilon_{sh \infty} [1 - \exp(-0.108(t - t_0)^{0.56})]$$

$$\varepsilon_{sh \infty} = -50 + 78(1 - \exp(RH/100)) + 38(\ln(w)) - 5(\ln(V/S)/10)^2 10^{-5}$$

where, w = water content of concrete (lb/yd³); V/S = volume-to-surface area ratio.

Two statistical analyses were performed to determine which model was better: the summation of the residuals squared test and an error percentage analysis. The analysis showed that Gardner/Lockman Model was the best predictor of drying shrinkage for the fly ash and slag cement mixtures followed by the Bazant B3, and CEB 90 Models. However, considering microsilica mixture to be Type I cement mixtures, ACI 209 Model was the best model followed by Bazant B3 and CEB 90 Models. The Bazant, CEB 90, and Gardner/Lockman Models tended to underestimate the shrinkage while ACI 209 and Sakata Models gave overestimated shrinkage values. It should be noted that some models containing 28-day compressive strength which were assumed that a higher compressive strength would have less shrinkage may not happen for all the cases [16].

Shrinkage testing methodology

Although most shrinkage related experiments are measured based on free shrinkage, such as ASTM C 157, shrinkage is more or less restrained in some ways and the strain capacity of mortar or concrete have a profound role in the cracking process. Therefore, restrained shrinkage tests have been developed to evaluate the restrained shrinkage of concrete, such as bar test, plate test, and ring test [21].

The advantages of using the bar test are uniaxial stress and the possibility of using large size aggregate in both free and restrained condition. The disadvantages, however, are the challenges to provide a constant restraint. Autogeneous shrinkage measurement could be assessed by using the restrained bar test. Stainless steel gage studs are embedded on both sides of fresh concrete to provide a 350 mm gage length. Two detachable mechanical gages are used to measure the shrinkage based on ASTM C 341 [23]. A similar uniaxial restrained shrinkage test was used in the study of “*Effect of mineral admixtures and curing periods on shrinkage and cracking under restrained condition*”. Bolts and dowels were used to fix both ends of the concrete specimen with dimensions of 100 by 100 by 350 mm. The restrained frame was made of two commercial steel channels with the total sectional area 1764 mm^2 and cross-section of $75 \text{ by } 75 \text{ mm}^2$. The apparatus for this external restrained shrinkage frame is shown in Figure 2. The displacement transducers (PI gauge), having a 100-mm gauge length, were attached to the bolts glued on the tensile surface in the constant moment span of the specimen. An electrical circuit was used to detect the crack. The portable data logger could record every second and the cracking was revealed by an abrupt change of voltage [24].

The plate test is another test method to determine the cracking potential due to drying shrinkage of concrete. However, it is very hard to be consistent because it can provide a biaxial restraint but highly depended on the geometry and boundary conditions [25]. Researchers investigated cracking potential with different concrete mixtures by using plate test. One panel was used as control and the other was a similar restrained plate panel except that a single material was altered to study its effect. Cracking length and cracking depth were then measured and the weighted value was as a parameter for cracking potential comparisons [22].

Ring test, either restrained or unrestrained, has become more popular in shrinkage testing field recently. Many advantages of ring tests include high and nearly constant restraint, applicable to both mortar and concrete samples, and lower effects of geometry and boundary conditions due to symmetry [25]. It is often assumed that cracking occurs when the stress that develops as a result of restraining the shrinkage exceeds the tensile strength of concrete [29]. However, “it should be noted that even if the ‘true’ tensile strength of concrete could be

determined, a strength-based failure criterion may not be appropriate in predicting the failure of restraint shrinkage specimens due to their failure is also depended on size and geometry” [29]. Although the tensile splitting and flexural strength are normally used as an approximation of tensile strength, it has been approved that this case is only valid for small specimen geometries, such as the tests used in laboratory and for quality assurance. Researchers suggested that the differences between the measured strength in different geometry could be better explained using fracture mechanics concepts [26-28]. Also, thicker steel rings with higher restraint caused cracking at an earlier age and higher interface pressures between the inner steel ring and concrete. Boundary condition series were investigated and the apparatus of restrained ring specimens is shown in Figure 3. The conclusions drawn from different boundary conditions were that drying from top and bottom had a higher surface to volume ratio which may lead a later age cracking even though it had lower interface pressures [30].

Limited literature reports uses of the concrete ring test to investigate the free shrinkage of concrete. An unrestrained ring test was used to understand the effect of boundary condition on free shrinkage and find out the relationship between using unrestrained ring specimens and linear specimens according to ASTM C 157. The unrestrained specimen apparatus is shown in Figure 4. It was allowed to dry only from the outer circumference and a linear variable differential transformer (LVDT) was used to measure the change in diameter of free rings. By converting the diametric deformation of the ring measured by LVDT to an equivalent free shrinkage strain, researchers found that the surface to volume ratio of specimens had a significant influence on the rate of free shrinkage [30].

A summarized shrinkage testing methodology is shown in Table 2.

References

- [1] Tia M, Liu Y, Brown D. Modulus of elasticity, creep and shrinkage of concrete. Gainesville: Department of Civil & Coastal Engineering, College of Engineering, 2005.

- [2] Holt E. Contribution of mixture design to chemical and autogenous shrinkage of concrete at early ages. *Cement and Concrete Research*, 2005: 464-472.
- [3] Boivin S, Acker P, Clavaud B. Experimental assessment of chemical shrinkage of hydrating cement pastes. In *Autogenous Shrinkage of Concrete*, by Ei-ichi Tazawa. New York: Routledge, 1999.
- [4] ACI. Report on factors affecting shrinkage and creep of hardened concrete. ACI Standards, ACI 209.1R-2005, Farmington Hills, MI: American Concrete Institute, 2005.
- [5] Khatri RP, Sirivivatn AV, and Gross W. Effect of different supplementary cementitious materials on mechanical properties of high performance concrete. *Cement and Concrete Research*, 25(1) (1995), 209-220.
- [6] Malhotra VM, Mehta PK. Pozzolanic and cementitious materials. *Advances in Concrete Technology*, v. 1, 1996.
- [7] Neville AM. *Properties of Concrete*. John Wiley & Sons, New York, 1998.
- [8] RILEM TC 107. Guidelines for characterizing concrete creep and shrinkage in structural design codes or recommendations, *Materials and structures* 28 (1995), 52-55. See also RILEM TC69, Conclusions for structural analysis and for formulation of standard design recommendations, Chapter 6 in *Mathematical Modeling of Creep and Shrinkage of Concrete*, ed. by Z.P. Bazant, John Wiley and Sons, Chichester and New York, 1988; reprinted in *Materials and Structures (RILEM, Paris)* 20 (1987), 395-398, and in *ACI Materials Journal* 84 (1987), 578-581.
- [9] Pickett G. Effect of aggregate on shrinkage of concrete and hypothesis concerning shrinkage, *Journal of the American Concrete Institute*, Vol. 27, No. 5, Jan., 1956. pp. 581-590.
- [10] Troxell GE, Davis HE, Kelly JW. *Composition and properties of concrete*, 2nd. Ed., McGraw-Hill Book Co., New York. 1968
- [11] Rao GA. Long-term drying shrinkage of mortar – influence of silica fume and size of fine aggregate. *Indian Institution of Science. Cement Concrete Research* 31 (2000) 171- 175

- [12] Güneysi E, Özturan T, Gesoğlu M. Laboratory investigation of chloride permeability for high performance concrete containing fly ash and silica fume. *Innovation and Developments in Concrete Materials and Construction*, 2002, p. 295-305.
- [13] Jawed I, Skalny J. Alkalies in cement: a review II. Effects of alkalis on hydration and performance of portland cement. *Cement and Concrete Research*, 1978; 37-52.
- [14] Kosmatka SH, Kerkhoff B, Panarese WC. Design and control of concrete mixtures, 14th Edition, Portland Cement Association (2002).
- [15] Alsayed SH. Influence of superplasticizer and silica fume on the drying shrinkage of high strength concrete subjected to hot-dry field conditions. *Cement & Concrete Research*, Vol. 28, Issue 10, 1998. pp. 1405-1415.
- [16] Mokarem DW, Weyers RE, Lane DS. Development of a shrinkage performance specifications and prediction model analysis for supplemental cementitious material concrete mixtures. *Cement and Concrete Research*, 35 (2005) 918-925.
- [17] Bhal NS, Mital MK. Effect of relative humidity on creep and shrinkage of concrete, *India Concr. J.* 70 (1) (1996 January) 21-27.
- [18] Gardner NJ, Lockman MJ. Design provisions for drying shrinkage and creep of normal-strength concrete, *ACI Mater. J.* 98 (2001) 159-167.
- [19] Bazant ZP. Creep and shrinkage prediction model for analysis and design of concrete structures-model B3, *Mat. Struct.* 28 (1995) 357-365.
- [20] Sakata K. Prediction of concrete creep and shrinkage, creep and shrinkage of concrete. *Proceedings of the Fifth International RILEM Symposium, Barcelona, Spain, September 6-9, 1993*, pp. 649-654.
- [21] Li Z, Kulkarni K., Shah SP. New test method for determining post peak response of concrete specimens under uniaxial tension, *Experimental Mechanics* 33 (1993) 181-188.
- [22] Kraai PP. A proposed test to determine the cracking potential due to drying shrinkage of concrete. San Jose State University. Publication No. C850775. The Aberdeen Group. Copy right ©1985.

- [23] Akkaya Y, Ouyang C, Shah SP. Effect of supplementary cementitious materials on shrinkage and crack development in concrete. *Cement and Concrete Composites*. Volume 29, Issue 2, February 2007, Pages 117-123.
- [24] Tongaroonsri S, Tangtermsirikul S. Effect of mineral admixtures and curing periods on shrinkage and cracking age under restrained condition. *Construction and Building Materials*. 23 (2009) 1050-1056.
- [25] Tang T, Ouyang C, Shah SP. A simple method for determining material fracture parameters from peak loads. *ACI Mat. J.*, 93(2), 147-157, 1996.
- [26] Bazant ZP. Size effect in blunt fracture: Concrete, rock and metal. *J. Engrg. Mech., ASCE*, 110(4), 518-535
- [27] John R, Shah SP. Fracture mechanics analysis of high strength concrete. *J. Mat. in Civ. Engrg., ASCE*, 1(4), 185-198.
- [28] Planas J, Guinea GV, Elices M. Rupture modulus and fracture properties of concrete. *Fracture mechanics of concrete structures*, Wittman F, ed., Aedificato Publishers, Freiburg, Germany. 1995.
- [29] Weiss J, Yang W, Shah SP. Influence of specimen size/geometry on shrinkage cracking of rings. *Journal of Engineering Mechanics*, 2000: Vol. 126.
- [30] Hossain AB, Weiss J. The role of specimen geometry and boundary conditions on stress development and cracking in the restrained ring test. *Cement and Concrete Research*, 2006: 189-199.
- [31] Idiart, AE. Coupled analysis of degradation processes in concrete specimens at the meso-level. Master Thesis: Universitat Politecnica De Catalunya, 2009, 45-48.
- [32] Gesoğlu M, Güneyisi E, Özbay E. Properties of self-compacting concretes made with binary, ternary, and quaternary cementitious blends of fly ash, blast furnace slag cement, and silica fume. *Construction and Building Materials*. 23 (2009) 1847-1854.
- [33] Haque MN, Kayali O. Properties of high-strength concrete using a fine fly ash. *Cement and Concrete Research*, Vol. 28, No. 10, pp. 1445-1452, 1998.
- [34] Collins F, Sanjayan JG. Cracking tendency of alkali-activated slag concrete subjected to restrained shrinkage. *Cement and Concrete Research* 30 (2000) 791-798.

- [35] Slag Cement Association. Effect of slag cement on shrinkage in concrete. Slag Cement in Construction. No. 27. 2005.
- [36] Whiting DA, Detwiler RJ, Lagergren ES. Cracking tendency and drying shrinkage of silica fume concrete for bridge deck applications. ACI Materials Journal. Title No. 96-M10. 2000.
- [37] Hooton RD. ACI Materials Journal, 90, 143, 1993.
- [38] Tazawa E and Yonekura A. Proc. of second international conference on fly ash, silica fume, slag and natural pozzolans in concrete, Madrid, Spain. ACI SP 91-43, 903, 1986.
- [39] Johnston C, Gamble B, Malhotra V. Effects of superplasticizers on properties of fresh and hardened concrete. Transportation Research Record, No. 720, pp. 1-7. 1979.
- [40] Brooks J. Influence of mix proportions, plasticizers, and superplasticizers on creep and drying shrinkage of concrete. Magazine of Concrete Research, Sep., 1989, Vol. 41, No. 148, pp. 145-153.
- [41] Qi M, Li Z, Ma B. Shrinkage and cracking behavior of high performance concrete containing chemical admixtures. Journal of Zhejiang University SCIENCE, Jun., 2002. Vol. 3, No. 2, pp. 188-193.
- [42] Guneyisi E, Gesoglu M, Ozbay E. Shtrength and drying shrinkage properties of self-compacting concretes incorporating multi-system blended minearal admixtures. Construction and Building Materials, 2010: 1878-1887.
- [43] Gesoğlu M, Güneyisi E, Özbay E. Properties of self-compacting concretes made with binary, ternary, and quaternary cementitious blends of fly ash, blast furnace slag, and silica fume. Construction and Building Materials. 23 (2009) 1847-1854.
- [44] Deshpande S, Darwin D, Browning J. Evaluating free shrinkage of concrete or control of cracking in bridge decks. Structural Engineering and Engineering Materials SM Report No. 89. The University of Kansas Center for Research, Inc. Lawrence, Kansas. Jan. 2007.
- [45] Hindy E, Miao B, Chaallal O, Aitcin P. Drying shrinkage of ready-mixed high-performance concrete. ACI Structural Journal, May-Jun., Vol. 91, No. 3, pp. 300-305. 1994.

- [46] Bissonnette B, Pierre P, Pigeon M. Influence of key parameters on drying shrinkage of cementitious materials. *Cement and Concrete Research*, Oct., Vol. 29, No.10, pp. 1655-1662. 1999.
- [47] Bloom R, Bentur A. Free and restrained shrinkage of normal and high-strength concretes. *ACI Materials Journal*, Mar-Apr., 1995. Vol. 92, No. 2, pp. 211-217.
- [48] Wang J, Yang Z, Niu K, KE G, Zhou M. Influence of MB-value of manufactured sand on the shrinkage and cracking of high strength concrete. *Journal of Wuhan University of Technology-Mater. Sci. Ed.* Apr. 2009.
- [49] Mindess S, Young JF, Darwin D. *Concrete*. 2nd Ed., Prentice-Hall Inc., Englewood Cliffs, New Jersey.
- [50] Lomboy G, Wang K, Ouyang C. Shrinkage and fracture properties of semi-flowable self-consolidating concrete. *Journal of Material in Civil Engineering*. 2010.
- [51] Raki L, Beaudoin J, Alizadeh R, Makar J, Sato T. Cement and concrete nanoscience and nanotechnology. *Materials*. 2010, 3, 918-942; ISSN 1996-1944.
- [52] Selvam RP, Subramani VJ, Murray S, Hall K. Potential application of nanotechnology on cement based materials. Project Number: MBTC DOT 2095/3004. August 06, 2009.
- [53] Feldman RF, Sereda PJ. *Sereda, Eng. J. (Canada)*, Vol. 53, No. 8/9, pp. 53-59, 1970.
- [54] Taylor HF. *Cement Chemistry*. Thomas Telford Ltd. 2nd edition. 1997.
- [55] Feldman RF, Sereda PJ. *Sereda, Eng. J. (Canada)*, Vol. 53, No. 8/9, pp. 53-59, 1970.

List of figures

- Fig. 1. Diagrammatic model of the types of water associated with the calcium silicate hydrate [55].
- Fig. 2. External restraint shrinkage apparatus [24].
- Fig. 3. Restrained ring specimens apparatus [30].
- Fig. 4. Unrestrained ring specimen apparatus [30].

List of Tables

- Table 1. Summary of influence factors on concrete shrinkage
- Table 2. Summary of shrinkage testing methodology

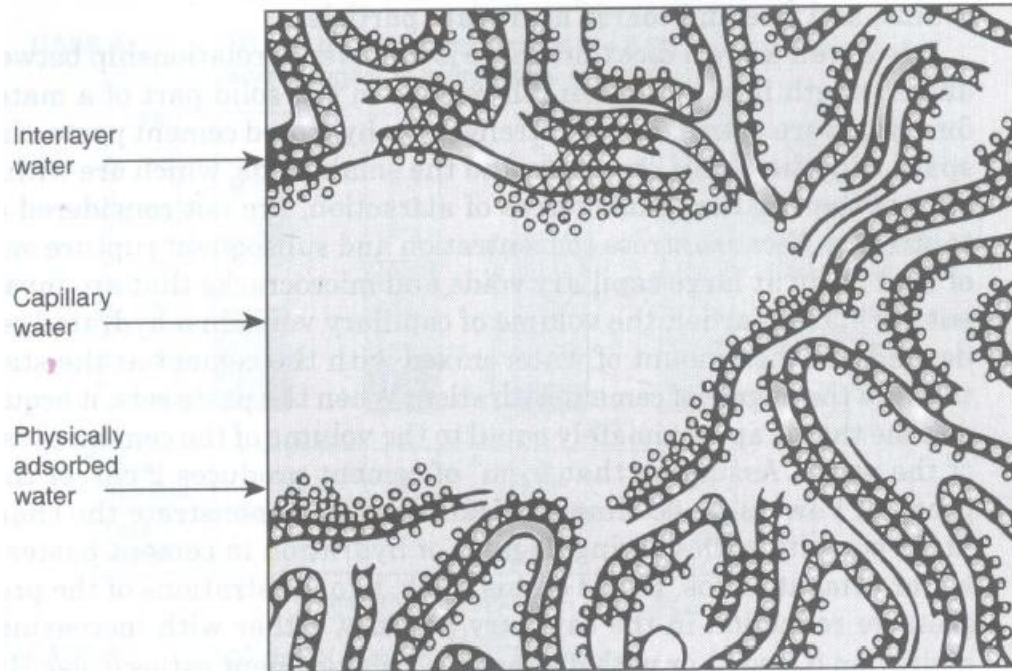


Fig. 1. Diagrammatic model of the types of water associated with the calcium silicate hydrate [55].

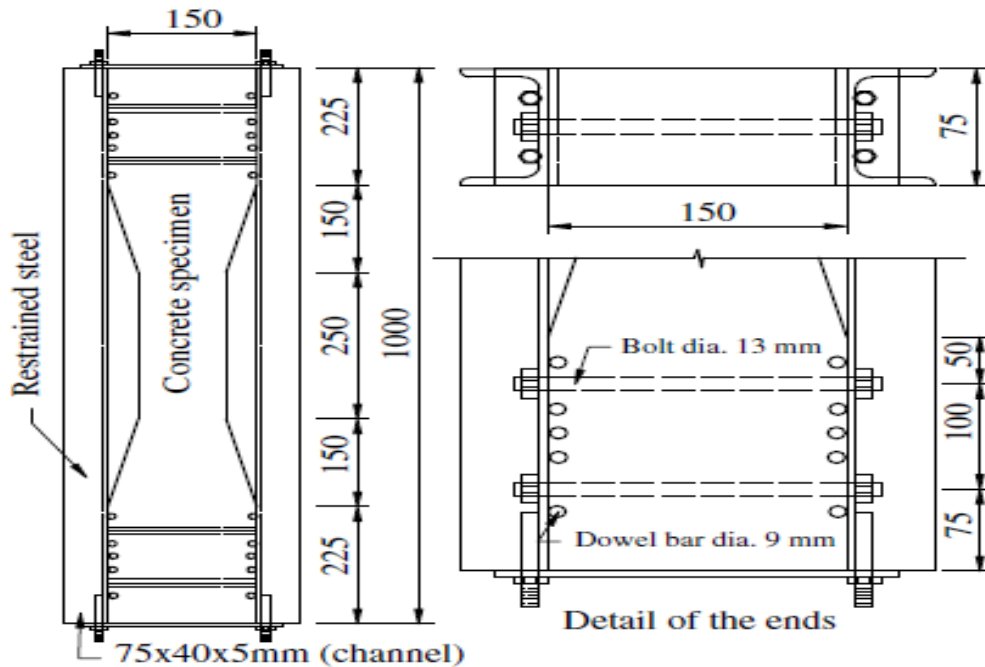


Fig. 2. External restraint shrinkage apparatus [24].

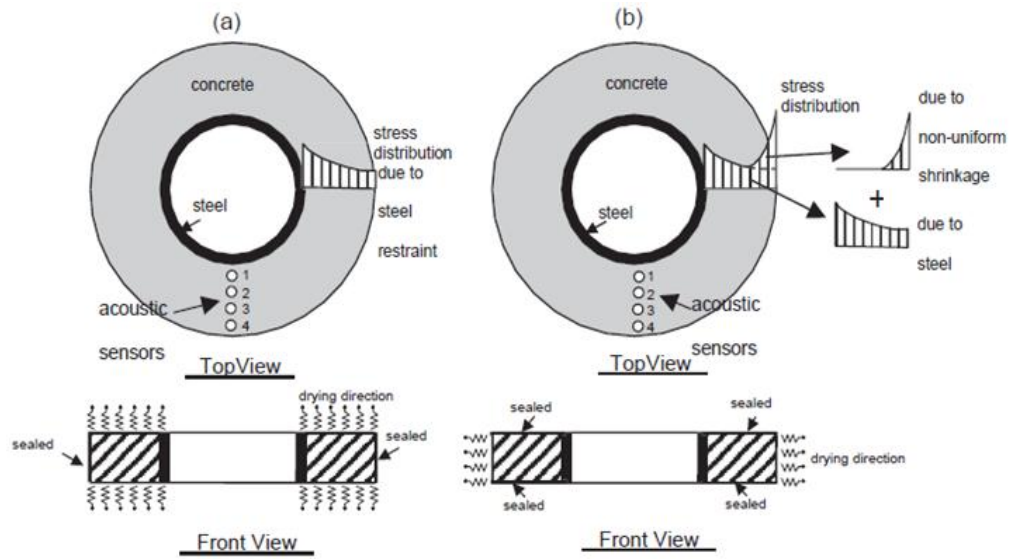


Fig. 3. Restrained ring specimens apparatus [30].

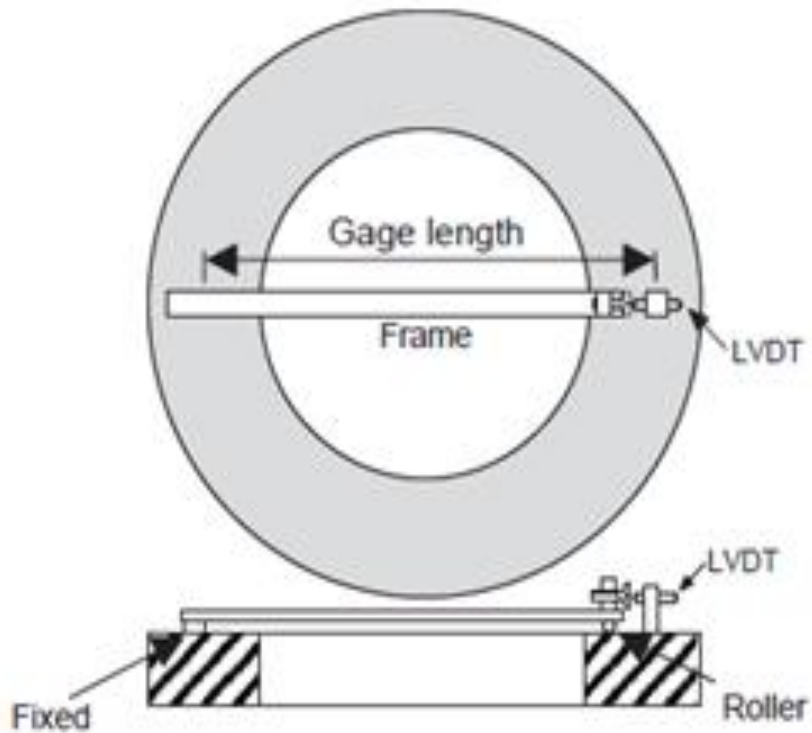


Fig. 4. Unrestrained ring specimen apparatus [30].

Table 1 Summary of influence factors on concrete shrinkage

Categories	Factors affect shrinkage	Specific factors	Findings and conclusions on shrinkage	Reference
	Quantity of aggregate		Increase with increased volume of aggregate content	4, 9, 14
	Size of grading of aggregate		Increase with decreased size of aggregate	4, 14
	Clay content of fine aggregate	Methylene Blue Index		
	Water to cement ratio		Increase with increased MBI, especially MBI higher than 1.45	48
	Paste content		Increase with increased w/c ratio, while others found little or no clear effect	4, 14, 44, 45, 46, 47, 49
	Elastic properties of aggregate		Higher modulus of elasticity aggregate tends to have a low drying shrinkage	4, 14, 44
	Cement characteristics		Lower sulfate content and finely ground cements increase shrinkage	4, 44
	Aggregate types		Higher water demand and higher absorption aggregate increases shrinkage	44
Materials	Aggregate gradation		No influence	44
	Air content		As long as the air content less than 8%, then no significant influence	4, 10
	Supplementary cementitious material	Silica fume	Increase the drying shrinkage for short term w/ higher replacement but no influence on long term	5, 11, 32, 36, 37, 38, 49
		Slag cement	May decrease or increase with increased amount, marginal effect	32, 34, 36, 40
		Fly ash	Increase with increased amount of replacement	32, 33, 40
	Chemical admixture	Water reducer	Increased with increased amount of dosages for most cases, however, high dosage may exhibit low shrinkage.	14, 15, 39, 40, 41
	Size and shape of specimen		Increasing the volume-to-surface area ratio decreases the shrinkage	14, 49
	Degree of hydration		Increase hydration will increase shrinkage	6, 14, 49
	Relative humidity		Higher relative humidity causes lower shrinkage	14, 49
Environment	Curing period		Extended curing period normally reduce shrinkage	4, 14
	Heat and steam curing		Reduce drying shrinkage	4
	Temperature		Shrinkage reduce with lower temperature	6, 14

Table 2 Summary of shrinkage testing methodology

Test Method	Brief description	Advantages	Disadvantages	Reference
Prism test in free condition	ASTM C 157	Most commonly used; easy to conduct	Hardly to correlate lab test to realistic condition, shrinkage is more or less restrained in some ways; strain capacity is hardly to accurately detect concrete cracking process.	21
Prism test in restrained condition	ASTM C 341	Uniaxial stress testing; possibility of using large size aggregate; easy to use portable data logger to detect cracking by an abrupt change of voltage	Not easy to set up equipment	23, 24
Plate test	Cracking length and depth can be measured and so does weighted value for cracking potential comparisons	Can be used to determining the cracking potential due to drying shrinkage; easy to conduct.	Very hard to be consistent because it can provide a biaxial restraint but highly depended on the geometry and boundary conditions	22, 25
Ring test in free condition	Geometry can be the same as restrained condition for comparisons	High and nearly constant restraint; applicable on both mortar and concrete test; lower effects of geometry and boundary conditions due to symmetric geometry	Hard to set up; somehow depends on geometry and boundary conditions when investigating cracking potential;	25, 30, 50
Ring test in restrained condition	ASTM C 1581, associated with fracture mechanics theory or mechanism of concrete specimens	Same as ring test in free condition; axisymmetric nature of geometry eliminates the need to consider tractions on the inner surface of steel ring; effect of creep has been taken into account when collecting strains results from strain gages	Hard to set up; level of restraint of concrete cause non-consistent of cracking potential; linear elasticity may not be accurate for such a non-linear relationship for cracking potential estimation	25, 26, 27, 28, 29, 30

Chapter 3

Drying Shrinkage Behavior of Mortars Made with Ternary Blends

A paper to be submitted to Journal of ASTM International

Xuhao Wang¹, Peter Taylor², Fatih Bektas³, Kejin Wang⁴, and Paul J. Tikalsky⁵

Abstract

In this paper, shrinkage behavior of mortar mixes made with various ternary blends is discussed. Ternary blends consisting of different combinations of portland or blended cement, slag cement, fly ash (class C and F) and/or silica fume were considered. The amounts of slag cement, fly ash and silica fume ranged between 15-35%, 13-30%, and 3-10% by mass of cementitious, respectively. Mortar bars were made with the ternary blends and subjected to a drying condition (i.e., $T = 73 \pm 3$ °F and $RH = 50 \pm 4\%$) after standard curing for 28 days. Free shrinkage of the mortar bars was measured up to 28 days. Based on the test results, a response surface analysis was determined to examine the effects of blend proportions on shrinkage behavior of the mortars. A statistical model was also developed for predicting the mortar shrinkage behavior. To validate this model, shrinkage strains of an independent group of mortar mixes were measured, and the measured values were compared with the predicted shrinkage values. The results indicated that among the three supplementary cementitious

¹ Graduate Student, Iowa State University, Civil, Construction and Environmental Engineering, 136 Town Engineering, Ames, IA 50011, Tel: 515-451-2145, Email: wangxh@iastate.edu

² Associate Director, National Concrete Pavement Technology Center, Iowa State University, Ames, IA 50011, Tel: 515-294-9333, Email: ptaylor@iastate.edu

³ Researcher, National Concrete Pavement Technology Center, Iowa State University, Ames, IA 50011, Tel: 515-294-5857, Email: fbektas@iastate.edu

⁴ Associate Professor, Iowa State University, Civil, Construction and Environmental Engineering, 492 Town Engineering, Ames, IA 50011, Tel: 515-294-5126, Fax: 515-294-8216, Email: kejinw@iastate.edu

⁵ Professor, University of Utah, Civil and Environmental Engineering, 2002 MCE, Salt Lake City, Utah, 84322, Tel: 801-581-6931, Email: tikalsky@civil.utah.edu

materials in the ternary blends studied, slag cement showed a dominant effect on mortar shrinkage. The contribution of class C fly ash to the mortar free shrinkage was slightly less than that of slag cement. Increasing silica fume content slightly increased free shrinkage, while an increase in class F fly ash content slightly decreased free shrinkage of the mortar. There was a good correlation between the measured shrinkage strain and the strain predicted from the shrinkage model developed from the response surface analysis.

Keywords: ternary blend, supplementary cementitious materials, shrinkage

Introduction

Concrete shrinkage, especially drying shrinkage, is of concern to engineers because of its direct influence on cracking risk. Supplementary cementitious materials (SCMs), such as class C fly ash (CFA), class F fly ash (FFA), slag cement (S), natural pozzolans and silica fume (SF) improve concrete performance by nature of their pozzolanic or combined pozzolanic and cementitious reactions [1]. The advantages of using SCMs are mostly in improving concrete durability, economy, and sustainability with reduced environmental impacts [2]. However, disadvantages also exist due to the nature of SCMs, such as slower hydration, accompanied by slower setting and a reported higher risk of drying shrinkage cracking [3].

Current literature focuses on investigating how binary systems affect drying shrinkage. Gesoğlu et al. replaced PC by FFA at levels of 20%, 40%, and 60% and observed that the free shrinkage was reduced by using FFA and this beneficial effect appeared to be more pronounced with increasing replacement levels [4]. In another study, FFA was used to investigate the drying shrinkage behavior in six mixtures cast with total cementitious contents of 400 and 500 kg/m³. The use of the FFA in 500 kg/m³ cementitious content mixtures resulted in a nominal reduction in shrinkage strain [1].

Free shrinkage was reduced by using slag cement in a binary system compared to an ordinary PC mixture. The shrinkage decreased with increased amounts of slag cement [4]. On the other hand, an alkali-activated slag concrete had higher drying shrinkage than plain PC concrete by 1.6 to 2.1 times [5]. In order to assess the influence of slag cement on drying

shrinkage behavior, the Slag Cement Association (SCA) performed a critical review based on published shrinkage research. Slag cement was incorporated either as a separately SCM or as a component in blended cement. The authors concluded that given a similar mixture, slag cement appears to have a marginal effect on increasing shrinkage [6].

A research project using 5% to 15% mass replacement of PC concluded that SF increased the drying shrinkage [4]. Similar conclusions were reached in another study that the ultimate drying shrinkage of mortar increases with increased of SF content at 28 days, but the long-term drying shrinkage after 365 days was not affected significantly by the addition of SF [7]. One study showed that at early ages, the amount of shrinkage showed an increased sensitivity to changes in water-to-cementitious ratio (w/c ratio) as the SF content was increased, while high levels of SF (i.e., over 8%) in mixtures may dramatically increase drying shrinkage [8]. However, some conflicting results were found in other studies: the drying shrinkage of SF incorporated concrete was 10 to 22% higher than that of ordinary PC of same w/c ratio and same binder content for short term [9]; on the other hand, SF concrete had lower shrinkage than that of normal portland cement concrete with the same w/c ratio but marginally lower binder content [10]. The lower drying shrinkage of SF concrete could be attributed to its lower w/c ratio used in the study [11].

Some researches into the effects of drying shrinkage with the use of ternary mixtures have been published. For ternary blends of PC, S, and SF, the adverse effect of the SF was reduced and the shrinkage values compared to control mixture were reduced [4]. Khatri et al. conducted research on shrinkage behavior of the addition of SF to slag cement concrete. It was established that strain due to drying shrinkage was caused by the removal of adsorbed water and the addition of SF to slag cement concrete refined the pore size distribution of the cement paste. The pore refinement could be the cause of reduced loss of water and thus decreased the shrinkage strain [11]. Compared to control mixtures, shrinkage was reduced by using 10% S and 10% FFA, 20% S and 20% FFA, and 30% S and 30% FFA as replacement dosages of PC in ternary blends [4].

The work discussed in this paper was aimed at developing a model of the drying shrinkage behavior of mortars produced with ternary blends. Shrinkage of mortar bars was

determined as 28-day length change. A statistical analysis software package was used to develop models and the validity of the models was tested [12].

Experimental program

Materials

This study consisted of two phases: developing the shrinkage models based on statistical analysis and verification of the proposed models using different materials. The first phase of statistical analysis was conducted based on the data published in reference 13 along with supplementary data obtained as a result of an additional group of mortar bars tested by the authors. The second phase included casting a series of mortar bars to verify the model obtained in phase I. The ternary percentages within the valid range of the model were randomly selected and different cementitious materials were used in Phase II.

Phase I

In order to perform the statistical analysis, the data reported in reference 13 (36 mortar mixtures) was complemented with additional data obtained in the current study (14 mortar mixtures). Mortar bars were cast with the same mix parameters used in reference 13. The mortar mixtures were proportioned with an aggregate to cementitious materials ratio of 2.75 and a w/c ratio of 0.45. The fine aggregate used in reference 13 reportedly complied with the requirements of ASTM C 33 had a specific gravity of 2.61 and a fineness modulus of 2.90, while the sand used in the additional lab study had a specific gravity of 2.62 and a fineness modulus of 3.09 [14]. A trithanolamine based water reducing admixture was utilized to maintain a flow between 80 and 120 in accordance with ASTM C 1437 [15]. All the mixes also included a vinsol resin air entraining agent. Chemistry of the cementitious materials used in both reference 13 and in the laboratory study is given in Table 1.

The ternary mixes are grouped into three series – (1) Type I portland cement (PC), slag cement (15-35%), class F fly ash (13-30%); (2) Type I portland cement, slag cement (15-35%), class C fly ash (15-30%); and (3) Type I portland cement, slag cement (15-35%), silica fume (3-10%). The ternary combinations are given in Table 3(a), 3(b), and

3(c). The ternary components could be either separately blended or a combination of a commercially blended Type IP or IS with an added SCM.

Four 1 × 1 × 1 ¼ inch mortar bars were prepared from each mortar mix in accordance with the method in ASTM C 157 [16]. The bars were moist cured for 28 days and the initial readings were recorded. Then, the mortar bars transferred to a room maintained at 50 ± 4% relative humidity and a temperature of 73 ± 3 F for 28 days. Shrinkage measurements were taken up to 28 days of drying and used for analysis.

Phase II

In this phase of the study, mortar mixes were cast following the same procedures as phase I and the 28-day shrinkage values were compared. Four verification mixes were used for each series using different cementitious materials. The river sand used as fine aggregate was the same as the one used in phase I, and the procedures to prepare and cure mixes were the same as those in phase I. Proportions of the cementitious materials in the verification mixes are given in Table 4. Chemistry of the cementitious materials is given in Table 2.

Results and discussion

Statistical analysis software was used to develop a quadratic response surface model for each series of ternary mixes – PC+S+FFA, PC+S+CFA and PC+S+SF. It is worth noting that in the same series class F fly ash and slag cement are represented by different materials varying in chemistry (e.g., class F fly ash 1 and 2) or in physical properties (e.g., interground or externally blended slag cements).

Since the three cementitious materials contents add up to 100 percent by mass, ternary plots are used to display the distribution of the materials used in each mixture. The ternary display is a triangle with sides scaled from 0 to 1. Data and trends were not extrapolated beyond the bounds of mixtures tested (Figure 1).

Ternary mixtures series I: Type I cement, Class F fly ash, and slag cement

A prediction equation was derived using statistical analysis software. The R² value was determined to be 74%. T-tests showed that slag cement content and the product of Type

I portland cement and slag cement content in series I mortar mixtures have statistically significant effects on 28-day drying shrinkage strain.

$$\varepsilon_{\text{free}} = -5051 \times \text{FFA} + 16041 \times \text{S} + 1605 \times \text{PC} - 17561 \times \text{FFA} \times \text{S} + 6645 \times \text{FFA} \times \text{PC} - 34835 \times \text{S} \times \text{PC}$$

where, $\varepsilon_{\text{free}}$ = drying shrinkage at 28 days, in./in.; FFA = class F fly ash content, %; S = slag cement content, %; PC = Type I Portland cement content, %.

Figure 1 shows the estimated 28-day drying shrinkage strain values. This ternary plot gives a shrinkage range for a specific ternary blend. Figure 2 (a) shows that for a given slag replacement level, shrinkage strain has an increasing trend with the increasing class F fly ash content. However, the findings seem to be in conflict with class F fly ash effects in binary blends systems reported in the literature [1, 4]. The discrepancy may be caused by interactive effect of using slag cement and class F fly ash as ternary blends. The contour lines developed from the response surface analysis in Figure 2 (b) shows that slag content has a significant effect on drying shrinkage strain compared to class F fly ash content. Moreover, it can be observed that drying shrinkage is increasing with increased slag cement content regardless the class F fly ash content between 13% to 30%. A similar trend has been reported in the literature [4-6].

Ternary mixtures series II: Type I cement, Class C fly ash, and slag cement

A prediction equation was derived using statistical analysis software. The R^2 value was determined to be 79%. The high R^2 value indicates a good correlation between predicted shrinkage strain and actual measured shrinkage strain. T-tests found that slag cement content and the product of class C fly ash and slag cement content have a statistically significant effect on 28-day drying shrinkage strain.

$$\varepsilon_{\text{free}} = 6595 \times \text{CFA} + 5303 \times \text{S} - 370 \times \text{PC} - 30030 \times \text{CFA} \times \text{S} + 7043 \times \text{CFA} \times \text{PC} - 8303 \times \text{S} \times \text{PC}$$

where, $\varepsilon_{\text{free}}$ = drying shrinkage at 28 days, in./in.; CFA = class C fly ash content, %; S = slag cement content, %; PC = Type I Portland cement content, %.

Predicted shrinkage of ternary blends in this series is shown in a ternary plot (Figure 3). Figure 4 (a) shows that when mortar mixtures have low slag cement content (i.e., 15-20%), shrinkage decreases as class C fly ash content increases. However, when slag cement

content is between 20 and 35%, the shrinkage tends to increase and this trend is observed to be more distinctive with the increased slag cement content. One of the reasons might be that the lower replacement dosage of slag cement (i.e., <20%) is not as active as higher dosage replacement level (i.e., >20%). Therefore, class C fly ash plays a dominant effect on shrinkage until slag cement content is greater than 20%. The pozzolanic index for class C fly ash listed in Table 1 indicates a high activity which is close to grade 120 slag cement and higher than the class F fly ash. The chemical composition of class C fly ash is closer to portland cement. Figure 4(b) is a 2-D contour plot developed from the response surface analysis to better illustrate the observations from response surface plot of Figure 4(a).

Ternary mixtures series III: Type I cement, silica fume, and slag cement

A prediction equation was derived using statistical analysis software. The R^2 value was determined to be 66%. T-tests found that slag cement content and the product of Type I portland cement and slag cement content have statistically significant effects on 28-day drying shrinkage strain.

$$\varepsilon_{\text{free}} = -7613 \times \text{SF} + 10477 \times \text{S} + 940.1 \times \text{PC} - 2713 \times \text{SF} \times \text{S} + 5039 \times \text{SF} \times \text{PC} - 22725 \times \text{S} \times \text{PC}$$

where, $\varepsilon_{\text{free}}$ = drying shrinkage at 28 days, in./in.; SF = silica fume content, %; S = slag cement content, %; PC = Type I Portland cement content, %.

Predicted shrinkage in this series is shown in a ternary plot (Figure 5). Figure 6 (a) shows that at the constant slag replacement level, shrinkage strain has an increasing trend with increasing silica fume content. This confirms the observations in the literature that silica fume increases shrinkage with increased replacement levels [4, 7-9, 11]. On the other hand, at a constant silica fume replacement dosage, shrinkage increases as the slag cement content increases. The 2-D contour lines developed from the response surface analysis in Figure 6 (b) shows that slag cement content has a significant effect on drying shrinkage strain compared to silica fume content. It also provides a quantitative view on how slag cement content affects drying shrinkage at different silica fume replacement levels.

Table 5 shows measured and predicted 28-day drying shrinkage strains for the ternary mixes. The relationship between measured shrinkage strains and predicted values derived from statistical models is shown in Figure 7. The shrinkage strains of verification mixtures

from phase II versus model predicted shrinkage strain points for series I, II, and III from phase I are highlighted in this figure as well. The R^2 value of 74% indicates that the model predicted shrinkage strains have a good correlation with the measured shrinkage values for the materials tested in this work.

Analysis on Ca/Si ratio and alkali content on drying shrinkage

In order to investigate the relationship between cementitious chemistry and drying shrinkage, the oxide compositions were normalized to 100% based on the percentage of the each ternary component. For example, the ternary mixture I-20 contains 68% Type I portland cement, 15% class F fly ash, and 17% slag. For a specific oxide, Type I, class F fly ash and slag cement contribute 68%, 15%, and 17%, respectively.

Table 6 summarizes the Ca/Si ratio and equivalent alkali content (i.e., $\text{Na}_2\text{O} + 0.658 \text{K}_2\text{O}$) for the mixtures in phase I. Figure 8 shows a plot of 28-day shrinkage strain vs Ca/Si ratio for series I, II, and III. The trend line in the plot shows that ternary blended mixtures with higher Ca/Si ratio tend to exhibit a lower shrinkage strain. However, the low value of R^2 indicates that a model based on these data may not be reliable. The alkali content for phase I mixtures of series I, II, and III are plotted against the 28-day shrinkage strain in Figure 9. This plot shows that the increasing alkali content in ternary blended mixtures tends to increase shrinkage strain. Again the R^2 is low indicating that the relationship is likely tenuous.

Discussion

From a microstructural point of view, solids in the hydrated cement paste include four principal solid phases, calcium silica hydrate (40 to 50%); calcium hydroxide (20 to 25%); calcium sulfoaluminate hydrates (15 to 20%) and unhydrated clinker grains [18].

Water can exist in many forms in the hydrated cement paste and they can be classified depending on the degree of ease with which it can be removed from the paste (Figure 10):

The capillary voids that represent the voids not filled by solid hydration products, initially filled with excess unhydrated water. Such voids will retain water by capillary tension. Water in the larger voids ($>50 \text{ nm}$) is considered to be “free water” because its removal does not result in volume change. However, water in small capillary voids (5 to 50 nm) may result

in large shrinkage strains when water is forced to leave the system [18]. The size and volume of the capillary voids are determined by the initial w/c ratio and the degree of cement hydration. At a constant w/c ratio, increasing the degree of hydration decreases the size and volume of the capillary voids. Subsequent drying then will result in reduced shrinkage strain [18].

Adsorbed water is the water bonded to but not reacted with the surface of hydration products. Water molecules are physically adsorbed onto the surface of solids in hydrate cement by influence of attractive forces such as hydrogen bonding. The removal of adsorbed water will result in shrinkage strains, but such removal will not occur when the RH of the pore system is low (less than about 40% RH) [21].

Interlayer water is the water held within the calcium silica hydrate (CSH) nano-structure. The water in the interlayer space of CSH voids is held by Van der Waals forces [22]. Because of the extremely small size of the so-called gel pores, removal of interlayer water will only occur under very dry conditions (about 10% RH) [18, 21]. The size and volume of gel pores vary depending on the Ca/Si ratio, type of molecules (non-ionic, anionic or cationic), concentration and pH while they are independent of the initial w/c ratio and degree of hydration [22, 23]. Therefore, increasing the Ca/Si ratio may decrease the size and volume of gel pores and so increase resistance to water removal [19].

Based on these mechanisms, the following discussion addresses how the changes in cementitious materials may be affecting shrinkage strain:

Class F fly ash with low-calcium content in series I have been reported to contain nonreactive crystalline minerals, such as quartz, mullite and magnetite [18]. These crystalline minerals tend to reduce the pozzolanic activity of class F fly ash. However, class C fly ash with high-calcium content in series II is generally considered to be more reactive because it contains reactive crystalline compounds, such as C_3A and free lime. As a result, class C fly ashes are generally more reactive than class F ashes. Subsequently, the volume of capillary voids in mixtures containing class C fly ashes may be less than those containing class F fly ashes and exhibit reduced drying shrinkage [18]. In addition, the chemical characteristics of class C fly ash will result in high Ca/Si ratio in the mixture which reduces the size and

volume of gel pores in CSH system. The removal of interlayer water from CSH system is likely reduced therefore reducing shrinkage strain [23].

Slag cement is similar to high-calcium fly ashes in the mineralogical composition and reactivity [18]. The high reactivity of slag cement may increase the degree of hydration result in reduced volume of capillary voids in a mixture so as to reduce drying shrinkage. The chemical composition of slag cement generally includes very low alkali contents. Previous research reported that a decrease of alkali content could decrease the shrinkage strain [20]. The low alkali content in slag cement plays a beneficial role in reducing drying shrinkage in a mixture.

It has been demonstrated that the particle size distributions of silica fume are about two orders of magnitude finer than typical fly ashes [18]. It is a high reactive pozzolanic material due to this fineness and its composition comprising mostly silica. Silica fume is reported to react with CH crystal hydrates to create additional CSH. This makes the concrete more resistance to drying shrinkage caused by force applied to it, such as surface tension and capillary tension [17]. On the other hand a decreased Ca/Si ratio in the cementitious system will likely increase shrinkage [23].

Therefore, the shrinkage of a cementitious system at a constant w/c ratio appears to be affected by degree of hydration depending on material reactivity. The reactivity is determined by cementitious material particle size distributions and chemical composition, such as alkali content and crystalline compounds content. Ca/Si ratio of cementitious material is another important influence factor that changes volume of gel pores in CSH system so as to drying shrinkage in a ternary blend mixture.

Conclusions

The following conclusions can be drawn from the present study:

- Slag cement shows a dominant effect on increasing mortar shrinkage in all three series. An increase of class C fly ash in series II is likely to decrease the mortar shrinkage. It also has a dominant effect although the effect of slag cement is slightly stronger. Silica fume in series III does not have a very strong effect while increasing in silica fume content still slightly increases free shrinkage of the mortar in ternary blends. An increase of class F fly ash in series I tends to increase the mortar shrinkage.

However, this behavior is likely tenuous and class F fly ash shows the least dominant effect on the shrinkage in ternary blended slag cement mixture.

- The mineralogical and chemical composition promotes the reactivity of slag cement. The low alkali content in slag cement plays a beneficial role on drying shrinkage in a mixture. Class C fly ash with high-calcium content is similar to slag cement in the mineralogical composition and reactivity. In addition, the chemical characteristics of class C fly ash will result in high Ca/Si ratio in the mixture which reduces the size and volume of gel pores in CSH system. The removal of interlayer water from CSH system is likely reduced therefore reducing shrinkage strain. The particle size distributions play a significant role on increasing pozzolanic reactivity of silica fume. The slightly increased mortar free shrinkage of silica fume in ternary blends is mainly due to the high pozzolanic reactivity and pore size refinement mechanisms. Class F fly ash with low calcium content results in low pozzolanic reactivity that plays the least effect on drying shrinkage of mortar in ternary blends.
- The shrinkage measurements from a group of verification mortar mixes have evidenced a good correlation between the measured shrinkage strain and the strain predicted from the shrinkage model developed from the response surface analysis.

Acknowledgements

The present study is a part of the research project, Development of Performance Properties of Ternary Mixtures, which is pool funded by Federal Highway Administration (FHWA), nine state departments of transportation (California, Illinois, Iowa, Kansas, Mississippi, New Hampshire, Pennsylvania, Wisconsin, and Utah), some concrete admixture companies, and the National Center of Concrete Pavement Technology (CP Tech Center). The authors acknowledge the research sponsorship and the collaboration between Iowa State University (ISU) and the University of Utah. Parts of the work were conducted in Pennsylvania State University which is gratefully acknowledged and help from Dr. Robert Stephenson from statistical department of ISU are earnestly appreciated.

References

- [1] Haque MN, Kayali O. Properties of high-strength concrete using a fine fly ash. *Cement and Concrete Research*, Vol. 28, No. 10, pp. 1445-1452, 1998.
- [2] Shiathas C, Muntasser TZ, Nwaubani SO. A comparative study of the properties and durability of binary and ternary cementitious systems. *Durability of Concrete*. SP-212-29. pp. 459-468.
- [3] Wang K. Sustainable benefits of utilizing supplementary cementing materials in concrete in desert environment. Iowa State University.
- [4] Gesoğlu M, Güneyisi E, Özbay E. Properties of self-compacting concretes made with binary, ternary, and quaternary cementitious blends of fly ash, blast furnace slag, and silica fume. *Construction and Building Materials*. 23 (2009) 1847-1854.
- [5] Collins F, Sanjayan JG. Cracking tendency of alkali-activated slag concrete subjected to restrained shrinkage. *Cement and Concrete Research* 30 (2000) 791-798.
- [6] Slag Cement Association. Effect of slag cement on shrinkage in concrete. *Slag Cement in Construction*. No. 27. 2005.
- [7] Rao GA. Long-term drying shrinkage of mortar – influence of silica fume and size of fine aggregate. *Indian Institution of Science. Cement Concrete Research* 31 (2000) 171- 175.
- [8] Whiting DA, Detwiler RJ, Lagergren ES. Cracking tendency and drying shrinkage of silica fume concrete for bridge deck applications. *ACI Materials Journal*. Title No. 96-M10. 2000.
- [9] Hooton RD. *ACI Materials Journal*, 90, 143, 1993.
- [10] Tazawa E and Yonekura A. Proc. of second international conference on fly ash, silica fume, slag and natural pozzolans in concrete, Madrid, Spain. *ACI SP 91-43*, 903, 1986.
- [11] Khatri RP, Sirivivatn AV, and Gross W. Effect of different supplementary cementitious materials on mechanical properties of high performance concrete. *Cement and Concrete Research*, 25(1) (1995), 209-220.
- [12] JMP 8.0.0. *Statistical Discovery*. From SAS. SAS Institute Inc. 2005.

- [13] Tikalsky P, Taylor P, Hanson S, Ghosh P. Development of performance properties of ternary mixes: laboratory study on concrete. Report No. DTFH61-06-H-00011 Work Plan 12 Pooled Fund Study TPF-5(117). Ames: National Center for Concrete Pavement Technology. March 2011.
- [14] ASTM Standard C33-03. Standard specification for concrete aggregates. Annual Book of Standards, Vol. 4.02, ASTM International, WestConshohocken, PA. 2008.
- [15] ASTM Standard C1437-01. Standard test method for flow of hydraulic cement mortar. Annual Book of Standards, Vol. 4.02, ASTM International, WestConshohocken, PA. 2008.
- [16] ASTM Standard C157-06. Standard test method for length change of hardened hydraulic-cement mortar and concrete. Annual Book of Standards, Vol. 4.02, ASTM International, WestConshohocken, PA. 2008.
- [17] Liu J, Yao Y. A study on creep and drying shrinkage of high performance concrete. Cement and Concrete Research, v. 31, n. 8, 2001, p. 1203-1206.
- [18] Malhotra VM, Mehta PK. Pozzolan and cementitious materials. Advances in Concrete Technology, v. 1, 1996.
- [19] Taylor HF. Cement Chemistry. Thomas Telford Ltd. 2nd edition. 1997.
- [20] Jawed I, Skalny J. Alkalies in cement: a review II. Effects of alkali on hydration and performance of portland cement. Cement and Concrete Research, 1978; 37-52.
- [21] Idiart, AE. Coupled analysis of degradation processes in concrete specimens at the meso-level. Master Thesis: Universitat Politecnica De Catalunya, 2009, 45-48.
- [22] Raki L, Beaudoin J, Alizadeh R, Makar J, Sato T. Cement and concrete nanoscience and nanotechnology. Materials. 2010, 3, 918-942; ISSN 1996-1944.
- [23] Selvam RP, Subramani VJ, Murray S, Hall K. Potential application of nanotechnology on cement based materials. Project Number: MBTC DOT 2095/3004. August 06, 2009.
- [24] Feldman RF, Sereda PJ. Sereda, Eng. J. (Canada), Vol. 53, No. 8/9, pp. 53-59, 1970.

List of Figures

- Figure 1. Ternary plot for series I.
- Figure 2. (a) Response surface plot for series I.
- Figure 2. (b) 2-D Contour plot developed from the response surface plot for series I.
- Figure 3. Ternary plot for series II.
- Figure 4. (a) Response surface plot for series II.
- Figure 4. (b) 2-D Contour plot developed from the response surface plot for series II.
- Figure 5. Ternary plot for series III.
- Figure 6. (a) Response surface plot for series III.
- Figure 6. (b) 2-D Contour plot developed from response surface plot for series III.
- Figure 7. Designed and verification mixtures shrinkage strain versus model predicted shrinkage strain.
- Figure 8. Relationship between Ca/Si ratio and 28-day shrinkage strain.
- Figure 9. Relationship between alkali content and 28-day shrinkage strain.
- Figure 10. Diagrammatic model of the types of water associated with the calcium silicate hydrate [24].

List of Tables

- Table 1. Chemical and physical properties of cementitious materials
- Table 2. Chemical and physical properties of cementitious materials used for model verification
- Table 3 (a). Ternary blends SCMs compositions and verification mixtures for series I
- Table 3 (b). Ternary blends SCMs compositions and verification mixtures for series II
- Table 3 (c). Ternary blends SCMs compositions and verification mixtures for series III
- Table 4. Proportions of the cementitious materials in phase II
- Table 5. 28-day drying shrinkage strain and model predicted shrinkage strain for series I, II, and III mortar mixes
- Table 6. Ca/Si ratio and equivalent alkali content for mixtures in phase I

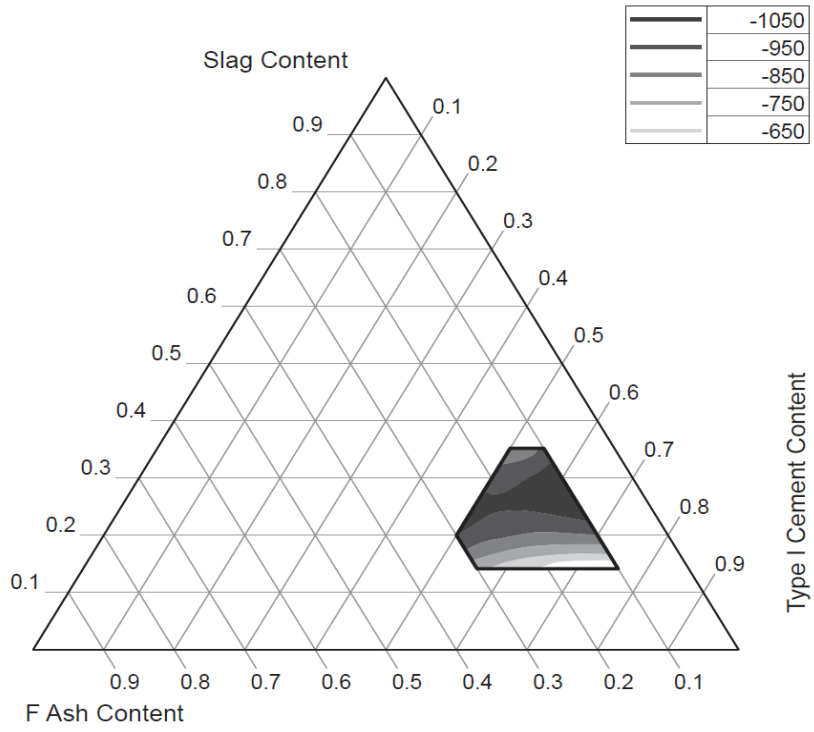


Figure 1. Ternary plot for series I.

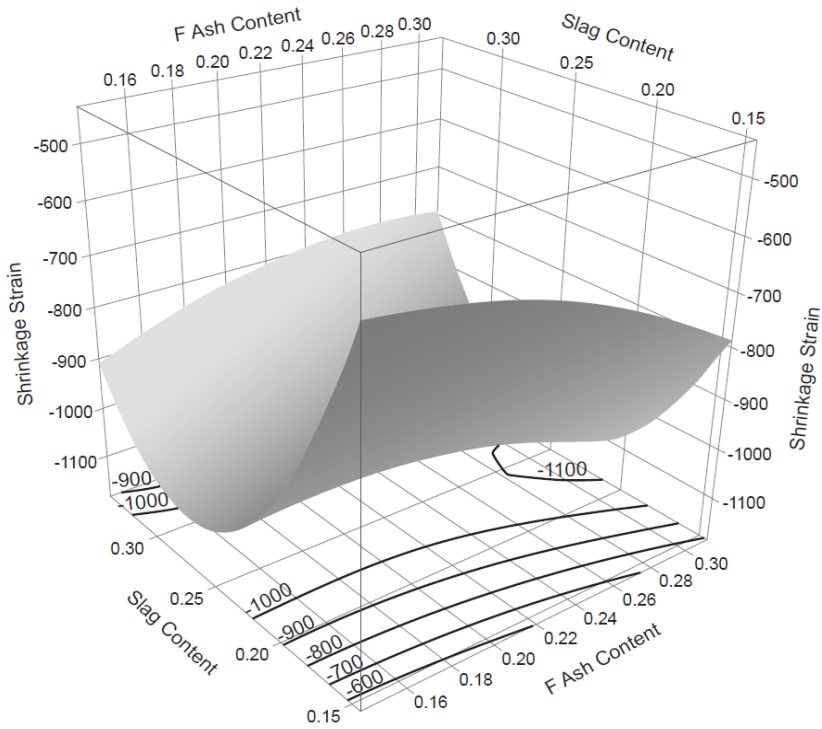


Figure 2. (a) Response surface plot for series I.

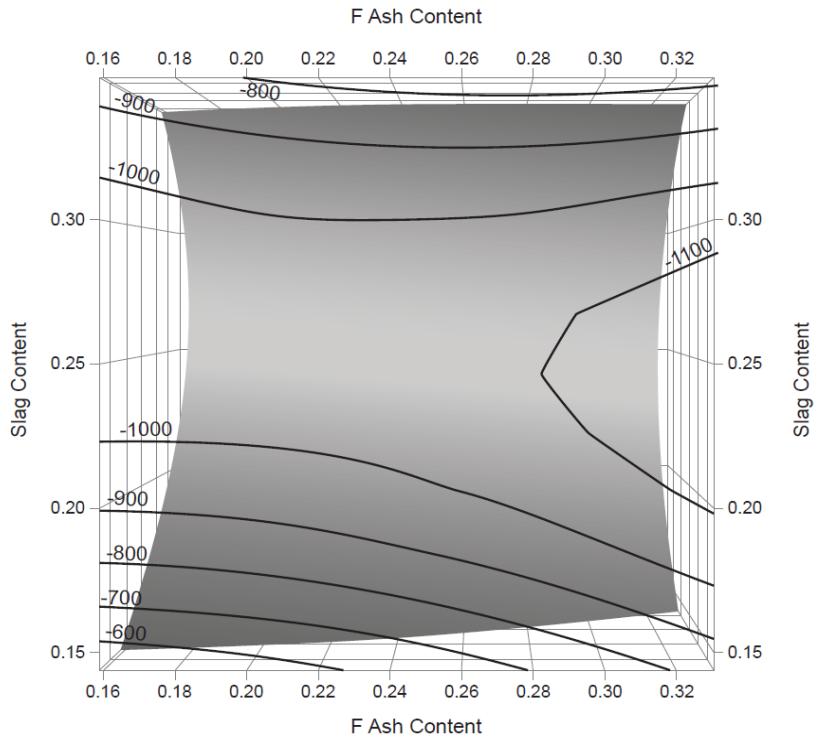


Figure 2. (b) 2-D Contour plot developed from the response surface plot for series I.

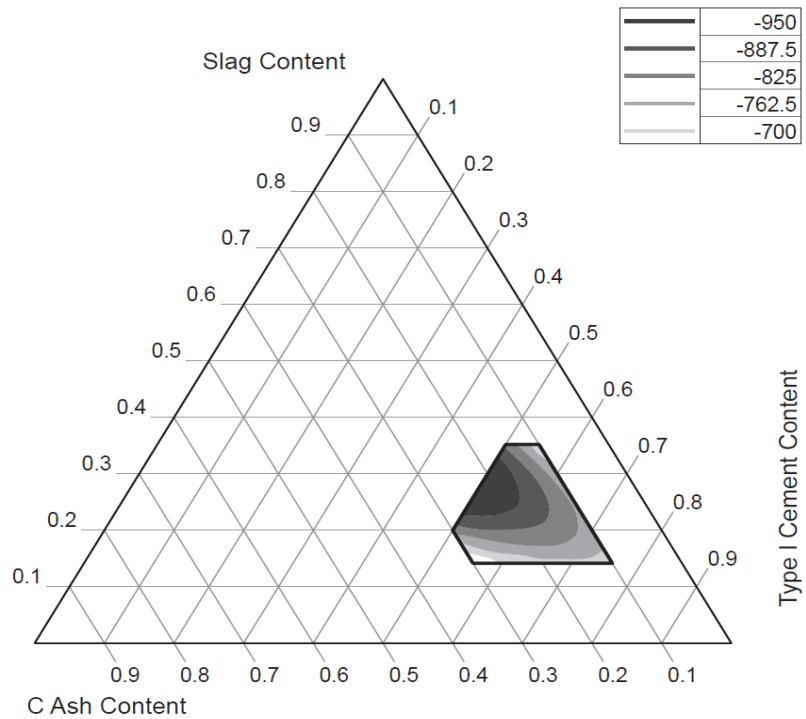


Figure 3. Ternary plot for series II.

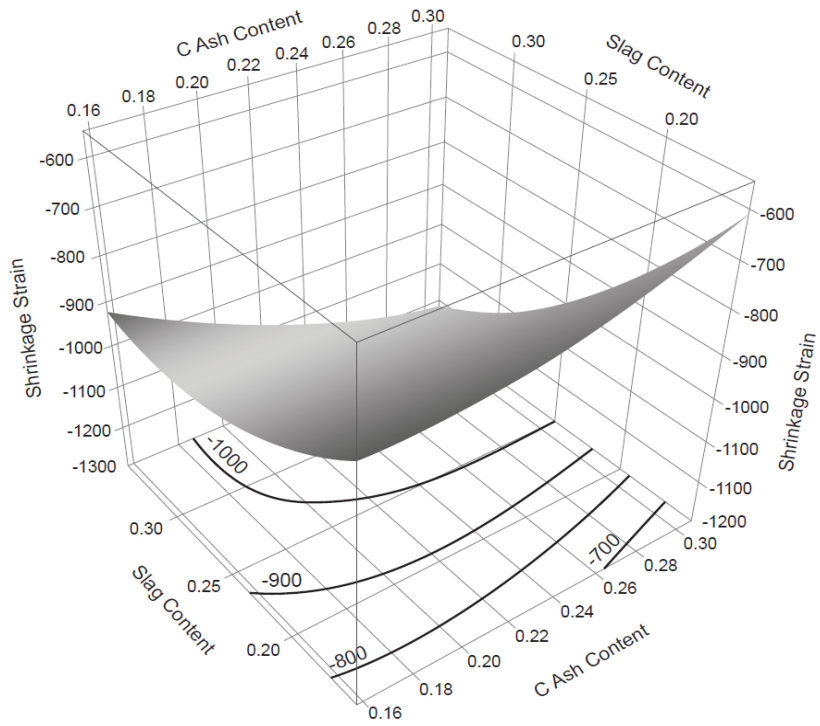


Figure 4. (a) Response surface plot for series II.

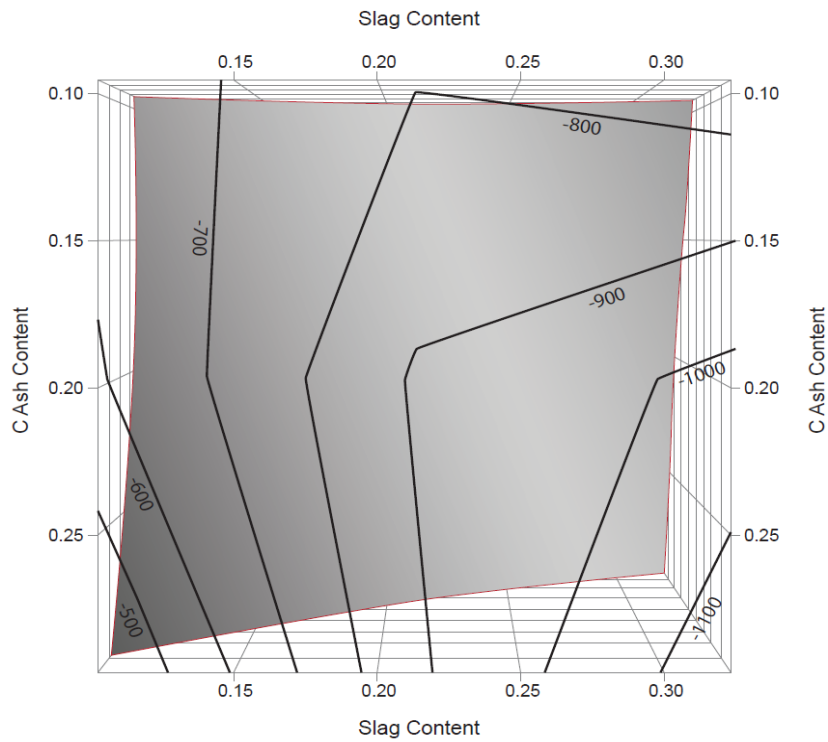


Figure 4. (b) 2-D Contour plot developed from the response surface plot for series II.

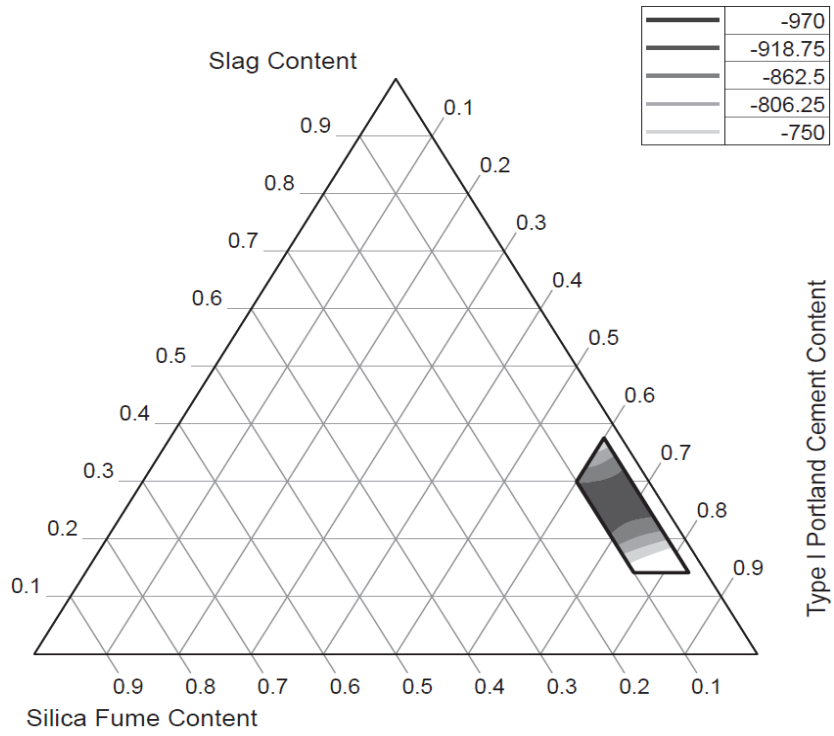


Figure 5. Ternary plot for series III.

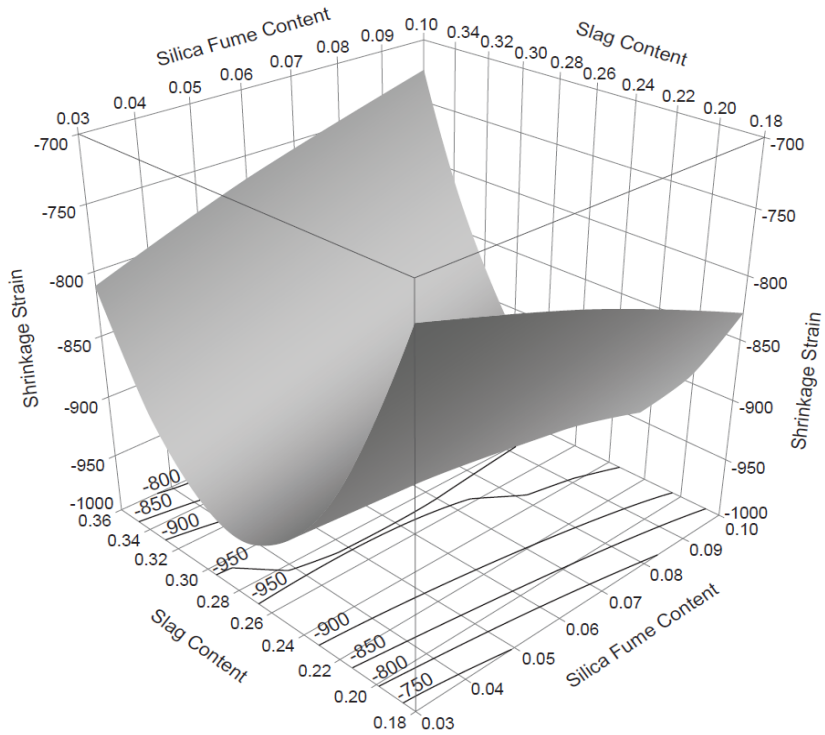


Figure 6. (a) Response surface plot for series III.

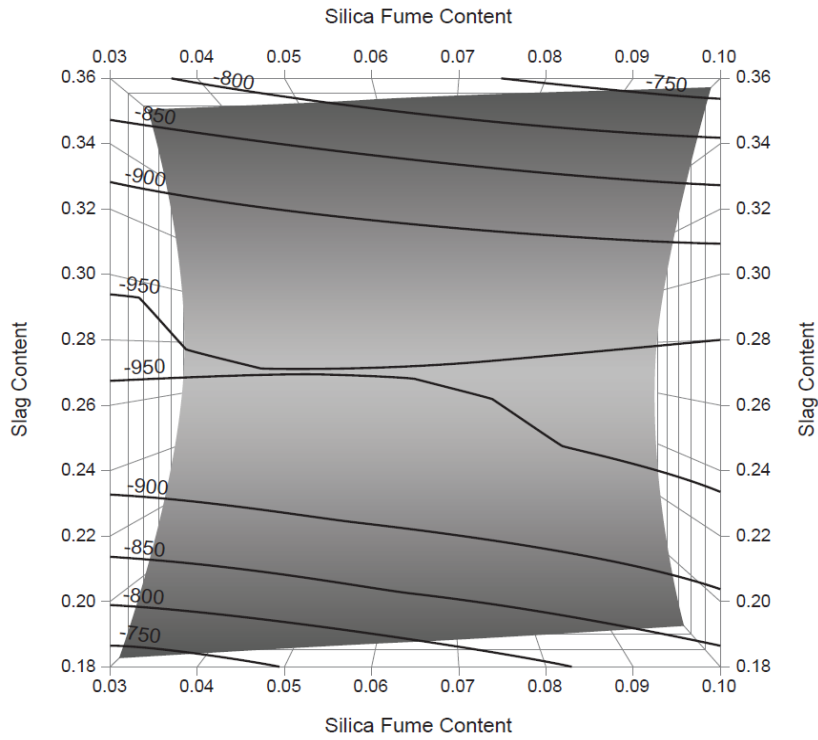


Figure 6. (b) 2-D Contour plot developed from response surface plot for series III.

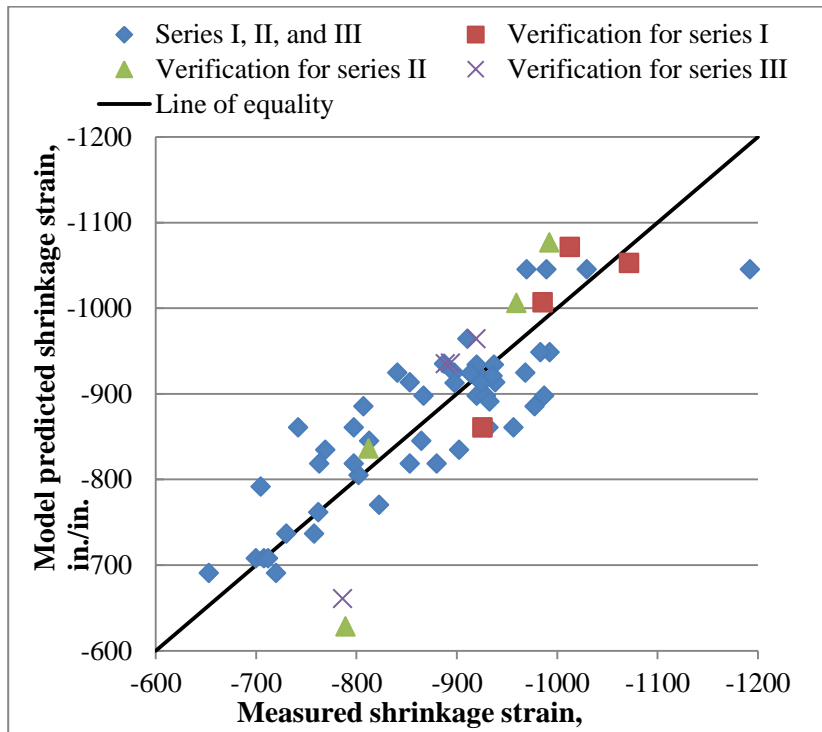


Figure 7. Designed and verification mixtures shrinkage strain vs. predicted shrinkage strain.

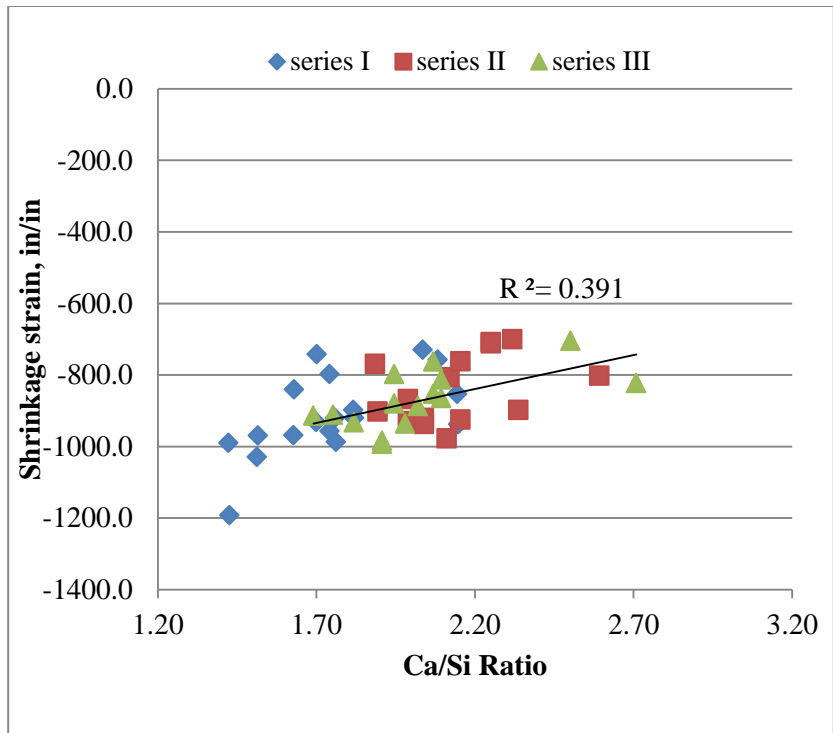


Figure 8. Relationship between Ca/Si ratio and 28-day shrinkage strain.

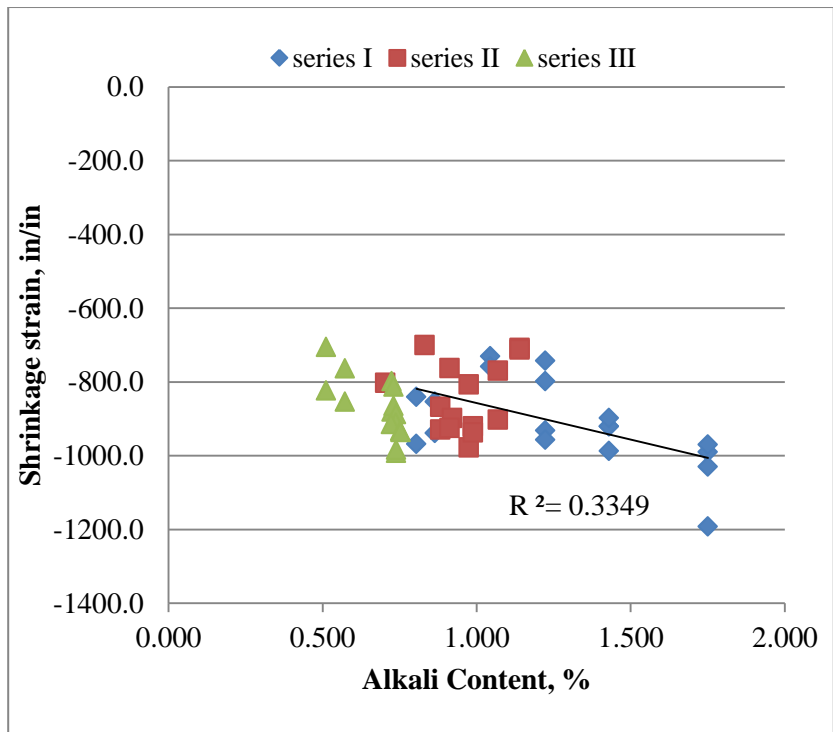


Figure 9. Relationship between alkali content and 28-day shrinkage strain.

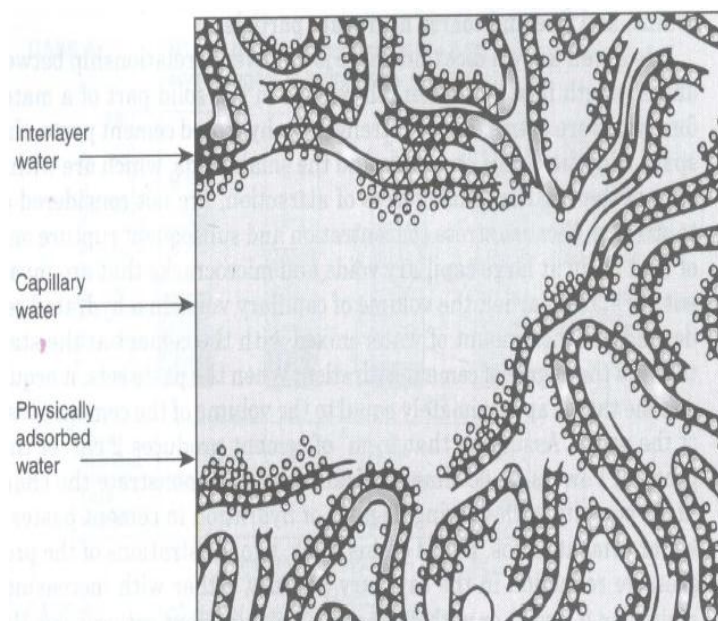


Figure 10. Diagrammatic model of the types of water associated with the calcium silicate hydrate [24].

Table 1. Chemical and physical properties of cementitious materials

Chemical, %	Type I-1	Type IS(20)	Type IP(20)	Type IP(7)	CFA	FFA1	FFA2	S100	S120	SF1
CaO	61.71	58.19	50.88	59.15	27.18	3.78	13.15	36.86	36.77	0.42
SiO ₂	19.80	23.53	28.88	24.91	34.02	45.05	51.40	37.40	36.81	97.90
Al ₂ O ₃	6.18	5.29	8.19	4.38	18.20	23.71	16.21	8.98	9.66	0.18
Fe ₂ O ₃	2.50	2.97	3.70	3.12	6.59	16.43	6.73	0.76	0.61	0.07
MgO	2.76	4.34	1.60	1.36	5.06	0.88	4.41	10.60	10.03	0.21
K ₂ O	0.74	0.58	0.90	0.56	0.35	1.46	2.33	0.40	0.35	0.59
Na ₂ O	0.36	0.13	0.35	0.22	1.56	0.80	2.86	0.29	0.31	0.12
SO ₃	2.63	2.88	2.74	3.33	2.70	0.68	0.80	-	-	0.17
P ₂ O ₅	0.21	0.09	0.22	0.11	1.29	0.24	0.15	0.02	0.01	0.12
TiO ₂	0.28	0.41	0.44	0.29	1.57	1.15	0.63	0.38	0.49	-
SrO	0.24	0.04	0.20	0.10	0.50	0.18	0.33	0.04	0.05	0.01
Mn ₂ O ₃	0.11	0.50	0.20	0.18	0.06	0.03	0.05	0.73	0.39	0.03
LOI	2.37	0.70	1.14	1.60	0.27	5.39	0.05	-	-	-
Specific gravity	3.04	2.95	3.11	3.08	2.62	2.37	2.41	2.82	2.96	2.21
Pozzolanic Index					108	86	107	97	112	125

Note: FFA1 and FFA2 denote different Class F fly ashes. S100 and S120 denote different grade of slag cement.

Table 2. Chemical and physical properties of cementitious materials used for model verification

Chemical, %	Type I-2	S	CFA	FFA1	SF2
CaO	63.22	42.25	27.18	3.78	0.46
SiO ₂	20.97	38.82	34.02	45.05	94.32
Al ₂ O ₃	4.47	7.27	18.20	23.71	0.28
Fe ₂ O ₃	2.93	0.81	6.59	16.43	0.31
MgO	2.30	9.02	5.06	0.88	0.75
K ₂ O	0.60	0.50	0.35	1.46	0.48
Na ₂ O	0.16	0.31	1.56	0.80	0.08
SO ₃	2.63	-	2.70	0.68	0.05
P ₂ O ₅	0.12	0.03	1.29	0.24	0.09
TiO ₂	0.31	0.41	1.57	1.15	0.01
SrO	0.08	0.05	0.50	0.18	-
Mn ₂ O ₃	0.04	0.52	0.06	0.03	-
LOI	2.17	-	0.27	5.39	2.58
Specific gravity	3.15	2.87	2.62	2.37	2.25

Table 3 (a). Ternary blends SCMs compositions and verification mixtures for series I

Mix ID	FFA1, %	FFA2, %	FFA in IP(20)	S100, %	S120, %	Slag in IS(20)	Type I-1, %
I-1	30	-	-	20	-	-	50
I-2	30	-	-	-	20	-	50
I-3	-	30	-	20	-	-	50
I-4	-	30	-	-	20	-	50
I-5	15	-	-	35	-	-	50
I-6	-	15	-	35	-	-	50
I-7	15	-	-	-	35	-	50
I-8	-	15	-	-	35	-	50
I-9	20	-	-	20	-	-	60
I-10	20	-	-	-	20	-	60
I-11	-	20	-	20	-	-	60
I-12	-	20	-	-	20	-	60
I-13	-	-	13	35	-	-	52
I-14	-	-	13	-	35	-	52
I-15	25	-	-	-	-	15	60
I-16	-	25	-	-	-	15	60
I-17	-	-	16	20	-	-	64
I-18	-	-	16	-	20	-	64
I-19	15	-	-	-	-	17	68
I-20	-	15	-	-	-	17	68

Note: Mixtures I-1 to I-20 are from reference [13].

Table 3 (b) Ternary blends SCMs compositions and verification mixtures for series II

Mix ID	CFA, %	S100, %	S120, %	S in IS(20)	Type I-1
II-1	30	20	-	-	50
II-2	30	-	20	-	50
II-3	15	35	-	-	50
II-4	15	-	35	-	50
II-5	20	20	-	-	60
II-6	20	-	20	-	60
II-7	25	-	-	15	60
II-8	15	-	-	17	68
II-9	22	-	22	-	56
II-10	22	22	-	-	56
II-11	15	-	15	-	70
II-12	15	-	25	-	60
II-13	15	25	-	-	60
II-14	25	15	-	-	60
II-15	25	-	15	-	60

Note: Mixtures II-1 to II-8 are from reference [13].

Table 3 (c). Ternary blends SCMs compositions and verification mixtures for series III

Mix ID	S100, %	S120, %	S in IS(20)	SF1, %	Type I-1
III-1	35	-	-	5	60
III-2	-	35	-	5	60
III-3	35	-	-	5	60
III-4	-	35	-	5	60
III-5	35	-	-	3	62
III-6	-	35	-	3	62
III-7	-	-	19	5	76
III-8	-	-	19	3	78
III-9	-	30	-	5	65
III-10	-	25	-	10	65
III-11	-	30	-	10	60
III-12	-	28	-	7	65
III-13	28	-	-	7	65
III-14	-	20	-	10	70
III-15	-	23	-	7	70

Note: Mixtures III-1 to III-8 are from reference [13].

Table 4. Proportions of the cementitious materials in phase II

Mix ID	FFA1, %	Type I-2, %	S, %	CFA, %	SF2, %
V-I-1	15	55	30	-	-
V-I-2	15	50	35	-	-
V-I-3	22	56	22	-	-
V-I-4	25	50	25	-	-
V-II-1	-	64	18	18	-
V-II-2	-	50	25	25	-
V-II-3	-	55	15	30	-
V-II-4	-	44	28	28	-
V-III-1	-	65	30	-	5
V-III-2	-	71	25	-	4
V-III-3	-	65	25	-	10
V-III-4	-	77	15	-	8

Table 5. 28-day drying shrinkage strain and model predicted shrinkage strain for series I, II, and III mortar mixes

Mix ID	Measured shrinkage strain, in./in.	Model predicted shrinkage strain, in./in.	Mix ID	Measured shrinkage strain, in./in.	Model predicted shrinkage strain, in./in.	Mix ID	Measured shrinkage strain, in./in.	Model predicted shrinkage strain, in./in.
I-1	-1192	-1045	II-1	-902	-835	III-1	-798	-818
I-2	-990	-1045	II-2	-769	-835	III-2	-880	-818
I-3	-970	-1045	II-3	-929	-898	III-3	-763	-818
I-4	-1030	-1045	II-4	-867	-898	III-4	-853	-818
I-5	-932	-861	II-5	-807	-885	III-5	-813	-845
I-6	-957	-861	II-6	-978	-885	III-6	-865	-845
I-7	-742	-861	II-7	-700	-708	III-7	-705	-791
I-8	-798	-861	II-8	-802	-805	III-8	-823	-770
I-9	-987	-898	II-9	-920	-934	III-9	-887	-935
I-10	-920	-898	II-10	-937	-934	III-10	-911	-964
I-11	-920	-924	II-11	-898	-913	III-11	-914	-924
I-12	-898	-924	II-12	-925	-913	III-12	-993	-948
I-13	-968	-924	II-13	-762	-761	III-13	-983	-948
I-14	-841	-924	II-14	-708	-708	III-14	-933	-891
I-15	-653	-691	II-15	-712	-708	III-15	-936	-921
I-16	-720	-691	V-II-1	-812	-836	V-III-1	-889	-935
I-17	-938	-913	V-II-2	-960	-1006	V-III-2	-894	-936
I-18	-853	-913	V-II-3	-789	-628	V-III-3	-919	-964
I-19	-730	-736	V-II-4	-992	-1076	V-III-4	-786	-661
I-20	-758	-736						
V-I-1	-1072	-1053						
V-I-2	-926	-861						
V-I-3	-986	-1006						
V-I-4	-1013	-1071						

Table 6. Ca/Si ratio and equivalent alkali content for mixtures in phase I

Mix ID	Ca/Si	Eq. alkali content, %	Mix ID	Ca/Si	Eq. alkali content, %	Mix ID	Ca/Si	Eq. alkali content, %
I-1	1.43	1.750	II-1	1.89	1.069	III-1	1.95	0.724
I-2	1.42	1.750	II-2	1.89	1.069	III-2	1.95	0.724
I-3	1.52	1.750	II-3	1.99	0.882	III-3	2.07	0.573
I-4	1.51	1.750	II-4	1.99	0.882	III-4	2.07	0.573
I-5	1.70	1.223	II-5	2.12	0.975	III-5	2.09	0.731
I-6	1.74	1.223	II-6	2.11	0.975	III-6	2.09	0.731
I-7	1.70	1.223	II-7	2.32	0.831	III-7	2.50	0.511
I-8	1.74	1.223	II-8	2.59	0.703	III-8	2.71	0.511
I-9	1.63	1.429	II-9	2.04	0.988	III-9	2.02	0.739
I-10	1.63	1.429	II-10	2.04	0.988	III-10	1.75	0.737
I-11	1.76	1.429	II-11	2.34	0.920	III-11	1.69	0.722
I-12	1.76	1.429	II-12	2.15	0.913	III-12	1.91	0.738
I-13	1.82	0.805	II-13	2.15	0.913	III-13	1.91	0.738
I-14	1.82	0.805	II-14	2.25	1.140	III-14	1.82	0.752
I-15	1.69	1.399	II-15	2.25	1.140	III-15	1.98	0.753
I-16	1.75	1.399						
I-17	2.15	0.865						
I-18	2.14	0.865						
I-19	2.04	1.044						
I-20	2.08	1.044						

Chapter 4

Drying Shrinkage of Ternary Blend Concrete in Transportation Structures

A paper to be submitted to Construction and Building Materials

Xuhao Wang⁶, Kejin Wang⁷, Fatih Bektas⁸, and Peter Taylor⁹

Abstract

In this paper, factors affecting drying shrinkage behavior of ternary blend concretes are studied. Five concrete mixes used for either pavement or bridge deck construction in different states are tested for both restrained and unrestrained shrinkages. The effects of blend materials and mix proportion on the concrete shrinkages are assessed. The results indicate that shrinkage strain rate linearly increases with clay content of fine aggregate, cementitious material content, paste-to-void ratio (by volume), and dosage of water reducer of the concrete mixes.

Keywords: ternary blends, drying shrinkage, cracking potential

⁶ Graduate Student, Iowa State University, Civil, Construction and Environmental Engineering, 136 Town Engineering, Ames, IA 50011, Tel: 515-451-2145, Email: wangxh@iastate.edu

⁷ Associate Professor, Iowa State University, Civil, Construction and Environmental Engineering, 492 Town Engineering, Ames, IA 50011, Tel: 515-294-5126, Fax: 515-294-8216, Email: kejinw@iastate.edu

⁸ Researcher, National Concrete Pavement Technology Center, Iowa State University, Ames, IA 50011, Tel: 515-294-5857, Email: fbektas@iastate.edu

⁹ Associate Director, National Concrete Pavement Technology Center, Iowa State University, Ames, IA 50011, Tel: 515-294-9333, Email: ptaylor@iastate.edu

Introduction

Concrete shrinkage, especially drying shrinkage, is of concern to engineers because of its direct influence on cracking risk. The drying shrinkage occurs when the specimen is exposed to a drying environment and allowed to have volumetric changes [1]. It is considered that the shrinkage strain in normal strength concrete (i.e., < 6000 psi at 28 days) primarily results from drying shrinkage and any contribution from autogenous shrinkage is marginal [1, 2]. Decreasing concrete volume with time due to moisture loss (drying shrinkage) is unavoidable [3, 4]. The shrinkage cracking of concrete may accelerate the deterioration of concrete used in transportation structures. For instance, deicer salts may reach to the steel surface through cracks or by capillary action and cause corrosion which leads to further cracking, delamination, and spalling of the concrete [5].

From a microstructural point of view, although the loss of moisture plays a significant role on drying shrinkage, an increase in water loss does not correspond to a proportional decrease in volume. The removal of capillary water in larger capillary voids (i.e., > 50 nm) of hydrated cement does not cause drying shrinkage. The loss of capillary water held by capillary tension in small voids (i.e., < 50 nm) contributes to shrinkage strain [3]. The volume of capillary voids is influenced by water-to-cementitious ratio (w/c ratio) and the degree of cement hydration. At constant w/c ratio, increasing the degree of hydration may cause a considerable decrease in the volume of capillary voids while the shrinkage strain may be reduced significantly [3].

The adsorbed water is removed in the concrete drying process by surface tension. Due to asymmetry of water molecules in contact with the surface of the material, referred to as surface tension, a resultant force perpendicular to the surface causes contraction as capillaries are drained. This phenomenon is only valid in the low RH regime (up to 40% of RH) [4].

Interlayer water is the water held by hydrogen bonding within the calcium silica hydrates (CSH) structures. The removal of interlayer water will contribute to drying shrinkage but only under strong drying conditions (i.e., RH about 10%) [4].

Factors that affect drying shrinkage are usually interrelated although they can be grouped into two main categories – material characteristics and ambient conditions [3].

Because the drying process involves moisture loss from the surface, drying shrinkage mainly

depends on the size and configuration of the element [6]. Increasing the volume-to-specimen surface area ratio may cause decrease in drying shrinkage [30]. Quantity of paste is one of the main parameters affecting the shrinkage potential of a mixture. For a given w/c ratio, decreasing paste content, and so increasing aggregate content leads to reduced shrinkage strain [7]. The methylene blue index (MBI) can be used as an indicator of clay content of fine aggregate in concrete. The drying shrinkage of concrete increases with the increasing MBI values, especially when MBI value is greater than or equal to 1.45 because clay particles coating aggregate particles will deform significantly with changing moisture content [32]. The elastic properties of the aggregate will also affect concrete shrinkage – the lower the modulus of elasticity of aggregate, the higher the drying shrinkage of the concrete may be [1].

Cement characteristics, such as reduced sulfate content, increasing fineness will reportedly increase drying shrinkage potential [1]. Proper, prompt, and sufficient curing period helps to reduce shrinkage [1, 10].

Both supplementary cementitious materials (SCMs) and chemical admixtures can dramatically affect the shrinkage of a mixture. The available literature indicates that for a similar mixture, inclusion of slag cement appears to have marginal effect on increasing shrinkage [31]. A high silica fume content may increase the drying shrinkage in the short term. However, silica fume may not cause an increase in shrinkage with lower replacement dosage over the long term (i.e., 365 days) [9]. Use of slag cement and silica fume in ternary mixes provides the best performance compared to binary mixtures where slag cement and silica fume are used alone [2]. Class F fly ash used in binary mixtures may reduce drying shrinkage with increasing replacement dosages compared to plain portland cement concrete [8]. Compared to class F fly ash, class C fly ash reportedly causes more shrinkage than control concrete mixtures in most cases, apparently due to low alkali contents and higher Ca/Si ratios [10]. However, both types of fly ash combined with slag cement or silica fume in ternary blends diminish the adverse effects of silica fume or slag cement [2].

A water reducer agent is used to achieve a higher strength at the same workability or to maintain strength at a higher workability. Most researchers have found that drying shrinkage increases when water reducer agent dosage increases regardless of the curing conditions [11, 12, 27, 28]. However, Qi et al. reported the shrinkage of concrete with a

higher water reducer content (2.37 percent by weight of cement) was lower than that with lower water reducer content (1.39 percent by weight of cement). The test results also showed that the high water reducer content was effective in inhibiting crack opening and propagation in concrete specimens tested in a restrained condition [26].

The work discussed in this paper is aimed at investigating the drying shrinkage behavior of ternary blend concretes that are used in transportation structures. Five different concrete mixes from field demonstration projects in the Midwest were included in the study. Both restrained and unrestrained shrinkage testing methodologies are used to analyze the factors that influence shrinkage in mixtures with large differences in materials and proportions.

Experimental program

Concrete mixtures for five transportation structures have been studied and project descriptions are listed in Table 1. The laboratory study employed the same materials that had been used in the job mixes. Shrinkage tests, either free shrinkage or restrained shrinkage were run with as-built mixture proportions, and also with mixes containing varying cementitious content. Additionally, the mechanical properties (i.e., modulus of elasticity, compressive strength, and splitting tensile strength) were also determined for the five as-built mixtures.

Materials and mix proportion

Raw materials from ready mix plants were collected to perform shrinkage related tests in a lab environment. The mixtures represent a wide variety of material combinations. Chemistry of the cementitious materials and the aggregate properties are given in Table 2 and 3, respectively. Combined aggregate gradations are plotted in Figure 1. The mix proportions for the as-built mixtures are summarized in Table 4(a). Additional mixtures were prepared with 450 and 700 pcy total cementitious materials contents, and w/c ratio of 0.45 without fiber and chemical admixtures are shown in Tables 4(b), (c), and (d), respectively. These added mixtures were used to investigate the effect of changing w/c ratio, water reducer agent dosages, and cementitious material content on the five mixtures.

Test Methods

Concrete strength and elastic modulus test

Compressive strength, splitting tensile strength, and elastic modulus specimens were prepared from each field concrete mixture in accordance with ASTM C 39, ASTM C 496, and ASTM C 469, respectively. Specimens for these tests were moist cured for seven days and then tested at ages of 1, 3, 7, 28, and 56 days [13-15].

Free shrinkage test

Three 3x3x11 ¼ inches concrete prisms were prepared from each mixture shown in Table 4(a) to 4(d). In addition, four 1x1x11 ¼ inch mortar bars were prepared based on the cementitious materials shown in Table 4(a). The mortar mixtures were proportioned with an aggregate to cementitious materials ratio of 2.75 and a w/c ratio of 0.45. The fine aggregate types used in mortar tests were the same as those used in field mixtures. The mortar mixes were mixed and compacted by hand. The prisms and bars were moisture cured for seven days, and then stored at 50±4% relative humidity and 73 ±3 °F. Testing was conducted in accordance with ASTM C 157, except that initial reading was taken at the end of seven days moist storage and drying readings were taken at ages of 1, 4, 7, 14, 28, and 56 days after the specimens were exposed to the drying environment [16].

Restrained ring test

Four restrained concrete rings for each as-built mixture (Table 4a) were cast in order to assess the potential for shrinkage induced cracking in accordance to ASTM C 1581 [17]. The geometry of the restrained ring was shown in Figure 2. Paraffin wax was used to seal the top surface of rings in order to allow the moisture loss only from the exterior surface. Two strain gages for each ring were used to measure the strains of the steel ring after casting and continued recording up to 28 days or until the concrete cracked. The recording interval was every 10 minutes.

Methylene blue index test

Because the clay content of fine aggregate may be a factor that affects concrete drying shrinkage, the relationship between MBI values and drying shrinkage of five field

mixtures was investigated [32]. The MBI was used as an indicator of clay content or the surface area of clay from different sources of fine aggregate in accordance with ASTM C 837 [22].

Paste-to-void ratio (by volume)

The effect of paste-to-void ratio was investigated to assess its relationship with drying shrinkage. Combined aggregate voids were determined in accordance with ASTM C 29 [20]. Paste content by volume and voids of combined aggregate were used to derive the voids of each designed mixture. The paste-to-void ratio is the simple ratio of paste content to void content within mixture.

Results and discussion

Mechanical properties of concrete

The development of compressive strength, elastic modulus, and tensile split strength are shown in Figure 3 to Figure 5. The compressive strength of Mix 4 was highest for later ages (i.e., > 7 days). This is most likely due to the combined effect of the lowest w/c ratio of 0.38 and silica fume which will improve the long term strength [9]. Mixes 1 and 2 had a relatively low compressive strength which may be caused by relatively high w/c ratio. The differences of splitting tensile strengths among five mixes were not significant. Compared to Mixes 1, 2 and 4 mixtures, higher coarse aggregate contents of 41% and 42% in Mixes 3 and 5 generate higher modulus of elasticity of concrete mixtures.

Unrestrained shrinkage

The average strain rate factor and average maximum length change are two parameters used to evaluate the drying shrinkage in an unrestrained condition. The shrinkage strain ϵ_s was plotted against the square root of elapse time t to compute the average strain rate factor α . Equation 1 describes that the strain factor α is the slope of a regression line that was used to fit the data in the shrinkage strain versus square root of elapse time plot [17].

$$\epsilon_{\text{steel}(t)@r=R_{IS}} = \alpha\sqrt{t} + k \quad (1)$$

where, $\epsilon_{\text{steel}(t)@r=R_{IS}}$ is equivalent to the measured strain from strain gages attached at the inner surface of the steel ring, and k is a regression constant.

Unrestrained shrinkage for concrete

Figure 6 provides the shrinkage strain for each as-built mixture. It can be observed that Mix 5 has the lowest shrinkage strain followed by Mixes 3, 2, 1 and 4 after 7 days.

Mixtures with different cementitious materials contents were prepared to investigate the effect on drying shrinkage. Figure 7 and 8 show that both lower cementitious content (450 pcy) and higher cementitious content mixtures (700 pcy) have similar trends to those in Figure 6, that is, Mix 5 is found to have the least shrinkage followed by Mixes 3, 2, 1, and 4. Figure 9 provides five linear relationships of 56-day shrinkage for mixes with 450, as-built, and 700 pcy cementitious materials. This figure clearly shows that increasing cementitious material content leads to higher shrinkage strain values but does not change the overall trends. Figure 10 presents the mixes with fixed w/c ratio of 0.45 for all five mixtures without adding chemical and fiber admixtures.

By comparing Figures 10 and Figure 6, it is found that the shrinkage strain of the as-built mixtures with high water reducer dosages, such as Mixes 4, 1 and 2, are significantly reduced when chemical admixtures are left out. However, the shrinkage strain of Mix 5 without adding chemical admixtures (as shown in Figure 10) is higher than that of the Mix 5 as-built mixture (as shown in Figure 6). This is likely because increasing w/c ratio from 0.40 to 0.45 leads to a higher free shrinkage strain [1]. The water reducer effect on shrinkage can be considered to be not significant in this case due to a very small amount of water reducer used in the Mix 5 as-built mixture.

Unrestrained shrinkage for mortar

Figure 11 shows the average free shrinkage results of four mortar bars. The mortar mix proportions effectively eliminate the influence of factors including w/c ratio, coarse aggregate size and types, chemical and fiber admixtures. In this case, cementitious material variations in terms of chemical and physical characteristics (i.e., Ca/Si ratio, alkali content, and hydration properties) likely play a dominant role on shrinkage strain. For example, Mix 3 with silica fume and slag cement performs better than Mix 1 with class F fly ash and slag cement. This may be attributed to different hydration properties between silica fume and class F fly ash.

Previous researchers have demonstrated that silica fume and slag cement will promote hydration of cement and react with CH particles. The hydration products can increase the density of hardened cement paste and so reduce drying shrinkage [29]. When compared to the concrete mixes in Figure 10, Mixture 5 mortar mixture shown in Figure 11 has an increased shrinkage strain and is similar to the other mortar mixtures. This may be due to removal of the high elastic modulus aggregate (i.e., quartzite) [1, 10, 11].

Restrained shrinkage

The restrained shrinkage strain development of ring samples is shown in Figure 12. The curves represent the average strain of four samples for each as-built field mixture. The positive shrinkage values indicate an expansion process during the first day. As shown in Figure 12, it is noted that Mixes 2, 5, 1, and 3 do not have significant changes in strain values after 18 days and did not crack up to 28 days except for the Mix 4 which cracked at 6.8 days. Mix 4 had the highest shrinkage strain rate up to 7 day, while Mix 5 exhibited the lowest average strain rate.

Data from all of the tests are summarized in Table 5. The average strain rate factor was determined up to 18 days for the restrained ring tests. The average strain rate factors for as-built mixture prisms are consistent with those for restrained rings. The results imply a good relationship between restrained and free shrinkage for each mixture. Good relationships between strain rate factors and prisms of 450, 700 pcy cementitious materials mixtures and restrained rings can be observed as well.

Shrinkage cracking potential of concrete

Previous publications have provided a method to compute the residual stress in the concrete rings and a tool to determine the cracking potential Θ_{CR} (i.e., the measure of how close the ring specimens are to failure) by comparing the actual residual stress with the strength of the material [23, 25]. Since the restrained ring can be separated into a steel cylinder pressurized at outer surface and a concrete cylinder loaded with opposite and equal tensile stresses at inner surface. This equilibrium consideration can be used to derive the interface pressure p on the outer surface of the steel ring or inner surface of concrete ring expressed in Equation 3 as:

$$p(t) = -\varepsilon_{\text{steel}(t)@r=R_{IS}} \times E_S \times \frac{R_{OS}^2 - R_{IS}^2}{2R_{OS}^2} \quad (2)$$

where, E_S is the modulus elasticity of steel, R_{OS} and R_{IS} are the outer and inner radii of steel ring refer to Figure 1, respectively [22]. It is noted that the actual measured strain from strain gages has taken the effect of creep into account. The axi-symmetric nature of the geometry eliminates the need to consider the circumferential tractions on the inner surface of steel ring. The interface pressure p can be directly related to the circumferential tensile stress at any point along the radial direction. Therefore, the shrinkage maximum induced stress (i.e., circumferential maximum tensile stress) is directly determined by Equation 3 at any time, t .

$$\sigma_{\text{Actual-Max}} = p \left(\frac{R_{OS}^2 + R_{OC}^2}{R_{OC}^2 - R_{OS}^2} + \nu \right) \quad (3)$$

where, $\sigma_{\text{Actual-Max}}$ is the shrinkage maximum induced stress, ν is the Poisson ration and R_{OS} and R_{OC} are the outer and inner radii of steel and concrete refer to Figure 1, respectively.

In this study, the simple ratio of the shrinkage maximum induced stress and the tensile split strength are presented to determine the cracking potential and expressed by Equation 4 [23].

$$\Theta_{CR} = \frac{\sigma_{\text{Actual-Max}}}{f_{sp(t)}} \quad (4)$$

where, $\sigma_{\text{Actual-Max}}$ is the shrinkage maximum induced stress, and $f_{sp(t)}$ is the splitting tensile strength developed with time t .

The calculated cracking potential values are shown in Figure 13. Concrete cracking will be expected to occur when the cracking potential reaches 1 meaning when the shrinkage maximum induced stress is close to splitting tensile strength [23]. However, it is observed that only the Mix 4 cracked when the cracking potential reached 2.1, while the cracking potentials of other mixtures all exceeded 1.0 and did not crack up to 28 days. It might be attributed to the assumption used in this study: the splitting tensile strength shown in Table 6 was calculated based on non-linear relationship while the shrinkage induced stress was estimated based on linear elasticity for simplicity [24]. The simple linear elasticity may overestimate the shrinkage maximum induced stress in the concrete under restrained conditions. Also, geometry and boundary conditions dramatically affect

the shrinkage induced stress due to the dependency of stress to geometry [25]. Therefore, the geometry of ring specimens used in this study may cause no cracking of concrete although cracking potentials are larger than 1.0. Equation 3 gave the relationship between geometry of specimen, such as outer and inner radii of steel and concrete in terms of concrete and steel ring thickness, and shrinkage induced stress. In another words, the levels of restraint of concrete may be an important factor to explain the inconsistent cracking potential values compared to theoretical failure potential, 1.0 [25]. Thus, further study is needed for a nonlinear approach to assess the shrinkage induced stress if using this approach to evaluate the cracking potential of concrete with restrained concrete rings.

Despite the inability of the cracking potential to predict cracking, Figure 13 provides a good stress-to-strength relationship with concrete ages of concrete rings for five field mixtures. It is interesting that the cracking potential value of Mix 2 was close to Mix 4 but did not crack. This may be attributed to fiber reinforcement within Mix 2.

Effects of concrete materials on shrinkage

Test results of methylene blue index (MBI), paste-to-void ratio, water reducer agent dosage, and modulus of elasticity at 28 days are given in Table 7. The linear relationships between restrained stress rate of as-built mixtures and the test results are shown in Figure 14(a) to (d). The other two linear relationships can also be observed in Figure 15 (a) and (b) including modulus of elasticity at 28 days and cracking potential and splitting tensile strength at either crack time or 28 days and cracking potential for five as-built mixtures.

Figure 14(a) shows that the higher MBI indicates a higher potential for shrinkage. The MBI values exhibit a good correlation with average strain rate factors. This is consistent with what has been found in previous research [32].

The relationship between paste-to-void ratio and average strain rate factor is shown in Figure 14(b). The strain rate factor increases with increased paste-to-void ratio. It is because greater distances between the aggregate particles, the less resistance will be to the movement of concrete caused by shrinkage [19]. It is also not surprising that a system with proportionately higher paste contents will shrink more because it is the paste that shrinks and not the aggregate.

Water reducing admixture dosage appears to play a significant role shown in Figure 14 (c). Higher water reducer agent dosage sufficiently increases the potential of drying shrinkage and this finding is consistent with most previous research [11, 12, 27, 28].

Figure 14(d) illustrates the relationship between modulus of elasticity of mixtures and their strain rate factors. Concrete mixtures with higher modulus of elasticity may resist drying shrinkage and so reduce the average strain rate factor [1, 10, 11]. Thus, Mix 5 tends to have a relatively higher modulus of elasticity because of the quartzite as coarse aggregate.

Figure 15(a) indicates that concrete mixtures with higher modulus of elasticity not only resist drying shrinkage, but also reduce the cracking potential. Shrinkage cracking potential decreases with increased splitting tensile strength can be observed in Figure 15(b) and this relationship is linear with R^2 value of 83%.

Conclusion

Based on the test results in this paper, the following conclusions can be drawn.

- Water reducing admixture dosage plays a dominant role in the five ternary blend concrete mixtures.
- Cementitious material content has a significant effect on shrinkage strain. All as-built mixtures showed that free shrinkage linearly increases with the increased cementitious material content at an age of 56 days.
- Shrinkage strain rate linearly increases with clay content in aggregate and paste-to-void ratio of as-built concrete mixes.
- Splitting tensile strength and modulus of elasticity affect cracking potential. Shrinkage cracking potential decreases with increased splitting tensile strength and modulus of elasticity.
- Use of fibers appears to have reduced cracking risk.
- Free shrinkage strain rate factors demonstrate good correlation with shrinkage rate factors for restrained conditions.

Acknowledgements

The present study is a part of the research project, Development of Performance Properties of Ternary Mixtures, which is pool funded and supported by Federal Highway Administration (FHWA), nine state departments of transportation (California, Illinois, Iowa, Kansas, Mississippi, New Hampshire, Pennsylvania, Wisconsin, and Utah), some concrete admixture companies, and the National Center of Concrete Pavement Technology (CP Tech Center). The authors are greatly thankful to research engineers, Bob Steffes, Bryan Zimmerman and Paul Jeremy McIntyre, from CP Tech Center and Doctor of Philosophy candidate Gilson Lowboy from ISU.

References

- [1] ACI. Report on factors affecting shrinkage and creep of hardened concrete. ACI Standards, ACI 209.1R-2005, Farmington Hills, MI: American Concrete Institute, 2005.
- [2] Guneyisi E, Gesoglu M, Ozbay E. Shtrength and drying shrinkage properties of self-compacting concretes incorporating multi-system blended minearal admixtures. *Construction and Building Materials*, 2010: 1878-1887.
- [3] Malhotra VM, Mehta PK. Pozzolanic and Cementitious Materials. *Advances in Concrete Technology*, v. 1, 1996.
- [4] Idiart, AE. Coupled analysis of degradation processes in concrete specimens at the meso-level. Master Thesis: Universitat Politecnica De Catalunya, 2009, 45-48.
- [5] Mokarem DW, Richard EW, Lane DS. Development of a shrinkage performance specifications and prediction model analysis for supplemental cementitious material concrete mixtures. *Cement and Concrete Research*, 2005: 918-925.
- [6] RILEM TC 107. Guidelines for characterizing concrete creep and shrinkage in structural designcodes or recommendations, *Materials and structures* 28 (1995), 52-55. See also RILEM TC69, Conclusions for structural analysis and for formulation of standard design recommendations, Chapter 6 in *Mathematical Modeling of Creep and Shrinkage of Concrete*, ed. by Z.P. Bazant, John Wiley and Sons, Chichester and New

- York, 1988; reprinted in *Materials and Structures (RILEM, Paris)* 20 (1987), 395-398, and in *ACI Materials Journal* 84 (1987), 578-581.
- [7] Pickett G. Effect of aggregate on shrinkage of concrete and hypothesis concerning shrinkage, *Journal of the American Concrete Institute*, Vol. 27, No. 5, Jan., 1956. pp. 581-590.
- [8] Gesoğlu M, Güneyisi E, Özbay E. Properties of self-compacting concretes made with binary, ternary, and quaternary cementitious blends of fly ash, blast furnace slag, and silica fume. *Construction and Building Materials*. 23 (2009) 1847-1854.
- [9] Rao GA. Long-term drying shrinkage of mortar – influence of silica fume and size of fine aggregate. *Indian Institution of Science, Cement Concrete Research* 31 (2000) 171- 175.
- [10] Deshpande S, Darwin D, Browning J. Evaluating free shrinkage of concrete for control of cracking in bridge decks. *Structural Engineering and Engineering Materials SM Report No. 89*. The University of Kansas Center for Research, Inc. Lawrence, Kansas. Jan. 2007.
- [11] Kosmatka SH, Kerkhoff B, Panarese WC. Design and control of concrete mixtures, 14th Edition, Portland Cement Association (2002).
- [12] Alsayed SH. Influence of superplasticizer and silica fume on the drying shrinkage of high strength concrete subjected to hot-dry field conditions. *Cement & Concrete Research*, Vol. 28, Issue 10, 1998. pp. 1405-1415.
- [13] ASTM Standard C39 -01. Standard test method for compressive strength of cylindrical concrete specimens. *Annual Book of Standards*, Vol. 4.02, ASTM International, WestConshohocken, PA. 2008.
- [14] ASTM Standard C469-02. Standard test method for static of elasticity and poisson's ratio of concrete in compression. *Annual Book of Standards*, Vol. 4.02, ASTM International, WestConshohocken, PA. 2008.
- [15] ASTM Standard C496-96. Standard test method for splitting tensile strength of cylindrical concrete specimens. *Annual Book of Standards*, Vol. 4.02, ASTM International, WestConshohocken, PA. 2008.

- [16] ASTM Standard C157-06. Standard test method for length change of hardened hydraulic-cement mortar and concrete. Annual Book of Standards, Vol. 4.02, ASTM International, WestConshohocken, PA. 2008.
- [17] ASTM Standard C1581-04. Standard test method for determining age at cracking and induced tensile stress characteristics of mortar and concrete under restrained shrinkage. Annual Book of Standards, Vol. 4.02, ASTM International, WestConshohocken, PA. 2008.
- [18] ASTM Standard C837-99. Standard test method for methylene blue index of clay. Annual Book of Standards, Vol. 4.02, ASTM International, WestConshohocken, PA. 2008.
- [19] Tia M, Liu Y, Brown D. Modulus of elasticity, creep and shrinkage of concrete. Gainesville: Department of Civil & Coastal Engineering, College of Engineering, 2005.
- [20] ASTM Standard C29 -97. Standard test method for bulk density (“unit weight”) and voids in aggregate. Annual Book of Standards, Vol. 4.02, ASTM International, WestConshohocken, PA. 2008.
- [21] Weiss J, Yang W, Shah SP. Influence of specimen size/geometry on shrinkage cracking of rings. Journal of Engineering Mechanics, 2000: Vol. 126.
- [22] Timoshenko S, Goodier JN. Theory of Elasticity. McGraw-Hill, 1951
- [23] Hossain AB, Weiss J. Assessing residual stress development and stress relaxation in restrained concrete ring specimens. Cement and Concrete Composites, 2004: 531-540.
- [24] Lomboy G, Wang K, Ouyang C. Shrinkage and fracture properties of semi-flowable self-consolidating concrete. Journal of Material in Civil Engineering. 2010.
- [25] Hossain AB, Weiss J. The role of specimen geometry and boundary conditions on stress development and cracking in the restrained ring test. Cement and Concrete Research, 2006: 189-199.
- [26] Qi M, Li Z, Ma B. Shrinkage and cracking behavior of high performance concrete containing chemical admixtures. Journal of Zhejiang University SCIENCE, Jun., 2002. Vol. 3, No. 2, pp. 188-193.

- [27] Johnston C, Gamble B, Malhotra V. Effects of superplasticizers on properties of fresh and hardened concrete. Transportation Research Record, No. 720, pp. 1-7. 1979.
- [28] Brooks J. Influence of mix proportions, plasticizers, and superplasticizers on creep and drying shrinkage of concrete. Magazine of Concrete Research, Sep., 1989, Vol. 41, No. 148, pp. 145-153.
- [29] Li J, Yao Y. A study on creep and drying shrinkage of high performance concrete. Cement and Concrete Research, v. 31, n. 8, 2001, p. 1203-1206.
- [30] Mindess S, Young JF, Darwin D. Concrete. 2nd Ed., Prentice-Hall Inc., Englewood Cliffs, New Jersey.
- [31] Slag Cement Association. Effect of slag cement on shrinkage in concrete. Slag Cement in Construction. No. 27. 2005.
- [32] Wang J, Yang Z, Niu K, KE G, Zhou M. Influence of MB-value of manufactured sand on the shrinkage and cracking of high strength concrete. Journal of Wuhan University of Technology-Mater. Sci. Ed. Apr. 2009.

List of Figures

- Figure 1. Combined aggregate gradations.
- Figure 2. Configuration of restrained concrete ring samples [24].
- Figure 3. Compressive strength development of concrete.
- Figure 4. Splitting tensile strength development of concrete.
- Figure 5. Modulus of elasticity development of concrete.
- Figure 6. Designed mixtures free shrinkage of prisms.
- Figure 7. 450 pcy cementitious materials mixtures free shrinkage of prisms.
- Figure 8. 700 pcy cementitious materials mixtures free shrinkage of prisms.
- Figure 9. Free shrinkage strain at 56 days versus cementitious material content at 450, designed, and 700 pcy.
- Figure 10. w/c of 0.45 and without chemical and fiber admixtures free shrinkage of prisms.
- Figure 11. Free shrinkage of bars for mortar mixtures.
- Figure 12. Strains of steel rings resulting from concrete shrinkage.

Figure 13. Shrinkage stress-to-tensile strength ratio (cracking potential Θ_{CR}) of restrained concrete rings with time.

Figure 14(a). Methylene blue index versus average strain rate factor.

Figure 14(b). Paste-to-void ratio versus average strain rate factor.

Figure 14(c). Water reducer dosage versus average strain rate factor.

Figure 14(d). 28-day modulus of elasticity of concrete versus average strain rate factor.

Figure 15(a). 28-day modulus of elasticity of concrete versus cracking potential Θ .

Figure 15(b). Splitting tensile strength of concrete versus cracking potential Θ .

List of Tables

Table 1. Project descriptions.

Table 2. Chemical and physical properties of cementitious materials

Table 3. Properties for coarse and fine aggregates

Table 4(a). Designed mix proportions for field mixtures

Table 4(b). Mix proportions for 450 pycementitious material content

Table 4(c). Mix proportions for 700 pycementitious material content

Table 4(d). Mix proportions for w/c of 0.45 and without fiber and chemical admixtures

Table 5. Average strain rate factor, maximum strain and time of cracking

Table 6. Concrete ring splitting tensile strength and failure strength at concrete crack time or 28 days

Table 7. Test results of methylene blue index, paste-to-void ratio, water reducer agent dosage and 28-day MOE and average strain rate factors

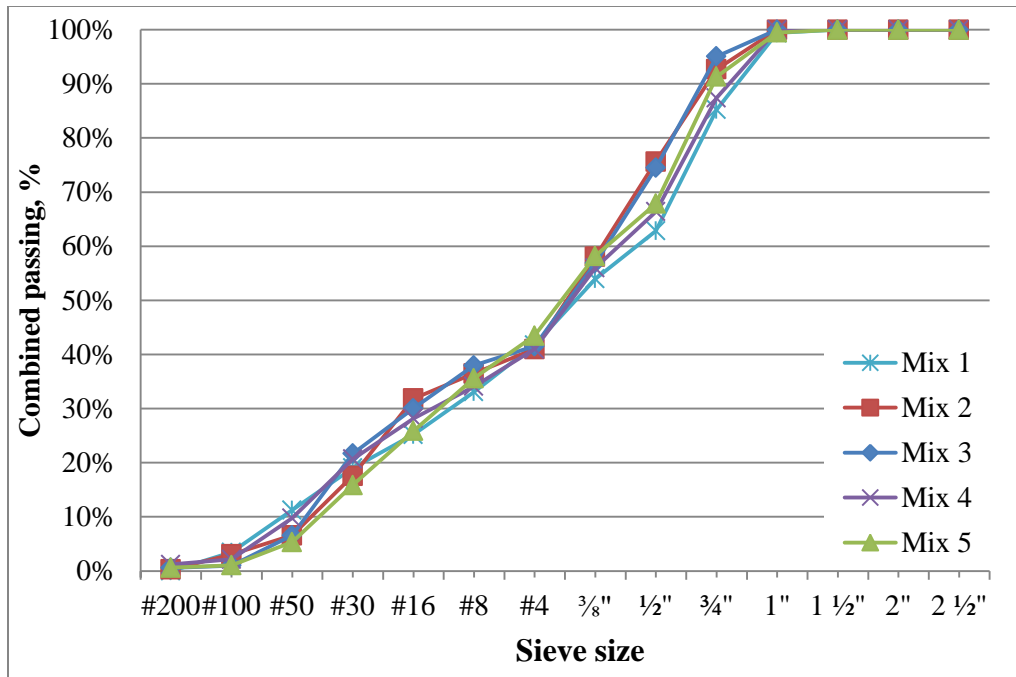


Figure 1. Combined aggregate gradations.

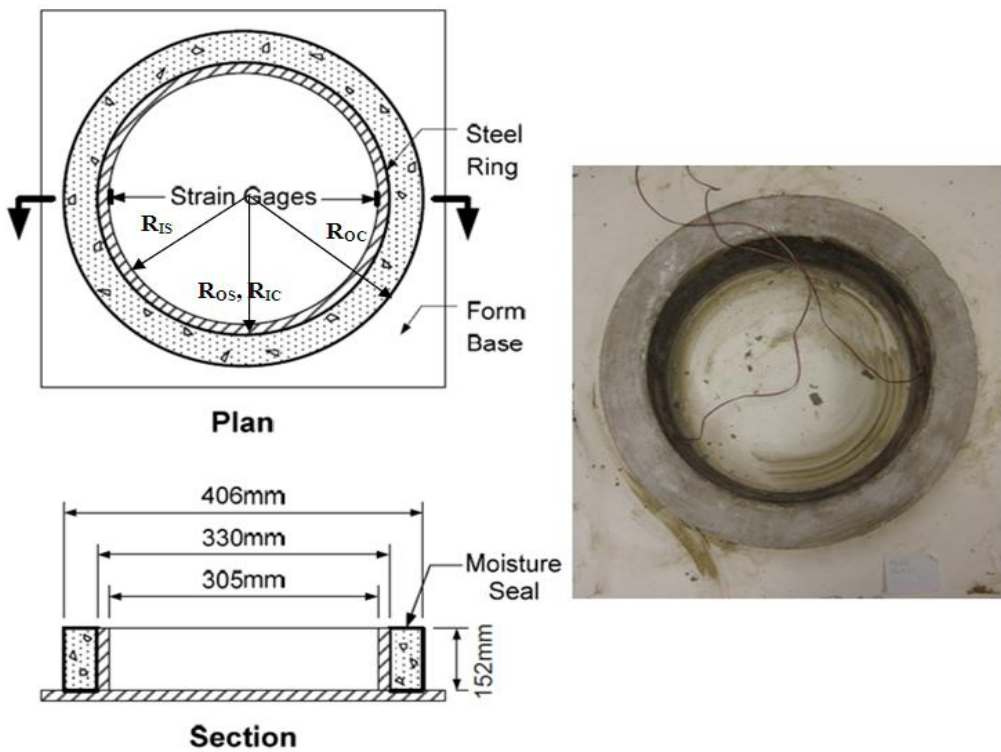


Figure 2. Configuration of restrained concrete ring samples [24].

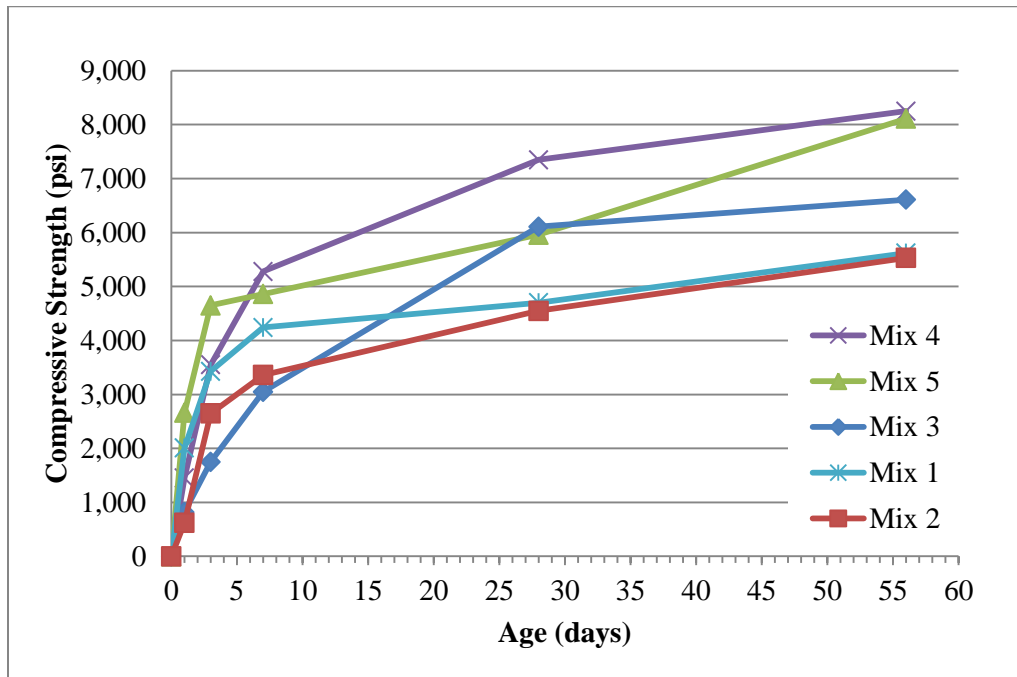


Figure 3. Compressive strength development of concrete.

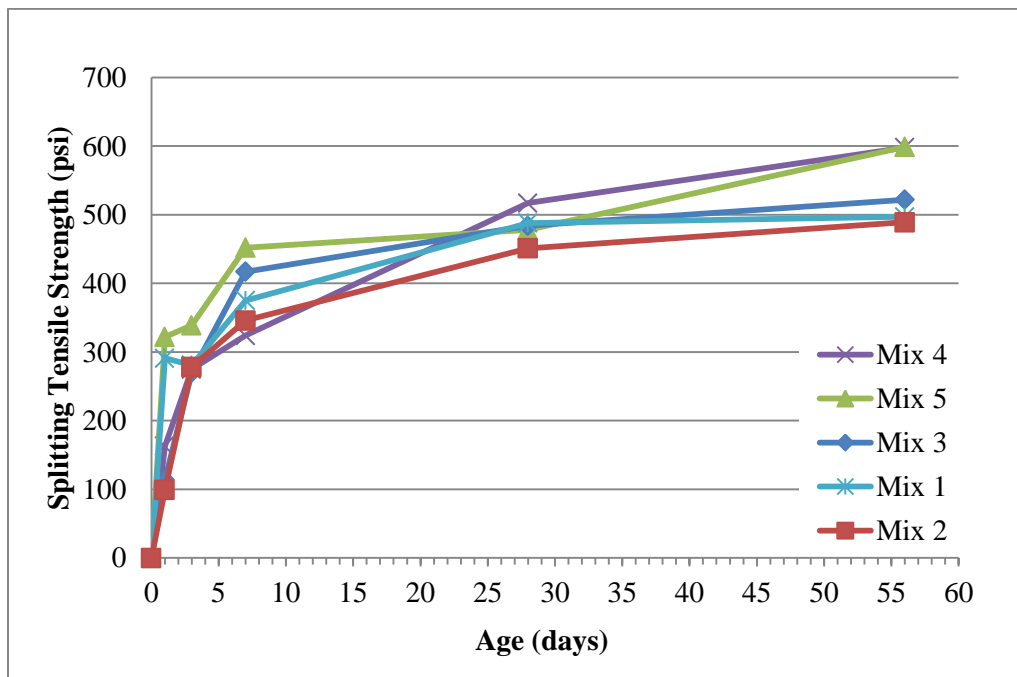


Figure 4. Splitting tensile strength development of concrete.

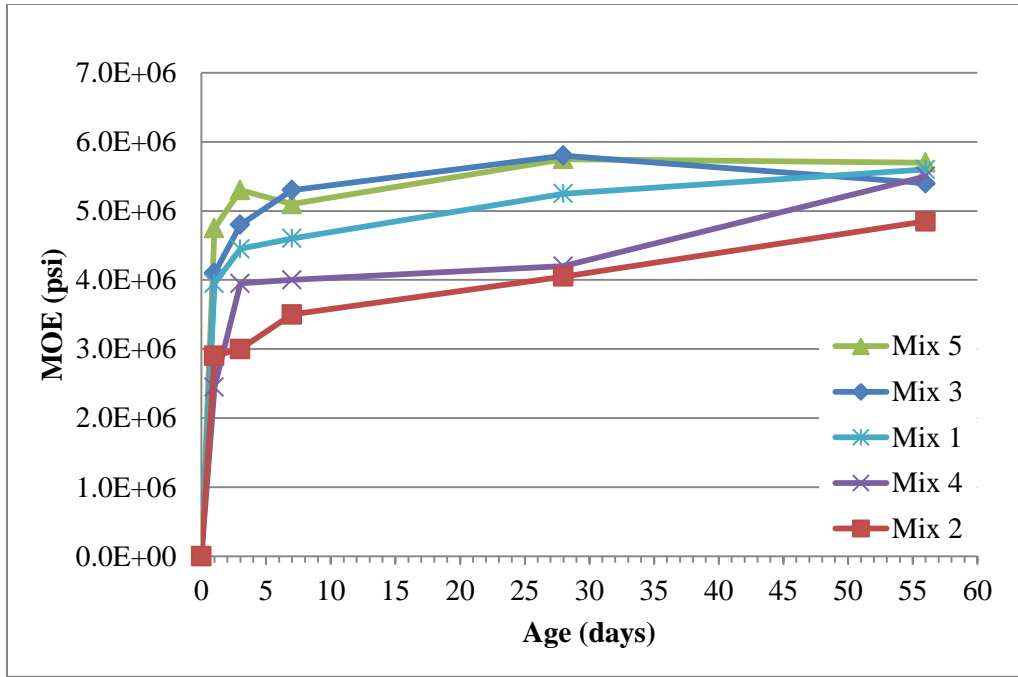


Figure 5. Modulus of elasticity development of concrete.

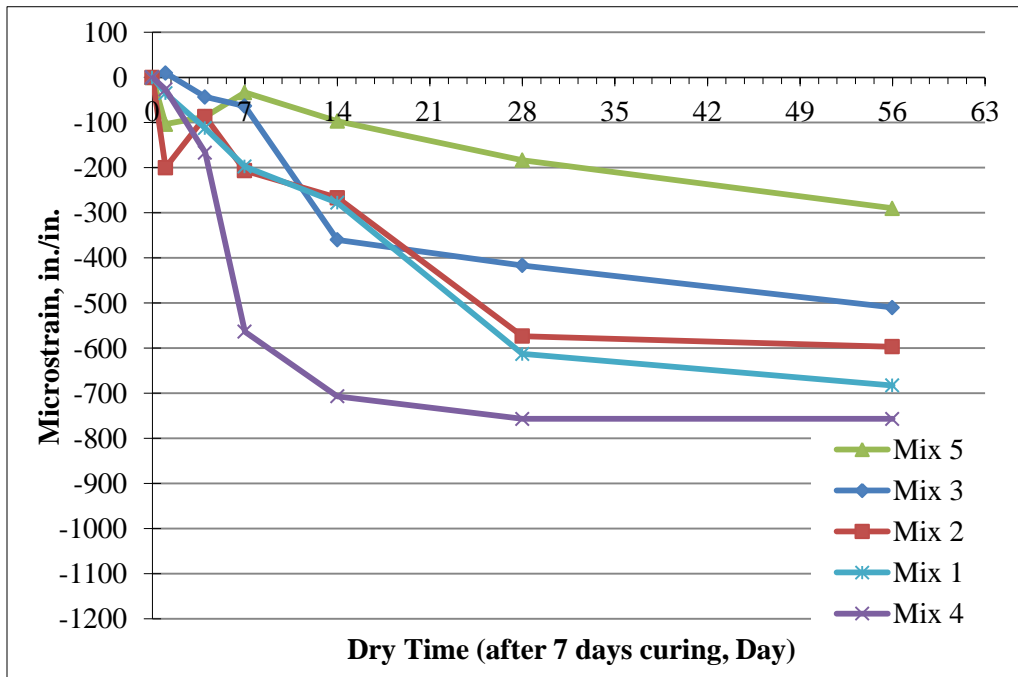


Figure 6. Designed mixtures free shrinkage of prisms.

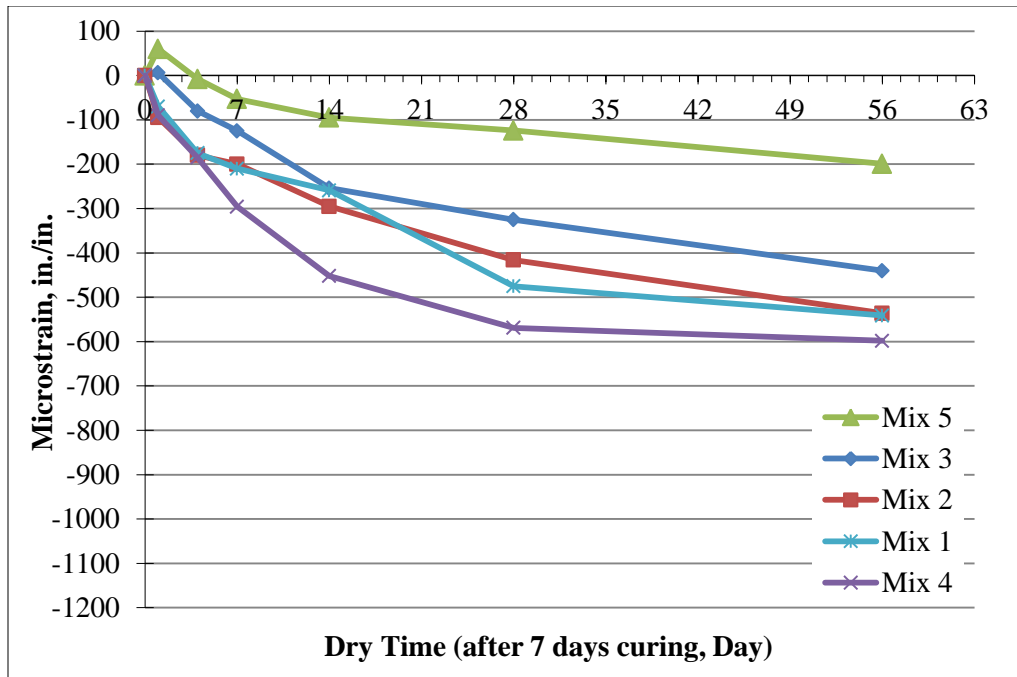


Figure 7. 450 pcy cementitious materials mixtures free shrinkage of prisms.

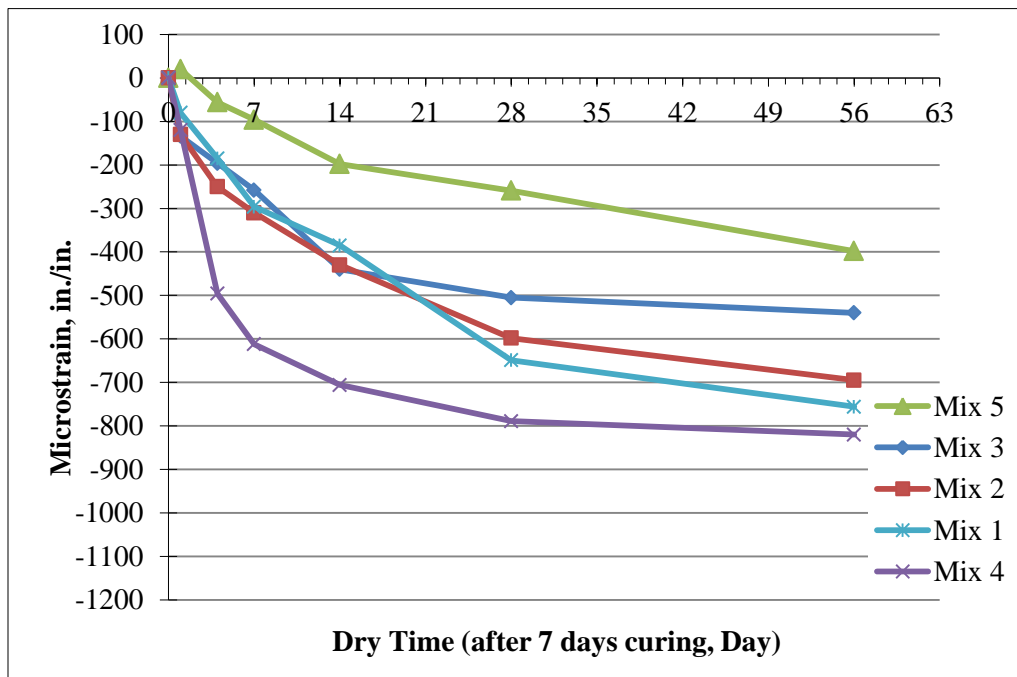


Figure 8. 700 pcy cementitious materials mixtures free shrinkage of prisms.

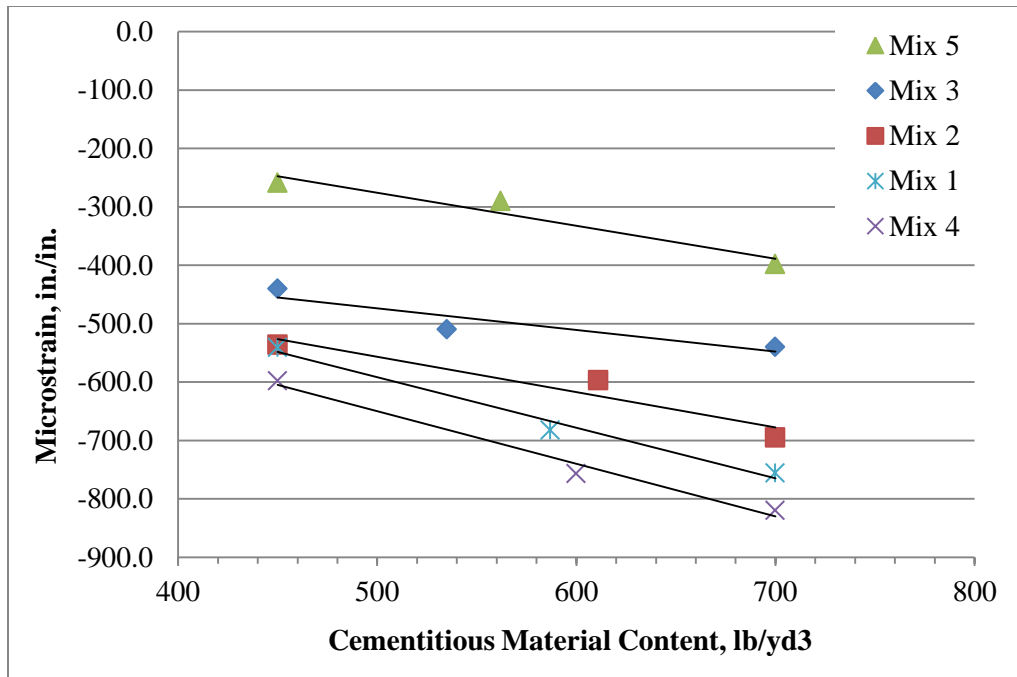


Figure 9. Free shrinkage strain at 56 days versus cementitious material content at 450, designed, and 700 pcy.

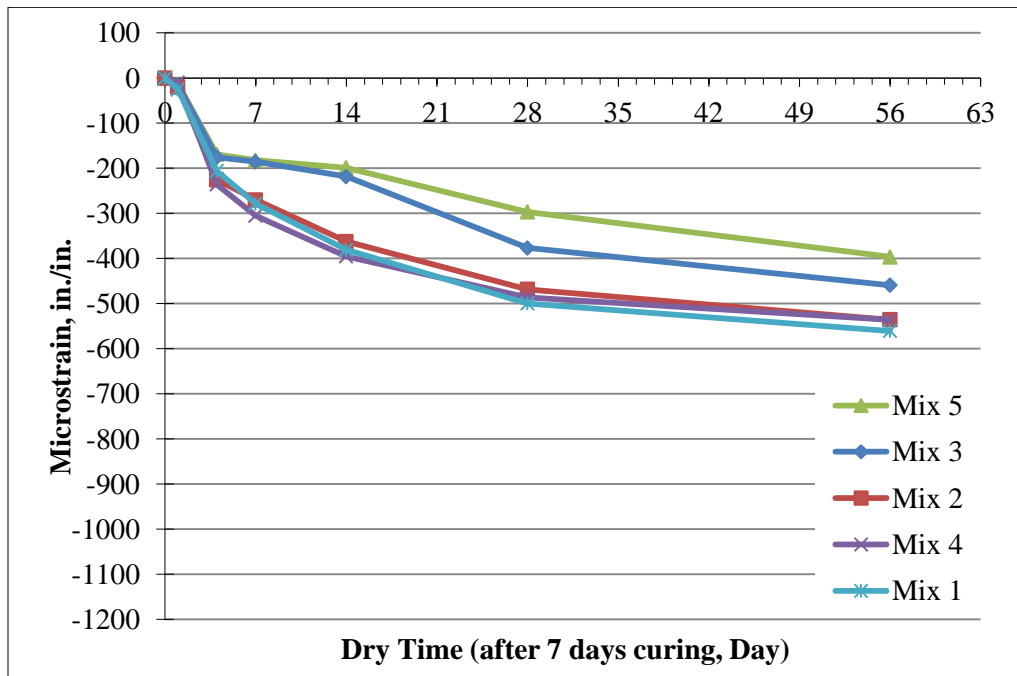


Figure 10. w/c of 0.45 and without chemical and fiber admixtures free shrinkage of prisms.

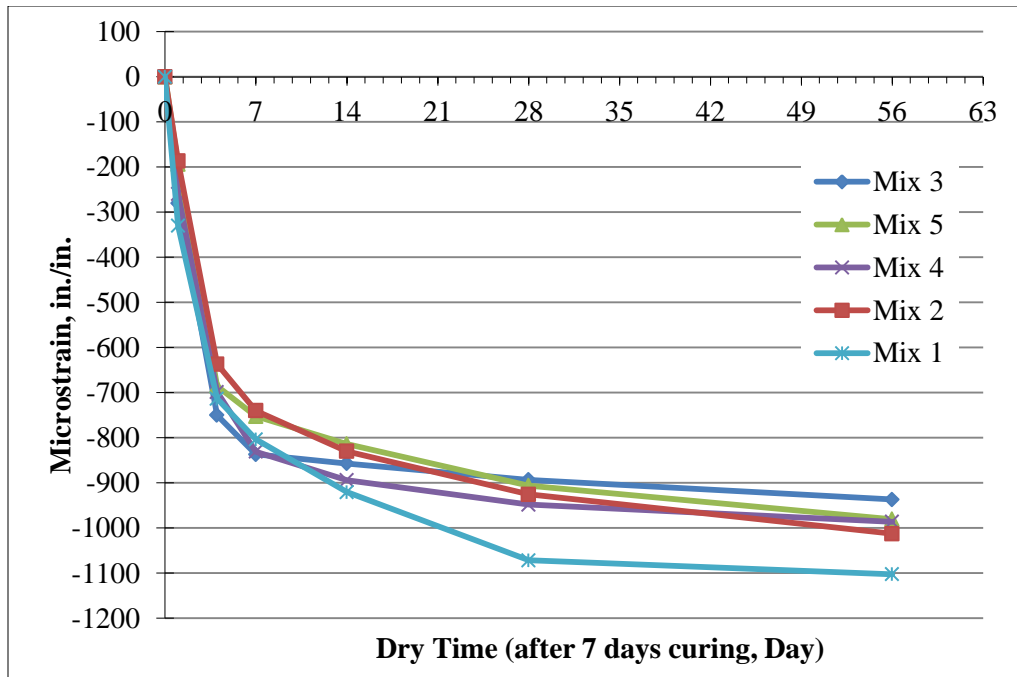


Figure 11. Free shrinkage of bars for mortar mixtures.

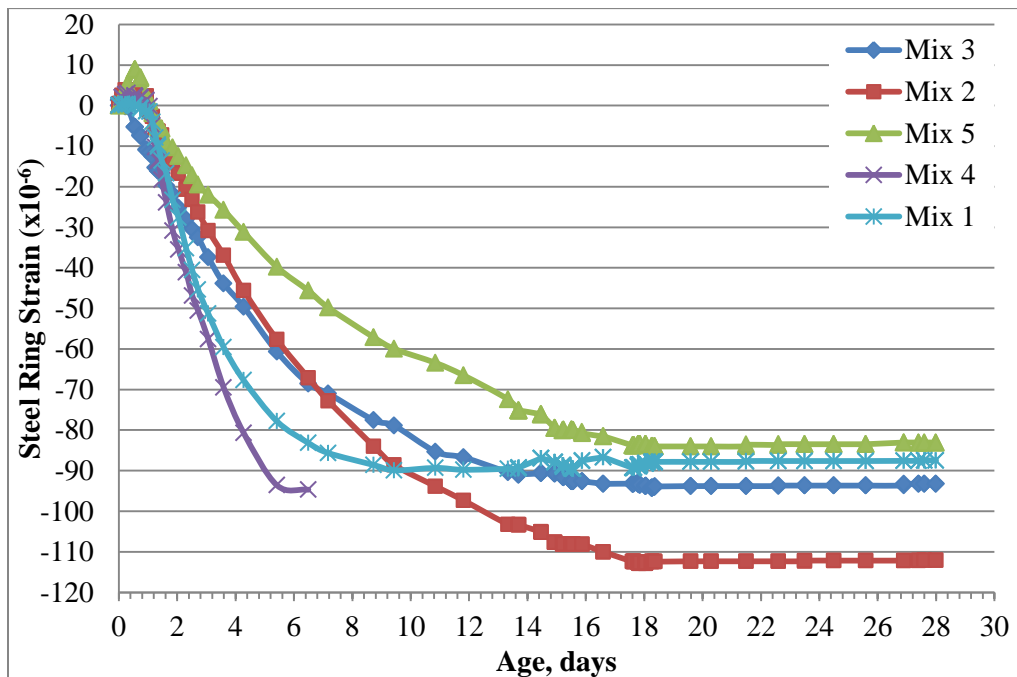


Figure 12. Strains of steel rings resulting from concrete shrinkage.

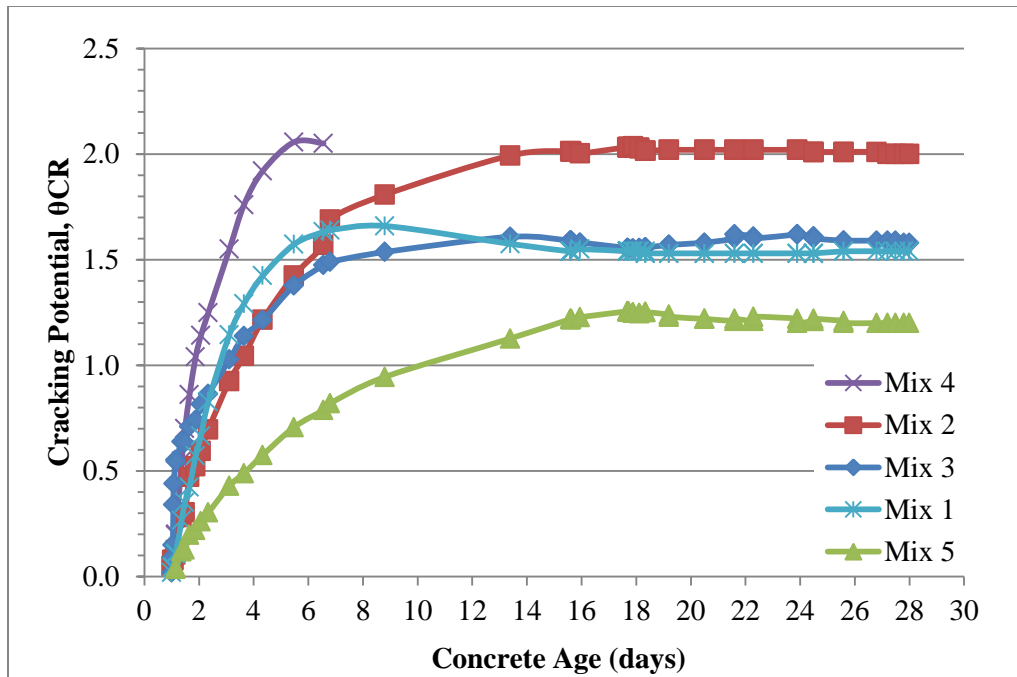


Figure 13. Shrinkage stress-to-tensile strength ratio (cracking potential Θ_{CR}) of restrained concrete rings with time.

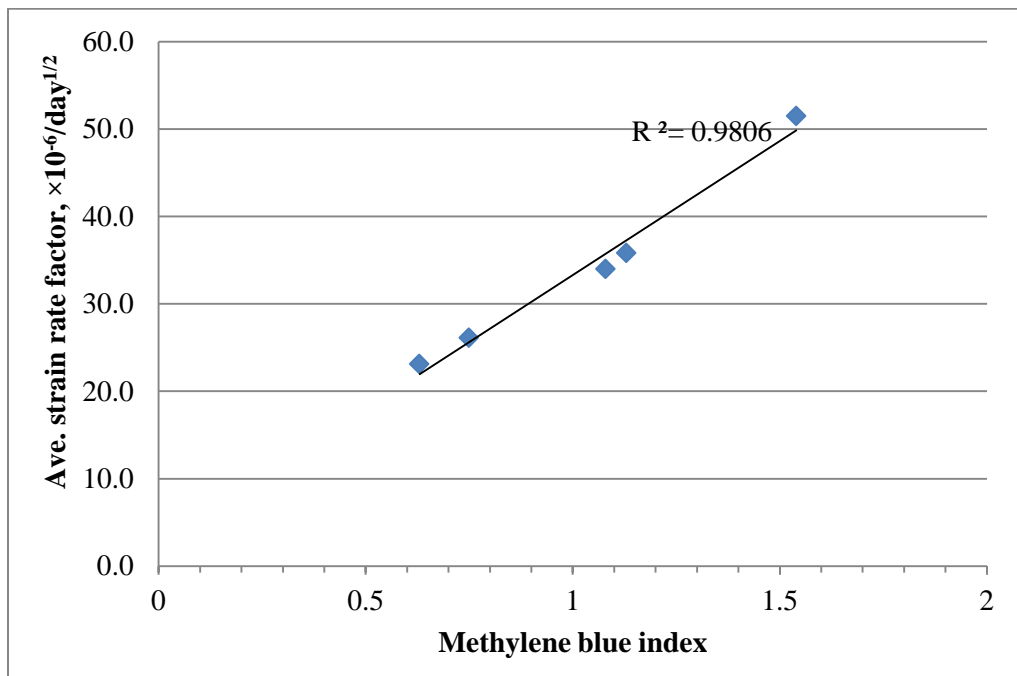


Figure 14(a). Methylene blue index versus average strain rate factor.

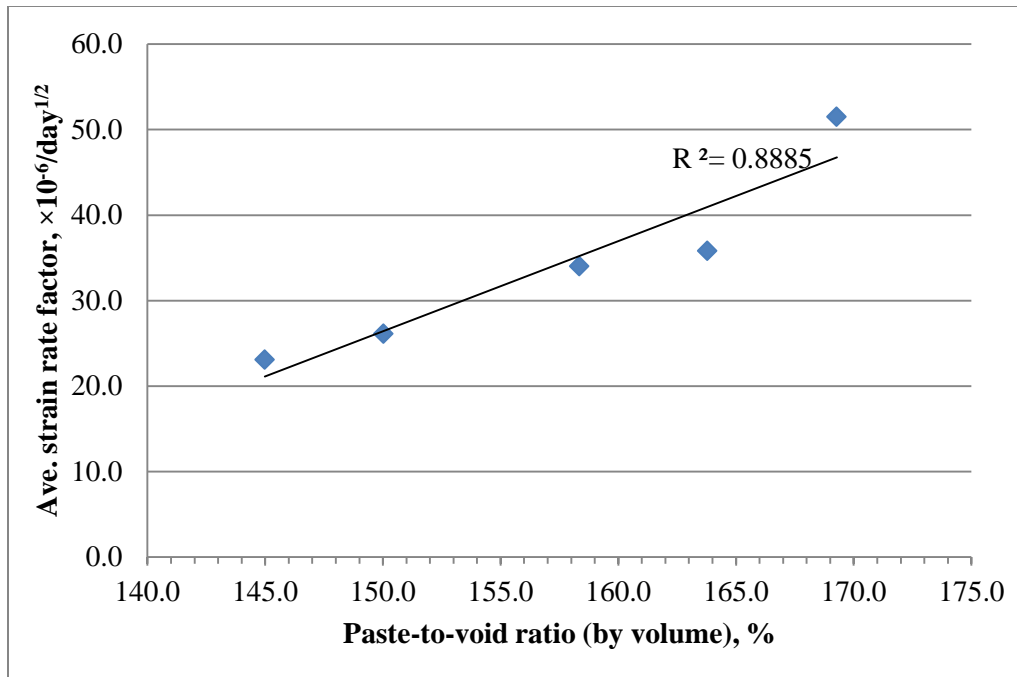


Figure 14(b). Paste-to-void ratio versus average strain rate factor.

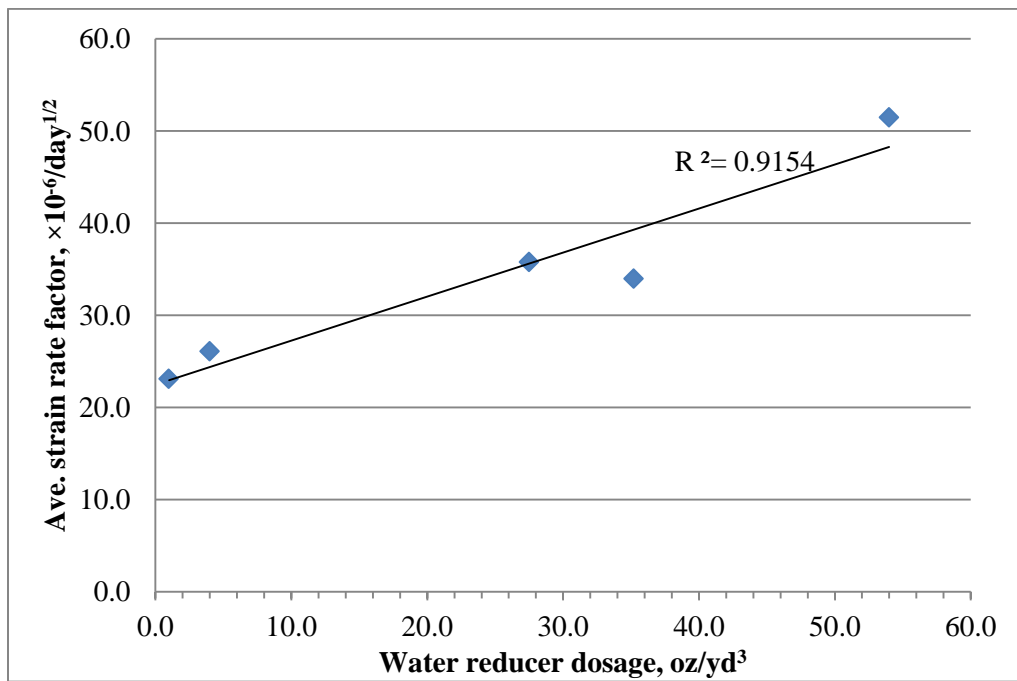


Figure 14(c). Water reducer dosage versus average strain rate factor.

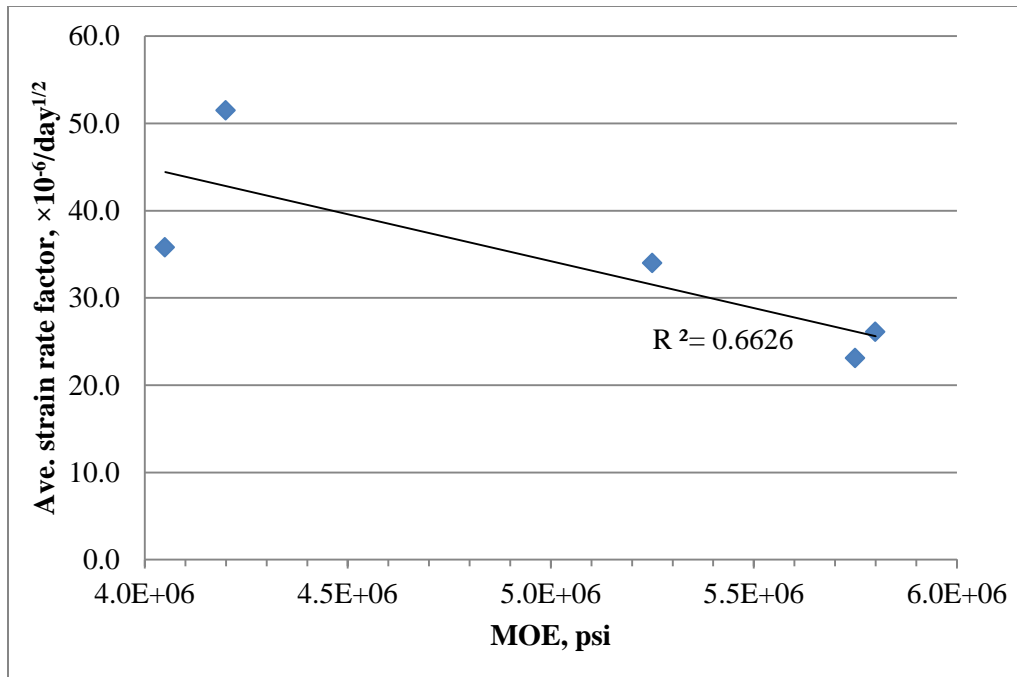


Figure 14(d). 28-day modulus of elasticity of concrete versus average strain rate factor.

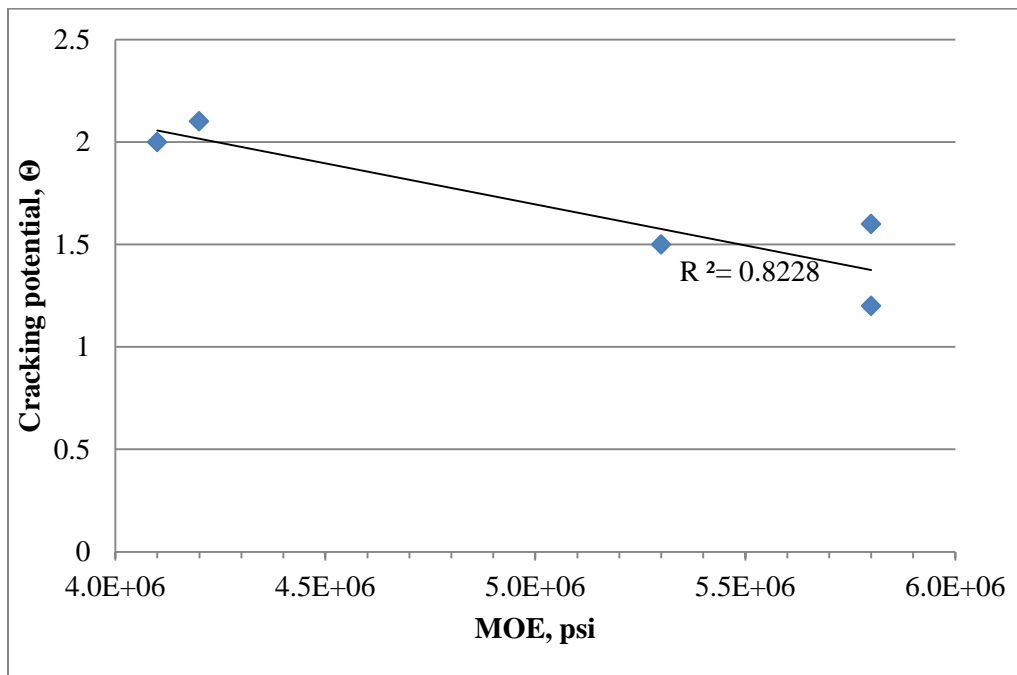


Figure 15(a). 28-day modulus of elasticity of concrete versus cracking potential Θ .

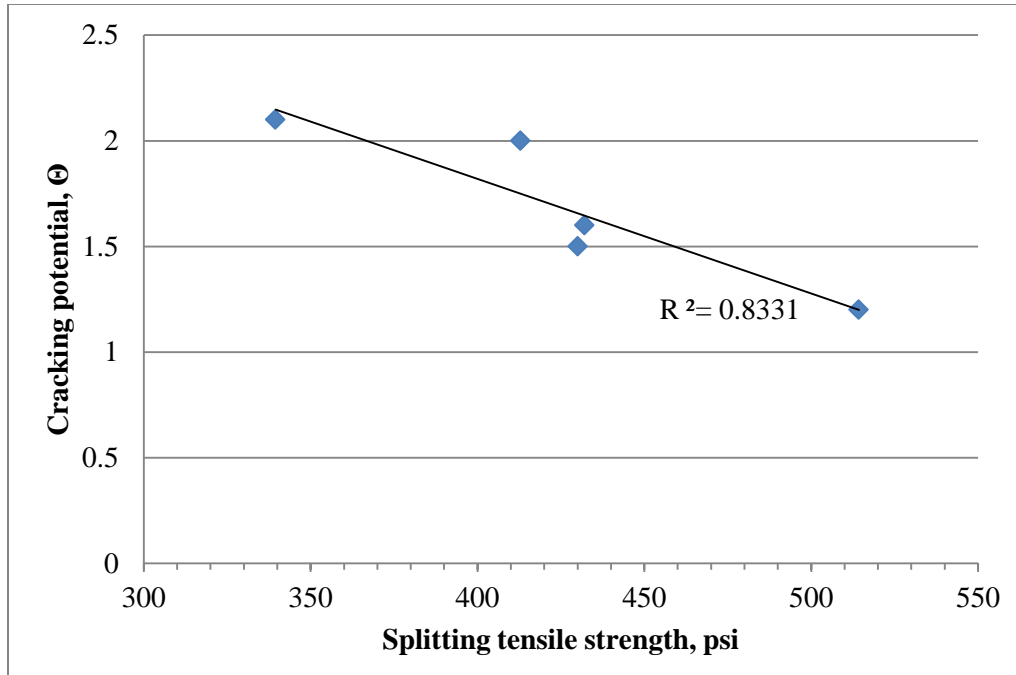


Figure 15(b). Splitting tensile strength of concrete versus cracking potential Θ .

Table 1. Project descriptions.

Project	Project Description
Mix 1	Bridge deck placement
Mix 2	Bridge deck placement
Mix 3	Bridge deck placement
Mix 4	Bridge deck placement
Mix 5	Rigid Pavement

Table 2. Chemical and physical properties of cementitious materials

Chemical, %	Mix 1			Mix 2			Mix 3			Mix 4	Mix 5	
	Type I/II cement	Class F fly ash	Grade 100 slag cement	Type II cement	Class F fly ash	Grade 120 slag cement	Type I/II cement	Silica fume	Slag cement	II(P4)(S25)	Type IP(25)	Class C fly ash
Ternary blends composition, %	55	15	30	50	15	35	60	5	35	71 PC + 4 SF + 25 Slag cement	64 PC+21 F ash	15
CaO	62.40	7.29	41.90	61.30	1.65	41.54	63.22	0.46	42.25	53.30	48.83	26.34
SiO₂	20.10	45.07	34.20	19.40	57.36	35.98	20.97	94.32	38.82	28.70	29.19	35.13
Al₂O₃	4.60	23.83	11.17	4.90	26.57	12.89	4.47	0.28	7.27	5.86	8.62	19.95
Fe₂O₃	2.70	15.02	0.68	3.70	5.40	0.52	2.93	0.31	0.81	1.98	3.80	5.74
MgO	4.00	1.58	6.89	2.30	-	6.11	2.30	0.75	9.02	4.68	3.04	4.88
K₂O	-	-	0.29	-	-	0.27	0.60	0.48	0.50	0.48	0.89	0.42
Na₂O	-	0.55	0.32	-	0.81	0.29	0.16	0.08	0.31	0.18	0.39	1.75
SO₃	3.40	1.30	-	3.80	0.33	1.09	2.63	0.05	-	2.52	3.14	1.45
P₂O₅	-	-	0.02	-	-	0.04	0.12	0.09	0.03	0.08	-	-
TiO₂	-	-	0.44	-	-	0.44	0.31	0.01	0.41	0.27	-	-
SrO	-	-	0.07	-	-	-	0.08	-	0.05	0.05	-	-
Mn₂O₃	-	-	0.38	-	-	0.45	0.04	-	0.52	0.18	-	-
Eq. Alkalies	0.89	0.67	0.51	0.85	-	0.47	0.55	0.40	0.64	0.49	0.97	2.03
LOI	2.10	1.91	-	1.80	1.97	-	2.17	2.58	-	1.60	1.26	0.11
Specific gravity	3.15	2.40	2.90	3.15	2.91	2.37	3.15	2.25	2.87	-	2.95	2.62

Table 3. Properties for coarse and fine aggregates

Field mixtures	Coarse aggregate type	Maximum aggregate size, in.	Specific gravity	Absorption, %	Passing #4 sieve, %	Fine aggregate type	Specific gravity	Fineness modulus
Mix 1	dolomitic limestone	3/4	2.84	0.32	2.0	sandstone	2.61	2.83
Mix 2	granite	3/4	2.67	0.65	3.6	sandstone	2.67	2.66
Mix 3	granite	3/4	2.60	0.80	3.0	natural sand	2.61	2.66
	granite	-	2.60	0.80	5.0			
Mix 4	high calcium limestone	3/4	2.70	1.73	3.0	natural sand	2.61	2.80
	granite	-	2.60	2.33	5.0			
Mix 5	quartzite	3/4	2.64	0.30	0.7	natural sand	2.65	3.00
	p-gravel	-	2.67	1.60	39			

Table 4(a). Designed mix proportions for field mixtures

Field Mixtures	Cement pcy	Fly Ash pcy	Slag cement pcy	Silica Fume pcy	FA pcy	CA 1 pcy	CA 2 pcy	w/c ratio	AEA oz/yd ³	WR oz/yd ³	Retarder oz/yd ³	Accelerator oz/yd ³	Fiber pcy
Mix 1	323	88	176	-	1210	1928	-	0.41	7.04	35.22	11.74	-	-
Mix 2	306	92	213	-	1160	1800	-	0.44	3.80	27.50	-	-	7
Mix 3	321	-	187	27	1217	1371	463	0.42	1.00	4.00	1.00	1	-
Mix 4	426	-	150	24	1234	1435	299	0.38	11.40	54.00	18.00	-	-
Mix 5	478	84	-	-	1235	1568	280	0.40	1.50	1.00	4.00	-	-

Table 4(b). Mix proportions for 450 pcy cementitious material content

Mixtures	Cement pcy	Fly Ash pcy	Slag pcy	Silica Fume pcy	FA pcy	CA 1 pcy	CA 2 pcy	w/c ratio	ARA oz/yd ³	WR oz/yd ³	Retarder oz/yd ³	Accelerator oz/yd ³	Fiber pcy
Mix 1	248	68	135	-	1319	2102	-	0.41	7.04	35.22	11.74	-	-
Mix 2	225	68	157	-	1302	2028	-	0.44	3.80	27.50	-	-	7
Mix 3	270	-	157	23	1284	1446	488	0.42	1.00	4.00	1.00	1	-
Mix 4	320	-	113	18	1363	1638	329	0.38	11.40	54.00	18.00	-	-
Mix 5	383	67	-	-	1323	1681	300	0.40	1.50	1.00	4.00	-	-

Table 4(c). Mix proportions for 700 pcy cementitious material content

Mixtures	Cement pcy	Fly Ash pcy	Slag pcy	Silica Fume pcy	FA pcy	CA 1 pcy	CA 2 pcy	w/c ratio	ARA oz/yd ³	WR oz/yd ³	Retarder oz/yd ³	Accelerator oz/yd ³	Fiber pcy
Mix 1	385	105	210	-	1120	1785	-	0.41	7.04	35.22	11.74	-	-
Mix 2	351	105	244	-	1097	1709	-	0.44	3.80	27.50	-	-	7
Mix 3	420	-	245	35	1088	1225	414	0.42	1.00	4.00	1.00	1	-
Mix 4	497	-	175	28	1170	1406	282	0.38	11.40	54.00	18.00	-	-
Mix 5	595	105	-	-	1126	1430	255	0.40	1.50	1.00	4.00	-	-

Table 4(d). Mix proportions for w/c of 0.45 and without fiber and chemical admixtures

Mixtures	Cement pcy	Fly Ash pcy	Slag pcy	Silica Fume pcy	FA pcy	CA 1 pcy	CA 2 pcy	w/c ratio	ARA oz/yd ³	WR oz/yd ³	Retarder oz/yd ³	Accelerator oz/yd ³	Fiber pcy
Mix 1	323	88	176	-	1210	1928	-	0.45	-	-	-	-	-
Mix 2	306	92	213	-	1160	1800	-	0.45	-	-	-	-	-
Mix 3	321	-	187	27	1217	1371	463	0.45	-	-	-	-	-
Mix 4	426	-	150	24	1234	1435	299	0.45	-	-	-	-	-
Mix 5	478	84	-	-	1235	1568	280	0.45	-	-	-	-	-

Table 5. Average strain rate factor, maximum strain and time of cracking

Mix	Designed mixture prisms	Restrained rings	Prisms of w/c=0.45 & w/o admixture			Mortar bars
			Prisms of 450 pcycementitious	Prisms of 700 pcycementitious		
Ave. strain rate factor α (strain $\times 10^{-6}/\text{day}^{1/2}$)						
Mix 1	83.0	34.0	81.9	76.1	108.5	140.6
Mix 2	102.9	35.8	77.1	71.5	95.0	132.7
Mix 3	81.2	26.1	64.6	65.1	75.4	113.5
Mix 4	118.9	51.5	78.3	87.5	112.1	125.0
Mix 5	34.0	23.1	53.6	31.9	58.0	125.9
Ave. maximum strain ($\times 10^{-6}$)						
Mix 1	682.5	87.9	560.5	541.0	756.0	1102.3
Mix 2	596.7	112.4	535.9	536.0	695.0	1012.5
Mix 3	510.0	93.9	459.3	440.0	540.0	936.9
Mix 4	756.7	94.7	535.8	598.0	820.0	986.2
Mix 5	290.0	83.8	396.3	199.0	398.0	980.3

Table 6. Concrete ring splitting tensile strength and failure strength at concrete crack time or 28 days

Mix	Cracking Potential, Θ	Concrete crack time, days	Shrinkage induced stress, psi	Splitting tensile strength, psi
Mix 1	1.5	No cracking	645.2	430.1
Mix 2	2.0	No cracking	825.7	412.9
Mix 3	1.6	No cracking	691.4	432.1
Mix 4	2.1	6.8	696.0	339.5
Mix 5	1.2	No cracking	617.1	514.3

Table 7. Test results of methylene blue index, paste-to- void ratio, water reducer agent dosage and 28-day MOE and average strain rate factors

Mix	Methylene blue index	Paste-to-void ratio (by volume), %	Water reducer content, oz/yd ³	28-day MOE, psi	Ave. strain rate factor, $\times 10^{-6}/\text{day}^{1/2}$
Mix 1	1.08	158.3	35.2	5.3E+06	34.0
Mix 2	1.13	163.8	27.5	4.1E+06	35.8
Mix 3	0.75	150.0	4.0	5.8E+06	26.1
Mix 4	1.54	169.3	54.0	4.2E+06	51.5
Mix 5	0.63	145.0	1.0	5.8E+06	23.1

Chapter 5

Conclusion

This study was aimed at developing a model of the drying shrinkage behavior of mortars produced with ternary blends. Shrinkage of mortar bars was determined as 28-day length change. A statistical analysis software package was used to develop models and the validity of the models was tested. In addition, the drying shrinkage behavior of ternary blend concretes that were used in transportation structures was investigated. Five different concrete mixes from field demonstration projects in the Midwest were included in the study. The mixtures represented a wide variety of material combinations. Raw materials from ready mix plants were collected to perform shrinkage related tests in a lab environment. Both restrained and unrestrained shrinkage testing methodologies were used to analyze the factors that influence shrinkage in mixtures with large differences in materials and proportions. The risk for cracking of as-built ternary blended concrete mixtures was assessed. In addition, compressive and splitting tensile strengths testing, and modulus of elasticity determination were carried out to investigate the correlations to drying shrinkage and cracking potential.

The main conclusions of the study are as follows:

- Slag cement shows a dominant effect on increasing mortar shrinkage in all three series. An increase of class C fly ash in series II is likely to decrease the mortar shrinkage. It also has a dominant effect although the effect of slag cement is slightly stronger. Silica fume in series III does not have a very strong effect while increasing in silica fume content still slightly increases free shrinkage of the mortar in ternary blends. An increase of class F fly ash in series I tends to increase the mortar shrinkage. However, this behavior is likely tenuous and class F fly ash shows the least dominant effect on the shrinkage in ternary blended slag cement mixture.
- The mineralogical and chemical composition promotes the reactivity of slag cement. The low alkali content in slag cement plays a beneficial role on drying shrinkage in a mixture. Class C fly ash with high-calcium content is similar to slag cement in the mineralogical composition and reactivity. In addition, the chemical characteristics of

class C fly ash will result in high Ca/Si ratio in the mixture which reduces the size and volume of gel pores in CSH system. The removal of interlayer water from CSH system is likely reduced therefore reducing shrinkage strain. The particle size distributions play a significant role on increasing pozzolanic reactivity of silica fume. The slightly increased mortar free shrinkage of silica fume in ternary blends is mainly due to the high pozzolanic reactivity and pore size refinement mechanisms. Class F fly ash with low calcium content results in low pozzolanic reactivity that plays the least effect on drying shrinkage of mortar in ternary blends.

- Literature provided general trends on concrete drying shrinkage when cement was replaced by single SCMs, such as class C fly ash, class F fly ash, slag cement, and silica fume. Reportedly, class C fly ash tended to increase drying shrinkage while class F fly ash may have a decrease trend on drying shrinkage strain without changing the w/cm ratio and aggregate content. Researchers concluded that given a similar binary system of slag cement mixture, slag cement tended to have a marginal effect on increasing drying shrinkage. The ultimate drying shrinkage of mortar increased with increase of SF content at 28 days, but the long-term drying shrinkage after 365 days was not affected significantly by the addition of SF.
- Class C and F fly ash have conflict effects on drying shrinkage in accordance with previous research of binary concrete system, while the silica fume and slag cement have agreements on literature. The conflicts may be caused by complex chemical and physical ternary mixing system, microstructural of ternary system, different mix proportion and w/cm ratio compared with literature, coarse aggregate effect on drying shrinkage, and differential effect between mortar and concrete mixtures.
- The shrinkage measurements from a group of verification mortar mixes have evidenced a good correlation between the measured shrinkage strain and the strain predicted from the shrinkage model developed from the response surface analysis.
- Water reducing admixture dosage plays a dominant role in the five ternary blend concrete mixtures.

- Cementitious material content has a significant effect on shrinkage strain. All as-built mixtures showed that free shrinkage linearly increases with the increased cementitious material content at an age of 56 days.
- Shrinkage strain rate linearly increases with clay content in aggregate and paste-to-void ratio of as-built concrete mixes.
- Splitting tensile strength and modulus of elasticity affect cracking potential. Shrinkage cracking potential decreases with increased splitting tensile strength and modulus of elasticity.
- Use of fibers appears to have reduced cracking risk.
- Free shrinkage strain rate factors demonstrate good correlation with shrinkage rate factors for restrained conditions.

Chapter 6

Recommendations for Future Research

The work presented in this thesis has provided a comprehensive study on drying shrinkage behavior of ternary blended mortar and concrete mixtures. However, further research is still needed, especially from the economic feasibility of the material point of view. The sources' availability plays a dominant role to determine different supplementary cementitious materials (SCMs) used in pavement and bridge deck structures. Some materials used to make good performance concrete are expensive. This is, for instance, true of silica fume. Therefore, the economic decisions will depend on some specific cases which may need accurate assessments.

From the technical point of view, statistical design and analysis can be introduced and contribute to mortar and concrete research. Design of mixture and response surface model, for example, can be beneficial to develop binary, ternary, or quantitative blended concrete testing matrix and perform a comprehensive analysis on different concrete properties, respectively.

Some other supplementary materials, such as rice husks, ground clay brick, and metakaolin, can be investigated on their effects of concrete durability and sustainability. Further research can also focus on other concrete properties caused by supplementary materials. Fracture mechanics and creep corresponding to concrete shrinkage and cracking, air and rapid chloride permeability, freeze-thaw resistance, alkali silica reaction (ASR) durability, and sulfate attack resistance are other realms that can be studied.

Appendix: Technical Reports from Additional Research

POOLED FUND STUDY

UNITED STATES DEPARTMENT OF TRANSPORTATION

FEDERAL HIGHWAY ADMINISTRATION



**DEVELOPMENT OF PERFORMANCE PROPERTIES OF TERNARY
MIXTURES**

**A Field Application of Ternary Mixtures
-An experience in construction of a bridge
deck in Kansas**

October 2009

U OF UTAH IOWA STATE UNIVERSITY


THE UNIVERSITY OF UTAH

National Concrete Pavement
Technology Center 
Tech Center

Introduction

This document is a report of the activities and observations of a research team that performed on-site testing of a ternary mixture placed on a bridge deck in Kansas. The purpose of this research project is a comprehensive study of how supplementary cementitious materials (SCMs) can be used to improve the performance of concrete mixtures when used in ternary blends. This is the third phase of a project which intends to provide consulting to states and contractors on the use and field management of ternary mixtures. A state-of-the-art 44-foot long PCC mobile laboratory equipped for on-site cement and concrete testing was provided by the CP Tech Center to collect data and field observations.

Project Information

- Project No. K 7888-01
- Douglas County, Kansas
- Contractor: Ames Construction
- US-59 Northbound bridge approximately 1½ mile south of US-56
- Bridge deck placement (3 span – structural steel girders with concrete deck) (Figure 1)

Site Location

An area at the bridge site was prepared by the contractor for the PCC mobile lab. The location of the project site and the mobile lab is shown in Figure 2.

Sampling and Testing Activities

The mobile lab arrived on site on October 27, 2009. Concrete placement, sampling and testing took place on October 28, 2009. Hardened samples were transported to Iowa State University on October 29, 2009 for further testing. The following tests were conducted either in the field or in the laboratory:

- Calorimetry test (ASTM C 1679)
- Slump, unit weight, temperature and air content of fresh concrete – 2 test (ASTM C 143, ASTM C 138, ASTM C 231)
- Microwave w/c ratio – 2 test (AASHTO T 318)

- Air Void Analyzer, Taylor et al. (2006)
- Initial set and final set of concrete – 1 test (ASTM C 403)
- Compressive strength, splitting tensile strength, static modulus of elasticity - 4” x 8” cylinders at 1-day, 3-days, 7-days, 28-days, and 56-days (ASTM C 39, ASTM C 496, ASTM C 469)
- Rapid chloride permeability - 4” x 8” cylinders at 56 days (ASTM C 1202)
- Air void analysis of hardened concrete - 4” x 8” cylinders (ASTM C 457)
- Porosity analysis (boil test) of hardened concrete - 4” x 8” cylinders (ASTM C 642)
- Free shrinkage test – 3 beams (ASTM C 157)
- Restrained rings – 4 samples (ASTM C 1581)

Observations of the Research Team

The following observations were made in this field study:

- The overall deck thickness is 8 ½ inches. The cover for top mat of epoxy coated grade 60 steel is 3 inches and cover from top surface for bottom mat of steel is 6 ½ inches.
- Removable wood formwork was used in the deck construction.
- The concrete was mixed at a central mix plant (Penny’s concrete) and transported by ready mix trucks.
- The mix design was from Ames Construction Inc., and approved by Kansas Department of Transportation. The accepted mix proportions are given in the project data section.
- Cementitious materials include Type I/II cement (Buzzi Unicem), grade 120 slag cement (Holcim), and silica fume (WR Grace). Two types of coarse granite aggregate were used together with a natural sand as fine aggregate.
- Setting time of the mix was determined as a single measurement: initial set occurred at 3.66 hours and the final set was achieved at 11.66 hours.
- According to the Workability Factor & Coarseness Factor graph (Page 13), combined aggregate gradation for this project falls in the well-graded region. However, from 0.45 Power Curve and Combined Percent Retained Curve, the aggregate gradation is slightly lacking in the amount of material retained on the #8 sieve. This did not

adversely affect workability or hardened properties of the mixture as observed in the field.

- A brief summary of weather conditions recorded by the PCC mobile lab is tabulated in Table 1 and presented graphically in Figures 3 to 5. The relative humidity ranged from 60% to 84%; the ambient temperature ranged from 48°F to 62 °F; the wind speed varied from 2.4 mph to 11.2 mph; the concrete temperature ranged from 55.0 °F to 66 °F during the recorded period (i.e., from 8am to 11:30am).
- Figures 6 through 10 illustrate some activities during the testing process.
- The fresh concrete tests include slump cone, unit weight, and water-cementitious materials ratio by microwave. Nine groups of samples were tested during the construction period. Slump results varied from a maximum of 7.5 inches to a minimum of 3.0 inches. The unit weight ranged from 142.4 lb/ft³ to 135.6 lb/ft³ with an average value of 138.9 lb/ft³. Two microwave w-cm ratio tests were performed at 8:20 AM and 10:50 AM, and the results were 0.44 and 0.45, respectively. The design value is 0.42. The data are provided on page 15.
- The air content ranged from 5.2% to 9.0% with an average of 7.3% over the nine tests conducted. The specified minimum was 6.5%.
- The air void test (Rapid Air Test) results for 14 samples from the same concrete mix are given in Table 2. A spacing factor ≤ 0.20 mm measured using microscopical methods is an indication of a good concrete freeze-thaw resistance (Tanesi and Meininger 2006). Based on this criterion, the spacing factors are acceptable in 7 out of 14 samples.
- The rapid chloride permeability test measures the electrical conductance of a concrete sample as its resistance to chloride ion penetration. The test results shown in Table 3 indicate a classification of “very low” permeability of chloride.
- The strength development 28/7 day f_c ratios are reported in Table 3.
- Compressive strength, splitting tensile strength and modulus of elasticity results (ASTM C 39, ASTM C 496, and ASTM C 469) are given in Table 4 and development curves are plotted in Figures 11 to Figure 13.

- The porosity values obtained by the boiling test (ASTM C 642) results are given in Table 3.
- The feedback from contractor on workability and finishing properties was positive. Traditionally, KDOT has constructed bridge decks in two pours, a binary mixture approximately 6” thick, which is later capped with an approximately 2” high density silica fume mixture. However, the ternary mixture allowed the contractor to place a full depth deck in one pour.
- Free shrinkage test (ASTM C 157) was conducted in the laboratory. Three concrete beams were wet cured for seven days and then moved to a dry room at 23°C and 50% relative humidity. The drying shrinkage results are given in Table 5 and also plotted in Figure 14.
- Restrained shrinkage test was conducted based on ASTM C 1581. Four rings were cast. The rings were demolded and the top surface was covered with paraffin wax 24 hours from casting. The rings were allowed to dry at 23°C and 50% relative humidity immediately after demolding. Strains in the steel rings were recorded every 10 minutes up to 28 days or until the concrete cracked. The configuration of restrained concrete rings is shown in Figure 15. The cracking potential is listed in Table 6 and shown graphically in Figure 16. The cracking potential is classified as “moderate high” based on the average stress rate.

Acknowledgements

The research team at the National Concrete Pavement Technology Center at Iowa State University sincerely thanks the Kansas Department of Transportation for their cooperation and Penny’s Concrete and Ames Construction Inc. for supplying the materials and equipment.

Project Data

The following test data is provided for information only, comments and conclusions will be reported in the comprehensive Phase III report of the pooled fund project *Development of Performance Properties of Ternary Mixtures*.

Mix Design & Misc. Info.

General Information

Project:	Kansas - Ternary Mixtures
Contractor:	Ames
Mix Description:	535 lb Cementitious
Mix ID:	1PL5046A
Date(s) of Placement:	10/28/2009

Cementitious Materials	Source	Type	Spec. Gravity	lb/yd ³	% Replacement by Mass
Portland Cement:	Buzzi Unicem	I/II	3.150	321	
GGBFS:	Holcim		2.870	187	34.95%
Fly Ash:					
Silica Fume:	WR Grace		2.250	27	5.05%
Other Pozzolan:					
				535	lb/yd ³
				5.7	sacks/yd ³

Aggregate Information	Source	Type	Spec. Gravity SSD	Absorption (%)	% Passing #4
Coarse Aggregate:	Granite Mountain - Ark.	Granite	2.600	0.80%	3.0%
Intermediate Aggregate #1:	Granite Mountain - Ark.	Granite	2.600	0.80%	5.0%
Intermediate Aggregate #2:					
Fine Aggregate #1:	Penny's	Natural Sand	2.610	0.70%	99.0%
Coarse Aggregate %:	45.0%				
Intermediate Aggregate #1%:	15.2%				
Intermediate Aggregate #2%:					
Fine Aggregate #1 %:	39.8%				

Mix Proportion Calculations

Water/Cementitious Materials Ratio:	0.420
Air Content:	6.50%

	Volume (ft ³)	Batch Weights SSD (lb/yd ³)	Spec. Gravity	Absolute Volume (%)
Portland Cement:	1.633	321	3.150	6.048%
GGBFS:	1.044	187	2.870	3.867%
Fly Ash:				
Silica Fume:	0.192	27	2.250	0.712%
Other Pozzolan:				
Coarse Aggregate:	8.449	1,371	2.600	31.291%
Intermediate Aggregate #1:	2.854	463	2.600	10.569%
Intermediate Aggregate #2:				
Fine Aggregate #1:	7.472	1,217	2.610	27.675%
Water:	3.601	225	1.000	13.337%
Air:	1.755			6.500%
	27.000	3,810		100.000%
	Unit Weight (lb/ft³)	141.1	Paste	30.465%
			Mortar	59.330%

Admixture Information	Source/Description	oz/yd ³	oz/cw t
Air Entraining Admix.:	Daravair 1400 AEA	4.00	0.75
Admix. #1:	ADVA 140M Full Range WR	1.00	0.19
Admix. #2:	Daraset 200 Type C accelerator	1.00	0.19
Admix. #3:	Recover Type D Retarder	1.00	0.19

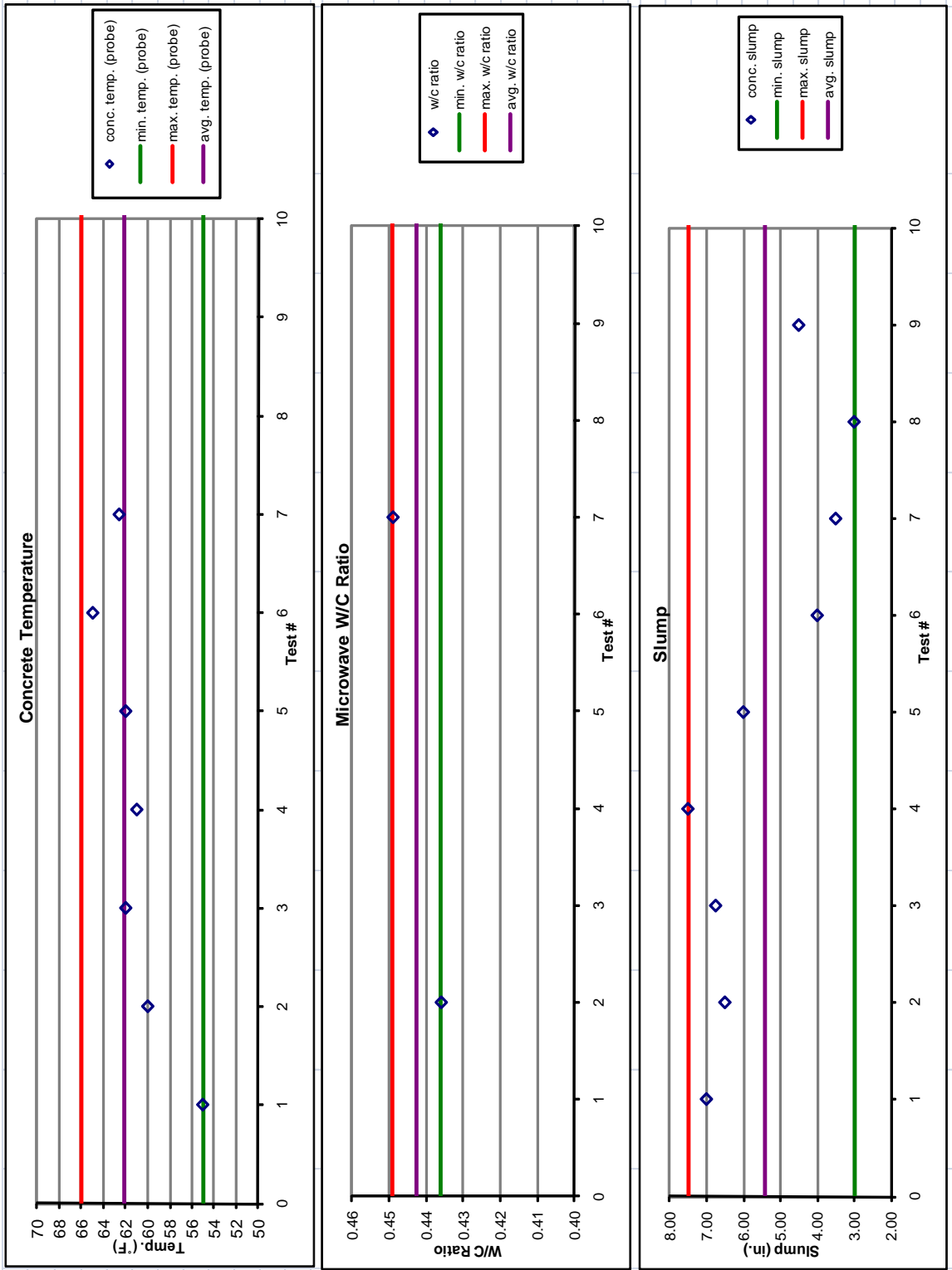
AVA Information

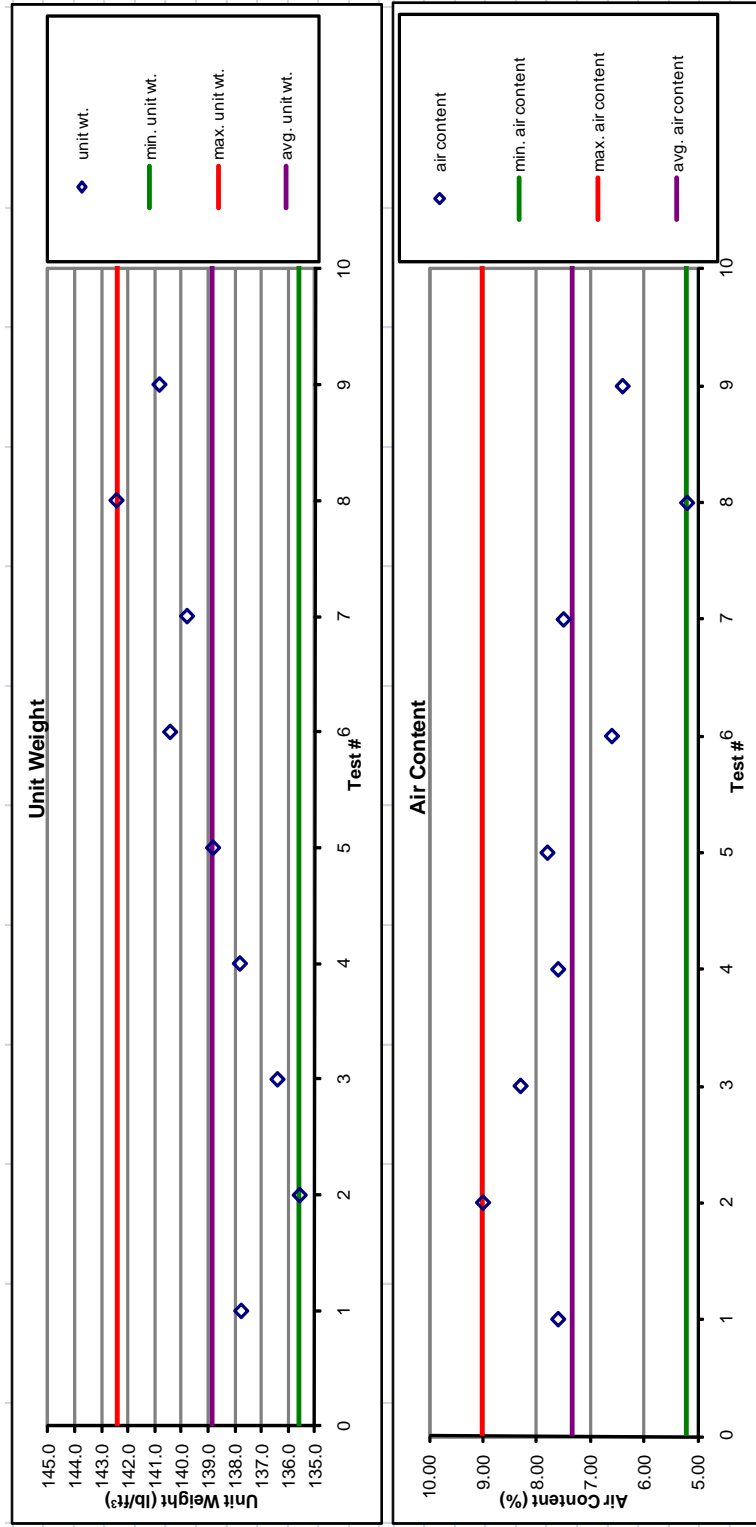
	Absolute Volume (%)
Air Free Paste:	23.965%
Air Free Mortar:	52.830%



Kansas - Ternary Mixtures
US-59 Bridge Deck

Sample Information & Identification			Environmental Conditions				Fresh Concrete Workability Properties			Pressure Air
Sample Date	Sample Time	Sample Comments	Relative Humidity (%)	Ambient Temp. (°F)	Wind Speed (mph)	Conc. Temp. (probe) (°F)	Slump (in)	Unit Weight (lb/ft ³)	Microwave W/C Ratio (%)	% Air Content
28-Oct-09	8:03 AM	kdot sample taken at pump discharge	65.0	48.0	2.4	55.0	7.00	137.8	n/a	7.6
28-Oct-09	8:20 AM	cp tech center sample taken at truck discharge	81.0	48.0	8.0	60.0	6.50	135.6	0.44	9.0
28-Oct-09	8:25 AM	kdot sample taken at pump discharge	84.0	49.0	4.5	62.0	6.75	136.4	n/a	8.3
28-Oct-09	9:20 AM	kdot sample taken at pump discharge	79.0	51.0	4.5	61.0	7.50	137.8	n/a	7.6
28-Oct-09	8:40 AM	kdot sample taken at pump discharge	81.0	53.0	11.2	62.0	6.00	138.8	n/a	7.8
28-Oct-09	10:10 AM	kdot sample taken at pump discharge	70.0	57.0	6.0	65.0	4.00	140.4	n/a	6.6
28-Oct-09	10:50 AM	cp tech center sample taken at truck discharge	60.0	57.0	5.0	62.6	3.50	139.8	0.45	7.5
28-Oct-09	11:04 AM	kdot sample taken at pump discharge	65.0	58.0	5.5	65.0	3.00	142.4	n/a	5.2
28-Oct-09	11:28 AM	kdot sample taken at pump discharge	62.0	62.0	3.5	66.0	4.50	140.8	n/a	6.4





Workability Factor & Coarseness Factor

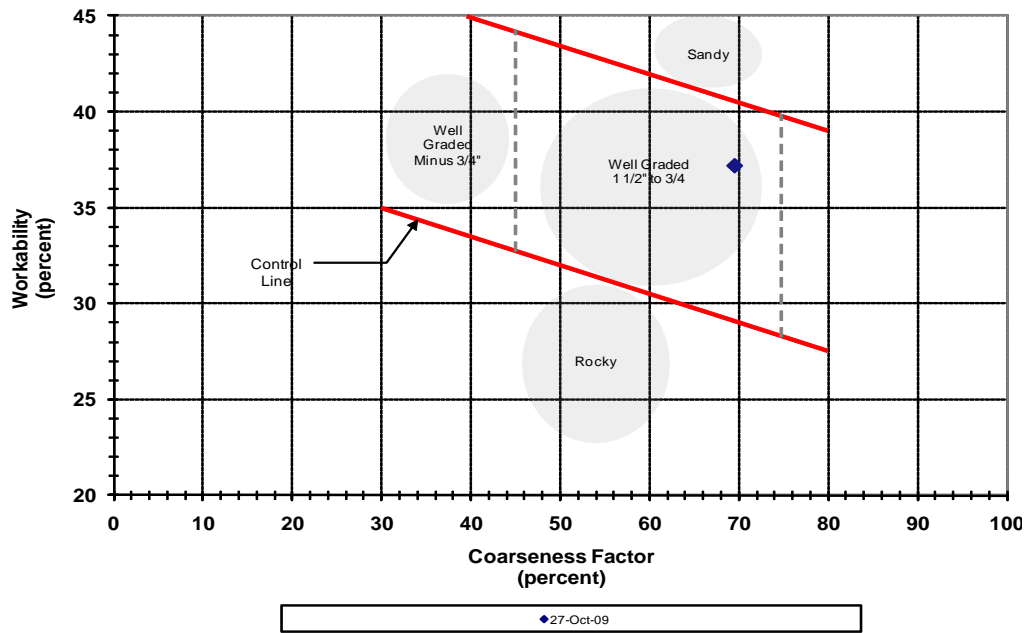
Project: **KDOT Ternary Mixtures**
 Mix ID: **Bridge Deck**
 Sample Comments: **KDOT Data**
 Test Date: **27-Oct-09**

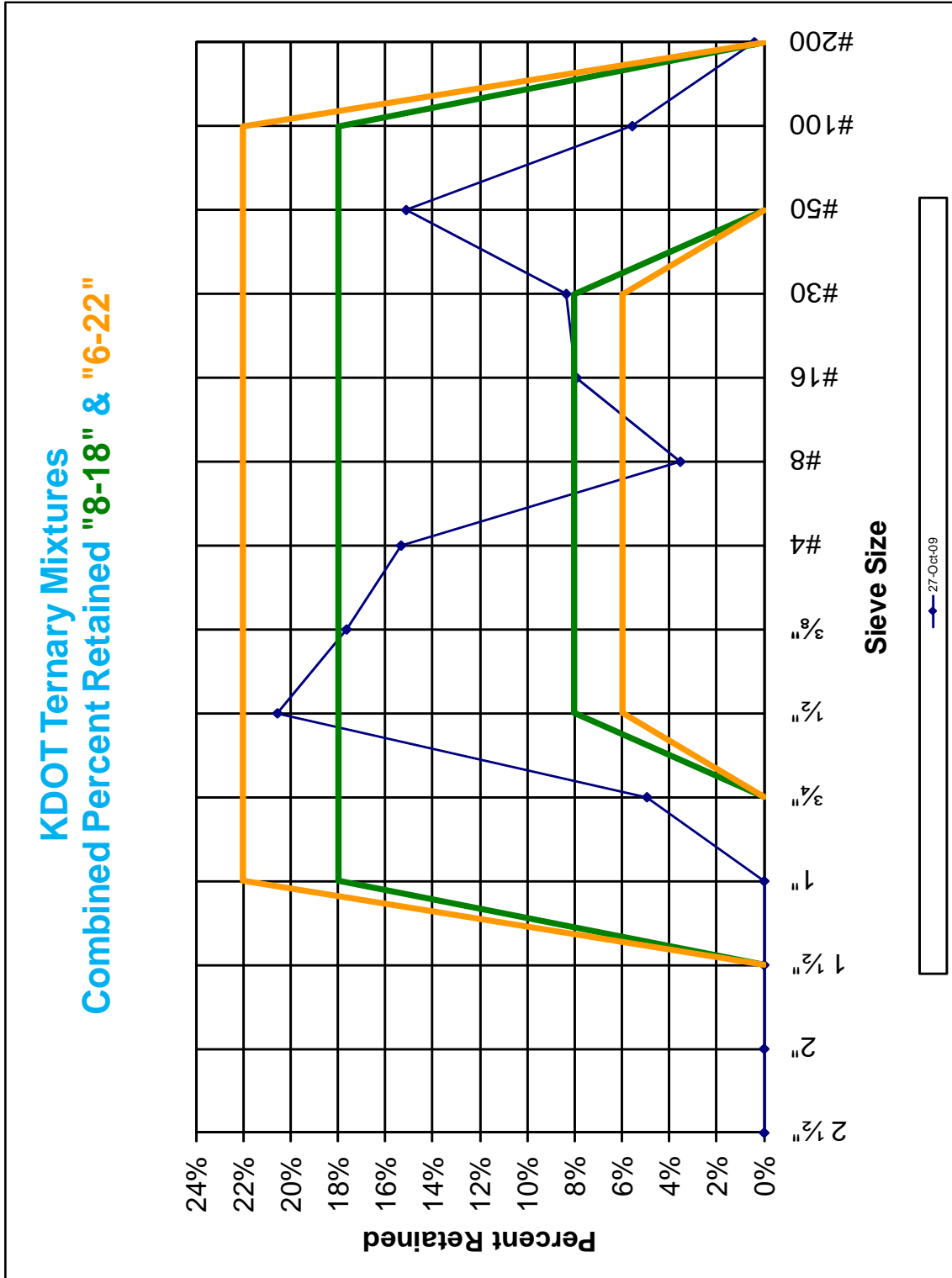
Total Cementitious Material: **535 lb/yd³**
 Agg. Ratios: **45.00%** **15.20%** **39.80%** **100.00%**

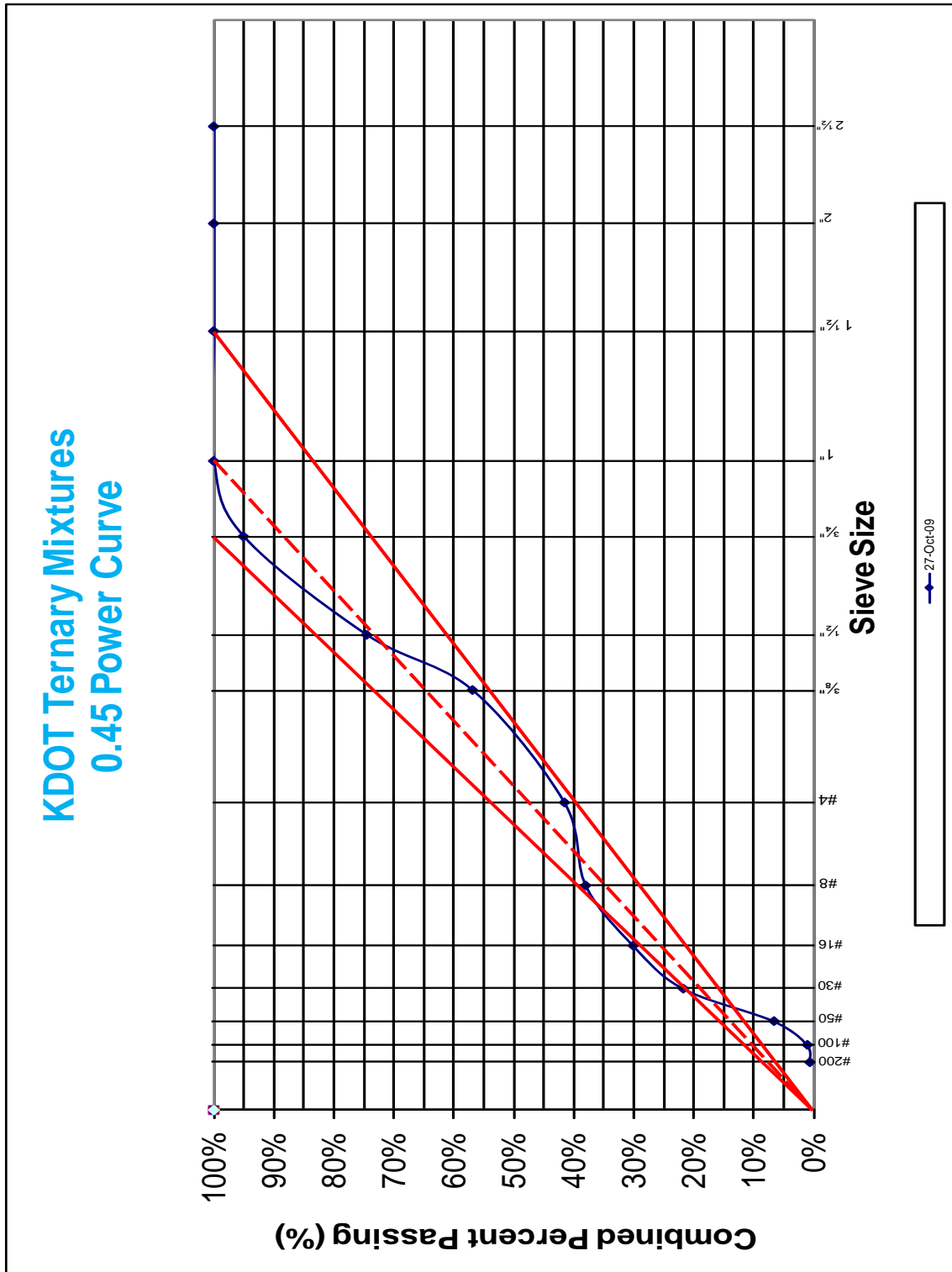
Sieve	Coarse	Intermediate	Fine #1	Fine #2	Combined % Retained	Combined % Retained On Each Sieve	Combined % Passing
2 1/2"	100%	100%	100%		0%	0%	100%
2"	100%	100%	100%		0%	0%	100%
1 1/2"	100%	100%	100%		0%	0%	100%
1"	100%	100%	100%		0%	0%	100%
3/4"	89%	100%	100%		5%	5%	95%
1/2"	45%	95%	100%		26%	21%	74%
3/8"	21%	50%	100%		43%	18%	57%
#4	3%	5%	99%		58%	15%	42%
#8	2%	3%	92%		62%	4%	38%
#16	1%	1%	74%		70%	8%	30%
#30	1%	1%	53%		78%	8%	22%
#50	1%	1%	15%		93%	15%	7%
#100	1%	1%	1%		99%	6%	1%
#200	0.7%	1.0%	0.3%		99.4%	0.4%	0.6%

Workability Factor: 37.2
Coarseness Factor: 69.6

KDOT Ternary Mixtures Workability Factor & Coarseness Factor









Kansas - Ternary Mixtures

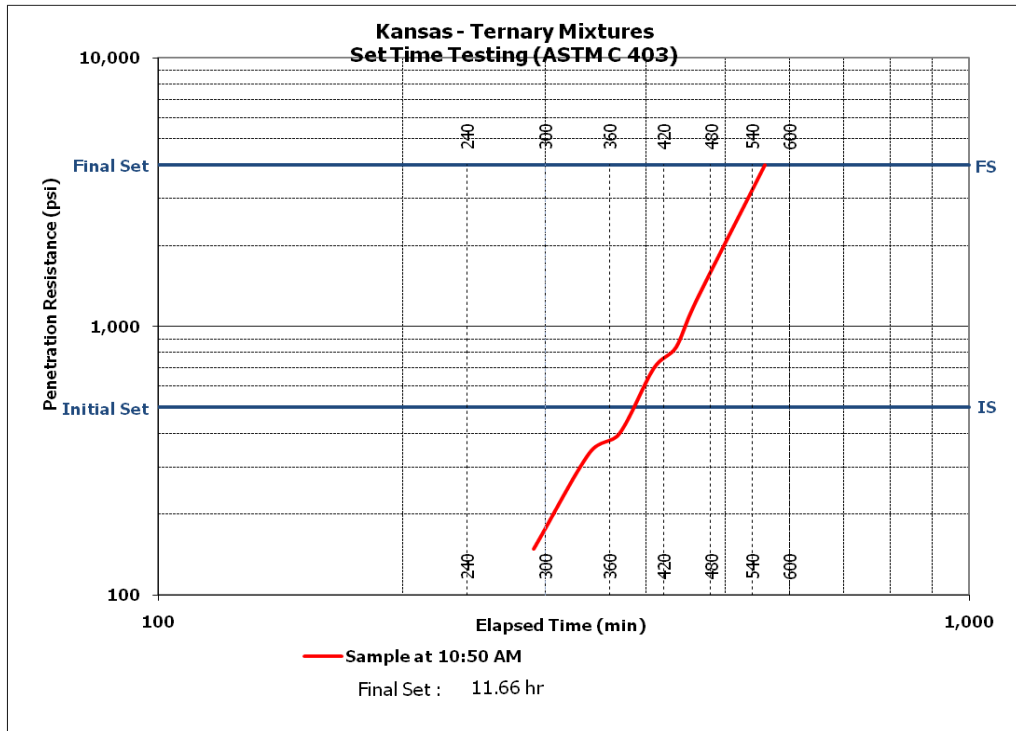
Set Time ASTM C 403

Project: US-59 Bridge Deck
 Date: 28-Oct-09 Start Time: 10:50 AM
 Sta: n/a

Test Data

Penetration Time (xx:xx-24 hr format)	Time (min)	Needle # (1, 2, 4, 10, 20 or 40)	Force (lb)	Penetration Resistance (psi)	Sample Temp. (°F)
3:40 PM	290.00	1	149	149.00	n/a
4:30 PM	340.00	4	85	340.00	n/a
5:00 PM	370.00	10	40	400.00	n/a
5:38 PM	408.00	10	70	700.00	n/a
6:05 PM	435.00	20	42	840.00	n/a
6:30 PM	460.00	20	62	1240.00	n/a
8:10 PM	560.00	40	100	4000.00	n/a
					n/a
					n/a

Initial Set (at 500 psi PR)	estimated times using forecast function	220 minutes	3.66 hours
Final Set (at 4,000 psi PR)		700 minutes	11.66 hours





Kansas - Ternary Mixtures

Microwave Water Content Worksheet

Project: US-59 Bridge Deck
 Date: 28-Oct-09 Time: 8:20 AM
 Sta: n/a


Test Data

Mass of tray+cloth+block+fresh test sample, W_F (g)	3,703.6
Mass of tray+cloth+block, W_S (g)	2,203.4
Mass of tray+cloth+dry sample, W_D (g) (5mins)	3,662.2
Mass of tray+cloth+dry sample, W_D (g) (7 mins)	3,611.0
Mass of tray+cloth+dry sample, W_D (g) (9 mins)*	3,603.2
Mass of tray+cloth+dry sample, W_D (g) (11 mins)*	3,601.1
Mass of tray+cloth+dry sample, W_D (g) (13 mins)*	3,599.6
Mass of tray+cloth+dry sample, W_D (g) (15 mins)*	3,598.8
Mass of tray+cloth+dry sample, W_D (g) (17 mins)*	3,598.5
Mass of tray+cloth+dry sample, W_D (g) (Final)**	3,598.5
Water content percentage, W_C (%)	7.0%
Unit weight of fresh concrete, UW (lb/ft ³)***	135.6
Total water content, W_T, (lb/yd³)	256.6
Total cementitious weight (lb/yd ³)	535
Fine aggregate weight (lb/yd ³)	1211
Coarse Aggregate weight (lb/yd ³)	1369
Intermediate Aggregate weight (lb/yd ³)	463
Fine aggregate absorption (%)	0.70%
Coarse aggregate absorption (%)	0.80%
Intermediate aggregate absorption (%)	0.80%
w/c	0.436

* If necessary (stop if the weight loss is less than 1g)

** Mass at test termination

***From unit weight test



Kansas - Ternary Mixtures

Compressive Strength Results

Catalog # KS ternary

Mix ID # 85TIP/15C

Date Cast: 28-Oct-09

Time Cast: 11 a.m.

Date Tested	Operator	1				2				3					
		Time of Test	Load (lb)	Diameter (in)	Load Rate (lb/sec)	f'_c (psi)	Time of Test	Load (lb)	Diameter (in)	Load Rate (lb/sec)	f'_c (psi)	Time of Test	Load (lb)	Diameter (in)	Load Rate (lb/sec)
4-Nov-09	PJM	7 day	41,490	4.00		3,300	7 day	39,630	4.00		3,150	7 day			3,225
				4.01		0			4.02		0				0
		28 day	74,310	4.01		5,880	28 day	68,180	4.01		5,400	28 day			5,640
		56 day	81,290	4.00		6,470	56 day	83,460	4.00		6,640	56 day			6,555

Boil Test (ASTM C 642)

KS A-1			KS B-1		
A	1032.5	g	A	1216.8	g
B	1061.86	g	B	1239.58	g
C	1072.3	g	C	1241.36	g
D	594.1	g	D	694.4	g
P	1	g/cm ³	P	1	g/cm ³
g1	2.1591	g/cm ³	g1	2.2247	g/cm ³
g2	2.3552	g/cm ³	g2	2.3292	g/cm ³
Volume of permeable pore space (voids), %		8.3229	Volume of permeable pore space (voids), %		4.4903
KS A-2			KS B-2		
A	1203.3	g	A	1207.8	g
B	1234.8	g	B	1227	g
C	1247.16	g	C	1227.71	g
D	694.8	g	D	695.1	g
P	1	g/cm ³	P	1	g/cm ³
g1	2.1785	g/cm ³	g1	2.2677	g/cm ³
g2	2.3664	g/cm ³	g2	2.3558	g/cm ³
Volume of permeable pore space (voids), %		7.9405	Volume of permeable pore space (voids), %		3.7382

Sample ID: CAST CYL A-1-122-S1

Sample Size (mm x mm) 90 x 85 Length Traversed (mm): 2413.1
 Paste Content (%): 27.00 Area Traversed (mm x mm): 80 x 75

Chord Length Distribution - Table

Class No.	Chord size (microns)	Number of Chords in Class	Number of Chords in Percent	Air Content in Class	Cumulated Air Content	Chord length frequenc	Air content, fraction	
1	0-10	18	1.78	0.010	0.010	0.02	0.010	0.00-0.01
2	10-20	82	8.11	0.050	0.060	0.08	0.050	0.01-0.02
3	20-30	52	8.11	0.060	0.110	0.05	0.060	0.02-0.03
4	30-40	43	4.25	0.060	0.180	0.04	0.060	0.03-0.04
5	40-50	45	4.45	0.080	0.260	0.04	0.080	0.04-0.05
6	50-60	42	4.15	0.100	0.360	0.04	0.100	0.05-0.06
7	60-80	74	7.32	0.210	0.570	0.07	0.210	0.06-0.08
8	80-100	72	7.12	0.270	0.840	0.07	0.270	0.08-0.10
9	100-120	67	6.63	0.300	1.140	0.07	0.300	0.10-0.12
10	120-140	58	5.74	0.310	1.450	0.06	0.310	0.12-0.14
11	140-160	44	4.35	0.270	1.720	0.04	0.270	0.14-0.16
12	160-180	44	4.35	0.310	2.030	0.04	0.310	0.16-0.18
13	180-200	40	3.96	0.320	2.350	0.04	0.320	0.18-0.20
14	200-220	20	1.98	0.170	2.520	0.02	0.170	0.20-0.22
15	220-240	33	3.26	0.320	2.840	0.03	0.320	0.22-0.24
16	240-260	25	2.47	0.260	3.100	0.02	0.260	0.24-0.26
17	260-280	22	2.18	0.250	3.340	0.02	0.250	0.26-0.28
18	280-300	21	2.08	0.250	3.590	0.02	0.250	0.28-0.30
19	300-350	38	3.76	0.510	4.100	0.04	0.510	0.30-0.35
20	350-400	26	2.57	0.400	4.500	0.03	0.400	0.35-0.40
21	400-450	22	2.18	0.390	4.890	0.02	0.390	0.40-0.45
22	450-500	16	1.58	0.320	5.210	0.02	0.320	0.45-0.50
23	500-1000	80	7.91	2.200	5.620	0.08	2.200	0.50-1.00
24	1000-1500	19	1.88	0.980	8.390	0.02	0.980	1.00-1.50
25	1500-2000	8	0.79	0.540	8.920	0.01	0.540	1.50-2.00
26	2000-2500	0	0.00	0.000	8.920	0.00	0.000	2.00-2.50
27	2500-3000	0	0.00	0.000	8.920	0.00	0.000	2.50-3.00
28	3000-4000	0	0.00	0.000	8.920	0.00	0.000	3.00-4.00
						1011		

Air Content (%): 8.92Specific Surface (mm⁻¹): 18.78Spacing Factor (mm): 0.161Void Frequency (mm⁻¹): 0.420Average Chord Length (r): 0.213Paste to Air Ratio: 3.03

Sample ID: CAST CYL A- 1 - 122 - S2

Sample Size (mm x mm 80 x 90 Length Traversed (mm): 2413.1

Paste Content (%): 27.00 Area Traversed (mm x mm): 70 x 80

Chord Length Distribution - Table

Class No.	Chord size (microns)	Number of Chords in Class	Number of Chords in Percent	Air Content in Class	Cumulated Air Content	Chord length frequency	Air content, fraction	
1	0-10	22	2.29	0.010	0.010	0.02	0.010	0.00-0.01
2	10-20	56	5.82	0.040	0.040	0.06	0.040	0.01-0.02
3	20-30	38	5.82	0.040	0.080	0.04	0.040	0.02-0.03
4	30-40	32	3.33	0.050	0.130	0.03	0.050	0.03-0.04
5	40-50	49	5.09	0.090	0.220	0.05	0.090	0.04-0.05
6	50-60	34	3.53	0.080	0.300	0.04	0.080	0.05-0.06
7	60-80	57	5.93	0.170	0.460	0.06	0.170	0.06-0.08
8	80-100	66	6.86	0.240	0.710	0.07	0.240	0.08-0.10
9	100-120	64	6.65	0.290	1.000	0.07	0.290	0.10-0.12
10	120-140	52	5.41	0.280	1.280	0.05	0.280	0.12-0.14
11	140-160	45	4.68	0.280	1.560	0.05	0.280	0.14-0.16
12	160-180	32	3.33	0.220	1.780	0.03	0.220	0.16-0.18
13	180-200	40	4.16	0.320	2.100	0.04	0.320	0.18-0.20
14	200-220	33	3.43	0.290	2.390	0.03	0.290	0.20-0.22
15	220-240	42	4.37	0.400	2.790	0.04	0.400	0.22-0.24
16	240-260	32	3.33	0.330	3.120	0.03	0.330	0.24-0.26
17	260-280	21	2.18	0.240	3.350	0.02	0.240	0.26-0.28
18	280-300	21	2.18	0.250	3.600	0.02	0.250	0.28-0.30
19	300-350	37	3.85	0.500	4.100	0.04	0.500	0.30-0.35
20	350-400	32	3.33	0.500	4.600	0.03	0.500	0.35-0.40
21	400-450	25	2.60	0.440	5.030	0.03	0.440	0.40-0.45
22	450-500	16	1.66	0.310	5.350	0.02	0.310	0.45-0.50
23	500-1000	82	8.52	2.230	5.870	0.09	2.230	0.50-1.00
24	1000-1500	22	2.29	1.090	8.670	0.02	1.090	1.00-1.50
25	1500-2000	9	0.94	0.640	9.310	0.01	0.640	1.50-2.00
26	2000-2500	3	0.31	0.280	9.590	0.00	0.280	2.00-2.50
27	2500-3000	0	0.00	0.000	9.590	0.00	0.000	2.50-3.00
28	3000-4000	0	0.00	0.000	9.590	0.00	0.000	3.00-4.00
						962		

Air Content (%): 9.59

Specific Surface (mm^{-1}): 16.63

Spacing Factor (mm): 0.169

Void Frequency (mm^{-1}): 0.400

Average Chord Length (n): 0.240

Paste to Air Ratio: 2.82

Sample ID: CAST CYL A- 1 - 122 - S3

Sample Size (mm x mm) 90 x 85 Length Traversed (mm): 2413.1

Paste Content (%): 27.00 Area Traversed (mm x mm): 80 x 75

Chord Length Distribution - Table

Class No.	Chord size (microns)	Number of Chords in Class	Number of Chords in Percent	Air Content in Class	Cumulated Air Content	Chord length frequency	Air content, fraction	
1	0-10	11	1.25	0.000	0.000	0.01	0.000	0.00-0.01
2	10-20	39	4.44	0.020	0.030	0.04	0.020	0.01-0.02
3	20-30	47	4.44	0.050	0.080	0.05	0.050	0.02-0.03
4	30-40	37	4.21	0.050	0.130	0.04	0.050	0.03-0.04
5	40-50	39	4.44	0.070	0.200	0.04	0.070	0.04-0.05
6	50-60	40	4.55	0.090	0.290	0.05	0.090	0.05-0.06
7	60-80	73	8.30	0.210	0.510	0.08	0.210	0.06-0.08
8	80-100	63	7.17	0.240	0.740	0.07	0.240	0.08-0.10
9	100-120	52	5.92	0.240	0.980	0.06	0.240	0.10-0.12
10	120-140	49	5.57	0.260	1.240	0.06	0.260	0.12-0.14
11	140-160	45	5.12	0.280	1.520	0.05	0.280	0.14-0.16
12	160-180	32	3.64	0.230	1.750	0.04	0.230	0.16-0.18
13	180-200	39	4.44	0.310	2.060	0.04	0.310	0.18-0.20
14	200-220	32	3.64	0.280	2.330	0.04	0.280	0.20-0.22
15	220-240	23	2.62	0.220	2.550	0.03	0.220	0.22-0.24
16	240-260	19	2.16	0.200	2.750	0.02	0.200	0.24-0.26
17	260-280	30	3.41	0.340	3.090	0.03	0.340	0.26-0.28
18	280-300	14	1.59	0.170	3.260	0.02	0.170	0.28-0.30
19	300-350	38	4.32	0.510	3.770	0.04	0.510	0.30-0.35
20	350-400	27	3.07	0.420	4.190	0.03	0.420	0.35-0.40
21	400-450	26	2.96	0.450	4.640	0.03	0.450	0.40-0.45
22	450-500	12	1.37	0.230	4.880	0.01	0.230	0.45-0.50
23	500-1000	66	7.51	1.920	5.010	0.08	1.920	0.50-1.00
24	1000-1500	16	1.82	0.800	7.600	0.02	0.800	1.00-1.50
25	1500-2000	4	0.46	0.300	7.900	0.00	0.300	1.50-2.00
26	2000-2500	2	0.23	0.190	8.100	0.00	0.190	2.00-2.50
27	2500-3000	2	0.23	0.220	8.320	0.00	0.220	2.50-3.00
28	3000-4000	2	0.23	0.270	8.590	0.00	0.270	3.00-4.00
						879		

Air Content (%): 8.59

Specific Surface (mm⁻¹): 16.96

Spacing Factor (mm): 0.185

Void Frequency (mm⁻¹): 0.360

Average Chord Length (r): 0.236

Paste to Air Ratio: 3.14

Sample Size (mm x mm) 75 x 100 Length Traversed (mm): 2413.1
 Paste Content (%): 27.00 Area Traversed (mm x mm): 65 x 90

Chord Length Distribution - Table

Class No.	Chord size (microns)	Number of Chords in Class	Number of Chords in Percent	Air Content in Class	Cumulated Air Content	Chord length frequency	Air content, fraction	
1	0-10	31	2.50	0.010	0.010	0.03	0.010	0.00-0.01
2	10-20	107	8.64	0.070	0.080	0.09	0.070	0.01-0.02
3	20-30	70	8.64	0.070	0.150	0.06	0.070	0.02-0.03
4	30-40	43	3.47	0.060	0.210	0.03	0.060	0.03-0.04
5	40-50	54	4.36	0.100	0.310	0.04	0.100	0.04-0.05
6	50-60	41	3.31	0.090	0.410	0.03	0.090	0.05-0.06
7	60-80	65	5.25	0.190	0.590	0.05	0.190	0.06-0.08
8	80-100	69	5.57	0.260	0.850	0.06	0.260	0.08-0.10
9	100-120	56	4.52	0.250	1.110	0.05	0.250	0.10-0.12
10	120-140	69	5.57	0.370	1.480	0.06	0.370	0.12-0.14
11	140-160	41	3.31	0.250	1.740	0.03	0.250	0.14-0.16
12	160-180	41	3.31	0.290	2.020	0.03	0.290	0.16-0.18
13	180-200	40	3.23	0.310	2.340	0.03	0.310	0.18-0.20
14	200-220	30	2.42	0.260	2.600	0.02	0.260	0.20-0.22
15	220-240	41	3.31	0.390	2.990	0.03	0.390	0.22-0.24
16	240-260	22	1.78	0.230	3.220	0.02	0.230	0.24-0.26
17	260-280	32	2.58	0.360	3.570	0.03	0.360	0.26-0.28
18	280-300	21	1.70	0.250	3.820	0.02	0.250	0.28-0.30
19	300-350	59	4.77	0.800	4.620	0.05	0.800	0.30-0.35
20	350-400	43	3.47	0.670	5.290	0.03	0.670	0.35-0.40
21	400-450	40	3.23	0.700	5.990	0.03	0.700	0.40-0.45
22	450-500	36	2.91	0.710	6.700	0.03	0.710	0.45-0.50
23	500-1000	153	12.36	4.380	7.220	0.12	4.380	0.50-1.00
24	1000-1500	24	1.94	1.190	12.270	0.02	1.190	1.00-1.50
25	1500-2000	5	0.40	0.370	12.650	0.00	0.370	1.50-2.00
26	2000-2500	1	0.08	0.090	12.740	0.00	0.090	2.00-2.50
27	2500-3000	4	0.32	0.450	13.190	0.00	0.450	2.50-3.00
28	3000-4000	0	0.00	0.000	13.190	0.00	0.000	3.00-4.00
						1238		

Air Content (%): 13.19

Specific Surface (mm^{-1}): 15.56

Spacing Factor (mm): 0.132

Void Frequency (mm^{-1}): 0.510

Average Chord Length (r) 0.257

Paste to Air Ratio: 2.05

Sample ID: CAST CYL A-2-122-S2

Sample Size (mm x mm) 90 x 80 Length Traversed (mm): 2413.1
 Paste Content (%): 27.00 Area Traversed (mm x mm): 80 x 70

Chord Length Distribution - Table

Class No.	Chord size (microns)	Number of Chords in Class	Number of Chords in Percent	Air Content in Class	Cumulated Air Content	Chord length frequency	Air content, fraction	
1	0-10	9	0.96	0.000	0.000	0.01	0.000	0.00-0.01
2	10-20	37	3.94	0.020	0.030	0.04	0.020	0.01-0.02
3	20-30	48	3.94	0.050	0.080	0.05	0.050	0.02-0.03
4	30-40	31	3.30	0.040	0.120	0.03	0.040	0.03-0.04
5	40-50	36	3.84	0.070	0.190	0.04	0.070	0.04-0.05
6	50-60	34	3.62	0.080	0.270	0.04	0.080	0.05-0.06
7	60-80	61	6.50	0.180	0.440	0.07	0.180	0.06-0.08
8	80-100	53	5.65	0.200	0.640	0.06	0.200	0.08-0.10
9	100-120	52	5.54	0.240	0.880	0.06	0.240	0.10-0.12
10	120-140	41	4.37	0.220	1.100	0.04	0.220	0.12-0.14
11	140-160	39	4.16	0.240	1.340	0.04	0.240	0.14-0.16
12	160-180	35	3.73	0.250	1.590	0.04	0.250	0.16-0.18
13	180-200	31	3.30	0.250	1.830	0.03	0.250	0.18-0.20
14	200-220	31	3.30	0.270	2.110	0.03	0.270	0.20-0.22
15	220-240	30	3.20	0.290	2.390	0.03	0.290	0.22-0.24
16	240-260	20	2.13	0.210	2.600	0.02	0.210	0.24-0.26
17	260-280	17	1.81	0.190	2.790	0.02	0.190	0.26-0.28
18	280-300	27	2.88	0.320	3.110	0.03	0.320	0.28-0.30
19	300-350	50	5.33	0.670	3.790	0.05	0.670	0.30-0.35
20	350-400	51	5.44	0.790	4.580	0.05	0.790	0.35-0.40
21	400-450	33	3.52	0.580	5.160	0.04	0.580	0.40-0.45
22	450-500	19	2.03	0.370	5.530	0.02	0.370	0.45-0.50
23	500-1000	119	12.69	3.300	6.120	0.13	3.300	0.50-1.00
24	1000-1500	22	2.35	1.110	9.940	0.02	1.110	1.00-1.50
25	1500-2000	6	0.64	0.430	10.370	0.01	0.430	1.50-2.00
26	2000-2500	3	0.32	0.280	10.650	0.00	0.280	2.00-2.50
27	2500-3000	3	0.32	0.330	10.990	0.00	0.330	2.50-3.00
28	3000-4000	0	0.00	0.000	10.990	0.00	0.000	3.00-4.00
						938		

Air Content (%): 10.99

Specific Surface (mm⁻¹): 14.15

Spacing Factor (mm): 0.174

Void Frequency (mm⁻¹): 0.390

Average Chord Length (r) 0.283

Paste to Air Ratio: 2.46

Sample ID: CAST CYL A-2-122-S3

Sample Size (mm x mm) 75 x 90 Length Traversed (mm): 2413.1
 Paste Content (%): 27.00 Area Traversed (mm x mm): 65 x 80

Chord Length Distribution - Table

Class No.	Chord size (microns)	Number of Chords in Class	Number of Chords in Percent	Air Content in Class	Cumulated Air Content	Chord length frequency	Air content, fraction	
1	0-10	29	2.50	0.010	0.010	0.02	0.010	0.00-0.01
2	10-20	101	8.70	0.060	0.070	0.09	0.060	0.01-0.02
3	20-30	75	8.70	0.080	0.150	0.06	0.080	0.02-0.03
4	30-40	52	4.48	0.080	0.230	0.04	0.080	0.03-0.04
5	40-50	43	3.70	0.080	0.310	0.04	0.080	0.04-0.05
6	50-60	40	3.45	0.090	0.400	0.03	0.090	0.05-0.06
7	60-80	73	6.29	0.210	0.610	0.06	0.210	0.06-0.08
8	80-100	63	5.43	0.240	0.850	0.05	0.240	0.08-0.10
9	100-120	64	5.51	0.290	1.140	0.06	0.290	0.10-0.12
10	120-140	49	4.22	0.260	1.400	0.04	0.260	0.12-0.14
11	140-160	43	3.70	0.270	1.670	0.04	0.270	0.14-0.16
12	160-180	46	3.96	0.320	1.990	0.04	0.320	0.16-0.18
13	180-200	31	2.67	0.240	2.230	0.03	0.240	0.18-0.20
14	200-220	29	2.50	0.250	2.490	0.02	0.250	0.20-0.22
15	220-240	26	2.24	0.250	2.740	0.02	0.250	0.22-0.24
16	240-260	32	2.76	0.330	3.070	0.03	0.330	0.24-0.26
17	260-280	22	1.89	0.240	3.310	0.02	0.240	0.26-0.28
18	280-300	30	2.58	0.360	3.670	0.03	0.360	0.28-0.30
19	300-350	38	3.27	0.510	4.180	0.03	0.510	0.30-0.35
20	350-400	37	3.19	0.570	4.750	0.03	0.570	0.35-0.40
21	400-450	36	3.10	0.640	5.390	0.03	0.640	0.40-0.45
22	450-500	40	3.45	0.790	6.170	0.03	0.790	0.45-0.50
23	500-1000	137	11.80	3.990	6.700	0.12	3.990	0.50-1.00
24	1000-1500	16	1.38	0.810	10.980	0.01	0.810	1.00-1.50
25	1500-2000	4	0.34	0.270	11.250	0.00	0.270	1.50-2.00
26	2000-2500	2	0.17	0.190	11.430	0.00	0.190	2.00-2.50
27	2500-3000	3	0.26	0.340	11.770	0.00	0.340	2.50-3.00
28	3000-4000	0	0.00	0.000	11.770	0.00	0.000	3.00-4.00
						1161		

Air Content (%): 11.77

Specific Surface (mm⁻¹): 16.35

Spacing Factor (mm): 0.140

Void Frequency (mm⁻¹): 0.480

Average Chord Length (r): 0.245

Paste to Air Ratio: 2.29

Sample ID: CAST CYL A-2-122-S4

Sample Size (mm x mm) 90 x 80 Length Traversed (mm): 2413.1

Paste Content (%): 27.00 Area Traversed (mm x mm): 80 x 70

Chord Length Distribution - Table

Class No.	Chord size (microns)	Number of Chords in Class	Number of Chords in Percent	Air Content in Class	Cumulated Air Content	Chord length frequency	Air content, fraction	
1	0-10	11	1.03	0.000	0.000	0.01	0.000	0.00-0.01
2	10-20	62	5.81	0.040	0.040	0.06	0.040	0.01-0.02
3	20-30	62	5.81	0.070	0.110	0.06	0.070	0.02-0.03
4	30-40	40	3.75	0.060	0.170	0.04	0.060	0.03-0.04
5	40-50	38	3.56	0.070	0.230	0.04	0.070	0.04-0.05
6	50-60	45	4.21	0.100	0.340	0.04	0.100	0.05-0.06
7	60-80	69	6.46	0.200	0.540	0.06	0.200	0.06-0.08
8	80-100	60	5.62	0.220	0.760	0.06	0.220	0.08-0.10
9	100-120	67	6.27	0.300	1.060	0.06	0.300	0.10-0.12
10	120-140	46	4.31	0.250	1.310	0.04	0.250	0.12-0.14
11	140-160	42	3.93	0.260	1.570	0.04	0.260	0.14-0.16
12	160-180	48	4.49	0.340	1.910	0.04	0.340	0.16-0.18
13	180-200	30	2.81	0.230	2.140	0.03	0.230	0.18-0.20
14	200-220	28	2.62	0.240	2.380	0.03	0.240	0.20-0.22
15	220-240	26	2.43	0.240	2.630	0.02	0.240	0.22-0.24
16	240-260	35	3.28	0.360	2.990	0.03	0.360	0.24-0.26
17	260-280	20	1.87	0.220	3.210	0.02	0.220	0.26-0.28
18	280-300	19	1.78	0.230	3.440	0.02	0.230	0.28-0.30
19	300-350	51	4.78	0.700	4.140	0.05	0.700	0.30-0.35
20	350-400	23	2.15	0.360	4.500	0.02	0.360	0.35-0.40
21	400-450	33	3.09	0.580	5.080	0.03	0.580	0.40-0.45
22	450-500	31	2.90	0.610	5.680	0.03	0.610	0.45-0.50
23	500-1000	135	12.64	3.840	6.400	0.13	3.840	0.50-1.00
24	1000-1500	32	3.00	1.540	11.060	0.03	1.540	1.00-1.50
25	1500-2000	9	0.84	0.660	11.710	0.01	0.660	1.50-2.00
26	2000-2500	4	0.37	0.360	12.070	0.00	0.360	2.00-2.50
27	2500-3000	2	0.19	0.230	12.300	0.00	0.230	2.50-3.00
28	3000-4000	0	0.00	0.000	12.300	0.00	0.000	3.00-4.00
						1068		

Air Content (%): 12.30

Specific Surface (mm⁻¹): 14.40

Spacing Factor (mm): 0.153

Void Frequency (mm⁻¹): 0.440

Average Chord Length (r): 0.278

Paste to Air Ratio: 2.20

Sample ID: CAST CYL B-1-133-S1

Sample Size (mm x mm): 120 x 80 Length Traversed (mm): 2413.1
 Paste Content (%): 27.00 Area Traversed (mm x mm): 100 x 70

Chord Length Distribution - Table

Class No.	Chord size (microns)	Number of Chords in Class	Number of Chords in Percent	Air Content in Class	Cumulated Air Content	Chord length frequency	Air content, fraction	
1	0-10	8	1.71	0.000	0.000	0.02	0.000	0.00-0.01
2	10-20	47	10.02	0.030	0.030	0.10	0.030	0.01-0.02
3	20-30	22	10.02	0.020	0.050	0.05	0.020	0.02-0.03
4	30-40	22	4.69	0.030	0.090	0.05	0.030	0.03-0.04
5	40-50	30	6.40	0.050	0.140	0.06	0.050	0.04-0.05
6	50-60	21	4.48	0.050	0.190	0.04	0.050	0.05-0.06
7	60-80	42	8.96	0.120	0.310	0.09	0.120	0.06-0.08
8	80-100	36	7.68	0.130	0.440	0.08	0.130	0.08-0.10
9	100-120	18	3.84	0.080	0.530	0.04	0.080	0.10-0.12
10	120-140	23	4.90	0.120	0.650	0.05	0.120	0.12-0.14
11	140-160	16	3.41	0.100	0.750	0.03	0.100	0.14-0.16
12	160-180	12	2.56	0.080	0.840	0.03	0.080	0.16-0.18
13	180-200	20	4.26	0.160	1.000	0.04	0.160	0.18-0.20
14	200-220	22	4.69	0.190	1.190	0.05	0.190	0.20-0.22
15	220-240	11	2.35	0.100	1.290	0.02	0.100	0.22-0.24
16	240-260	13	2.77	0.140	1.430	0.03	0.140	0.24-0.26
17	260-280	7	1.49	0.080	1.510	0.01	0.080	0.26-0.28
18	280-300	8	1.71	0.100	1.600	0.02	0.100	0.28-0.30
19	300-350	21	4.48	0.280	1.890	0.04	0.280	0.30-0.35
20	350-400	18	3.84	0.280	2.170	0.04	0.280	0.35-0.40
21	400-450	10	2.13	0.180	2.350	0.02	0.180	0.40-0.45
22	450-500	6	1.28	0.120	2.470	0.01	0.120	0.45-0.50
23	500-1000	30	6.40	0.820	2.600	0.06	0.820	0.50-1.00
24	1000-1500	4	0.85	0.200	3.490	0.01	0.200	1.00-1.50
25	1500-2000	2	0.43	0.130	3.620	0.00	0.130	1.50-2.00
26	2000-2500	0	0.00	0.000	3.620	0.00	0.000	2.00-2.50
27	2500-3000	0	0.00	0.000	3.620	0.00	0.000	2.50-3.00
28	3000-4000	0	0.00	0.000	3.620	0.00	0.000	3.00-4.00
						469		

Air Content (%): 3.62

Specific Surface (mm⁻¹): 21.50

Spacing Factor (mm): 0.259

Void Frequency (mm⁻¹): 0.190

Average Chord Length (mm): 0.186

Paste to Air Ratio: 7.46

Sample ID: CAST CYL B-1-133-S2

Sample Size (mm x mm): 90 x 100 Length Traversed (mm): 2413.1
 Paste Content (%): 27.00 Area Traversed (mm x mm): 80 x 90

Chord Length Distribution - Table

Class No.	Chord size (microns)	Number of Chords in Class	Number of Chords in Percent	Air Content in Class	Cumulated Air Content	Chord length frequency	Air content, fraction	
1	0-10	6	1.35	0.000	0.000	0.01	0.000	0.00-0.01
2	10-20	33	7.42	0.020	0.020	0.07	0.020	0.01-0.02
3	20-30	21	7.42	0.020	0.040	0.05	0.020	0.02-0.03
4	30-40	14	3.15	0.020	0.060	0.03	0.020	0.03-0.04
5	40-50	21	4.72	0.040	0.100	0.05	0.040	0.04-0.05
6	50-60	16	3.60	0.040	0.140	0.04	0.040	0.05-0.06
7	60-80	26	5.84	0.070	0.210	0.06	0.070	0.06-0.08
8	80-100	30	6.74	0.110	0.330	0.07	0.110	0.08-0.10
9	100-120	20	4.49	0.090	0.420	0.04	0.090	0.10-0.12
10	120-140	11	2.47	0.060	0.480	0.02	0.060	0.12-0.14
11	140-160	16	3.60	0.100	0.570	0.04	0.100	0.14-0.16
12	160-180	21	4.72	0.150	0.720	0.05	0.150	0.16-0.18
13	180-200	15	3.37	0.120	0.840	0.03	0.120	0.18-0.20
14	200-220	17	3.82	0.150	0.990	0.04	0.150	0.20-0.22
15	220-240	10	2.25	0.090	1.080	0.02	0.090	0.22-0.24
16	240-260	23	5.17	0.240	1.320	0.05	0.240	0.24-0.26
17	260-280	13	2.92	0.150	1.470	0.03	0.150	0.26-0.28
18	280-300	11	2.47	0.130	1.600	0.02	0.130	0.28-0.30
19	300-350	19	4.27	0.250	1.850	0.04	0.250	0.30-0.35
20	350-400	18	4.04	0.280	2.130	0.04	0.280	0.35-0.40
21	400-450	6	1.35	0.110	2.240	0.01	0.110	0.40-0.45
22	450-500	14	3.15	0.270	2.510	0.03	0.270	0.45-0.50
23	500-1000	48	10.79	1.340	2.710	0.11	1.340	0.50-1.00
24	1000-1500	6	1.35	0.300	4.150	0.01	0.300	1.00-1.50
25	1500-2000	5	1.12	0.340	4.490	0.01	0.340	1.50-2.00
26	2000-2500	0	0.00	0.000	4.490	0.00	0.000	2.00-2.50
27	2500-3000	2	0.45	0.230	4.720	0.00	0.230	2.50-3.00
28	3000-4000	3	0.67	0.380	5.100	0.01	0.380	3.00-4.00
						445		

Air Content (%): 5.10

Specific Surface (mm⁻¹): 14.46

Spacing Factor (mm): 0.329

Void Frequency (mm⁻¹): 0.180

Average Chord Length (mm): 0.277

Paste to Air Ratio: 5.29

Sample ID: CAST CYL B-1-133-S3

Sample Size (mm x mm): 80 x 110 Length Traversed (mm): 2413.1

Paste Content (%): 27.00 Area Traversed (mm x mm): 70 x 90

Chord Length Distribution - Table

Class No.	Chord size (microns)	Number of Chords in Class	Number of Chords in Percent	Air Content in Class	Cumulated Air Content	Chord length frequency	Air content, fraction
1	0-10	10	2.62	0.000	0.000	0.03	0.000 0.00-0.01
2	10-20	41	10.73	0.020	0.030	0.11	0.020 0.01-0.02
3	20-30	20	10.73	0.020	0.050	0.05	0.020 0.02-0.03
4	30-40	16	4.19	0.020	0.070	0.04	0.020 0.03-0.04
5	40-50	14	3.66	0.030	0.100	0.04	0.030 0.04-0.05
6	50-60	11	2.88	0.020	0.120	0.03	0.020 0.05-0.06
7	60-80	21	5.50	0.060	0.180	0.05	0.060 0.06-0.08
8	80-100	28	7.33	0.100	0.290	0.07	0.100 0.08-0.10
9	100-120	11	2.88	0.050	0.340	0.03	0.050 0.10-0.12
10	120-140	10	2.62	0.050	0.390	0.03	0.050 0.12-0.14
11	140-160	15	3.93	0.090	0.480	0.04	0.090 0.14-0.16
12	160-180	15	3.93	0.110	0.590	0.04	0.110 0.16-0.18
13	180-200	19	4.97	0.150	0.740	0.05	0.150 0.18-0.20
14	200-220	10	2.62	0.090	0.820	0.03	0.090 0.20-0.22
15	220-240	13	3.40	0.120	0.950	0.03	0.120 0.22-0.24
16	240-260	13	3.40	0.130	1.080	0.03	0.130 0.24-0.26
17	260-280	12	3.14	0.130	1.220	0.03	0.130 0.26-0.28
18	280-300	16	4.19	0.190	1.410	0.04	0.190 0.28-0.30
19	300-350	15	3.93	0.200	1.600	0.04	0.200 0.30-0.35
20	350-400	10	2.62	0.150	1.760	0.03	0.150 0.35-0.40
21	400-450	10	2.62	0.180	1.930	0.03	0.180 0.40-0.45
22	450-500	7	1.83	0.140	2.070	0.02	0.140 0.45-0.50
23	500-1000	28	7.33	0.750	2.240	0.07	0.750 0.50-1.00
24	1000-1500	9	2.36	0.480	3.300	0.02	0.480 1.00-1.50
25	1500-2000	7	1.83	0.490	3.790	0.02	0.490 1.50-2.00
26	2000-2500	1	0.26	0.090	3.880	0.00	0.090 2.00-2.50
27	2500-3000	0	0.00	0.000	3.880	0.00	0.000 2.50-3.00
28	3000-4000	0	0.00	0.000	3.880	0.00	0.000 3.00-4.00
						382	
Air Content (%):			3.88				
Specific Surface (mm ⁻¹):			16.33				
Spacing Factor (mm):			0.330				
Void Frequency (mm ⁻¹):			0.160				
Average Chord Length (mm):			0.245				
Paste to Air Ratio:			6.96				

Sample ID: CAST CYL B-1-133-S4

Sample Size (mm x mm): 100 x 90 Length Traversed (mm): 2413.1

Paste Content (%): 27.00 Area Traversed (mm x mm): 90 x 80

Chord Length Distribution - Table

Class No.	Chord size (microns)	Number of Chords in Class	Number of Chords in Percent	Air Content in Class	Cumulated Air Content	Chord length frequency	Air content, fraction	
1	0-10	13	3.66	0.000	0.000	0.04	0.000	0.00-0.01
2	10-20	48	13.52	0.030	0.030	0.14	0.030	0.01-0.02
3	20-30	34	13.52	0.040	0.070	0.10	0.040	0.02-0.03
4	30-40	18	5.07	0.030	0.090	0.05	0.030	0.03-0.04
5	40-50	13	3.66	0.020	0.120	0.04	0.020	0.04-0.05
6	50-60	9	2.54	0.020	0.140	0.03	0.020	0.05-0.06
7	60-80	21	5.92	0.060	0.200	0.06	0.060	0.06-0.08
8	80-100	15	4.23	0.060	0.250	0.04	0.060	0.08-0.10
9	100-120	18	5.07	0.080	0.340	0.05	0.080	0.10-0.12
10	120-140	10	2.82	0.050	0.390	0.03	0.050	0.12-0.14
11	140-160	11	3.10	0.070	0.460	0.03	0.070	0.14-0.16
12	160-180	7	1.97	0.050	0.510	0.02	0.050	0.16-0.18
13	180-200	8	2.25	0.060	0.570	0.02	0.060	0.18-0.20
14	200-220	11	3.10	0.100	0.670	0.03	0.100	0.20-0.22
15	220-240	10	2.82	0.090	0.760	0.03	0.090	0.22-0.24
16	240-260	6	1.69	0.060	0.820	0.02	0.060	0.24-0.26
17	260-280	8	2.25	0.090	0.910	0.02	0.090	0.26-0.28
18	280-300	7	1.97	0.080	0.990	0.02	0.080	0.28-0.30
19	300-350	11	3.10	0.150	1.140	0.03	0.150	0.30-0.35
20	350-400	12	3.38	0.190	1.330	0.03	0.190	0.35-0.40
21	400-450	12	3.38	0.210	1.540	0.03	0.210	0.40-0.45
22	450-500	8	2.25	0.160	1.700	0.02	0.160	0.45-0.50
23	500-1000	31	8.73	0.830	1.850	0.09	0.830	0.50-1.00
24	1000-1500	7	1.97	0.340	2.870	0.02	0.340	1.00-1.50
25	1500-2000	5	1.41	0.370	3.250	0.01	0.370	1.50-2.00
26	2000-2500	2	0.56	0.180	3.430	0.01	0.180	2.00-2.50
27	2500-3000	0	0.00	0.000	3.430	0.00	0.000	2.50-3.00
28	3000-4000	0	0.00	0.000	3.430	0.00	0.000	3.00-4.00
						355		

Air Content (%): 3.43

Specific Surface (mm⁻¹): 17.17

Spacing Factor (mm): 0.332

Void Frequency (mm⁻¹): 0.150

Average Chord Length (mm): 0.233

Paste to Air Ratio: 7.87

Sample Size (mm x mm):	80 x 90	Length Traversed (mm):	2413.1
Paste Content (%):	27.00	Area Traversed (mm x mm):	70 x 80

Chord Length Distribution - Table

Class No.	Chord size (microns)	Number of Chords in Class	Number of Chords in Percent	Air Content in Class	Cumulated Air Content	Chord length frequency	Air content, fraction	
1	0-10	13	3.08	0.000	0.000	0.03	0.000	0.00-0.01
2	10-20	36	8.53	0.020	0.030	0.09	0.020	0.01-0.02
3	20-30	25	8.53	0.030	0.050	0.06	0.030	0.02-0.03
4	30-40	19	4.50	0.030	0.080	0.05	0.030	0.03-0.04
5	40-50	20	4.74	0.040	0.120	0.05	0.040	0.04-0.05
6	50-60	19	4.50	0.040	0.160	0.05	0.040	0.05-0.06
7	60-80	32	7.58	0.090	0.250	0.08	0.090	0.06-0.08
8	80-100	29	6.87	0.110	0.360	0.07	0.110	0.08-0.10
9	100-120	15	3.55	0.070	0.430	0.04	0.070	0.10-0.12
10	120-140	20	4.74	0.110	0.540	0.05	0.110	0.12-0.14
11	140-160	22	5.21	0.140	0.670	0.05	0.140	0.14-0.16
12	160-180	26	6.16	0.180	0.860	0.06	0.180	0.16-0.18
13	180-200	16	3.79	0.130	0.980	0.04	0.130	0.18-0.20
14	200-220	18	4.27	0.160	1.140	0.04	0.160	0.20-0.22
15	220-240	5	1.18	0.050	1.190	0.01	0.050	0.22-0.24
16	240-260	5	1.18	0.050	1.240	0.01	0.050	0.24-0.26
17	260-280	9	2.13	0.100	1.340	0.02	0.100	0.26-0.28
18	280-300	8	1.90	0.100	1.430	0.02	0.100	0.28-0.30
19	300-350	12	2.84	0.160	1.600	0.03	0.160	0.30-0.35
20	350-400	5	1.18	0.080	1.670	0.01	0.080	0.35-0.40
21	400-450	10	2.37	0.180	1.850	0.02	0.180	0.40-0.45
22	450-500	8	1.90	0.160	2.010	0.02	0.160	0.45-0.50
23	500-1000	37	8.77	1.010	2.290	0.09	1.010	0.50-1.00
24	1000-1500	4	0.95	0.190	3.210	0.01	0.190	1.00-1.50
25	1500-2000	5	1.18	0.390	3.590	0.01	0.390	1.50-2.00
26	2000-2500	3	0.71	0.280	3.870	0.01	0.280	2.00-2.50
27	2500-3000	1	0.24	0.100	3.970	0.00	0.100	2.50-3.00
28	3000-4000	0	0.00	0.000	3.970	0.00	0.000	3.00-4.00
						422		

Air Content (%): 3.97

Specific Surface (mm^{-1}): 17.60

Spacing Factor (mm): 0.303

Void Frequency (mm^{-1}): 0.170

Average Chord Length (mm): 0.227

Paste to Air Ratio: 6.80

Sample ID: CAST CYL B-2-129-S2

Sample Size (mm x mm): 90 x 90 Length Traversed (mm): 2413.1
 Paste Content (%): 27.00 Area Traversed (mm x mm): 80 x 80

Chord Length Distribution - Table

Class No.	Chord size (microns)	Number of Chords in Class	Number of Chords in Percent	Air Content in Class	Cumulated Air Content	Chord length frequency	Air content, fraction	
1	0-10	11	2.34	0.000	0.000	0.02	0.000	0.00-0.01
2	10-20	41	8.72	0.030	0.030	0.09	0.030	0.01-0.02
3	20-30	28	8.72	0.030	0.060	0.06	0.030	0.02-0.03
4	30-40	15	3.19	0.020	0.080	0.03	0.020	0.03-0.04
5	40-50	24	5.11	0.040	0.120	0.05	0.040	0.04-0.05
6	50-60	22	4.68	0.050	0.170	0.05	0.050	0.05-0.06
7	60-80	32	6.81	0.090	0.270	0.07	0.090	0.06-0.08
8	80-100	39	8.30	0.150	0.410	0.08	0.150	0.08-0.10
9	100-120	28	5.96	0.130	0.540	0.06	0.130	0.10-0.12
10	120-140	19	4.04	0.100	0.640	0.04	0.100	0.12-0.14
11	140-160	22	4.68	0.140	0.780	0.05	0.140	0.14-0.16
12	160-180	23	4.89	0.160	0.940	0.05	0.160	0.16-0.18
13	180-200	23	4.89	0.180	1.120	0.05	0.180	0.18-0.20
14	200-220	15	3.19	0.130	1.250	0.03	0.130	0.20-0.22
15	220-240	15	3.19	0.140	1.390	0.03	0.140	0.22-0.24
16	240-260	5	1.06	0.050	1.440	0.01	0.050	0.24-0.26
17	260-280	6	1.28	0.070	1.510	0.01	0.070	0.26-0.28
18	280-300	11	2.34	0.130	1.640	0.02	0.130	0.28-0.30
19	300-350	12	2.55	0.160	1.810	0.03	0.160	0.30-0.35
20	350-400	15	3.19	0.230	2.040	0.03	0.230	0.35-0.40
21	400-450	13	2.77	0.230	2.270	0.03	0.230	0.40-0.45
22	450-500	13	2.77	0.250	2.520	0.03	0.250	0.45-0.50
23	500-1000	20	4.26	0.570	2.670	0.04	0.570	0.50-1.00
24	1000-1500	15	3.19	0.730	3.820	0.03	0.730	1.00-1.50
25	1500-2000	3	0.64	0.200	4.020	0.01	0.200	1.50-2.00
26	2000-2500	0	0.00	0.000	4.020	0.00	0.000	2.00-2.50
27	2500-3000	0	0.00	0.000	4.020	0.00	0.000	2.50-3.00
28	3000-4000	0	0.00	0.000	4.020	0.00	0.000	3.00-4.00
						470		

Air Content (%): 4.02

Specific Surface (mm⁻¹): 19.40

Spacing Factor (mm): 0.273

Void Frequency (mm⁻¹): 0.190

Average Chord Length (mm): 0.206

Paste to Air Ratio: 6.72

Sample ID: CAST CYL B-2-129-S3

Sample Size (mm x mm): 80 x 90 Length Traversed (mm): 2413.1
 Paste Content (%): 27.00 Area Traversed (mm x mm): 70 x 80

Chord Length Distribution - Table

Class No.	Chord size (microns)	Number of Chords in Class	Number of Chords in Percent	Air Content in Class	Cumulated Air Content	Chord length frequency	Air content, fraction	
1	0-10	14	3.02	0.000	0.000	0.03	0.000	0.00-0.01
2	10-20	36	7.78	0.020	0.030	0.08	0.020	0.01-0.02
3	20-30	37	7.78	0.040	0.060	0.08	0.040	0.02-0.03
4	30-40	13	2.81	0.020	0.080	0.03	0.020	0.03-0.04
5	40-50	23	4.97	0.040	0.120	0.05	0.040	0.04-0.05
6	50-60	20	4.32	0.050	0.170	0.04	0.050	0.05-0.06
7	60-80	38	8.21	0.110	0.280	0.08	0.110	0.06-0.08
8	80-100	27	5.83	0.100	0.380	0.06	0.100	0.08-0.10
9	100-120	23	4.97	0.100	0.490	0.05	0.100	0.10-0.12
10	120-140	24	5.18	0.130	0.620	0.05	0.130	0.12-0.14
11	140-160	17	3.67	0.110	0.720	0.04	0.110	0.14-0.16
12	160-180	20	4.32	0.140	0.860	0.04	0.140	0.16-0.18
13	180-200	18	3.89	0.140	1.000	0.04	0.140	0.18-0.20
14	200-220	7	1.51	0.060	1.060	0.02	0.060	0.20-0.22
15	220-240	10	2.16	0.100	1.160	0.02	0.100	0.22-0.24
16	240-260	10	2.16	0.110	1.260	0.02	0.110	0.24-0.26
17	260-280	4	0.86	0.050	1.310	0.01	0.050	0.26-0.28
18	280-300	7	1.51	0.080	1.390	0.02	0.080	0.28-0.30
19	300-350	12	2.59	0.160	1.550	0.03	0.160	0.30-0.35
20	350-400	14	3.02	0.210	1.770	0.03	0.210	0.35-0.40
21	400-450	12	2.59	0.210	1.980	0.03	0.210	0.40-0.45
22	450-500	15	3.24	0.300	2.270	0.03	0.300	0.45-0.50
23	500-1000	51	11.02	1.430	2.470	0.11	1.430	0.50-1.00
24	1000-1500	7	1.51	0.350	4.060	0.02	0.350	1.00-1.50
25	1500-2000	2	0.43	0.160	4.220	0.00	0.160	1.50-2.00
26	2000-2500	2	0.43	0.190	4.400	0.00	0.190	2.00-2.50
27	2500-3000	0	0.00	0.000	4.400	0.00	0.000	2.50-3.00
28	3000-4000	0	0.00	0.000	4.400	0.00	0.000	3.00-4.00
						463		

Air Content (%): 4.40

Specific Surface (mm⁻¹): 17.43

Spacing Factor (mm): 0.292

Void Frequency (mm⁻¹): 0.190

Average Chord Length (mm): 0.229

Paste to Air Ratio: 6.14



ASTM C 1202-97



Test-compagny
Testing street 45
CompagnyCity
Some Country

Your own logo.
size=20x80mm



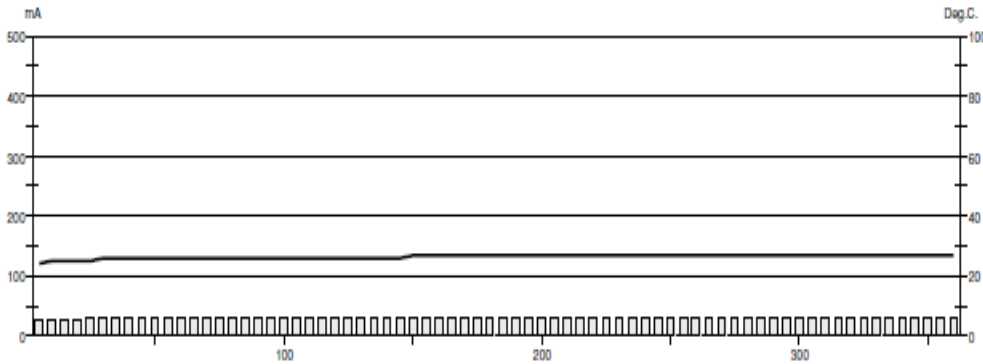
GERMANN INSTRUMENTS

DENMARK
Phone: +45 397 7117
Fax: +45 397 3167

USA
Phone: (947)325-9999
Fax: (947)325-9888

Test report

Voltage Used: 60
Testing time: 06:00 hour
Charge passed: 613
Adjusted Charge passed: 532
Permeability class: Very Low
Instrument number: 023907
Channel number: 1
Report date: 12/22/2009
Testing by: PJM
Reference: KS ternary A-1
Sample diameter: 102
Comment: --



Time	°C	mA	Time	°C	mA	Time	°C	mA	Time	°C	mA
00:05	24	26.3	01:35	26	29.0	03:05	27	28.2	04:35	27	28.3
00:10	25	26.9	01:40	26	28.9	03:10	27	28.2	04:40	27	28.5
00:15	25	26.9	01:45	26	28.8	03:15	27	28.2	04:45	27	28.9
00:20	25	27.4	01:50	26	28.7	03:20	27	28.2	04:50	27	28.8
00:25	25	28.0	01:55	26	28.6	03:25	27	28.4	04:55	27	28.8
00:30	26	28.1	02:00	26	28.5	03:30	27	28.9	05:00	27	28.7
00:35	26	28.3	02:05	26	28.4	03:35	27	28.9	05:05	27	28.6
00:40	26	28.3	02:10	26	28.5	03:40	27	28.9	05:10	27	28.4
00:45	26	28.5	02:15	26	28.4	03:45	27	28.8	05:15	27	28.3
00:50	26	28.4	02:20	26	28.4	03:50	27	28.7	05:20	27	28.2
00:55	26	28.4	02:25	26	28.3	03:55	27	28.6	05:25	27	28.1
01:00	26	28.4	02:30	27	28.3	04:00	27	28.5	05:30	27	28.1
01:05	26	28.6	02:35	27	28.3	04:05	27	28.4	05:35	27	28.1
01:10	26	28.9	02:40	27	28.3	04:10	27	28.3	05:40	27	28.1
01:15	26	29.1	02:45	27	28.2	04:15	27	28.3	05:45	27	28.1
01:20	26	29.1	02:50	27	28.2	04:20	27	28.4	05:50	27	28.0
01:25	26	29.1	02:55	27	28.3	04:25	27	28.5	05:55	27	28.2
01:30	26	29.1	03:00	27	28.3	04:30	27	28.4	06:00	27	28.9



ASTM C 1202-97



Test-compagny
Testing street 45
CompagnyCity
Some Country

Your own logo,
size=20x80pxmm



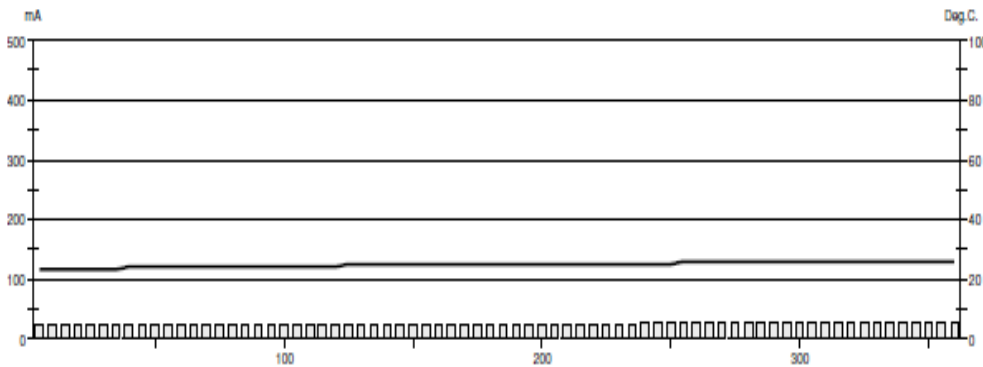
GERMANN INSTRUMENTS

GERMANY
Phone: +49 3907 7117
Fax: +49 3907 3107

USA
Phone: (847) 224-9999
Fax: (847) 224-4888

Test report

Voltage Used: 60
Testing time: 06:00 hour
Charge passed: 543
Adjusted Charge passed: 471
Permeability class: Very Low
Instrument number: 023907
Channel number: 2
Report date: 12/22/2009
Testing by: PJM
Reference: KS ternary A-2
Sample diameter: 102
Comment: ---



Time	°C	mA	Time	°C	mA	Time	°C	mA	Time	°C	mA
00:05	23	24.5	01:35	24	24.6	03:05	25	25.3	04:35	26	25.8
00:10	23	24.4	01:40	24	24.8	03:10	25	25.3	04:40	26	25.7
00:15	23	24.4	01:45	24	24.8	03:15	25	25.4	04:45	26	25.7
00:20	23	24.3	01:50	24	24.8	03:20	25	25.4	04:50	26	25.7
00:25	23	24.3	01:55	24	24.8	03:25	25	25.4	04:55	26	25.7
00:30	23	24.2	02:00	24	24.9	03:30	25	25.4	05:00	26	25.7
00:35	23	24.2	02:05	25	24.9	03:35	25	25.4	05:05	26	25.7
00:40	24	24.2	02:10	25	25.0	03:40	25	25.4	05:10	26	25.7
00:45	24	24.3	02:15	25	25.1	03:45	25	25.5	05:15	26	25.7
00:50	24	24.2	02:20	25	25.1	03:50	25	25.5	05:20	26	25.7
00:55	24	24.1	02:25	25	25.1	03:55	25	25.5	05:25	26	25.7
01:00	24	24.2	02:30	25	25.1	04:00	25	25.7	05:30	26	25.7
01:05	24	24.2	02:35	25	25.3	04:05	25	25.7	05:35	26	25.7
01:10	24	24.2	02:40	25	25.2	04:10	25	25.7	05:40	26	25.7
01:15	24	24.3	02:45	25	25.2	04:15	26	25.7	05:45	26	25.7
01:20	24	24.4	02:50	25	25.2	04:20	26	25.8	05:50	26	25.8
01:25	24	24.5	02:55	25	25.3	04:25	26	25.9	05:55	26	25.8
01:30	24	24.5	03:00	25	25.4	04:30	26	25.9	06:00	26	25.7



ASTM C 1202-97



Test-compagny
Testing street 45
CompagnyCity
Some Country

Your own logo.
size=20x80mm



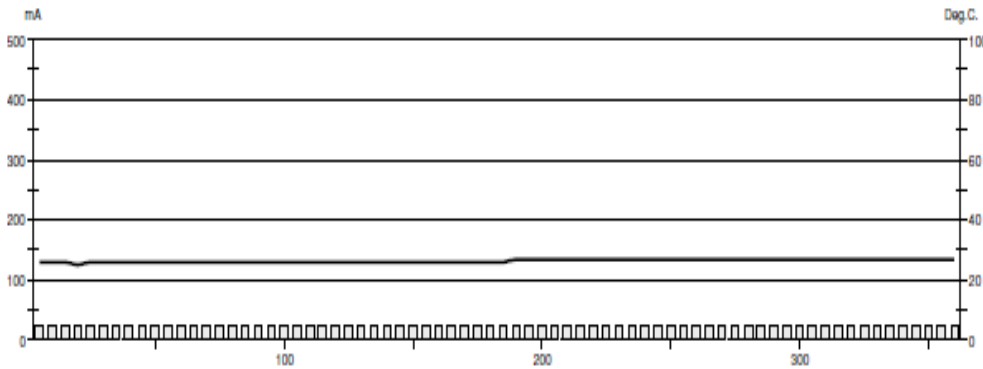
GERMANN INSTRUMENTS

DENMARK
Phone: +45 297 7117
Fax: +45 297 3167

USA
Phone: (877)254-9999
Fax: (847)321-4888

Test report

Voltage Used: 60
Testing time: 06:00 hour
Charge passed: 539
Adjusted Charge passed: 468
Permeability class: Very Low
Instrument number: 023907
Channel number: 3
Report date: 12/22/2009
Testing by: PJM
Reference: KS Ternary B-1
Sample diameter: 102
Comment: ---



Time	°C	mA	Time	°C	mA	Time	°C	mA	Time	°C	mA
00:05	26	25.1	01:35	26	24.9	03:05	26	24.7	04:35	27	25.2
00:10	26	24.8	01:40	26	24.9	03:10	27	24.8	04:40	27	25.2
00:15	26	24.6	01:45	26	24.9	03:15	27	24.8	04:45	27	25.2
00:20	25	24.6	01:50	26	24.9	03:20	27	24.8	04:50	27	25.2
00:25	26	24.7	01:55	26	24.9	03:25	27	24.8	04:55	27	25.2
00:30	26	24.7	02:00	26	24.9	03:30	27	24.8	05:00	27	25.2
00:35	26	24.7	02:05	26	24.9	03:35	27	24.9	05:05	27	25.1
00:40	26	24.7	02:10	26	24.9	03:40	27	25.1	05:10	27	25.1
00:45	26	24.7	02:15	26	24.9	03:45	27	25.1	05:15	27	25.1
00:50	26	24.7	02:20	26	24.8	03:50	27	25.1	05:20	27	25.1
00:55	26	24.7	02:25	26	24.8	03:55	27	25.1	05:25	27	25.3
01:00	26	24.7	02:30	26	24.8	04:00	27	25.1	05:30	27	25.3
01:05	26	24.7	02:35	26	24.8	04:05	27	25.2	05:35	27	25.3
01:10	26	24.7	02:40	26	24.7	04:10	27	25.2	05:40	27	25.3
01:15	26	24.7	02:45	26	24.7	04:15	27	25.2	05:45	27	25.4
01:20	26	24.9	02:50	26	24.7	04:20	27	25.2	05:50	27	25.4
01:25	26	24.9	02:55	26	24.7	04:25	27	25.2	05:55	27	25.4
01:30	26	24.9	03:00	26	24.7	04:30	27	25.2	06:00	27	25.4



ASTM C 1202-97



Test-compagny
Testing street 45
CompagnyCity
Some Country

Your own logo,
size=20x80pxmm



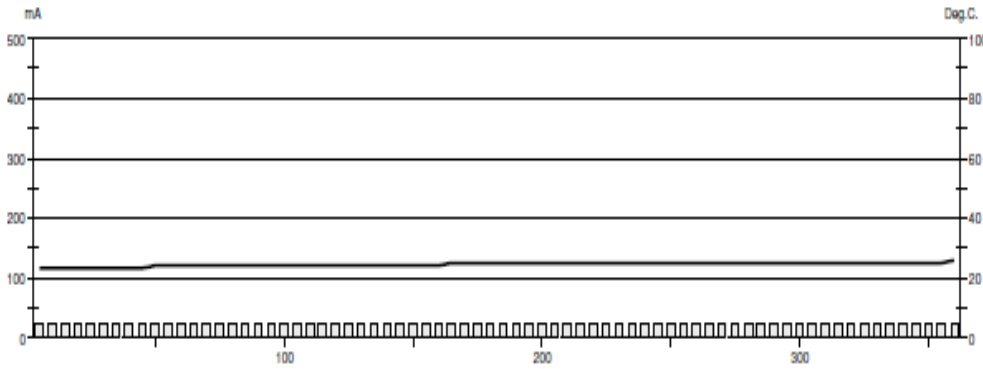
GERMANN INSTRUMENTS

GERMANY
Phone: +49 3907 7117
Fax: +49 3907 3107

USA
Phone: (847)224-9999
Fax: (847)321-4000

Test report

Voltage Used: 60
Testing time: 06:00 hour
Charge passed: 518
Adjusted Charge passed: 449
Permeability class: Very Low
Instrument number: 023907
Channel number: 4
Report date: 12/22/2009
Testing by: PJM
Reference: KS Ternary B-2
Sample diameter: 102
Comment: ---



Time	°C	mA	Time	°C	mA	Time	°C	mA	Time	°C	mA
00:05	23	23.6	01:35	24	23.3	03:05	25	23.8	04:35	25	24.6
00:10	23	23.7	01:40	24	23.4	03:10	25	23.8	04:40	25	24.7
00:15	23	23.7	01:45	24	23.3	03:15	25	23.8	04:45	25	24.7
00:20	23	23.9	01:50	24	23.3	03:20	25	24.1	04:50	25	24.7
00:25	23	23.9	01:55	24	23.4	03:25	25	24.3	04:55	25	24.5
00:30	23	23.9	02:00	24	23.4	03:30	25	24.3	05:00	25	24.5
00:35	23	23.8	02:05	24	23.5	03:35	25	24.3	05:05	25	24.5
00:40	23	23.6	02:10	24	23.4	03:40	25	24.3	05:10	25	24.6
00:45	23	23.5	02:15	24	23.5	03:45	25	24.3	05:15	25	24.6
00:50	24	23.5	02:20	24	23.5	03:50	25	24.3	05:20	25	24.7
00:55	24	23.4	02:25	24	23.6	03:55	25	24.4	05:25	25	24.7
01:00	24	23.3	02:30	24	23.6	04:00	25	24.4	05:30	25	24.7
01:05	24	23.4	02:35	24	23.6	04:05	25	24.4	05:35	25	24.7
01:10	24	23.4	02:40	24	23.6	04:10	25	24.5	05:40	25	24.7
01:15	24	23.3	02:45	25	23.6	04:15	25	24.5	05:45	25	24.7
01:20	24	23.3	02:50	25	23.6	04:20	25	24.6	05:50	25	24.7
01:25	24	23.3	02:55	25	23.7	04:25	25	24.6	05:55	25	24.8
01:30	24	23.4	03:00	25	23.7	04:30	25	24.6	06:00	26	24.7



Figure 1 US-59 Bridges (Southbound-left and Northbound-right).

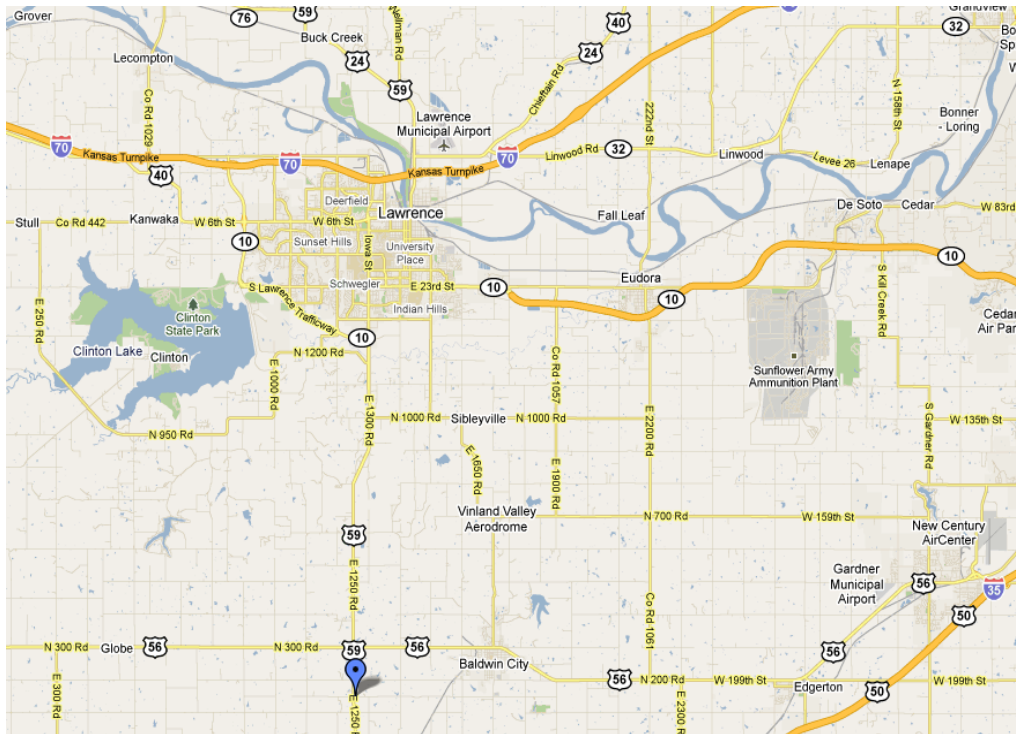


Figure 2 Project and Mobile Lab Location.

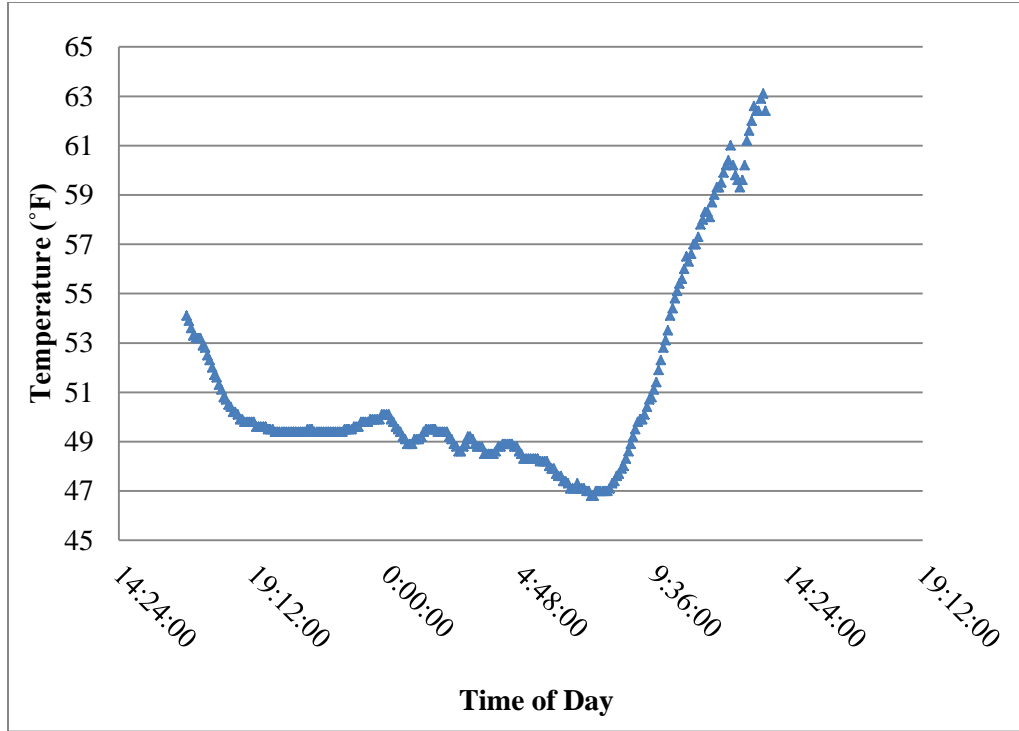


Figure 3 Ambient temperature versus time of day.

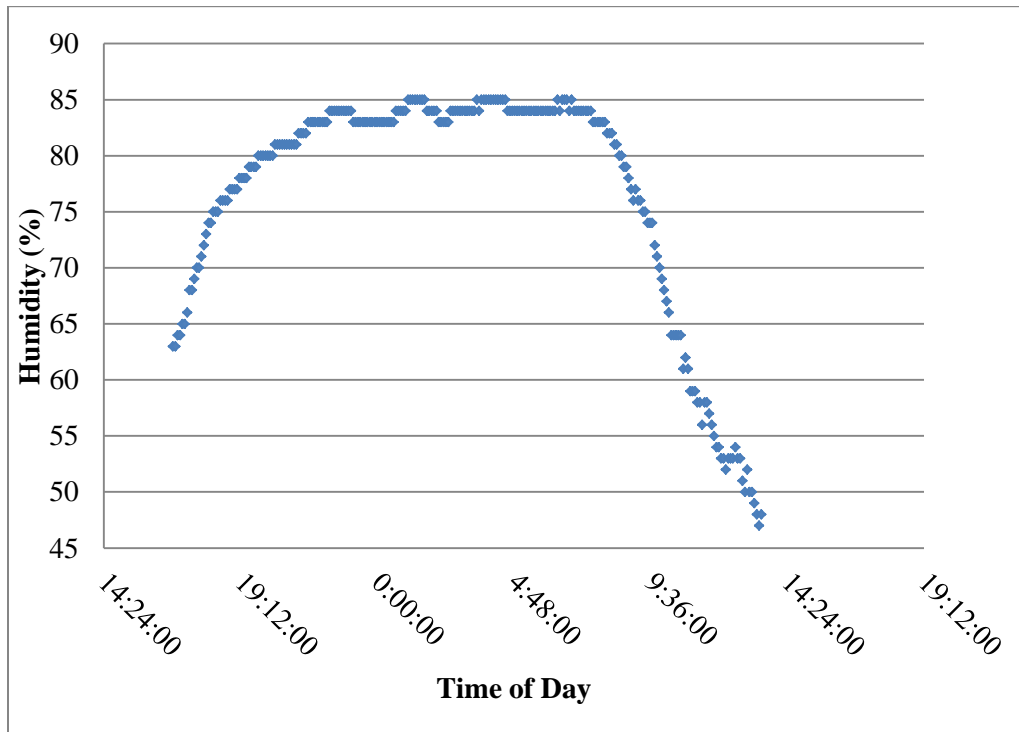


Figure 4 Relative humidity versus time of day.

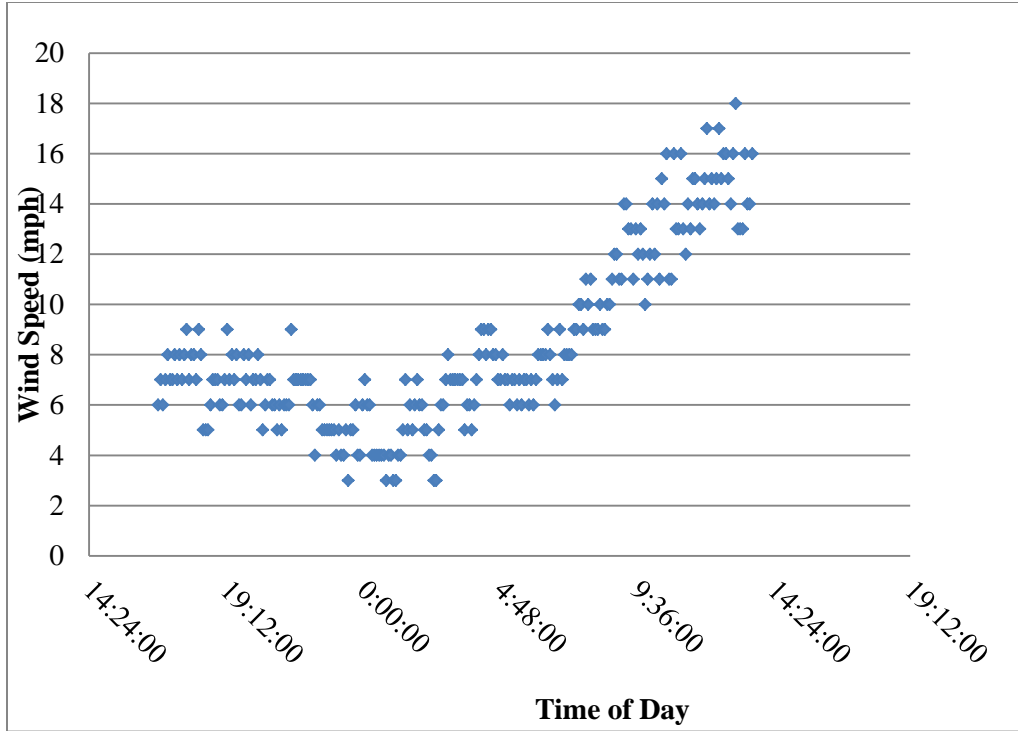


Figure 5 Wind speed versus time of day.



Figure 6 KDOT crew collecting samples.



Figure 7 Construction crew placing concrete pouring and vibrating.



Figure 8 Preparing concrete cylinder samples.



Figure 9 CP Tech Center PCC mobile lab.



Figure 10 Concrete being placed and vibrated.

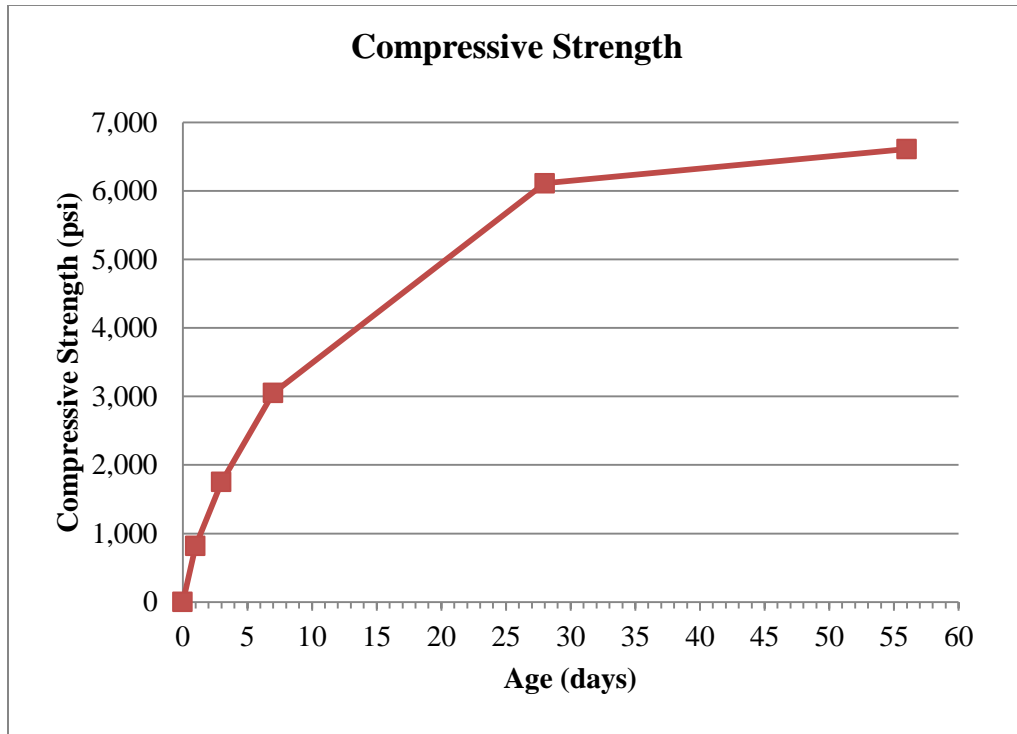


Figure 11 Compressive strength development with time.

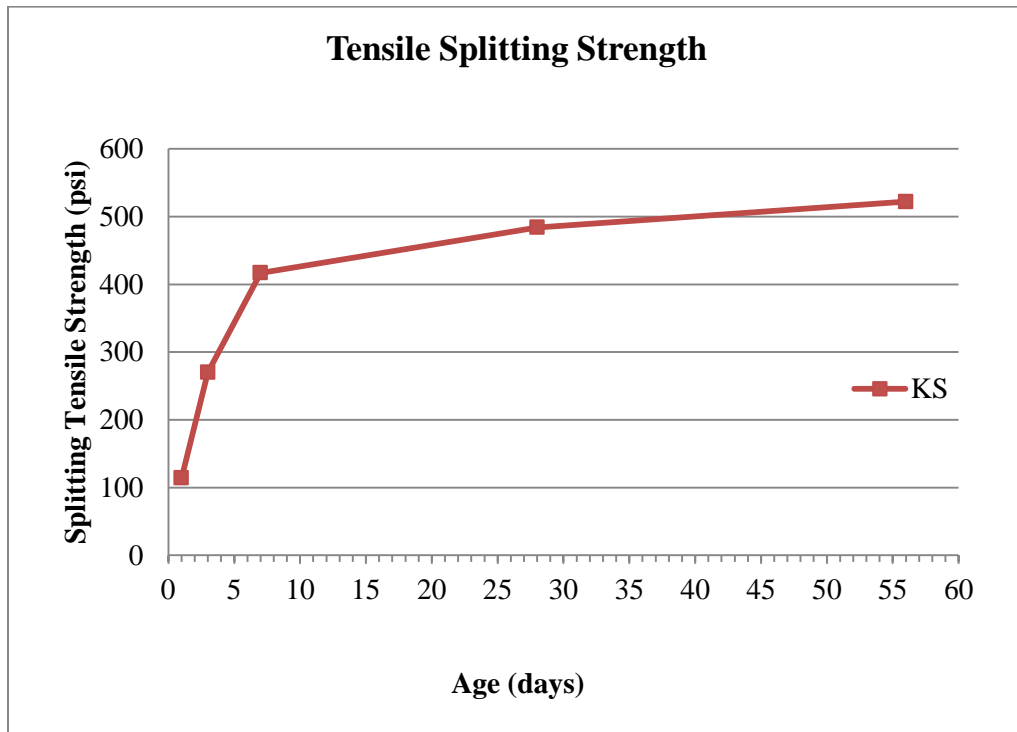


Figure 12 Tensile splitting strength development with time.

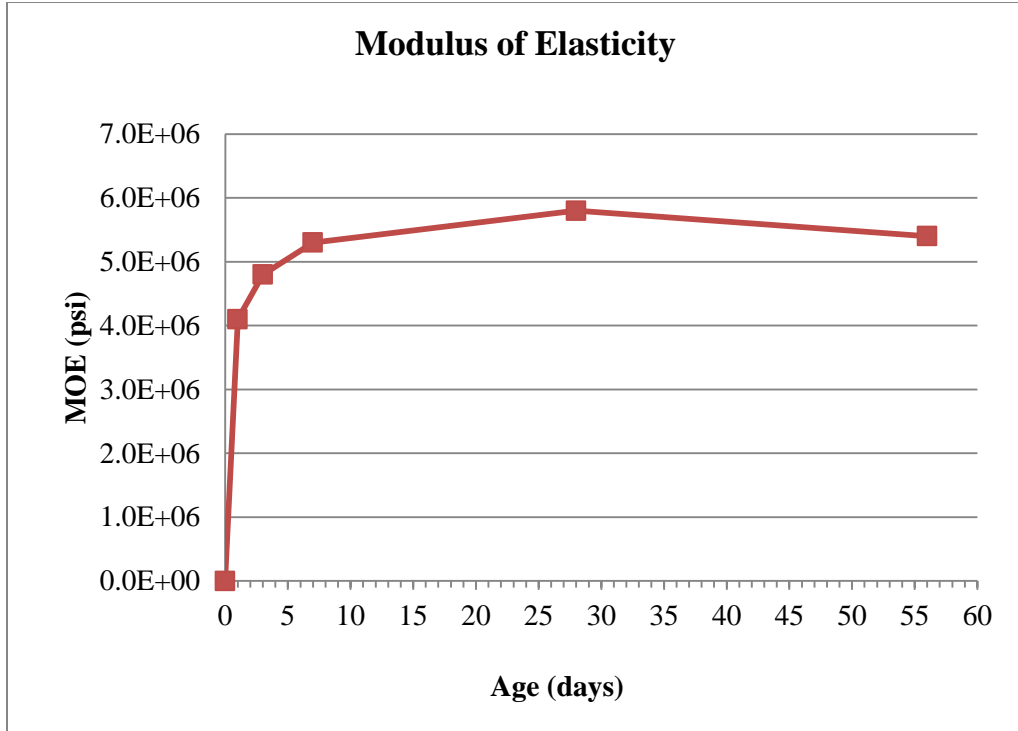


Figure 13 Modulus of elasticity development with time.

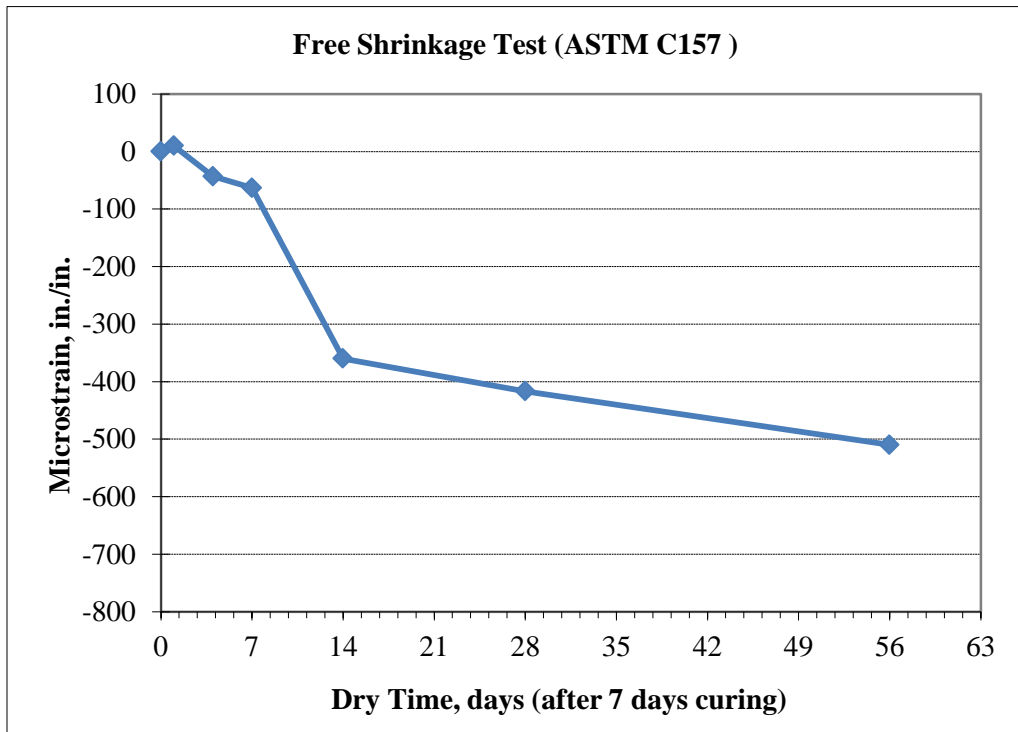


Figure 14 Free shrinkage test results (ASTM C 157).

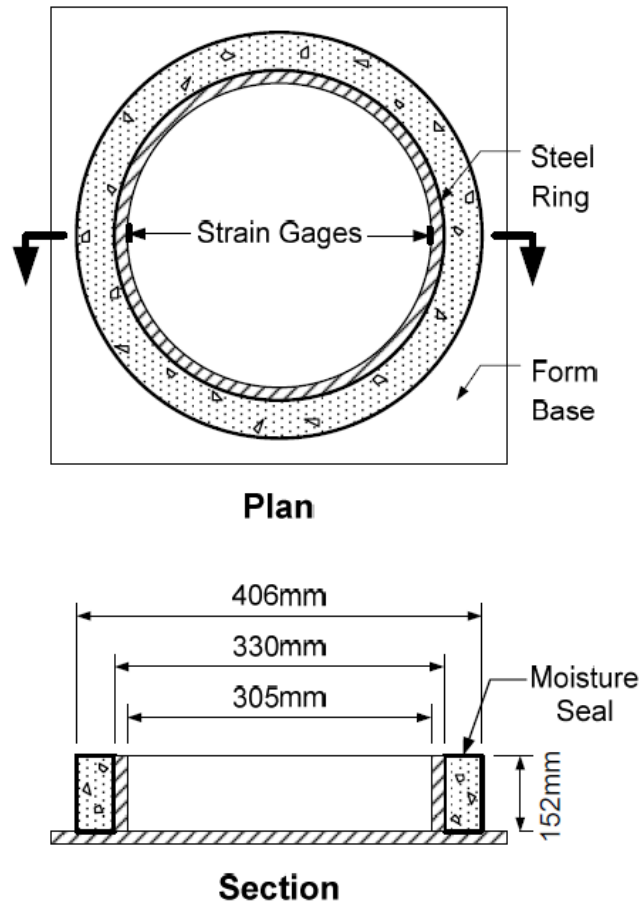


Figure 15 Configuration of restrained concrete ring samples.

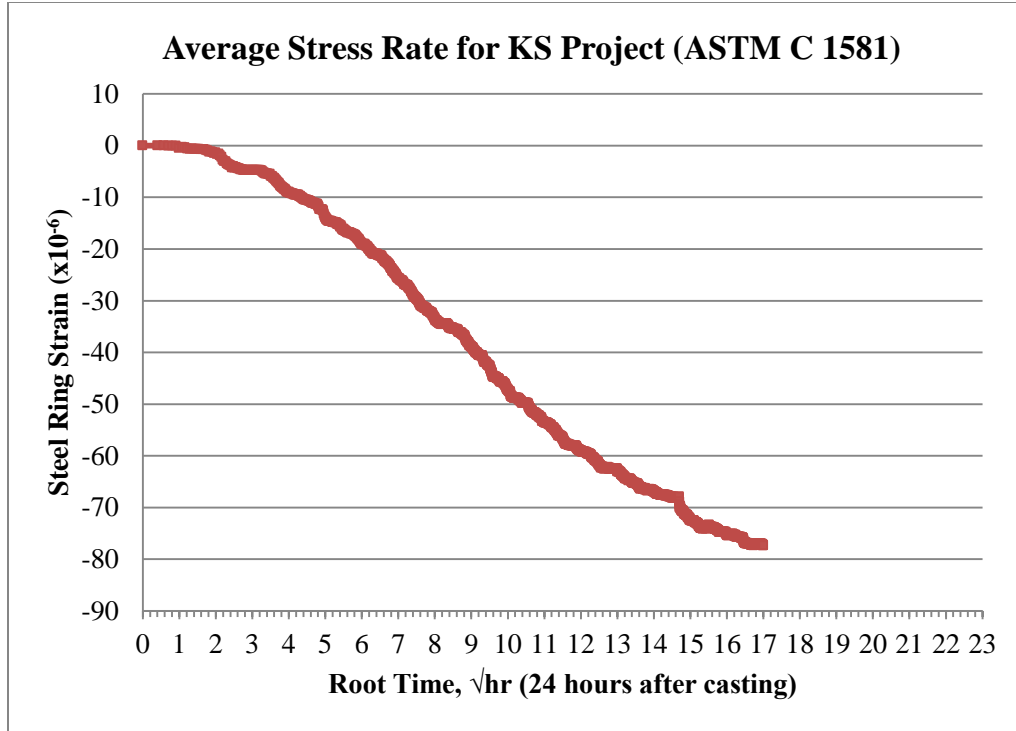


Figure 16 Stain of steel rings resulting from concrete shrinkage.

Table 1 Ambient conditions of US-59 bridge deck project

Kansas - Ternary Mixtures
US-59 Bridge Deck

Sample Information & Identification			Environmental Conditions			
Sample Date	Sample Time	Sample Comments	Relative Humidity (%)	Ambient Temp. (°F)	Wind Speed (mph)	Conc. Temp. (probe) (°F)
28-Oct-09	8:03 AM	kdot sample taken at pump discharge	65.0	48.0	2.4	55.0
28-Oct-09	8:20 AM	cp tech center sample taken at truck discharge	81.0	48.0	8.0	60.0
28-Oct-09	8:25 AM	kdot sample taken at pump discharge	84.0	49.0	4.5	62.0
28-Oct-09	9:20 AM	kdot sample taken at pump discharge	79.0	51.0	4.5	61.0
28-Oct-09	8:40 AM	kdot sample taken at pump discharge	81.0	53.0	11.2	62.0
28-Oct-09	10:10 AM	kdot sample taken at pump discharge	70.0	57.0	6.0	65.0
28-Oct-09	10:50 AM	cp tech center sample taken at truck discharge	60.0	57.0	5.0	62.6
28-Oct-09	11:04 AM	kdot sample taken at pump discharge	65.0	58.0	5.5	65.0
28-Oct-09	11:28 AM	kdot sample taken at pump discharge	62.0	62.0	3.5	66.0

Table 2 Air void structure results

Sample ID	Air Content (%)	Specific Surface (mm⁻¹)	Spacing Factor (mm)
A-1-122-S1	8.92	18.78	0.161
A-1-122-S2	9.59	16.63	0.169
A-1-122-S3	8.59	16.96	0.185
A-2-122-S1	13.19	15.56	0.132
A-2-122-S2	10.99	14.15	0.174
A-2-122-S3	11.77	16.35	0.140
A-2-122-S4	12.3	14.40	0.153
B-1-133-S1	3.62	21.50	0.259
B-1-133-S2	5.10	14.46	0.329
B-1-133-S3	3.88	16.33	0.330
B-1-133-S4	3.43	17.17	0.332
B-2-129-S1	3.97	17.60	0.303
B-2-129-S2	4.02	19.40	0.273
B-2-129-S3	4.40	17.43	0.292

Table 3 Properties of hardened concrete

	7-day	28-day	56-day		Rapid Chloride Permeability, (coulombs)	Porosity, (%)	Strength Development
	Compressive Strength, (psi)	Compressive Strength, (psi)	Compressive Strength, (psi)	Compressive Strength, (psi)			
A-1-122-S1							
A-1-122-S2	2100	5010	6020	532	8.3	2.39	
A-1-122-S3							
A-2-122-S1							
A-2-122-S2	2170	4950	5790	471	7.9	2.28	
A-2-122-S3							
A-2-122-S4							
B-1-133-S1							
B-1-133-S2	3300	5880	6470	468	4.5	1.78	
B-1-133-S3							
B-1-133-S4							
B-2-129-S1							
B-2-129-S2	3150	5400	6640	449	3.7	1.71	
B-2-129-S3							

Table 4 Summation of strength and modulus of elasticity

Location	Age, days	Compressive Strength, psi	Splitting Tensile Strength, psi	Modulus of Elasticity, psi
KS	1	820	114	4.1E+06
	3	1,750	270	4.8E+06
	7	3,050	417	5.3E+06
	28	6,110	484	5.8E+06
	56	6,610	522	5.4E+06

Table 5 Free shrinkage test results

Free Shrinkage (ASTM C 157)					
Dry Time	Beam 1 change%	Beam 2 change %	Beam 3 change %	Average	Microstrain
1	-0.001	0.004	0.000	0.001	10.0
4	-0.008	-0.003	-0.002	-0.004	-43.3
7	0.000	-0.009	-0.01	-0.006	-63.3
14	-0.031	-0.038	-0.039	-0.036	-360.0
28	-0.039	-0.044	-0.042	-0.042	-416.7
56	-0.050	-0.056	-0.047	-0.051	-510.0

Table 6 Cracking potential and average stress rate (ASTM C 1581)

Cracking Potential for KS Project (ASTM C 1581)			
	Ring 1	Ring 2	Ring 3
Strain Rate Factor (in./in.x10 ⁻⁶)/hours ^{1/2}	-5.09	-5.70	-5.21
G (psi)	10.47x10 ⁶	10.47x10 ⁶	10.47x10 ⁶
Absolute Value of α_{avg} (in./in.10 ⁻⁶)/day ^{1/2}	26.13		
Elapsed Time, tr (hours)	424.0	302.9	302.9
Elapsed Time, tr (days)	17.7	12.6	12.6
Stress Rate, q (psi/day) $q=GI\alpha_{avg}I/2\sqrt{t_r}$	32.5	38.5	38.5
Average Stress Rate, q (psi/day) $q=GI\alpha_{avg}I/2\sqrt{t_r}$	36.52		
Potential for cracking classification (ASTM 1581)	Moderate-high (25 ≤ q < 50)		

POOLED FUND STUDY

UNITED STATES DEPARTMENT OF TRANSPORTATION

FEDERAL HIGHWAY ADMINISTRATION



DEVELOPMENT OF PERFORMANCE PROPERTIES OF TERNARY MIXTURES

**A Field Application of Ternary Mixtures
-An experience in construction of a bridge
deck project in Battle Creek, MI**

December 2009

U OF UTAH IOWA STATE UNIVERSITY


THE UNIVERSITY OF UTAH

National Concrete Pavement
Technology Center 
Tech Center

Introduction

This document is a report of the activities and observations of a research team that performed on-site testing of a ternary mixture placed on I-94 Riverside Drive bridge deck in Battle Creek, Michigan. The cementitious system comprised a Type I cement, Grade 120 slag cement, and silica fume. The purpose of this research project is a comprehensive study of how supplementary cementitious materials (SCMs) can be used to improve the performance of concrete mixtures when used in ternary blends. This is the third phase of a project which intends to provide consulting to states and contractors on the use and field management of ternary mixtures. Due to severe weather condition, a state-of-the-art 44-foot long PCC mobile laboratory equipped for on-site cement and concrete testing was not provided by the CP Tech Center to collect data and field observations. However, samples were delivered by Michigan Department of Transportation and tested under laboratory condition.

Project Information

- Project: Tercem
- I-94, Riverside Drive, Battle Creek, Michigan
- Contractor: Anlaan Contracting.
- Bridge deck placement (Figure 1)

Site Location

An area at the bridge site was prepared by the contractor for the PCC mobile lab. The location of the project is shown as following Figure 2.

Sampling and Testing Activities

Concrete placement, sampling and testing took place on December 18, 2009. Hardened samples were transported to Iowa State University on December 30, 2010, for further testing. The following tests were conducted either in the field or in the laboratory:

- Slump, unit weight, temperature of fresh concrete – 1 test (ASTM C 143, ASTM C 138, ASTM C 231)

- Compressive strength, splitting tensile strength, static modulus of elasticity - 4" x 8" cylinders at 1-day, 3-days, 7-days, 28-days, and 56-days (ASTM C 39, ASTM C 496, ASTM C 469)
- Rapid chloride permeability - 4" x 8" cylinders at 56 days (ASTM C 1202)
- Air void analysis of hardened concrete - 4" x 8" cylinders (ASTM C 457)
- Free shrinkage test – 4 beams (ASTM C 157)
- Restrained rings – 4 samples (ASTM C 1581)

Observations of the Research Team

The following observations were made in this field testing:

- Two types of coarse aggregate were use: one type was 6AA high calcium limestone with 1.73% absorption and the other was 29A granite with 2.33% absorption. One type of fine aggregate 2NS natural sand with 1.2% absorption was used in the concrete. Micro-Air Type AR air entraining agent, Delvo retarding agent (ASTM Type D), and Rheobuild 1000 (Type MR) water reducer were used as chemical admixtures in order to achieve a better performance.
- According to the workability factor & coarseness factor graph (Page 14) combined aggregate gradation for this project fell in the well-graded region. Similarly, the aggregate gradation (Page 15) indicated a well graded system.
- Eight temperature sensors were used to track the concrete and ambient temperatures. Table 1 lists the name of sensors and description of location for each sensor. The specific locations of eight sensors are list from Figure 3 to Figure 6. The temperature sensor data reported by MI DOT are shown in Figure 7.
- The fresh concrete tests include slump cone, unit weight, and temperature measurement. MI DOT crew conducted the tests on site: the slump was 4 inches; unit weight was 147.2 lb/ft³; concrete placement temperature was 81 °F; and the ambient temperature is 33 °F.
- Figures 8 to 11 illustrate several activities during the testing process.
- The air void test (Rapid Air Test) results for 9 samples, which were tested by MI DOT, are given in Table 2.

- The air void test (Rapid Air Test) results for 10 samples, which were tested by the CPO Tech Center are given in Table 3. The average results for each cylinder are less than the expected values. Two of cylinders have lower specific surface results than desired.
- The strength development as 28/7 day compressive strength ratios is reported in Table 4.
- The rapid chloride permeability test measures the electrical conductance of a concrete sample as its resistance to chloride ion penetration. The test results shown in Table 4 indicate a classification of “very low” chloride permeability according to ASTM C1202.
- Compressive strength, splitting tensile strength and modulus of elasticity results (ASTM C 39, ASTM C 496, and ASTM C 469) are tabulated in Table 5 and also plotted in Figures 12 to 14.
- Free shrinkage test (ASTM C 157) was conducted in the laboratory. Three concrete beams were wet cured for seven days and then moved to a dry room at 23°C and 50% relative humidity. The drying shrinkage results are given in Table 6 and also plotted in Figure 15.
- Restrained shrinkage test was conducted based on ASTM C 1581. Four rings were cast. The rings were demolded and the top surface was covered with paraffin wax 24 hours from casting. The rings were allowed to dry at 23°C and 50% relative humidity immediately after demolding. Strains in the steel rings were recorded every 10 minutes up to 28 days or until the concrete cracked. The configuration of restrained concrete rings is shown in Figure 16. The cracking potential is listed in Table 4 and shown graphically in Figure 17. The cracking potential is classified as “moderate high” based on the average stress rate.

Acknowledgements

The research team at the National Concrete Pavement Technology Center at Iowa State University sincerely thanks the Michigan Department of Transportation for their cooperation and Anlaan Company for supplying the equipment and materials.

Project Data

The following test data is provided for information only, comments and conclusions will be reported in the comprehensive Phase III report of the pooled fund project *Development of Performance Properties of Ternary Mixtures*.

Mix Design & Misc. Info.

General Information

Project:	MI - Ternary Mixtures
Contractor:	
Mix Description:	600 lb Cementitious
Mix ID:	1PL5046A
Date(s) of Placement:	10/28/2009

Cementitious Materials	Source	Type	Spec. Gravity	lb/yd ³	% Replacement by Mass
Portland Cement:	Buzzi Unicem	I	3.150	426	
GGBFS:			2.870	150	25.00%
Fly Ash:					
Silica Fume:			2.250	24	4.00%
Other Pozzolan:					
				600	lb/yd³
				6.4	sacks/yd³

Aggregate Information	Source	Type	Spec. Gravity SSD	Absorption (%)	% Passing #4
Coarse Aggregate:	6AA	High calcium limestone	2.700	1.73%	3.0%
Intermediate Aggregate #1:	29A	Granite	2.600	2.33%	5.0%
Intermediate Aggregate #2:					
Fine Aggregate #1:	2NS	Natural Sand	2.610	1.20%	99.0%
Coarse Aggregate %:	48.3%				
Intermediate Aggregate #1%:	10.1%				
Intermediate Aggregate #2%:					
Fine Aggregate #1 %:	41.6%				

Mix Proportion Calculations

Water/Cementitious Materials Ratio:	0.380
Air Content:	6.50%

	Volume (ft ³)	Batch Weights SSD (lb/yd ³)	Spec. Gravity	Absolute Volume (%)
Portland Cement:	2.167	426	3.150	8.030%
GGBFS:	0.838	150	2.870	3.103%
Fly Ash:				
Silica Fume:	0.171	24	2.250	0.633%
Other Pozzolan:				
Coarse Aggregate:	8.895	1,435	2.700	32.954%
Intermediate Aggregate #1:	1.854	299	2.600	6.871%
Intermediate Aggregate #2:				
Fine Aggregate #1:	7.657	1,234	2.610	28.369%
Water:	3.654	228	1.000	13.537%
Air:	1.755			6.502%
	26.991	3,796		100.000%
	Unit Weight (lb/ft³)	140.6	Paste	31.806%
			Mortar	61.224%

Admixture Information

Source/Description	oz/yd ³	oz/cw t	
Air Entraining Admix.:	Micro-Air (type AR)	11.40	1.90
Admix. #1:	Delvo (Type D)	18.00	3.00
Admix. #2:	Rheobuild 1000 (Type MR)	54.00	9.00
Admix. #3:			

AVA Information

	Absolute Volume (%)
Air Free Paste:	25.304%
Air Free Mortar:	54.721%

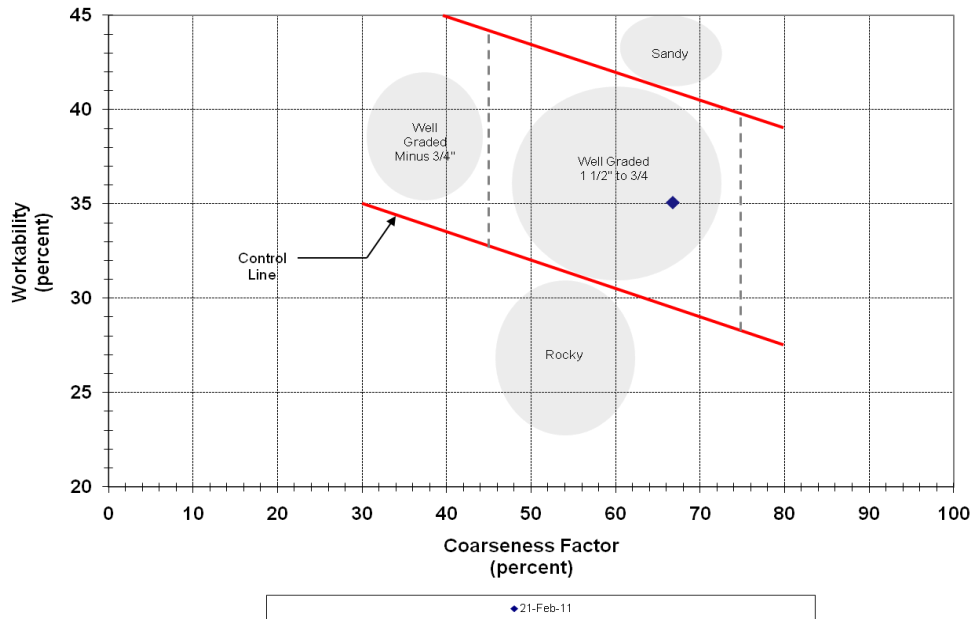
Project: **MIDOT Ternary Mixtures**
 Mix ID: **Bridge Deck**
 Sample Comments: **MIDOT Data**
 Test Date: **21-Feb-11**

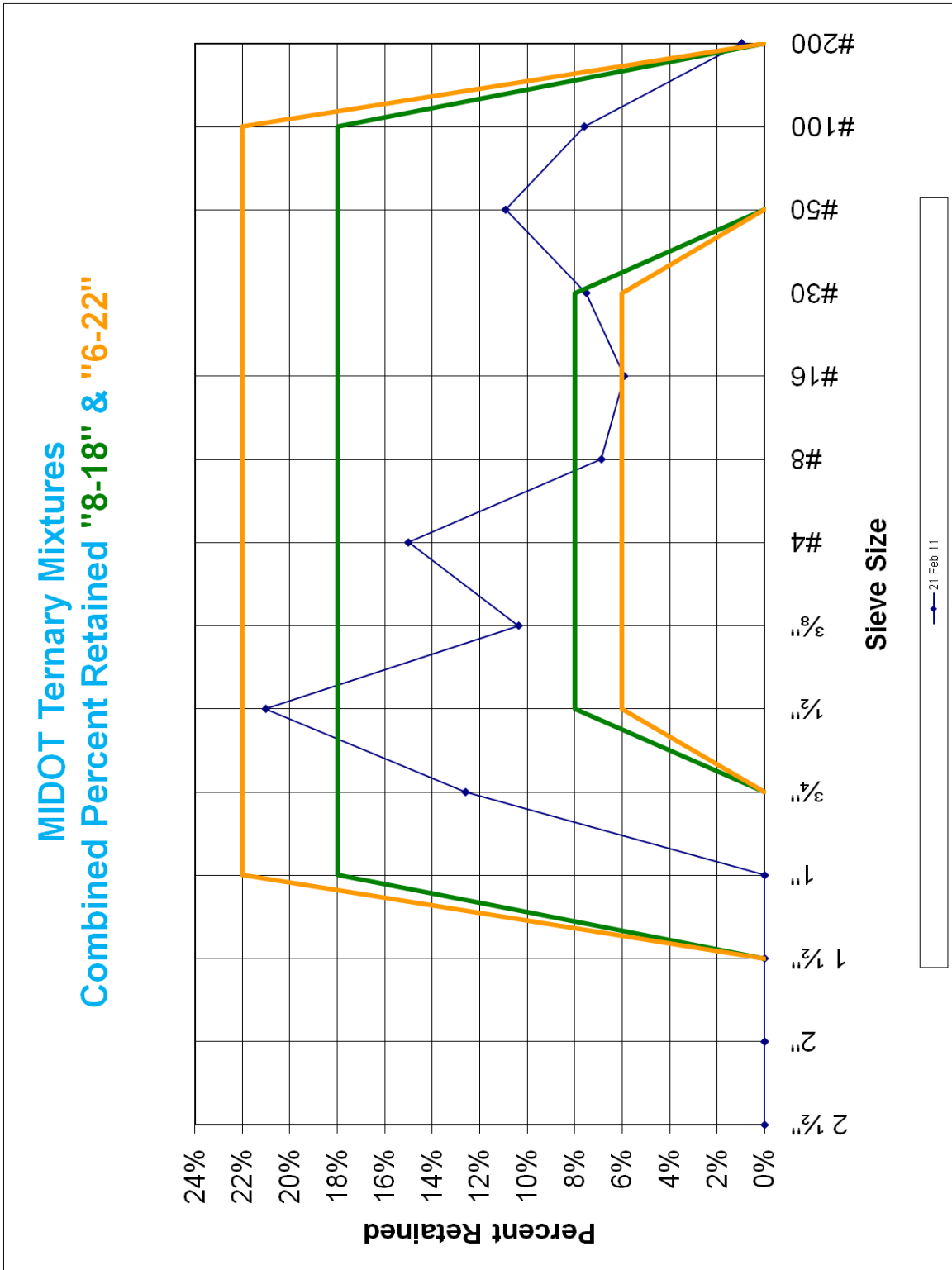
Total Cementitious Material: **600 lb/yd³**
 Agg. Ratios: **48.35%** **10.07%** **41.58%** **100.00%**

Sieve	Coarse	Intermediate	Fine #1	Fine #2	Combined % Retained	Combined % Retained On Each Sieve	Combined % Passing
2 1/2"	100%	100%	100%		0%	0%	100%
2"	100%	100%	100%		0%	0%	100%
1 1/2"	100%	100%	100%		0%	0%	100%
1"	100%	100%	100%		0%	0%	100%
3/4"	74%	100%	100%		13%	13%	87%
1/2"	30%	100%	100%		34%	21%	66%
3/8"	10%	96%	100%		44%	10%	56%
#4	0%	6%	97%		59%	15%	41%
#8	0%	1%	82%		66%	7%	34%
#16	0%	1%	67%		72%	6%	28%
#30	0%	1%	49%		79%	8%	21%
#50	0%	1%	23%		90%	11%	10%
#100	0%	1%	5%		98%	8%	2%
#200	0.0%	0.7%	2.7%		98.8%	1.0%	1.2%

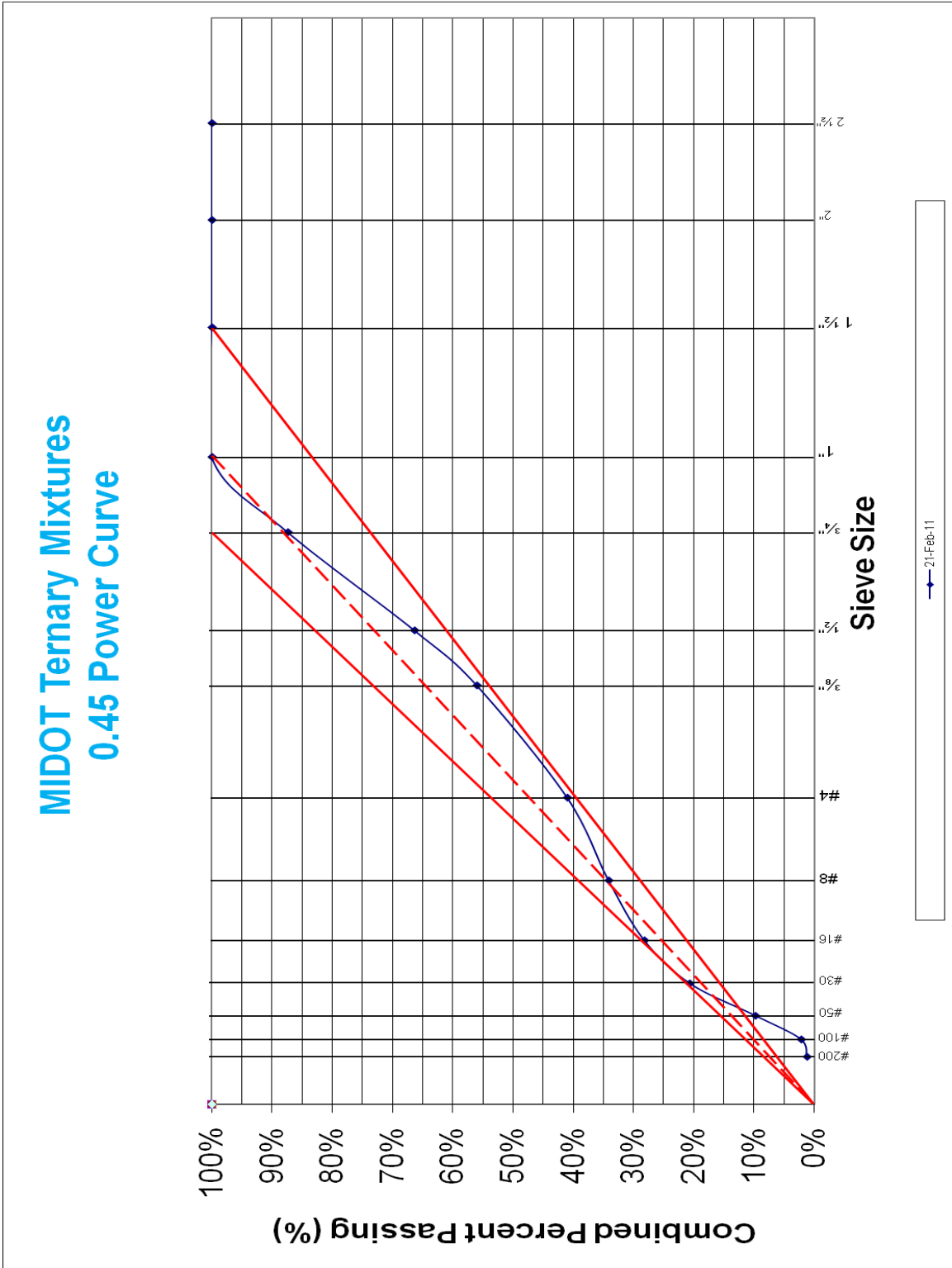
Workability Factor: 35.1
Coarseness Factor: 66.8

MIDOT Ternary Mixtures Workability Factor & Coarseness Factor





MIDOT Ternary Mixtures 0.45 Power Curve





ASTM C 1202-97



Test-compagny
Testing street 45
CompagnyCity
Some Country

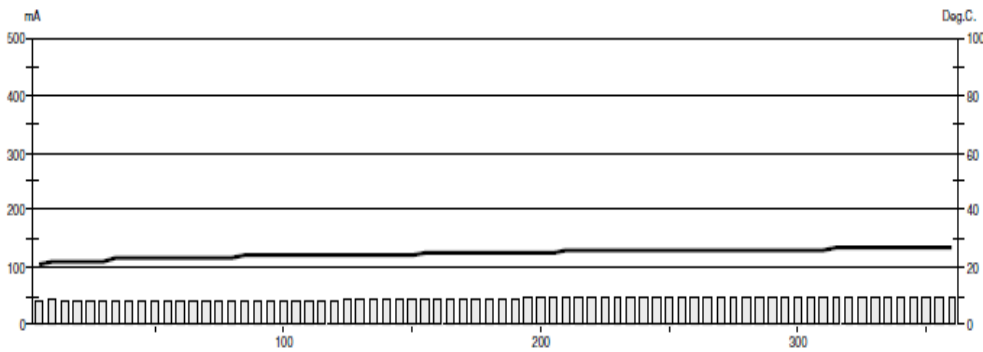
Your own logo,
size=20x80mm



GERMANN INSTRUMENTS
DENMARK
Phone: +45 3907 7117
Fax: +45 3907 3107
USA
Phone: (847)329-9999
Fax: (847)329-8888

Test report

Voltage Used: 60
Testing time: 06:00 hour
Charge passed: 977
Adjusted Charge passed: 848
Permeability class: Very Low
Instrument number: 023907
Channel number: 1
Report date: 2/11/2010
Testing by: PJM
Reference: MI ternary
Sample diameter: 102
Comment: ---



Time	°C	mA	Time	°C	mA	Time	°C	mA	Time	°C	mA
00:05	21	43.3	01:35	24	42.5	03:05	25	45.5	04:35	26	47.9
00:10	22	43.6	01:40	24	42.7	03:10	25	45.7	04:40	26	48.0
00:15	22	42.7	01:45	24	42.9	03:15	25	45.9	04:45	26	47.9
00:20	22	42.1	01:50	24	43.0	03:20	25	45.9	04:50	26	48.1
00:25	22	41.5	01:55	24	43.2	03:25	25	46.1	04:55	26	48.1
00:30	22	41.1	02:00	24	43.4	03:30	26	46.2	05:00	26	48.2
00:35	23	40.8	02:05	24	43.6	03:35	26	46.3	05:05	26	48.4
00:40	23	40.7	02:10	24	43.8	03:40	26	46.4	05:10	26	48.5
00:45	23	40.8	02:15	24	43.9	03:45	26	46.7	05:15	27	48.5
00:50	23	40.8	02:20	24	44.1	03:50	26	46.8	05:20	27	48.6
00:55	23	41.0	02:25	24	44.3	03:55	26	47.0	05:25	27	48.7
01:00	23	41.1	02:30	24	44.5	04:00	26	47.2	05:30	27	48.7
01:05	23	41.3	02:35	25	44.7	04:05	26	47.3	05:35	27	48.7
01:10	23	41.5	02:40	25	44.8	04:10	26	47.4	05:40	27	48.9
01:15	23	41.8	02:45	25	45.0	04:15	26	47.5	05:45	27	48.9
01:20	23	41.9	02:50	25	45.1	04:20	26	47.7	05:50	27	49.0
01:25	24	42.1	02:55	25	45.3	04:25	26	47.8	05:55	27	49.0
01:30	24	42.3	03:00	25	45.4	04:30	26	47.8	06:00	27	49.1



ASTM C 1202-97



Test-compagny
Testing street 45
CompagnyCity
Some Country

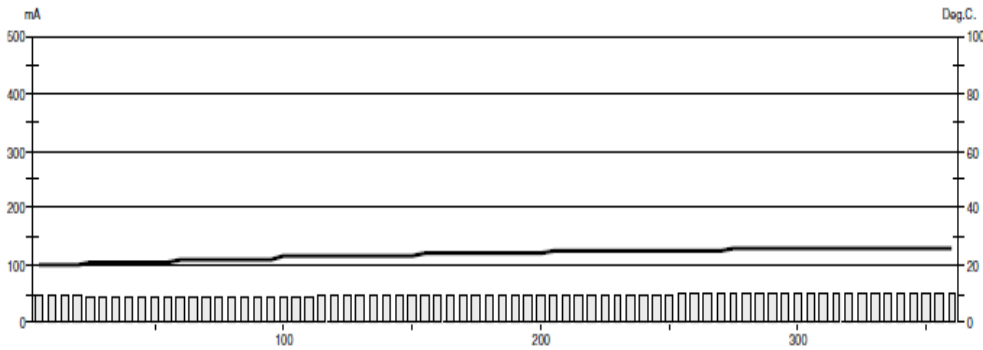
Your own logo,
size=20x80mm



GERMANN INSTRUMENTS
DENMARK
Phone: +45 39677117
Fax: +45 3967 3167
USA
Phone: (947)329-9999
Fax: (947)329-9888

Test report

Voltage Used: 60
Testing time: 06:00 hour
Charge passed: 1040
Adjusted Charge passed: 902
Permeability class: Very Low
Instrument number: 023907
Channel number: 2
Report date: 2/11/2010
Testing by: PJM
Reference: MI ternary 2
Sample diameter: 102
Comment: ---



Time	°C	mA	Time	°C	mA	Time	°C	mA	Time	°C	mA
00:05	20	49.2	01:35	22	45.1	03:05	24	48.2	04:35	26	50.7
00:10	20	47.8	01:40	23	45.3	03:10	24	48.4	04:40	26	50.7
00:15	20	46.7	01:45	23	45.4	03:15	24	48.6	04:45	26	50.8
00:20	20	46.1	01:50	23	45.6	03:20	24	48.8	04:50	26	50.9
00:25	21	45.7	01:55	23	45.8	03:25	25	49.0	04:55	26	51.0
00:30	21	45.4	02:00	23	46.0	03:30	25	49.2	05:00	26	51.1
00:35	21	45.1	02:05	23	46.1	03:35	25	49.3	05:05	26	51.2
00:40	21	44.8	02:10	23	46.3	03:40	25	49.4	05:10	26	51.2
00:45	21	44.5	02:15	23	46.4	03:45	25	49.5	05:15	26	51.4
00:50	21	44.2	02:20	23	46.6	03:50	25	49.6	05:20	26	51.5
00:55	21	44.0	02:25	23	46.7	03:55	25	49.7	05:25	26	51.5
01:00	22	43.9	02:30	23	46.9	04:00	25	49.9	05:30	26	51.7
01:05	22	44.1	02:35	24	47.1	04:05	25	50.0	05:35	26	51.7
01:10	22	44.3	02:40	24	47.3	04:10	25	50.2	05:40	26	51.8
01:15	22	44.4	02:45	24	47.5	04:15	25	50.3	05:45	26	51.7
01:20	22	44.5	02:50	24	47.6	04:20	25	50.4	05:50	26	51.8
01:25	22	44.7	02:55	24	47.8	04:25	25	50.4	05:55	26	51.9
01:30	22	44.9	03:00	24	48.0	04:30	25	50.5	06:00	26	51.8



ASTM C 1202-97



Test-compagny
Testing street 45
CompagnyCity
Some Country

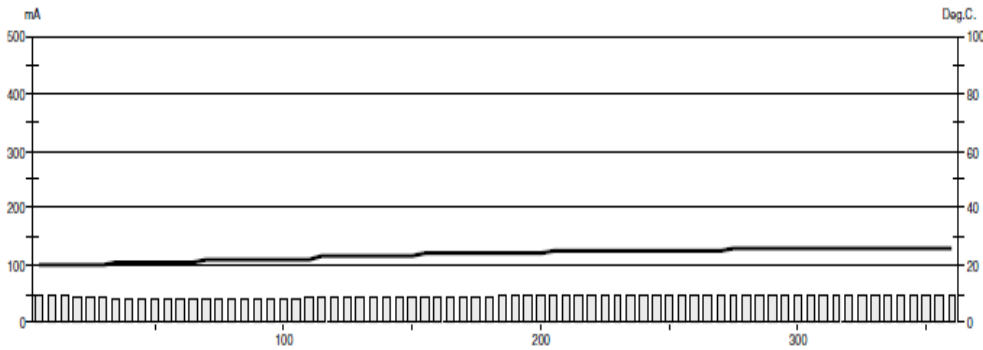
Your own logo,
size=20x80mm



GERMANN INSTRUMENTS
DENMARK
Phone: +45 39677117
Fax: +45 3967 3167
USA
Phone: (947)329-9999
Fax: (947)329-9888

Test report

Voltage Used: 60
Testing time: 06:00 hour
Charge passed: 987
Adjusted Charge passed: 856
Permeability class: Very Low
Instrument number: 023907
Channel number: 3
Report date: 2/11/2010
Testing by: PJM
Reference: MI Ternary 3
Sample diameter: 102
Comment: ---



Time	°C	mA	Time	°C	mA	Time	°C	mA	Time	°C	mA
00:05	20	50.0	01:35	22	42.9	03:05	24	45.9	04:35	26	47.6
00:10	20	48.0	01:40	22	43.0	03:10	24	46.0	04:40	26	47.6
00:15	20	46.6	01:45	22	43.1	03:15	24	46.0	04:45	26	47.7
00:20	20	45.5	01:50	22	43.7	03:20	24	46.0	04:50	26	47.8
00:25	20	44.6	01:55	23	43.8	03:25	25	46.1	04:55	26	47.9
00:30	20	43.8	02:00	23	43.7	03:30	25	46.2	05:00	26	47.9
00:35	21	43.0	02:05	23	43.8	03:35	25	46.4	05:05	26	48.0
00:40	21	42.4	02:10	23	43.8	03:40	25	46.5	05:10	26	48.2
00:45	21	42.0	02:15	23	43.9	03:45	25	46.8	05:15	26	48.1
00:50	21	42.0	02:20	23	44.1	03:50	25	46.7	05:20	26	48.1
00:55	21	42.1	02:25	23	44.3	03:55	25	46.8	05:25	26	48.3
01:00	21	42.1	02:30	23	44.5	04:00	25	46.9	05:30	26	48.3
01:05	21	42.1	02:35	24	44.6	04:05	25	47.2	05:35	26	48.3
01:10	22	42.2	02:40	24	44.8	04:10	25	47.5	05:40	26	48.5
01:15	22	42.3	02:45	24	45.1	04:15	25	47.4	05:45	26	48.5
01:20	22	42.5	02:50	24	45.1	04:20	25	47.3	05:50	26	48.5
01:25	22	42.8	02:55	24	45.2	04:25	25	47.4	05:55	26	48.5
01:30	22	42.8	03:00	24	45.4	04:30	25	47.7	06:00	26	48.5

Sample ID: Cast cyl Cylinder 1-3

Sample Size (mm x mm): 85 x 90 Length Traversed (mm): 2413.1

Paste Content (%): 30.20 Area Traversed (mm x mm): 75 x 80

Chord Length Distribution - Table

Class No.	Chord size (microns)	Number of Chords in Class	Number of Chords in Percent	Air Content in Class	Cumulated Air Content	Chord length frequency	Air content, fraction	
1	0-10	6	2.36	0.000	0.000	0.02	0.000	0.00-0.01
2	10-20	24	9.45	0.020	0.020	0.09	0.020	0.01-0.02
3	20-30	26	9.45	0.030	0.040	0.10	0.030	0.02-0.03
4	30-40	15	5.91	0.020	0.070	0.06	0.020	0.03-0.04
5	40-50	17	6.69	0.030	0.100	0.07	0.030	0.04-0.05
6	50-60	19	7.48	0.040	0.140	0.07	0.040	0.05-0.06
7	60-80	22	8.66	0.060	0.200	0.09	0.060	0.06-0.08
8	80-100	15	5.91	0.060	0.260	0.06	0.060	0.08-0.10
9	100-120	8	3.15	0.040	0.290	0.03	0.040	0.10-0.12
10	120-140	7	2.76	0.040	0.330	0.03	0.040	0.12-0.14
11	140-160	13	5.12	0.080	0.410	0.05	0.080	0.14-0.16
12	160-180	9	3.54	0.060	0.470	0.04	0.060	0.16-0.18
13	180-200	4	1.57	0.030	0.510	0.02	0.030	0.18-0.20
14	200-220	8	3.15	0.070	0.580	0.03	0.070	0.20-0.22
15	220-240	5	1.97	0.050	0.620	0.02	0.050	0.22-0.24
16	240-260	1	0.39	0.010	0.630	0.00	0.010	0.24-0.26
17	260-280	3	1.18	0.030	0.670	0.01	0.030	0.26-0.28
18	280-300	1	0.39	0.010	0.680	0.00	0.010	0.28-0.30
19	300-350	3	1.18	0.040	0.720	0.01	0.040	0.30-0.35
20	350-400	3	1.18	0.050	0.770	0.01	0.050	0.35-0.40
21	400-450	4	1.57	0.070	0.840	0.02	0.070	0.40-0.45
22	450-500	3	1.18	0.060	0.900	0.01	0.060	0.45-0.50
23	500-1000	16	6.30	0.470	0.940	0.06	0.470	0.50-1.00
24	1000-1500	6	2.36	0.290	1.660	0.02	0.290	1.00-1.50
25	1500-2000	7	2.76	0.530	2.180	0.03	0.530	1.50-2.00
26	2000-2500	4	1.57	0.350	2.530	0.02	0.350	2.00-2.50
27	2500-3000	0	0.00	0.000	2.530	0.00	0.000	2.50-3.00
28	3000-4000	5	1.97	0.730	3.270	0.02	0.730	3.00-4.00
						254		
Air Content (%):		3.27						
Specific Surface (mm ⁻¹):		12.89						
Spacing Factor (mm):		0.475						
Void Frequency (mm ⁻¹):		0.110						
Average Chord Length (mm):		0.310						
Paste to Air Ratio:		9.24						

Sample ID: Cast cyl Cylinder 2-1

Sample Size (mm x mm): 80 x 90 Length Traversed (mm): 2413.1

Paste Content (%): 30.20 Area Traversed (mm x mm): 70 x 80

Chord Length Distribution - Table

Class No.	Chord size (microns)	Number of Chords in Class	Number of Chords in Percent	Air Content in Class	Cumulated Air Content	Chord length frequency	Air content, fraction	
1	0-10	1	0.44	0.000	0.000	0.00	0.000	0.00-0.01
2	10-20	30	13.16	0.020	0.020	0.13	0.020	0.01-0.02
3	20-30	20	13.16	0.020	0.040	0.09	0.020	0.02-0.03
4	30-40	13	5.70	0.020	0.060	0.06	0.020	0.03-0.04
5	40-50	12	5.26	0.020	0.080	0.05	0.020	0.04-0.05
6	50-60	14	6.14	0.030	0.110	0.06	0.030	0.05-0.06
7	60-80	15	6.58	0.040	0.160	0.07	0.040	0.06-0.08
8	80-100	14	6.14	0.050	0.210	0.06	0.050	0.08-0.10
9	100-120	16	7.02	0.070	0.280	0.07	0.070	0.10-0.12
10	120-140	6	2.63	0.030	0.310	0.03	0.030	0.12-0.14
11	140-160	7	3.07	0.040	0.360	0.03	0.040	0.14-0.16
12	160-180	8	3.51	0.060	0.410	0.04	0.060	0.16-0.18
13	180-200	6	2.63	0.050	0.460	0.03	0.050	0.18-0.20
14	200-220	2	0.88	0.020	0.480	0.01	0.020	0.20-0.22
15	220-240	5	2.19	0.050	0.530	0.02	0.050	0.22-0.24
16	240-260	4	1.75	0.040	0.570	0.02	0.040	0.24-0.26
17	260-280	6	2.63	0.070	0.630	0.03	0.070	0.26-0.28
18	280-300	7	3.07	0.080	0.720	0.03	0.080	0.28-0.30
19	300-350	9	3.95	0.120	0.840	0.04	0.120	0.30-0.35
20	350-400	6	2.63	0.090	0.930	0.03	0.090	0.35-0.40
21	400-450	2	0.88	0.040	0.960	0.01	0.040	0.40-0.45
22	450-500	3	1.32	0.060	1.020	0.01	0.060	0.45-0.50
23	500-1000	16	7.02	0.440	1.130	0.07	0.440	0.50-1.00
24	1000-1500	1	0.44	0.040	1.500	0.00	0.040	1.00-1.50
25	1500-2000	2	0.88	0.160	1.660	0.01	0.160	1.50-2.00
26	2000-2500	3	1.32	0.260	1.920	0.01	0.260	2.00-2.50
27	2500-3000	0	0.00	0.000	1.920	0.00	0.000	2.50-3.00
28	3000-4000	0	0.00	0.000	1.920	0.00	0.000	3.00-4.00

228

Air Content (%): 1.92

Specific Surface (mm⁻¹): 19.66

Spacing Factor (mm): 0.394

Void Frequency (mm⁻¹): 0.090

Average Chord Length (mm): 0.203

Paste to Air Ratio: 15.73

Sample ID: Cast cyl Cylinder 2-2

Sample Size (mm x mm): 80 x 80 Length Traversed (mm): 2413.1

Paste Content (%): 30.20 Area Traversed (mm x mm): 70 x 80

Chord Length Distribution - Table

Class No.	Chord size (microns)	Number of Chords in Class	Number of Chords in Percent	Air Content in Class	Cumulated Air Content	Chord length frequency	Air content, fraction	
1	0-10	3	1.35	0.000	0.000	0.01	0.000	0.00-0.01
2	10-20	32	14.35	0.020	0.020	0.14	0.020	0.01-0.02
3	20-30	25	14.35	0.030	0.050	0.11	0.030	0.02-0.03
4	30-40	16	7.17	0.020	0.070	0.07	0.020	0.03-0.04
5	40-50	18	8.07	0.030	0.100	0.08	0.030	0.04-0.05
6	50-60	10	4.48	0.020	0.130	0.04	0.020	0.05-0.06
7	60-80	14	6.28	0.040	0.170	0.06	0.040	0.06-0.08
8	80-100	16	7.17	0.060	0.230	0.07	0.060	0.08-0.10
9	100-120	6	2.69	0.030	0.260	0.03	0.030	0.10-0.12
10	120-140	12	5.38	0.060	0.320	0.05	0.060	0.12-0.14
11	140-160	5	2.24	0.030	0.350	0.02	0.030	0.14-0.16
12	160-180	6	2.69	0.040	0.390	0.03	0.040	0.16-0.18
13	180-200	7	3.14	0.060	0.450	0.03	0.060	0.18-0.20
14	200-220	6	2.69	0.050	0.500	0.03	0.050	0.20-0.22
15	220-240	6	2.69	0.060	0.560	0.03	0.060	0.22-0.24
16	240-260	1	0.45	0.010	0.570	0.00	0.010	0.24-0.26
17	260-280	6	2.69	0.070	0.640	0.03	0.070	0.26-0.28
18	280-300	2	0.90	0.020	0.660	0.01	0.020	0.28-0.30
19	300-350	7	3.14	0.090	0.750	0.03	0.090	0.30-0.35
20	350-400	3	1.35	0.050	0.800	0.01	0.050	0.35-0.40
21	400-450	1	0.45	0.020	0.820	0.00	0.020	0.40-0.45
22	450-500	1	0.45	0.020	0.840	0.00	0.020	0.45-0.50
23	500-1000	10	4.48	0.250	0.940	0.04	0.250	0.50-1.00
24	1000-1500	4	1.79	0.220	1.300	0.02	0.220	1.00-1.50
25	1500-2000	2	0.90	0.130	1.440	0.01	0.130	1.50-2.00
26	2000-2500	1	0.45	0.100	1.540	0.00	0.100	2.00-2.50
27	2500-3000	1	0.45	0.110	1.650	0.00	0.110	2.50-3.00
28	3000-4000	2	0.90	0.290	1.940	0.01	0.290	3.00-4.00
						223		
Air Content (%):			1.94					
Specific Surface (mm ⁻¹):			19.09					
Spacing Factor (mm):			0.404					
Void Frequency (mm ⁻¹):			0.090					
Average Chord Length (mm):			0.209					
Paste to Air Ratio:			15.57					

Sample ID: Cast cyl Cylinder 2-3

Sample Size (mm x mm): 80 x 80 Length Traversed (mm): 2413.1

Paste Content (%): 30.20 Area Traversed (mm x mm): 70 x 70

Chord Length Distribution - Table

Class No.	Chord size (microns)	Number of Chords in Class	Number of Chords in Percent	Air Content in Class	Cumulated Air Content	Chord length frequency	Air content, fraction	
1	0-10	5	2.51	0.000	0.000	0.03	0.000	0.00-0.01
2	10-20	33	16.58	0.020	0.020	0.17	0.020	0.01-0.02
3	20-30	16	16.58	0.020	0.040	0.08	0.020	0.02-0.03
4	30-40	21	10.55	0.030	0.070	0.11	0.030	0.03-0.04
5	40-50	7	3.52	0.010	0.080	0.04	0.010	0.04-0.05
6	50-60	13	6.53	0.030	0.110	0.07	0.030	0.05-0.06
7	60-80	16	8.04	0.050	0.160	0.08	0.050	0.06-0.08
8	80-100	17	8.54	0.060	0.220	0.09	0.060	0.08-0.10
9	100-120	10	5.03	0.050	0.270	0.05	0.050	0.10-0.12
10	120-140	5	2.51	0.030	0.290	0.03	0.030	0.12-0.14
11	140-160	11	5.53	0.070	0.360	0.06	0.070	0.14-0.16
12	160-180	4	2.01	0.030	0.390	0.02	0.030	0.16-0.18
13	180-200	0	0.00	0.000	0.390	0.00	0.000	0.18-0.20
14	200-220	4	2.01	0.030	0.420	0.02	0.030	0.20-0.22
15	220-240	3	1.51	0.030	0.450	0.02	0.030	0.22-0.24
16	240-260	2	1.01	0.020	0.470	0.01	0.020	0.24-0.26
17	260-280	1	0.50	0.010	0.480	0.01	0.010	0.26-0.28
18	280-300	2	1.01	0.020	0.510	0.01	0.020	0.28-0.30
19	300-350	3	1.51	0.040	0.550	0.02	0.040	0.30-0.35
20	350-400	1	0.50	0.010	0.560	0.01	0.010	0.35-0.40
21	400-450	2	1.01	0.040	0.600	0.01	0.040	0.40-0.45
22	450-500	3	1.51	0.060	0.660	0.02	0.060	0.45-0.50
23	500-1000	17	8.54	0.460	0.720	0.09	0.460	0.50-1.00
24	1000-1500	3	1.51	0.150	1.260	0.02	0.150	1.00-1.50
25	1500-2000	0	0.00	0.000	1.260	0.00	0.000	1.50-2.00
26	2000-2500	0	0.00	0.000	1.260	0.00	0.000	2.00-2.50
27	2500-3000	0	0.00	0.000	1.260	0.00	0.000	2.50-3.00
28	3000-4000	0	0.00	0.000	1.260	0.00	0.000	3.00-4.00

199

Air Content (%): 1.26

Specific Surface (mm⁻¹): 26.13

Spacing Factor (mm): 0.355

Void Frequency (mm⁻¹): 0.080

Average Chord Length (mm): 0.153

Paste to Air Ratio: 23.97

Sample ID: Cast cyl Cylinder 2-4

Sample Size (mm x mm): 80 x 80 Length Traversed (mm): 2413.1

Paste Content (%): 30.20 Area Traversed (mm x mm): 70 x 70

Chord Length Distribution - Table

Class No.	Chord size (microns)	Number of Chords in Class	Number of Chords in Percent	Air Content in Class	Cumulated Air Content	Chord length frequency	Air content, fraction	
1	0-10	6	3.06	0.000	0.000	0.03	0.000	0.00-0.01
2	10-20	16	8.16	0.010	0.010	0.08	0.010	0.01-0.02
3	20-30	21	8.16	0.020	0.030	0.11	0.020	0.02-0.03
4	30-40	15	7.65	0.020	0.050	0.08	0.020	0.03-0.04
5	40-50	10	5.10	0.020	0.070	0.05	0.020	0.04-0.05
6	50-60	10	5.10	0.020	0.100	0.05	0.020	0.05-0.06
7	60-80	13	6.63	0.040	0.130	0.07	0.040	0.06-0.08
8	80-100	16	8.16	0.060	0.190	0.08	0.060	0.08-0.10
9	100-120	12	6.12	0.050	0.250	0.06	0.050	0.10-0.12
10	120-140	12	6.12	0.060	0.310	0.06	0.060	0.12-0.14
11	140-160	4	2.04	0.030	0.340	0.02	0.030	0.14-0.16
12	160-180	3	1.53	0.020	0.360	0.02	0.020	0.16-0.18
13	180-200	7	3.57	0.050	0.410	0.04	0.050	0.18-0.20
14	200-220	3	1.53	0.030	0.440	0.02	0.030	0.20-0.22
15	220-240	3	1.53	0.030	0.470	0.02	0.030	0.22-0.24
16	240-260	5	2.55	0.050	0.520	0.03	0.050	0.24-0.26
17	260-280	3	1.53	0.030	0.550	0.02	0.030	0.26-0.28
18	280-300	2	1.02	0.020	0.580	0.01	0.020	0.28-0.30
19	300-350	6	3.06	0.080	0.660	0.03	0.080	0.30-0.35
20	350-400	6	3.06	0.090	0.750	0.03	0.090	0.35-0.40
21	400-450	4	2.04	0.070	0.820	0.02	0.070	0.40-0.45
22	450-500	3	1.53	0.060	0.880	0.02	0.060	0.45-0.50
23	500-1000	11	5.61	0.320	0.900	0.06	0.320	0.50-1.00
24	1000-1500	5	2.55	0.250	1.440	0.03	0.250	1.00-1.50
25	1500-2000	0	0.00	0.000	1.440	0.00	0.000	1.50-2.00
26	2000-2500	0	0.00	0.000	1.440	0.00	0.000	2.00-2.50
27	2500-3000	0	0.00	0.000	1.440	0.00	0.000	2.50-3.00
28	3000-4000	0	0.00	0.000	1.440	0.00	0.000	3.00-4.00
						196		

Air Content (%): 1.44

Specific Surface (mm⁻¹): 22.56

Spacing Factor (mm): 0.388

Void Frequency (mm⁻¹): 0.080

Average Chord Length (mm): 0.177

Paste to Air Ratio: 20.97

Sample ID: Cast cyl Cylinder 3-2

Sample Size (mm x mm): 80 x 80 Length Traversed (mm): 2413.1

Paste Content (%): 30.20 Area Traversed (mm x mm): 70 x 70

Chord Length Distribution - Table

Class No.	Chord size (microns)	Number of Chords in Class	Number of Chords in Percent	Air Content in Class	Cumulated Air Content	Chord length frequency	Air content, fraction	
1	0-10	17	2.93	0.010	0.010	0.03	0.010	0.00-0.01
2	10-20	58	10.00	0.030	0.040	0.10	0.030	0.01-0.02
3	20-30	76	10.00	0.080	0.120	0.13	0.080	0.02-0.03
4	30-40	38	6.55	0.050	0.180	0.07	0.050	0.03-0.04
5	40-50	38	6.55	0.070	0.240	0.07	0.070	0.04-0.05
6	50-60	47	8.10	0.110	0.350	0.08	0.110	0.05-0.06
7	60-80	63	10.86	0.180	0.530	0.11	0.180	0.06-0.08
8	80-100	42	7.24	0.160	0.690	0.07	0.160	0.08-0.10
9	100-120	20	3.45	0.090	0.780	0.03	0.090	0.10-0.12
10	120-140	22	3.79	0.120	0.900	0.04	0.120	0.12-0.14
11	140-160	18	3.10	0.110	1.010	0.03	0.110	0.14-0.16
12	160-180	17	2.93	0.120	1.130	0.03	0.120	0.16-0.18
13	180-200	13	2.24	0.100	1.230	0.02	0.100	0.18-0.20
14	200-220	10	1.72	0.090	1.320	0.02	0.090	0.20-0.22
15	220-240	9	1.55	0.090	1.410	0.02	0.090	0.22-0.24
16	240-260	6	1.03	0.060	1.470	0.01	0.060	0.24-0.26
17	260-280	4	0.69	0.040	1.510	0.01	0.040	0.26-0.28
18	280-300	6	1.03	0.070	1.590	0.01	0.070	0.28-0.30
19	300-350	17	2.93	0.230	1.810	0.03	0.230	0.30-0.35
20	350-400	7	1.21	0.110	1.920	0.01	0.110	0.35-0.40
21	400-450	9	1.55	0.160	2.080	0.02	0.160	0.40-0.45
22	450-500	7	1.21	0.140	2.220	0.01	0.140	0.45-0.50
23	500-1000	24	4.14	0.690	2.330	0.04	0.690	0.50-1.00
24	1000-1500	8	1.38	0.400	3.300	0.01	0.400	1.00-1.50
25	1500-2000	4	0.69	0.300	3.600	0.01	0.300	1.50-2.00
26	2000-2500	0	0.00	0.000	3.600	0.00	0.000	2.00-2.50
27	2500-3000	0	0.00	0.000	3.600	0.00	0.000	2.50-3.00
28	3000-4000	0	0.00	0.000	3.600	0.00	0.000	3.00-4.00
						580		
Air Content (%):		3.60						
Specific Surface (mm ⁻¹):		26.68						
Spacing Factor (mm):		0.220						
Void Frequency (mm ⁻¹):		0.240						
Average Chord Length (mm):		0.150						
Paste to Air Ratio:		8.39						

Sample ID: Cast cyl Cylinder 3-3

Sample Size (mm x mm): 70 x 80 Length Traversed (mm): 2413.1

Paste Content (%): 30.20 Area Traversed (mm x mm): 60 x 70

Chord Length Distribution - Table

Class No.	Chord size (microns)	Number of Chords in Class	Number of Chords in Percent	Air Content in Class	Cumulated Air Content	Chord length frequency	Air content, fraction	
1	0-10	22	3.70	0.010	0.010	0.04	0.010	0.00-0.01
2	10-20	79	13.30	0.050	0.050	0.13	0.050	0.01-0.02
3	20-30	80	13.30	0.080	0.140	0.13	0.080	0.02-0.03
4	30-40	54	9.09	0.080	0.220	0.09	0.080	0.03-0.04
5	40-50	49	8.25	0.090	0.310	0.08	0.090	0.04-0.05
6	50-60	36	6.06	0.080	0.390	0.06	0.080	0.05-0.06
7	60-80	58	9.76	0.170	0.560	0.10	0.170	0.06-0.08
8	80-100	30	5.05	0.110	0.670	0.05	0.110	0.08-0.10
9	100-120	32	5.39	0.150	0.810	0.05	0.150	0.10-0.12
10	120-140	19	3.20	0.100	0.920	0.03	0.100	0.12-0.14
11	140-160	19	3.20	0.120	1.040	0.03	0.120	0.14-0.16
12	160-180	15	2.53	0.100	1.140	0.03	0.100	0.16-0.18
13	180-200	14	2.36	0.110	1.250	0.02	0.110	0.18-0.20
14	200-220	9	1.52	0.080	1.330	0.02	0.080	0.20-0.22
15	220-240	6	1.01	0.060	1.390	0.01	0.060	0.22-0.24
16	240-260	5	0.84	0.050	1.440	0.01	0.050	0.24-0.26
17	260-280	6	1.01	0.070	1.510	0.01	0.070	0.26-0.28
18	280-300	6	1.01	0.070	1.580	0.01	0.070	0.28-0.30
19	300-350	11	1.85	0.150	1.730	0.02	0.150	0.30-0.35
20	350-400	9	1.52	0.140	1.870	0.02	0.140	0.35-0.40
21	400-450	3	0.51	0.050	1.920	0.01	0.050	0.40-0.45
22	450-500	6	1.01	0.120	2.040	0.01	0.120	0.45-0.50
23	500-1000	24	4.04	0.670	2.060	0.04	0.670	0.50-1.00
24	1000-1500	2	0.34	0.110	2.810	0.00	0.110	1.00-1.50
25	1500-2000	0	0.00	0.000	2.810	0.00	0.000	1.50-2.00
26	2000-2500	0	0.00	0.000	2.810	0.00	0.000	2.00-2.50
27	2500-3000	0	0.00	0.000	2.810	0.00	0.000	2.50-3.00
28	3000-4000	0	0.00	0.000	2.810	0.00	0.000	3.00-4.00

594

Air Content (%): 2.81

Specific Surface (mm⁻¹): 34.98

Spacing Factor (mm): 0.187

Void Frequency (mm⁻¹): 0.250

Average Chord Length (mm): 0.114

Paste to Air Ratio: 10.75



Figure 1 I-94 Riverside drive bridge deck placement.

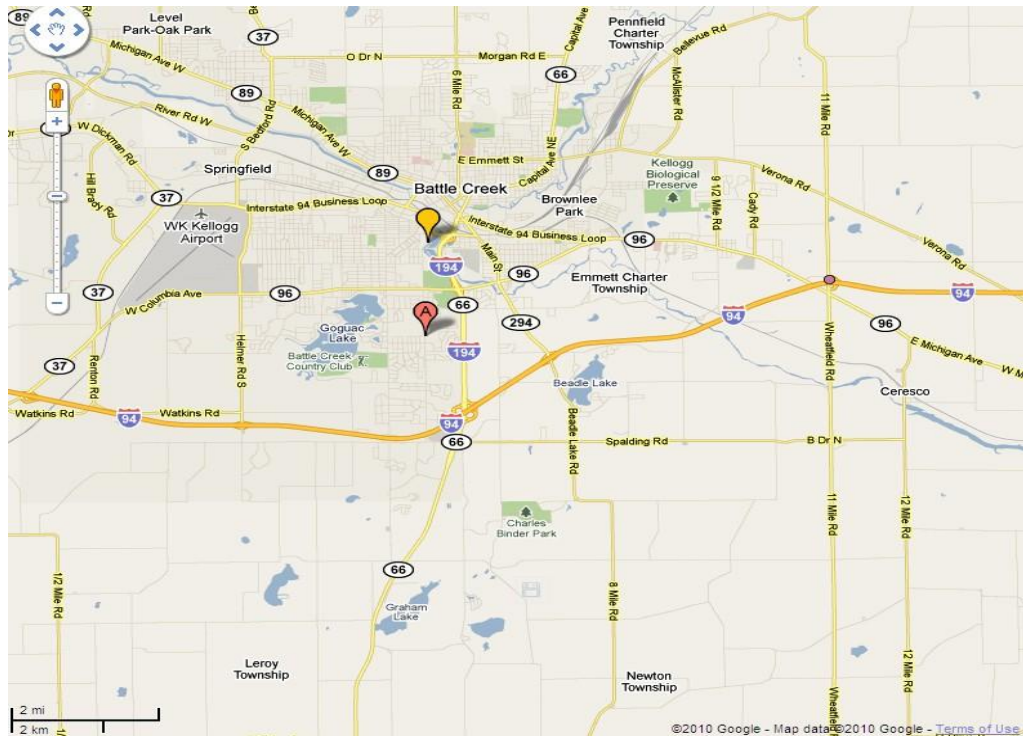


Figure 2 Project and mobile lab location.



Figure 3 Ambient sensor location.

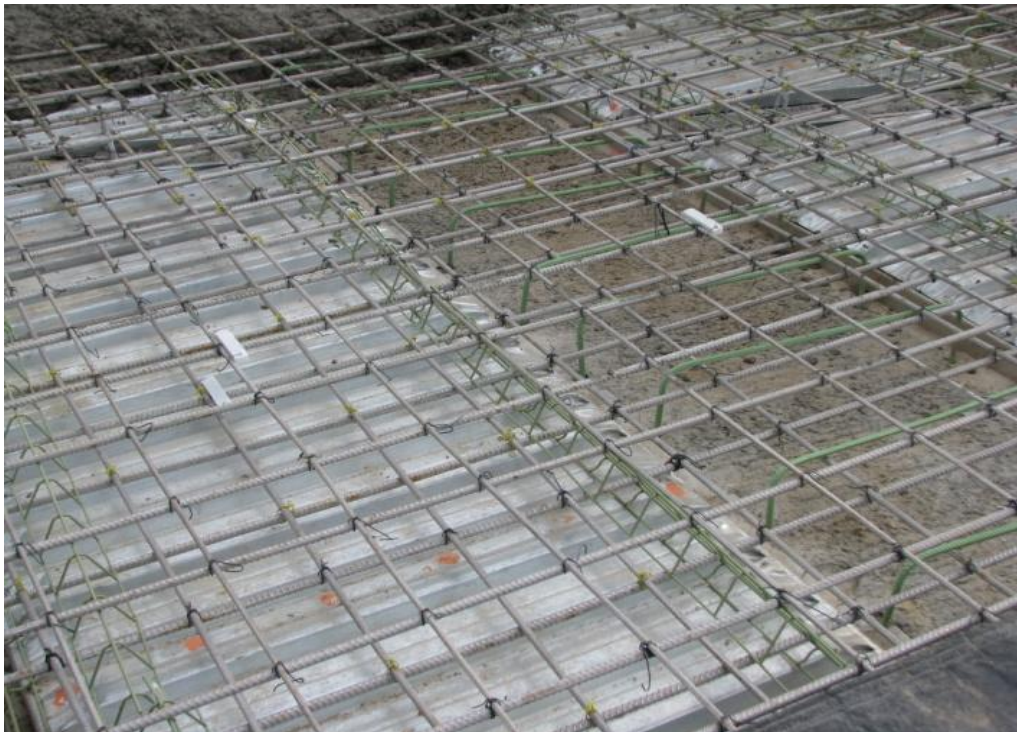


Figure 4 Locations of sensor #640, #641, and #644.



Figure 5 Locations of sensor #642 and #643.



Figure 6 Locations of sensor # 646 and #647.

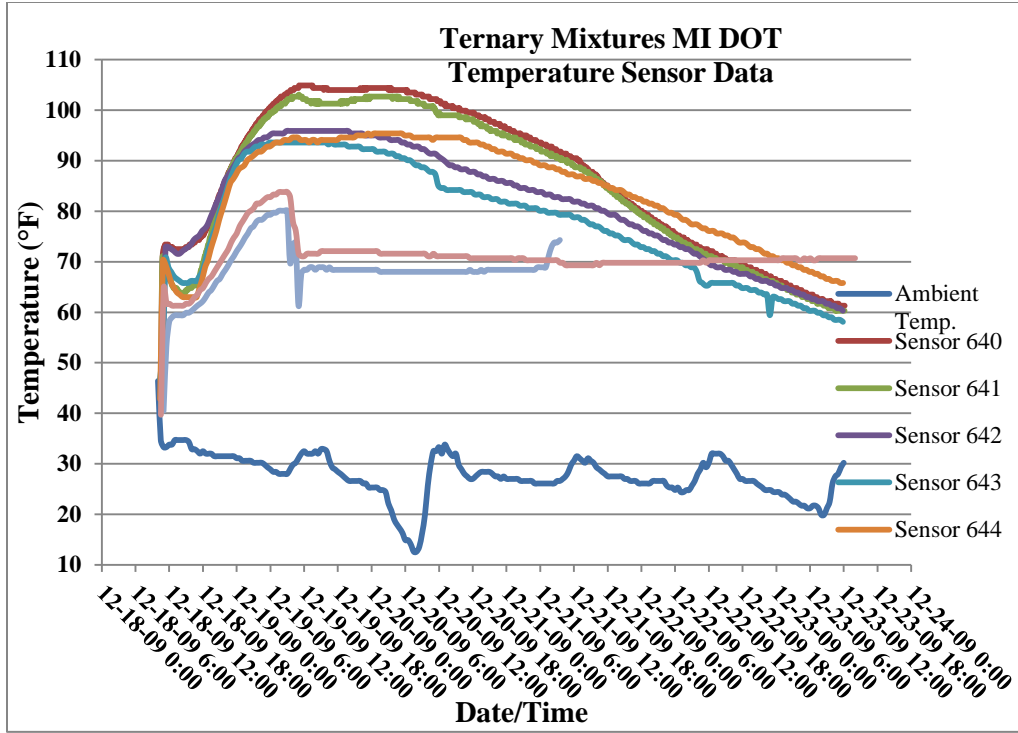


Figure 7 Temperature sensor data from MI DOT.



Figure 8 Concrete being placed.



Figure 9 Concrete being finished.



Figure 10 Concrete heated tent enclosure.



Figure 11 Curing blankets for concrete curing.

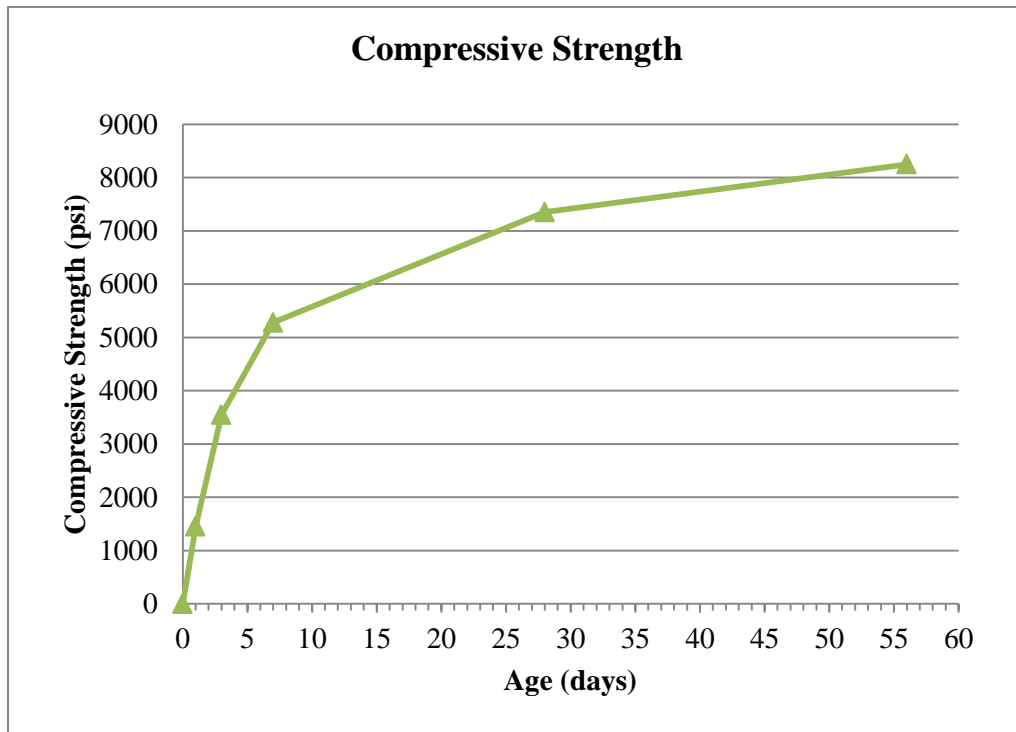


Figure 12 Compressive strength development with time.

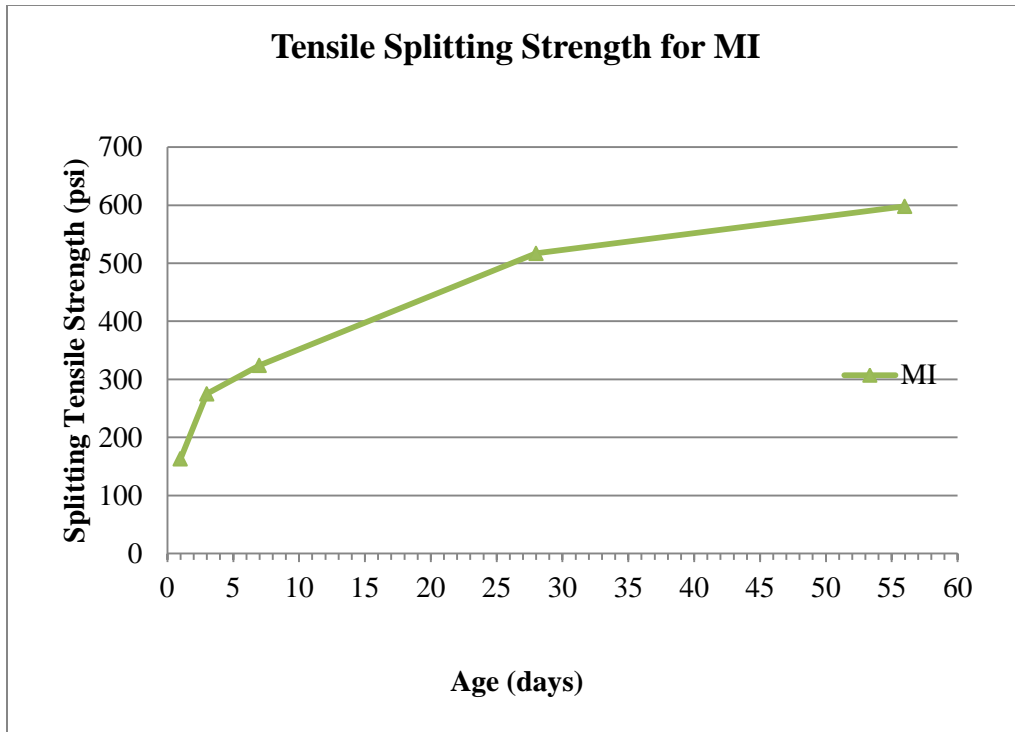


Figure 13 Tensile splitting strength development with time.

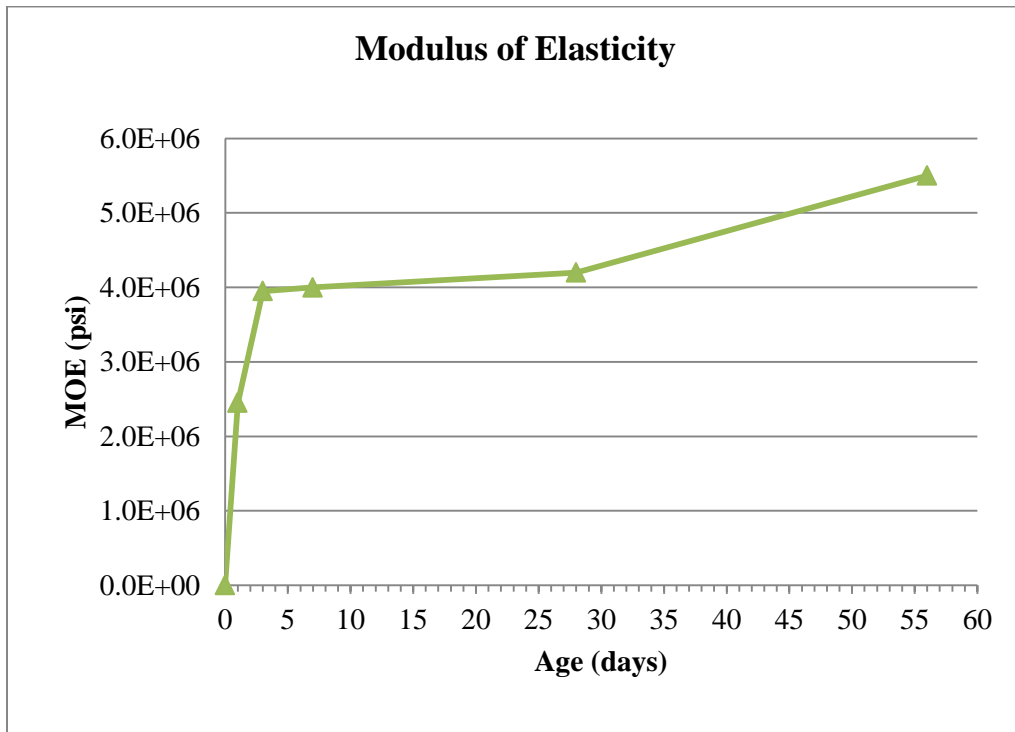


Figure 14 Modulus of elasticity development with time.

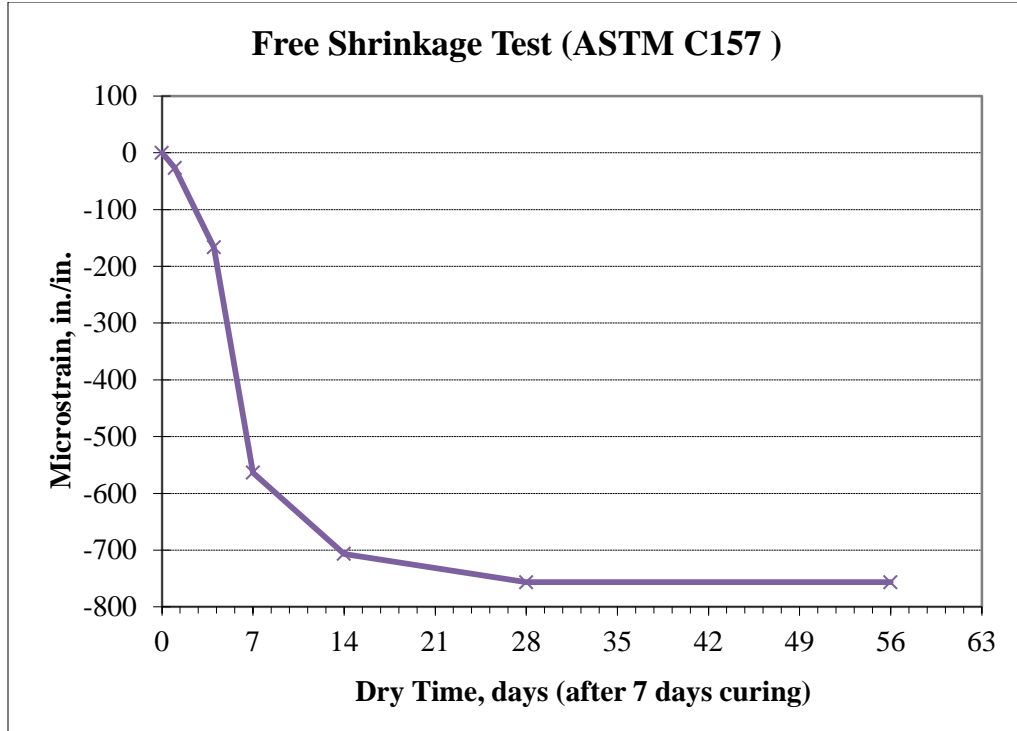


Figure 15 Free shrinkage of prisms (ASTM C 157).

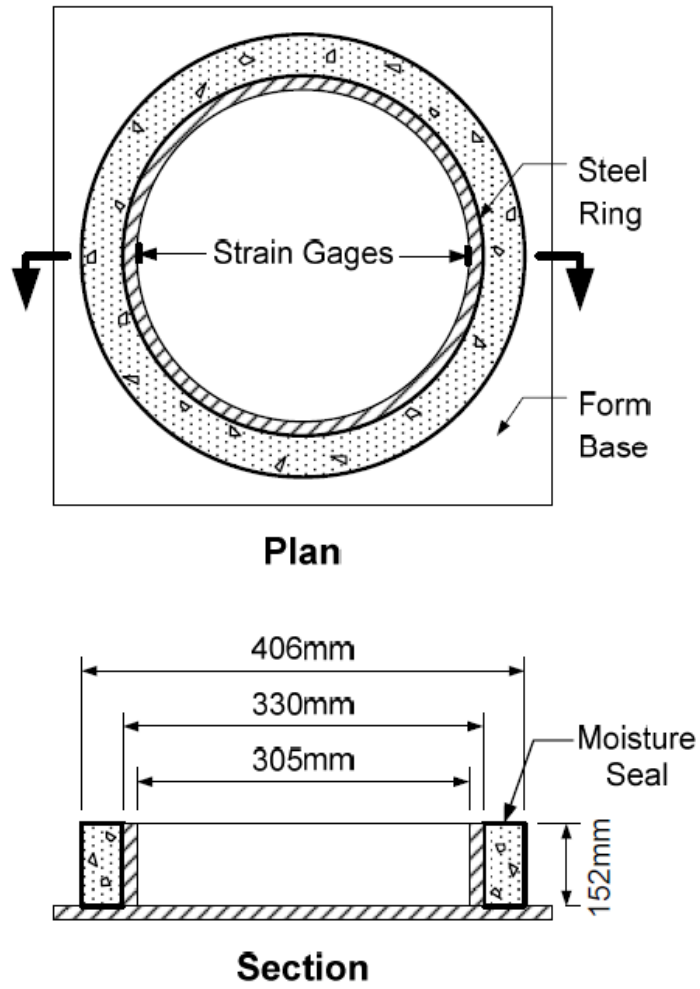


Figure 16 Configuration of restrained concrete ring samples.

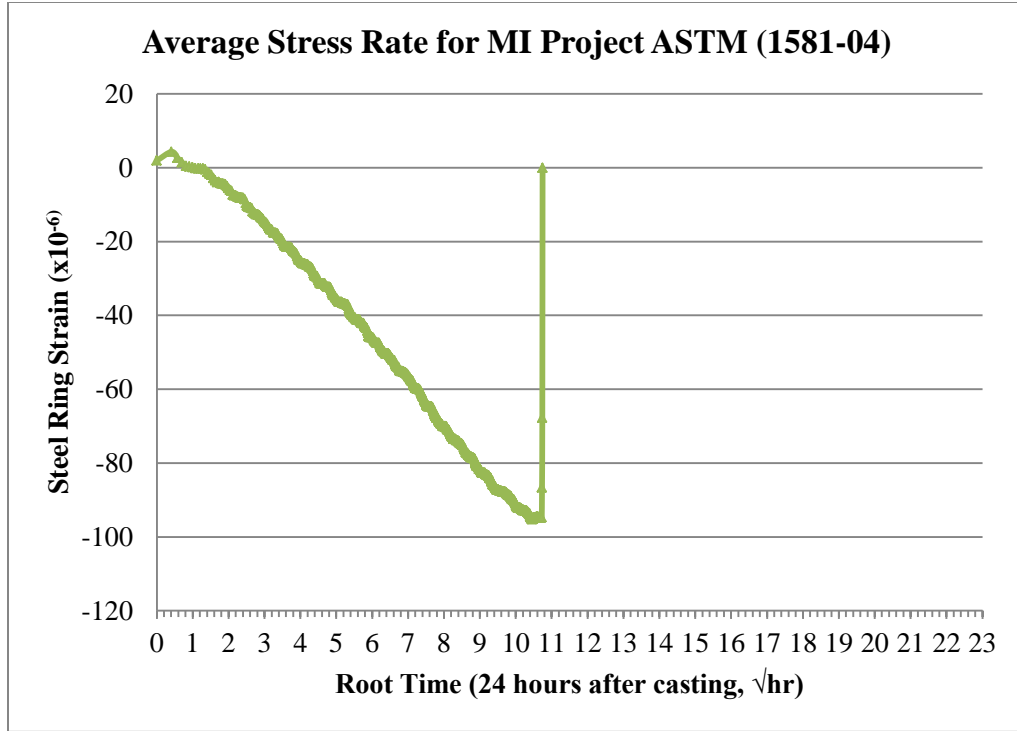


Figure 17 Strains of steel rings resulting from concrete shrinkage.

Table 1 Description of locations for each temperature sensor

Sensor	Location/Description
Ambient	Approximately 200' from structure, tied to a tree to protect from sunlight and exhaust
640	Mid-structure, on bottom mat, over a metal form
641	Mid-structure, on top mat, over a metal form
642	Where wood forms meet the fascia beam, on bottom mat
643	Where wood forms meet the fascia beam, on top mat
644	Mid-structure south of #640 & #641, on top mat, over middle of beam
646	Cure box, placed between cylinders
647	Inside a cylinder

Table 2 Air void test results conducted in MI DOT

Sample ID	Spacing Factor (mm)	Specific Surface (mm⁻¹)
Cylinder 1-1	0.308	24.720
Cylinder 1-2	0.352	27.110
Cylinder 1-3	0.475	12.890
Cylinder 2-1	0.394	19.660
Cylinder 2-2	0.355	26.130
Cylinder 2-3	0.388	22.560
Cylinder 3-1	0.192	33.390
Cylinder 3-2	0.220	26.680
Cylinder 3-3	0.187	34.980

Table 3 Air void test results conducted in ISU

Sample ID	Air Content	Specific Surface	Spacing Factor
	(%)	(mm ⁻¹)	(mm)
Cylinder 1-1	1.99	24.72	0.308
Cylinder 1-2	1.18	27.11	0.352
Cylinder 1-3	3.27	12.89	0.475
Cylinder 2-1	1.92	19.66	0.394
Cylinder 2-2	1.94	19.09	0.404
Cylinder 2-3	1.26	26.13	0.355
Cylinder 2-4	1.44	22.56	0.388
Cylinder 3-1	2.95	33.39	0.192
Cylinder 3-2	3.60	26.68	0.220
Cylinder 3-3	2.81	34.98	0.187

Table 4 Properties of hardened concrete

Tests	Results			
7-day Compressive Strength, psi	3050			
28-day Compressive Strength, psi	6110			
Rapid Chloride Permeability, Coulombs	Sample 1	Sample 2	Sample 3	Average
	977	1040	987	1001
Strength Development 28/7 day fc Ratio	2.00			
Shrinkage Microstrain @ 28 days, in/in	756.7			
Average Stress Rate by Restrained Ring Test, psi/day	92.63			

Table 5 Summation of strength and modulus of elasticity

Location	Age, days	Compressive Strength, psi	Splitting Tensile Strength, psi	Modulus Of Elasticity, psi
MI	1	820	114	4.10E+06
	3	1,750	270	4.80E+06
	7	3,050	417	5.30E+06
	28	6,110	484	5.80E+06
	56	6,610	522	5.40E+06

Table 6 Free shrinkage test results**MI Project Free Shrinkage Test (ASTM C 157)**

Dry					
Time	Beam 1 change%	Beam 2 change %	Beam 3 change %	Average	Microstrain
1	-0.002	-0.001	-0.005	-0.003	-26.7
4	-0.015	-0.015	-0.020	-0.017	-166.7
7	-0.073	-0.051	-0.045	-0.056	-563.3
14	-0.080	-0.064	-0.068	-0.071	-706.7
28	-0.089	-0.067	-0.071	-0.076	-756.7
56	-0.077	-0.070	-0.080	-0.076	-756.7

Table 7 Cracking potential and average stress rate (ASTM C 1581)**Cracking Potential for MI Project (ASTM C 1581)**

	Ring 1	Ring 2	Ring 3
Strain Rate Factor (in./in.x10 ⁻⁶)/hours ^{1/2}	-11.57	-10.48	-9.47
G (psi)	10.47x10 ⁶	10.47x10 ⁶	10.47x10 ⁶
Absolute Value of α_{avg} (in./in.10 ⁻⁶)/day ^{1/2}	51.47		
Elapsed Time, tr (hours)	176.0	138.0	400.0
Elapsed Time, tr (days)	7.3	5.8	16.7
Stress Rate, q (psi/day) $q=GI\alpha_{avg}I/2\sqrt{t_r}$	99.5	112.4	66.0
Average Stress Rate, q (psi/day) $q=GI\alpha_{avg}I/2\sqrt{t_r}$	92.63		
Potential for cracking classification (ASTM 1581)	High (50 ≤ q)		

POOLED FUND STUDY

UNITED STATES DEPARTMENT OF TRANSPORTATION

FEDERAL HIGHWAY ADMINISTRATION



DEVELOPMENT OF PERFORMANCE PROPERTIES OF TERNARY MIXTURES

**A Field Application of Ternary Mixtures
-An experience in construction of a rigid pavement project in Monona, Iowa**

June 2010

U OF UTAH IOWA STATE UNIVERSITY


THE UNIVERSITY OF UTAH

National Concrete Pavement
Technology Center

Tech Center

Introduction

This document is a report of the activities and observations of a research team that performed on-site testing of a ternary mixture placed on an interstate pavement in Iowa. The cementitious system comprised a Type 1P cement (25% fly ash) blended with 15% Class C fly ash. The purpose of this research project is a comprehensive study of how supplementary cementitious materials (SCMs) can be used to improve the performance of concrete mixtures when used in ternary blends. This is the third phase of a project which intends to provide consulting to states and contractors with the use and field management of ternary mixtures. A state-of-the-art 44-foot long PCC mobile laboratory equipped for on-site cement and concrete testing was provided by the CP Tech Center to collect data and field observations.

Project Information

- Project No. ESIMX-029-5(100)95-1S-43
- Monona County, Iowa
- Contractor: McCarthy Improvement Co.
- I-29 Grade/Replace, Monona, Iowa
- Rigid Pavement Improvement (Southbound of Interstate 29 in Iowa) (Figure 1)

Site Location

An area at the bridge site was prepared by the contractor for the PCC mobile lab. The location of the project (on Interstate 29 near the city of Onawa, IA) and the mobile lab is shown in Figure 2.

Sampling and Testing Activities

The mobile lab arrived on site on June 1, 2010. Concrete placement, sampling and testing took place on June 7, 2010. Hardened samples were transported to Iowa State University on June 8, 2010, for further testing. The following tests were conducted in the field or in the laboratory:

- Calorimetry test (ASTM C 1679)
- Slump, unit weight, temperature and air content of fresh concrete – 1 test (ASTM C 143, ASTM C 138, ASTM C 231)

- Microwave w/c ratio – 1 test (AASHTO T 318)
- Initial set and final set of concrete – 1 test (ASTM C 403)
- Compressive strength, splitting tensile strength, static modulus of elasticity - 4" x 8" cylinders at 1-day, 3-days, 7-days, 28-days, and 56-days (ASTM C 39, ASTM C 496, ASTM C 469)
- Rapid chloride permeability - 4" x 8" cylinders at 56 days (ASTM C 1202)
- Porosity analysis (boil test) of hardened concrete - 4" x 8" cylinders (ASTM C 642)
- Salt scaling – 3 samples (ASTM C 672)
- Shrinkage – 3 beams (ASTM C 157)
- Restrained rings – 4 samples (ASTM C 1581)

Observations of the Research Team

The following observations were made in this field testing:

- The sub-base for the entire project was recycled material: the old concrete slab had been crushed to create a granular sub-base of approximately 8-10 inches thick.
- The sub-grade was also a recycled section: the old asphalt overlay was crushed into sub-grade of 12 inches thick. All was installed on a 1% grade to the outside.
- Slab dimensions were 11 inches by 26 feet for mainline and 7 inches by 6 or 8 feet for shoulders which were tied to mainline by #4 bars.
- For mainline pavement, the contractor used a Guntert-Zimmerman 8500, while Gomaco Commander with a side kit was used for the shoulders.
- 1½ -inch dowel bars were used in baskets placed every 20 feet. The transverse joints were ¼ inches wide and approximately 2 inches deep cut using early entry saws. The center longitudinal joint was 1/8 inches wide by approximately 3 ½ inches deep cut using conventional water-cooled saws.
- The concrete was supplied from a fixed batch plant and was delivered to the job site in tandem trucks. The mix design was from McCarthy Improvement Company and approved by Iowa Department of Transportation. The specific accepted mix proportions are given in the project data section (page 14). The plant had a 90 second

mix time. Once in the truck, the mix had to be placed on the ground within 60 minutes without segregation.

- Workability factor & coarseness factors were 34.5 and 64.9, respectively. The combined aggregate gradation fell in the well-graded region (page 17). Similarly, the Combined Percent Retained Curve indicated a well graded system (page 18).
- The weather condition at the job site was recorded for a period of eight days from June 1st to June 8th. Data is shown in Figures 3 to 5. The relative humidity ranged between 21% and 89%. The ambient temperature ranged from 48 °F to 88°F. The wind speed varied from 3 mph to 20 mph.
- The fresh concrete properties testing include slump, unit weight, and water-cementitious materials ratio measured by microwave. Due to unexpected weather, only one group of sample was tested during the construction period. Slump was 2.0 inches. The unit weight was 135.6 lb/ft³. The water- cementitious material ratio was 0.35.
- The air content was 8.75% from the one test conducted at the batch plant, which was slightly higher than the specified minimum, 6%.
- Setting time of the mix was determined as a single measurement: initial set occurred at 2.32 hours and the final set was achieved at 8.41 hours.
- The rapid chloride permeability test measures the electrical conductance of a concrete sample as its resistance to chloride ion penetration. The test results shown in Table 1 indicate a classification of “very low” chloride permeability according to ASTM C1202.
- The compressive strengths at 7 and 28 days and the 28/7 days strength development ratio are reported in Table 1.
- The porosity values obtained by the boiling test (ASTM C 642) results are given in Table 1.
- Compressive strength, splitting tensile strength and modulus of elasticity results (ASTM C 39, ASTM C 496, and ASTM C 469) are given in Table 2 and development curves are plotted in Figures 12 to Figure 14.

- Free shrinkage test (ASTM C 157) was conducted in the laboratory. Three concrete beams were wet cured for seven days and then moved to a dry room at 23°C and 50% relative humidity. The drying shrinkage results are given in Table 3 and also plotted in Figure 15.
- Restrained shrinkage test was conducted based on ASTM C 1581. Four rings were cast. The rings were demolded and the top surface was covered with paraffin wax 24 hours from casting. The rings were allowed to dry at 23°C and 50% relative humidity immediately after demolding. Strains in the steel rings were recorded every 10 minutes up to 28 days or until the concrete cracked. The configuration of restrained concrete rings is shown in Figure 16. The cracking potential is listed in Table 4 and shown graphically in Figure 17. The cracking potential is classified as “moderate high” based on the average stress rate.
- Salt scaling test (ASTM C 672) was performed: the specimens were subjected to 16 to 18 hours freezing and then allowed to thaw at $23 \pm 2.0^\circ\text{C}$ and a relative humidity of 45 to 55% for 6 to 8 hours. The solution of 4 % calcium chloride was rinsed off and the surface was visually examined. The solution was replaced and the test was continued following visual examination. 50 freeze-thaw cycles were applied. The surface was rated on a scale of 0 to 5 with 0 having no scaling, 1 having very slight scaling of 3 mm depth maximum without coarse aggregate visible, 2 having slight to moderate scaling, 3 having moderate scaling with some coarse aggregate visible, 4 having moderate to severe scaling, and 5 having severe scaling with coarse aggregate visible over entire surface. The photograph after 50th cycle was taken and shown in Figure 18. The visual ratings assigned to each specimen for cycles 0, 5, 10, 15, 20, 25, and 50 are given in Table 5.

Acknowledgements

The research team at the Center for Concrete Pavement Technology, Iowa State University, sincerely thanks the Iowa Department of Transportation for providing the cooperation, McCarthy Improvement Company for supplying the materials and equipment. All of the contributions from job site and concrete design company are also gratefully acknowledged.

Project Data

The following test data is provided for information only, comments and conclusions will be reported in the comprehensive Phase III report of the pooled fund project *Development of Performance Properties of Ternary Mixtures*.

Mix Design & Misc. Info.

General Information

Project:	I-29 Grade/Replace Monona Co
Contractor:	McCarthy Improvement Company
Mix Description:	562 lb Cementitious
Mix ID:	ESIMX-029-5(100)951S-43
Date(s) of Placement:	6/7/2010

Cementitious Materials	Source	Type	Spec. Gravity	lb/yd ³	%
					Replacement by Mass
Portland Cement:	PC0008 Ash Grove Louisville, NE	IP (25)	2.950	478	
GGBFS:					
Fly Ash:	FA004C Headwater Resources Concl Bluffs, IA	Class C	2.620	84	14.95%
Silica Fume:					
Other Pozzolan:					
				562	lb/yd³
				6.0	sacks/yd³

Aggregate Information	Source	Type	Spec. Gravity	Absorption	% Passing
			SSD	(%)	#4
Coarse Aggregate:	ASD010 Everist, Inc. Dell Rapids, SD	Quartzite	2.640	0.30%	0.7%
Intermediate Aggregate #1:	A18528 Higman S&G Washta, IA	P-Gravel	2.670	1.60%	39.0%
Intermediate Aggregate #2:					
Fine Aggregate #1:	A18528 Higman S&G Washta, IA	Natural Sand	2.650	0.80%	99.0%
Coarse Aggregate %:	51.0%				
Intermediate Aggregate #1%:	9.0%				
Intermediate Aggregate #2%:					
Fine Aggregate #1 %:	40.0%				

Mix Proportion Calculations

Water/Cementitious Materials Ratio:	0.400
Air Content:	6.00%

	Batch Weights SSD			Absolute Volume
	Volume (ft ³)	(lb/yd ³)	Spec. Gravity	(%)
Portland Cement:	2.597	478	2.950	9.617%
GGBFS:				
Fly Ash:	0.514	84	2.620	1.903%
Silica Fume:				
Other Pozzolan:				
Coarse Aggregate:	9.520	1,568	2.640	35.260%
Intermediate Aggregate #1:	1.680	280	2.670	6.222%
Intermediate Aggregate #2:				
Fine Aggregate #1:	7.467	1,235	2.650	27.655%
Water:	3.603	225	1.000	13.343%
Air:	1.620			6.000%
	27.000	3,870		100.000%
	Unit Weight (lb/ft³)	143.3	Paste	30.863%
			Mortar	60.915%

Admixture Information	Source/Description	oz/yd ³	oz/cwt
Air Entraining Admix:	Euclid AEA 92/ AEA	1.00	0.18
Admix #1:	Euclid Eucon Retardent 100/ Retarder	1.50	0.27
Admix #2:	Euclid Eucon WR/ Water Reducer	4.00	0.71
Admix #3:			

AVA Information	Absolute Volume (%)
Air Free Paste:	24.863%
Air Free Mortar:	54.915%



Iowa - Ternary Mixtures

Sample Information:

Project: I-29 @ Blencoe

Date: 7-Jun-10

Time: 1:15 PM

Type of Paving: _____

Direction of Paving: _____

Sta: _____

Latitude: _____

Longitude: _____

Mix ID: _____

Truck IDs: _____

Sample Location Mark
& Comments: _____

Environmental Conditions:

Dew Point: _____

Relative Humidity: 65%

Wind Speed: _____

Ambient Temp.: 72.0

Concrete Properties:

Base/Soil Temp. (internal)(F): _____

Base Temp. (surface)(F): _____

Microwave Water Content Samples: _____

Calorimetry (ADIACAL Cylinders): 4

Set-Time (ASTMC403) Mortar Samples: _____

Cylinder for RCP & Perm. Voids Boil Test: use adiacal

Scaling Blocks: 3

Concrete Temp.(F): 74.1

Compressive, Tensile & MOR Cylinders: 30

Slump (in.): 2.00

Shrinkage Beams: 3

Air Content: 8.8%

Unit Weight (lb/ft³): 135.6

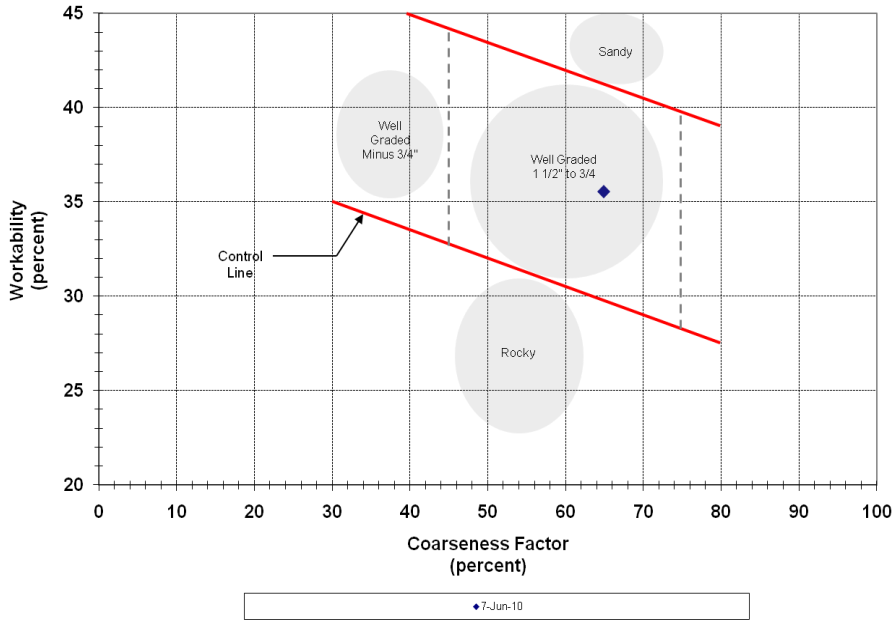
Project: I-29 Grade/Replace Monona Co @ Blencoe
 Mix ID: CDM
 Sample Comments:
 Test Date: 7-Jun-10

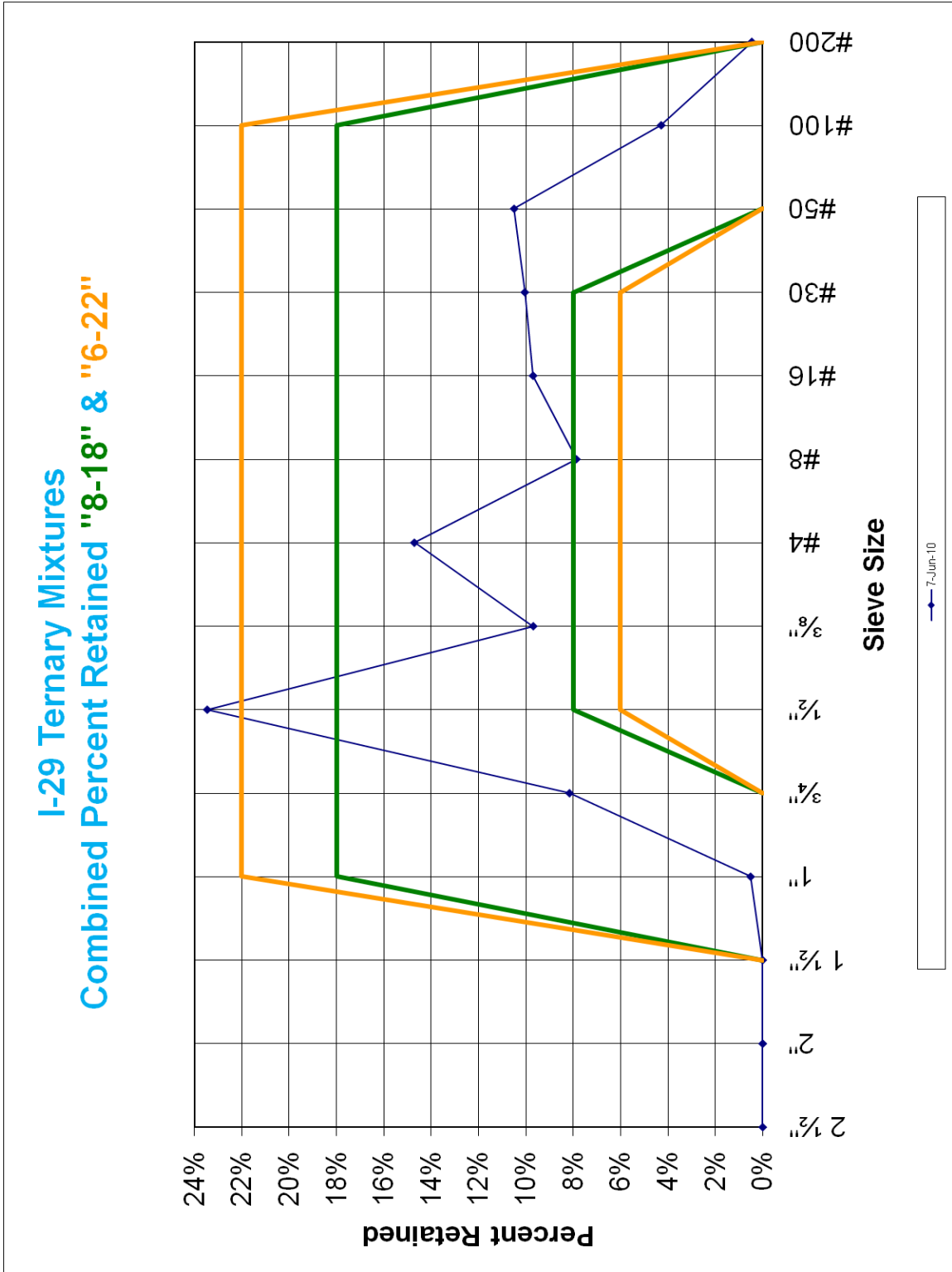
Total Cementitious Material: 562 lb/yd³
 Agg. Ratios: 51.00% 9.00% 40.00% 100.00%

Sieve	Coarse	Intermediate	Fine #1	Fine #2	Combined % Retained	Combined % Retained On Each Sieve	Combined % Passing
2 1/2"	100%	100%	100%		0%	0%	100%
2"	100%	100%	100%		0%	0%	100%
1 1/2"	100%	100%	100%		0%	0%	100%
1"	99%	100%	100%		1%	1%	99%
3/4"	83%	100%	100%		9%	8%	91%
1/2"	37%	100%	100%		32%	23%	68%
3/8"	18%	100%	100%		42%	10%	58%
#4	1%	39%	99%		57%	15%	43%
#8	1%	6%	87%		64%	8%	36%
#16	1%	5%	63%		74%	10%	26%
#30	1%	4%	38%		84%	10%	16%
#50	1%	3%	12%		95%	10%	5%
#100	1%	2%	1%		99%	4%	1%
#200	0.7%	0.5%	0.5%		99.4%	0.5%	0.6%

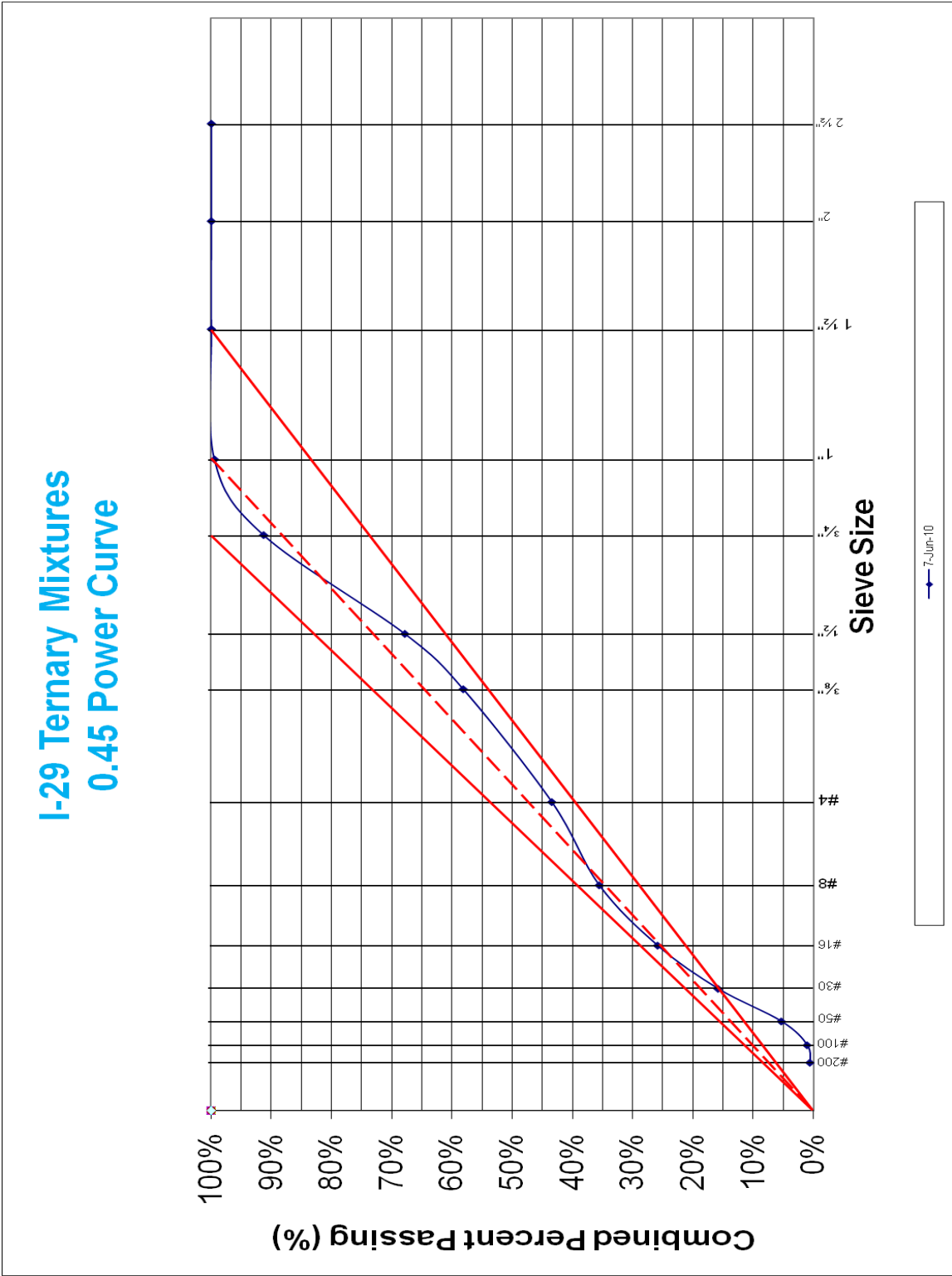
Workability Factor: 35.5
 Coarseness Factor: 64.9

I-29 Ternary Mixtures
 Workability Factor & Coarseness Factor





I-29 Ternary Mixtures
0.45 Power Curve





Iowa - Ternary Mixtures

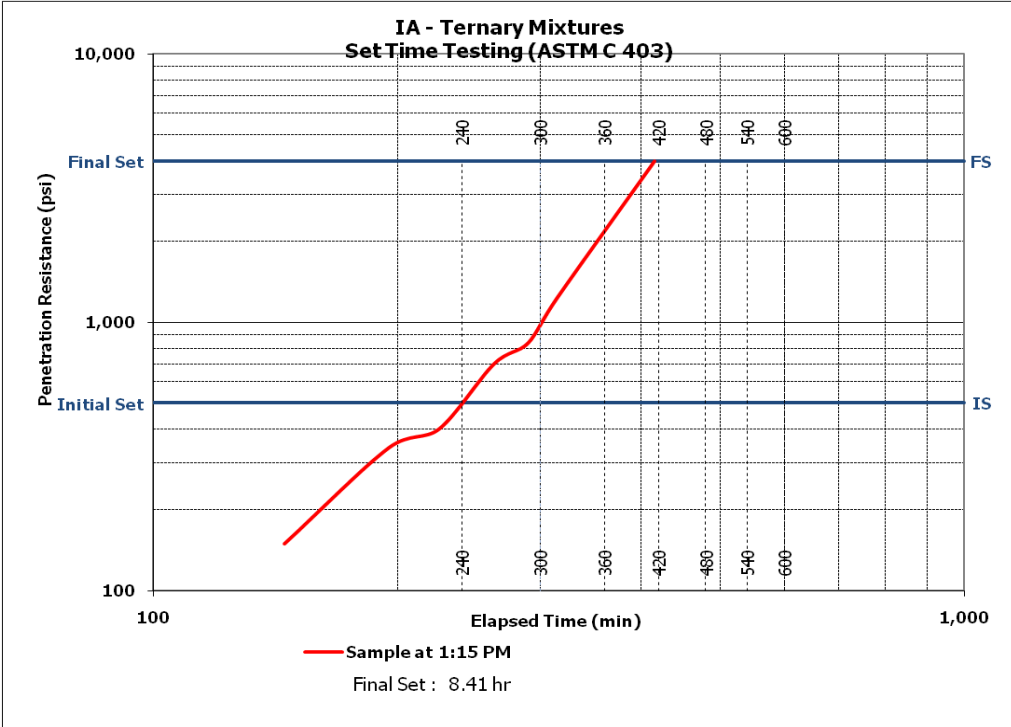
Set Time ASTM C 403


Project: I-29 Grade/Replace Monona Co
 Date: 7-Jun-10 Start Time: 1:15 PM
 Sta: n/a

Test Data

Penetration Time (xx:xx-24 hr format)	Time (min)	Needle # (1,2,4,10,20 or 40)	Force (lb)	Penetration Resistance (psi)	Sample Temp. (°F)
3:40 PM	145.00	1	149	149.00	n/a
4:30 PM	195.00	4	85	340.00	n/a
5:00 PM	225.00	10	40	400.00	n/a
5:38 PM	263.00	10	70	700.00	n/a
6:05 PM	290.00	20	42	840.00	n/a
6:30 PM	315.00	20	62	1240.00	n/a
8:10 PM	415.00	40	100	4000.00	n/a
					n/a
					n/a

Initial Set (at 500 psi PR)	estimated times using forecast function	139 minutes	2.32 hours
Final Set (at 4,000 psi PR)		505 minutes	8.41 hours



 Iowa - Ternary Mixtures Boil Test (ASTM C 642)		
IA #1		
A	944.4	g
B	966.61	g
C	967.18	g
D	557.5	g
P	1	g/cm ³
g1	2.3052	g/cm ³
g2	2.4409	g/cm ³
Volume of permeable pore space (voids), %		5.5604
IA #2		
A	982.7	g
B	1006.28	g
C	1006.91	g
D	581.1	g
P	1	g/cm ³
g1	2.3078	g/cm ³
g2	2.4470	g/cm ³
Volume of permeable pore space (voids), %		5.6856
IA #3		
A	1017.7	g
B	1044.53	g
C	1045.46	g
D	596.2	g
P	1	g/cm ³
g1	2.2653	g/cm ³
g2	2.4145	g/cm ³
Volume of permeable pore space (voids), %		6.1791



ASTM C 1202-97



Test-compagny
Testing street 45
CompagnyCity
Some Country

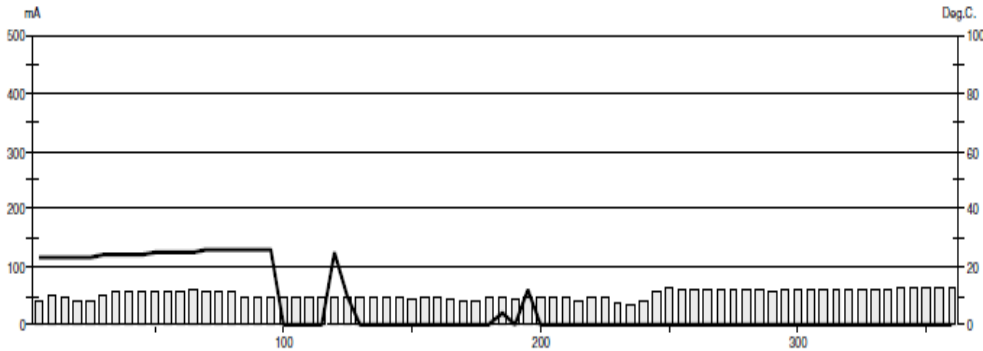
Your own logo.
size=20x80mm



GERMANN INSTRUMENTS
DENMARK
Phone: +45 3907 7117
Fax: +45 3907 3107
USA
Phone: (547)329-8999
Fax: (547)329-8988

Test report

Voltage Used: 60
Testing time: 06:00 hour
Charge passed: 1130
Adjusted Charge passed: 980
Permeability class: Very Low
Instrument number: 023907
Channel number: 1
Report date: 8/3/2010
Testing by: PJM
Reference: IA ternary 56day #1
Sample diameter: 102
Comment: ---



Time	°C	mA	Time	°C	mA	Time	°C	mA	Time	°C	mA
00:05	23	42.1	01:35	26	46.0	03:05	4	47.0	04:35	0	59.3
00:10	23	50.3	01:40	0	47.3	03:10	0	44.8	04:40	0	59.3
00:15	23	46.5	01:45	0	47.4	03:15	12	46.4	04:45	0	59.4
00:20	23	42.0	01:50	0	47.9	03:20	0	49.1	04:50	0	59.1
00:25	23	42.2	01:55	0	48.3	03:25	0	48.7	04:55	0	59.8
00:30	24	50.6	02:00	25	48.7	03:30	0	48.4	05:00	0	60.4
00:35	24	59.1	02:05	10	49.1	03:35	0	40.1	05:05	0	59.7
00:40	24	58.5	02:10	0	48.8	03:40	0	45.9	05:10	0	59.9
00:45	24	56.8	02:15	0	47.8	03:45	0	46.7	05:15	0	60.2
00:50	25	56.5	02:20	0	47.5	03:50	0	37.5	05:20	0	60.8
00:55	25	55.9	02:25	0	46.4	03:55	0	35.1	05:25	0	61.1
01:00	25	57.9	02:30	0	45.3	04:00	0	40.6	05:30	0	61.3
01:05	25	59.7	02:35	0	48.6	04:05	0	56.4	05:35	0	61.3
01:10	26	59.0	02:40	0	48.4	04:10	0	61.4	05:40	0	61.4
01:15	26	58.4	02:45	0	45.6	04:15	0	59.8	05:45	0	61.5
01:20	26	55.8	02:50	0	41.0	04:20	0	59.6	05:50	0	61.9
01:25	26	50.0	02:55	0	41.8	04:25	0	59.6	05:55	0	61.9
01:30	26	48.0	03:00	0	46.6	04:30	0	59.4	06:00	0	61.7



ASTM C 1202-97



Test-compagny
Testing street 45
CompagnyCity
Some Country

Your own logo.
size=20x80mm



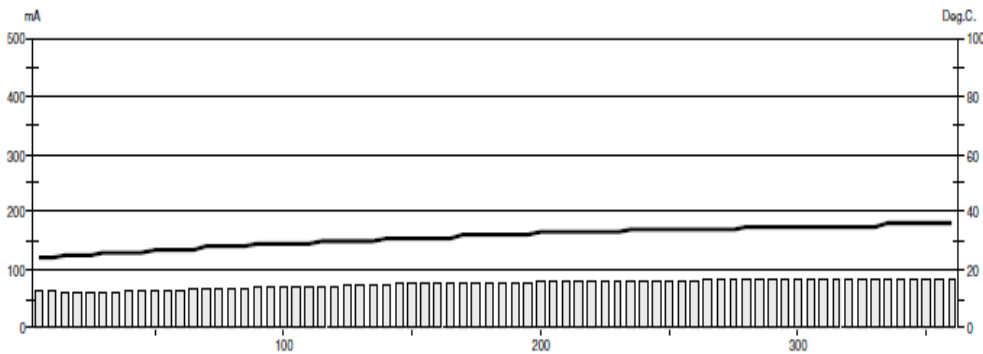
GERMANN INSTRUMENTS

DENMARK
Phone: +45 3907 7117
Fax: +45 3907 3107

USA
Phone: (547)329-8999
Fax: (547)329-8988

Test report

Voltage Used: 60
Testing time: 06:00 hour
Charge passed: 1629
Adjusted Charge passed: 1413
Permeability class: Low
Instrument number: 023907
Channel number: 2
Report date: 8/3/2010
Testing by: PJM
Reference: IA ternary 56day #2
Sample diameter: 102
Comment: ---



Time	°C	mA	Time	°C	mA	Time	°C	mA	Time	°C	mA
00:05	24	62.5	01:35	29	69.3	03:05	32	78.1	04:35	34	82.4
00:10	24	62.0	01:40	29	70.0	03:10	32	78.5	04:40	35	82.5
00:15	25	61.3	01:45	29	70.5	03:15	32	79.0	04:45	35	82.7
00:20	25	61.0	01:50	29	71.1	03:20	33	79.4	04:50	35	82.6
00:25	25	60.8	01:55	30	71.5	03:25	33	79.4	04:55	35	82.2
00:30	26	60.7	02:00	30	72.3	03:30	33	79.6	05:00	35	82.4
00:35	26	60.9	02:05	30	72.7	03:35	33	79.8	05:05	35	83.0
00:40	26	61.9	02:10	30	73.0	03:40	33	80.0	05:10	35	83.3
00:45	26	62.3	02:15	30	73.7	03:45	33	80.2	05:15	35	83.5
00:50	27	63.4	02:20	31	74.3	03:50	33	80.1	05:20	35	83.8
00:55	27	65.0	02:25	31	74.9	03:55	34	80.3	05:25	35	84.2
01:00	27	65.8	02:30	31	75.3	04:00	34	80.7	05:30	35	84.4
01:05	27	66.0	02:35	31	75.8	04:05	34	81.0	05:35	36	84.5
01:10	28	66.4	02:40	31	76.1	04:10	34	81.2	05:40	36	84.6
01:15	28	67.3	02:45	31	76.5	04:15	34	81.3	05:45	36	84.6
01:20	28	67.8	02:50	32	76.9	04:20	34	81.4	05:50	36	84.1
01:25	28	68.0	02:55	32	77.2	04:25	34	81.9	05:55	36	84.8
01:30	29	68.6	03:00	32	77.6	04:30	34	82.2	06:00	36	84.9



Figure 1 Interstate 29 in Iowa (Southbound).

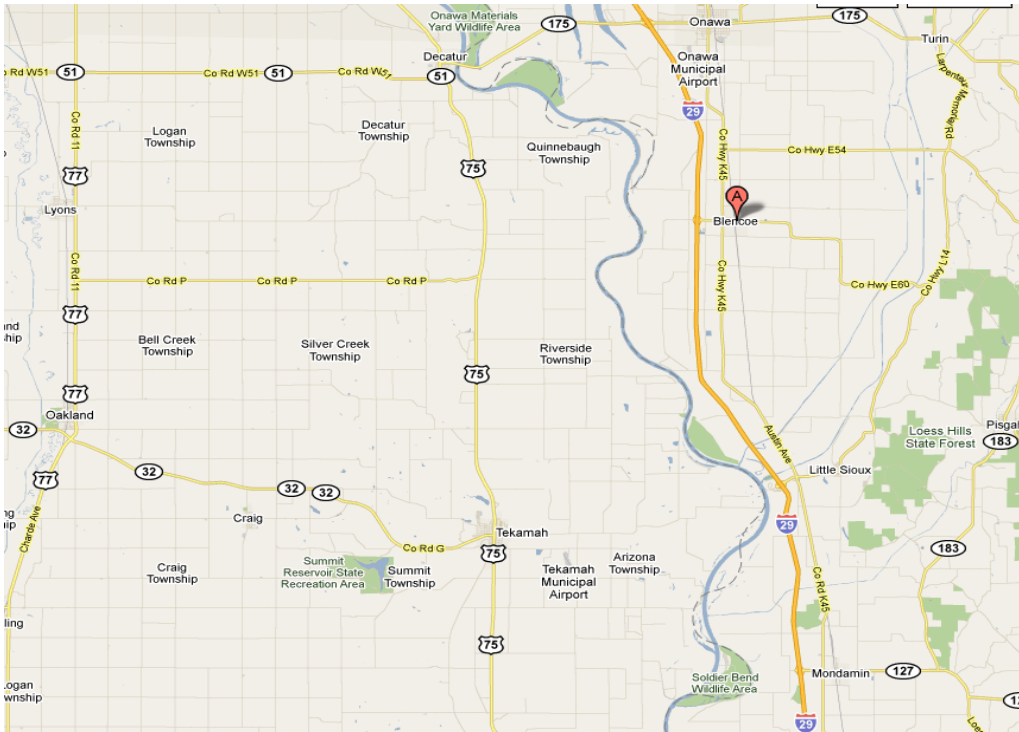


Figure 2 Project and mobile lab location.

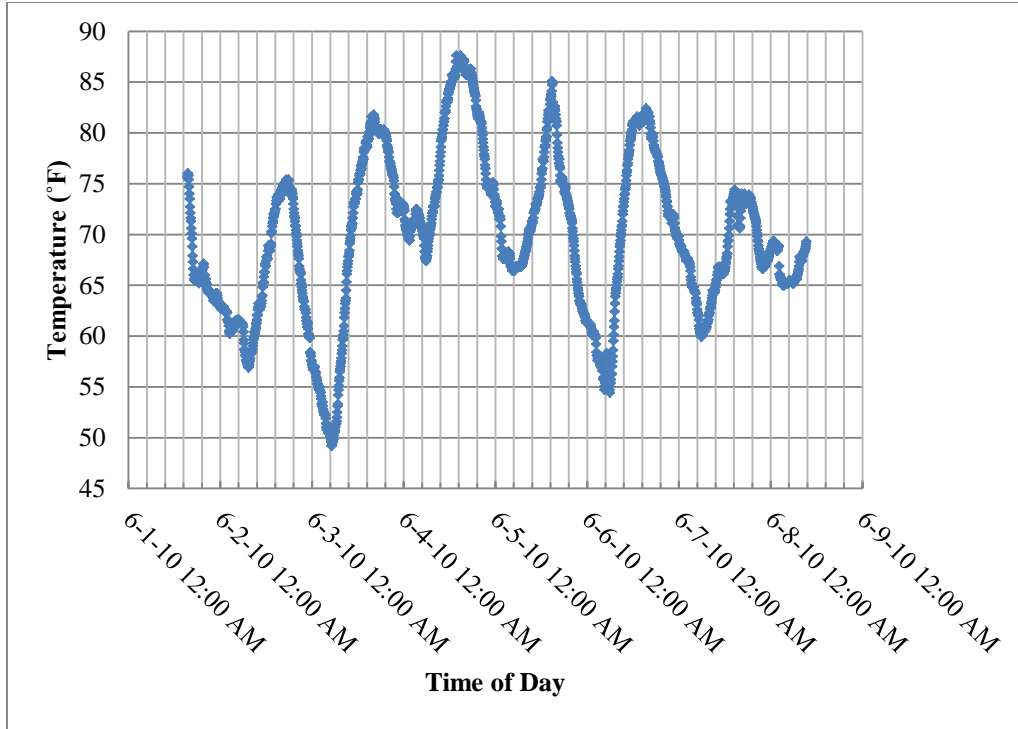


Figure 3 Ambient temperature versus time of day.

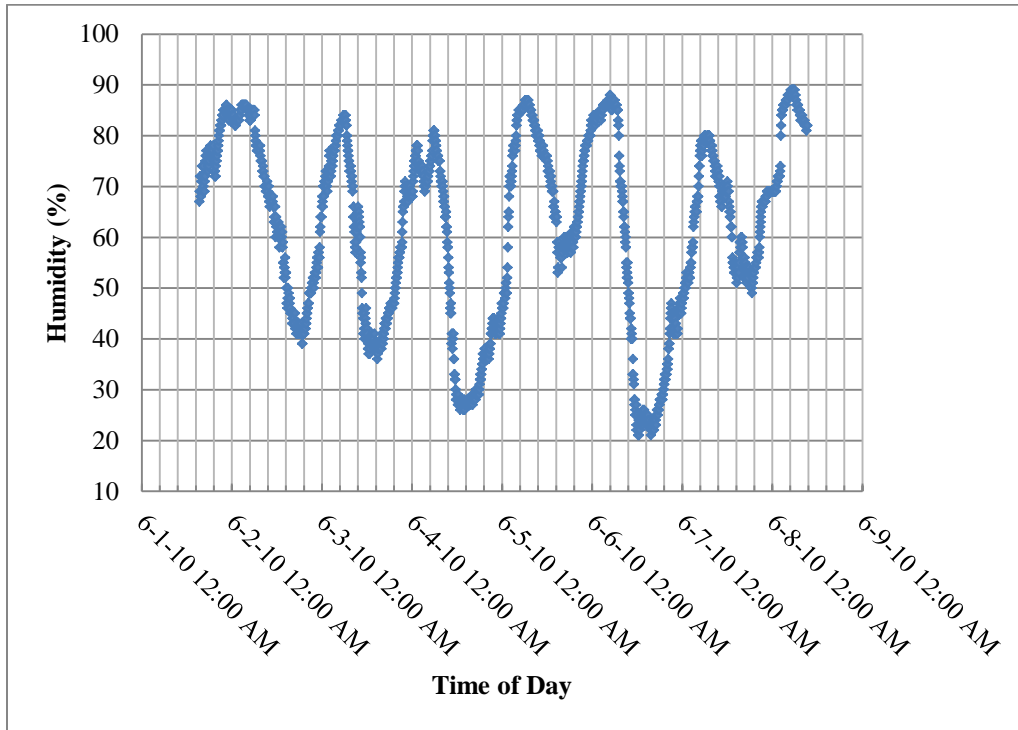


Figure 4 Relative humidity versus time of day.

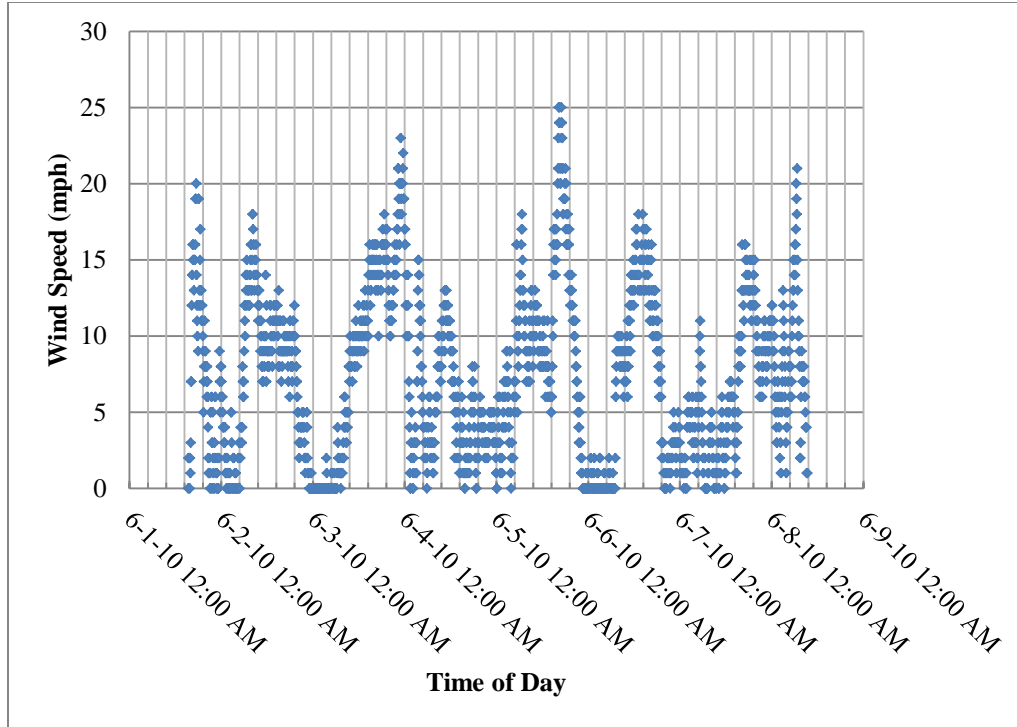


Figure 5 Wind speed versus time of day.



Figure 6 Concrete being dumped into a belt placer and spread by the placer.



Figure 7 Concrete being dumped into a belt placer and spread by the placer.



Figure 8 Concrete passing through the paver.



Figure 9 Concrete passing through the paver.



Figure 10 Concrete being finished and curing compound being applied.



Figure 11 Concrete being finished and curing compound being applied.

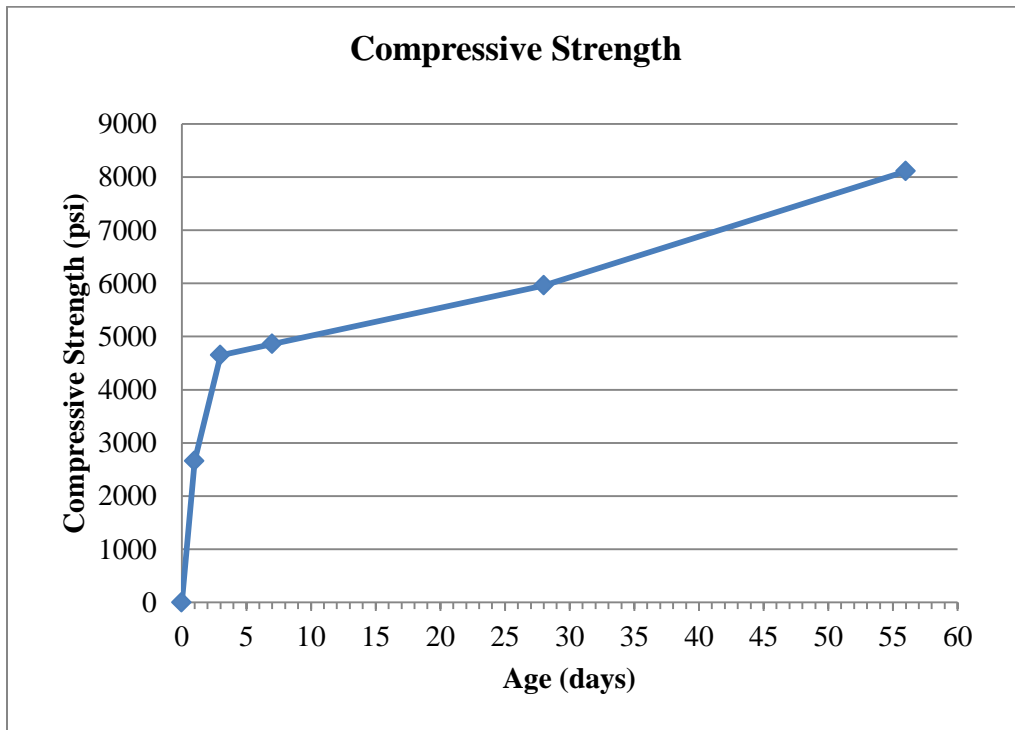


Figure 12 Compressive strength development with time.

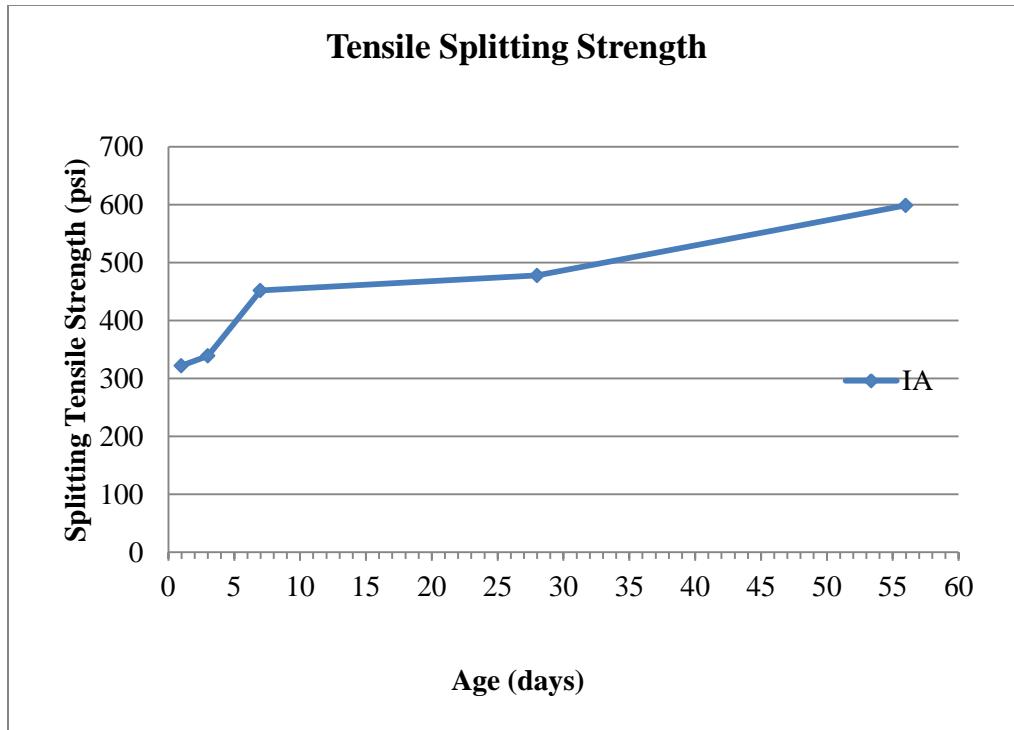


Figure 13 Tensile splitting strength development with time.

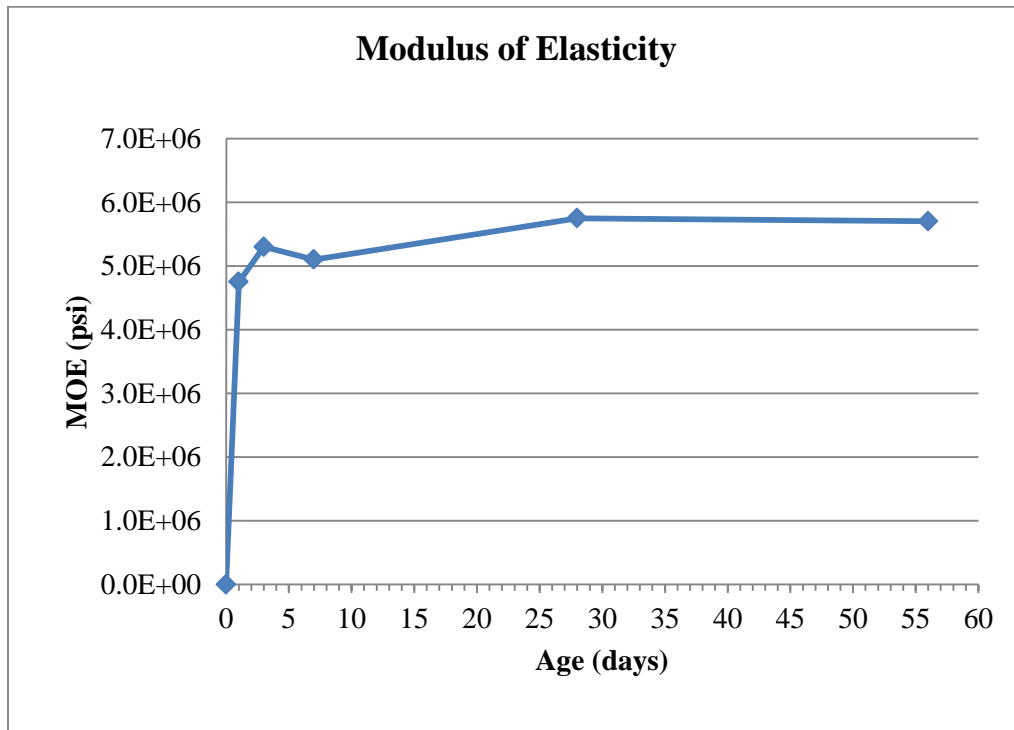


Figure 14 Modulus of elasticity development with time.

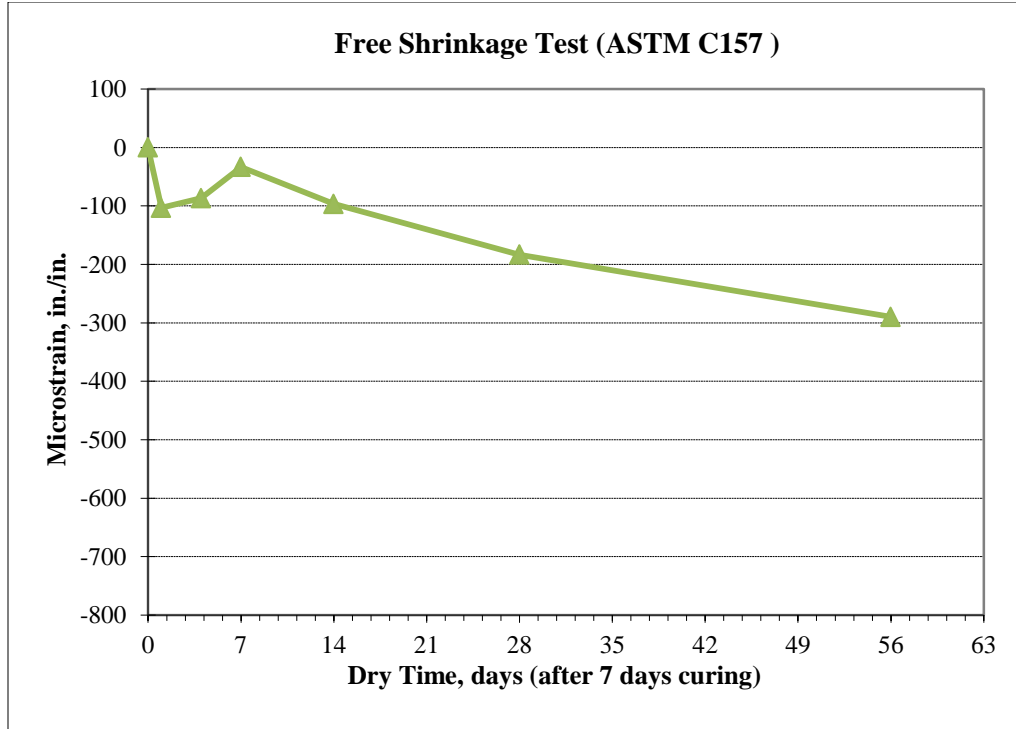


Figure 15 Free shrinkage of prisms (ASTM C 157).

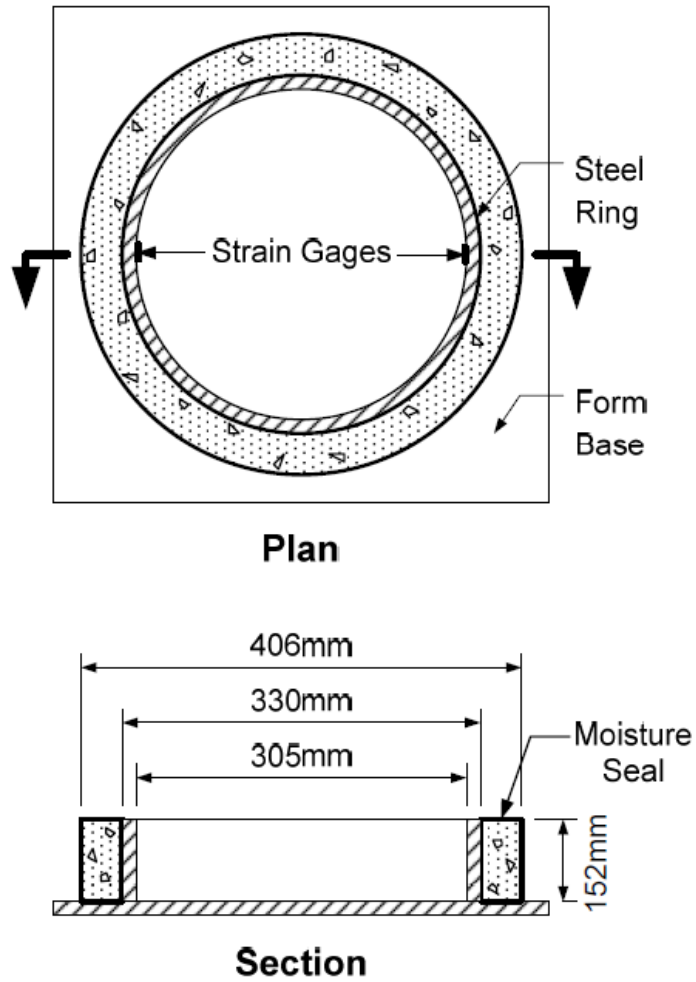


Figure 16 Configuration of restrained concrete ring samples.

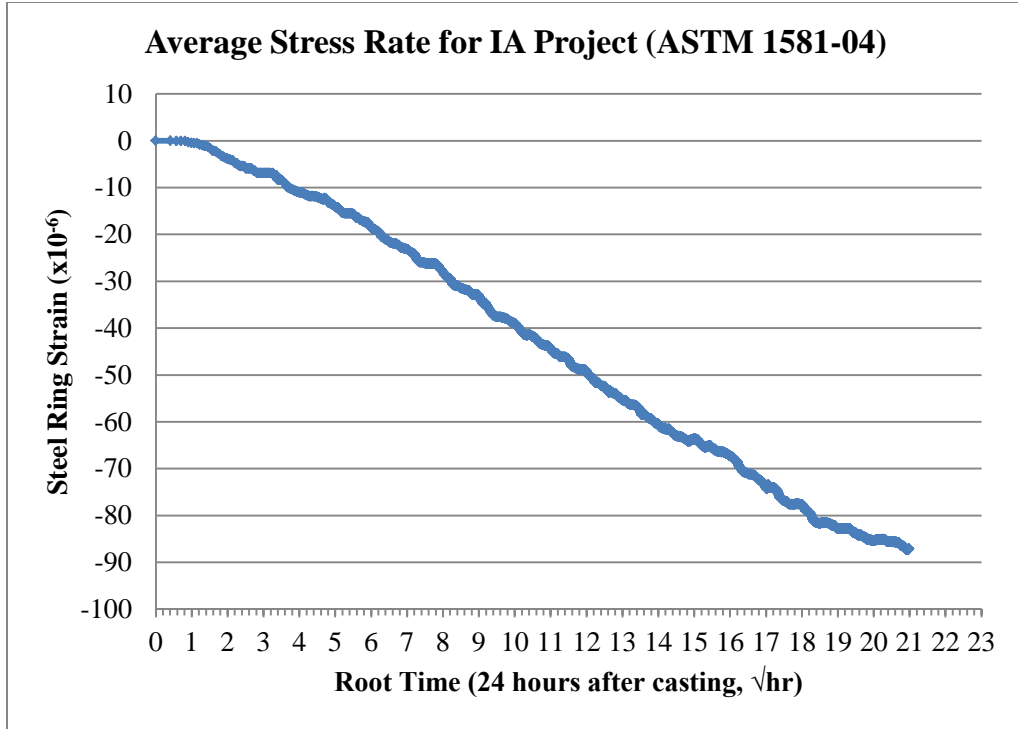


Figure 17 Average stress rate for KS project.



Figure 18 IA salt scaling sample after 50th freeze-thaw cycle.

Table 1 Properties of hardened concrete

Tests	Results			
7-day Compressive Strength, psi	4860			
28-day Compressive Strength, psi	5960			
Volume of Permeable Pore Space, %	Sample 1	Sample 2	Sample 3	Average
	5.56	5.68	6.18	5.81
Rapid Chloride Permeability, Coulombs	Sample 1	Sample 2	Average	
	980	1413	1197	
Strength Development 28/7 day fc Ratio	1.23			
Shrinkage Microstrain @ 28 days, in/in	183.3			
Average Stress Rate by Restrained Ring Test, psi/day	28.21			

Table 2 Summation of strength and modulus of elasticity

Location	Age, days	Compressive Strength, psi	Splitting Tensile Strength, psi	Modulus Of Elasticity, psi
IA	1	2,660	322	4.75E+06
	3	4,650	339	5.30E+06
	7	4,860	452	5.10E+06
	28	5,960	478	5.75E+06
	56	8,110	599	5.70E+06

Table 3 Free shrinkage test results

IA Project Free Shrinkage Test (ASTM C 157)					
Dry					
Time	Beam 1 change%	Beam 2 change %	Beam 3 change %	Average	Microstrain
0	0.000	0.000	0.000	0.000	0.000
1	-0.011	-0.010	-0.010	-0.010	-103.3
4	-0.010	-0.008	-0.008	-0.009	-86.7
7	-0.005	-0.005	0.000	-0.003	-33.3
14	-0.011	-0.012	-0.006	-0.010	-96.7
28	-0.017	-0.024	-0.014	-0.018	-183.3
56	-0.027	-0.031	-0.029	-0.029	-290.0

Table 4 Cracking potential and average stress rate (ASTM C 1581)

Cracking Potential for IA Project (ASTM C 1581)				
	Ring 1	Ring 2	Ring 3	Ring 4
Strain Rate Factor (in./in.x10 ⁻⁶)/hours ^{1/2}	-4.89	-4.23	-4.47	-5.27
G (psi)	10.47x10 ⁶	10.47x10 ⁶	10.47x10 ⁶	10.47x10 ⁶
Absolute Value of α_{avg} (in./in.10 ⁻⁶)/day ^{1/2}	23.10			
Elapsed Time, tr (hours)	441.0	441.0	441.0	441.0
Elapsed Time, tr (days)	18.4	18.4	18.4	18.4
Stress Rate, q (psi/day) $q=GI\alpha_{avg}I/2\sqrt{t_r}$	28.2	28.2	28.2	28.2
Average Stress Rate, q (psi/day) $q=GI\alpha_{avg}I/2\sqrt{t_r}$	28.21			
Potential for cracking classification (ASTM 1581)	Moderate-high (25 ≤ q < 50)			

Table 5 Salt scaling test visual condition of specimen

IA Salt Scaling Samples	Condition of Surface					
	Cycle 5	Cycle 10	Cycle 15	Cycle 20	Cycle 25	Cycle 50
No. 1	1	1	2	2	2	4
No. 2	1	1	2	2	2	4
No. 3	1	1	2	2	2	4

POOLED FUND STUDY

UNITED STATES DEPARTMENT OF TRANSPORTATION

FEDERAL HIGHWAY ADMINISTRATION



DEVELOPMENT OF PERFORMANCE PROPERTIES OF TERNARY MIXTURES

**A Field Application of Ternary Mixtures
-An experience in construction of a bridge
deck project in Roaring Spring, PA**

July 2010

U OF UTAH IOWA STATE UNIVERSITY


THE UNIVERSITY OF UTAH

National Concrete Pavement
Technology Center



Introduction

This document is a report of the activities and observations of a research team that performed on-site testing of a ternary mixture placed on a State Road 36, section 20, bridge deck in Pennsylvania. The cementitious system comprised a Type I/II cement, Grade 100 slag cement, and Class F fly ash. The purpose of this research project is a comprehensive study of how supplementary cementitious materials (SCMs) can be used to improve the performance of concrete mixtures when used in ternary blends. This is the third phase of a project which intends to provide consulting to states and contractors on the use and field management of ternary mixtures. A state-of-the-art 44-foot long PCC mobile laboratory equipped for on-site cement and concrete testing was provided by the CP Tech Center to collect data and field observations.

Project Information

- Project No. ECMS#21899
- Roaring Spring, Blair County, New07A42&07B42
- Contractor: Plum Contracting.
- State Route 36, section 20
- Bridge deck placement (1 span – structural steel girders with concrete deck) (Figure 1)

Site Location

An area at the bridge site was prepared by the contractor for the PCC mobile lab. The location of the project and mobile lab is shown as following Figure 2.

Sampling and Testing Activities

The mobile lab arrived on site on July 13, 2010. Concrete placement, sampling and testing took place on July 14, 2010. Hardened samples were transported to Iowa State University on July 16, 2010, for further testing. The following tests were conducted either in the field or in the laboratory:

- Calorimetry test (ASTM C 1679)

- Slump, unit weight, temperature and air content of fresh concrete – 2 test (ASTM C 143, ASTM C 138, ASTM C 231)
- Microwave w/c ratio – 2 test
- Initial set and final set – 1 test (ASTM C 403)
- Compressive strength, splitting tensile strength, static modulus of elasticity - 4” x 8” cylinders at 1-day, 3-days, 7-days, 28-days, and 56-days (ASTM C 39, ASTM C 496, ASTM C 469)
- Rapid chloride permeability - 4” x 8” cylinders at 56 days (ASTM C 1202)
- Porosity analysis (boil test) of hardened concrete - 4” x 8” cylinders (ASTM C 642)
- Salt scaling – 3 samples (ASTM C 672)
- Free shrinkage test – 4 beams (ASTM C 157)
- Restrained rings – 4 samples (ASTM C 1581)
- Two i-buttons are buried on top and bottom layer of reinforcement to investigate maturity of concrete. (ASTM C 1074)

Observations of the Research Team

The following observations were made in the field work:

- Concrete paving: Contractors were using Bid-Well 3600 typical form riding bridge deck paver for a rural bridge deck. The bridge deck was 8 inches deep with a 2 ½ inches cover on top layer of reinforcement and 1 inch cover on bottom layer of reinforcement.
- All concrete came from a fixed batch plant and was delivered to the job site in transit mix trucks or front-ready-mix trucks. A front-ready-mix truck was used to transfer material from a central mixed concrete to a rear-ready-mix truck. The concrete was placed using a conveyor belt.
- The mix design was from New Enterprise Stone & Lime Co., Inc, and approved by Pennsylvania Department of Transportation. The mix proportions are given in the project data section.
- Cementitious materials include Type I/II portland cement (Holcim-Hagerstown, MD), Grade 100 slag cement (GranCem-Camden, NJ) and Class F fly ash (Headwaters-

Sammiss Plant). Dolomitic limestone coarse aggregate (Class A57) was used and the fine aggregate was sandstone. MBVR air entraining agent, Glenium 3030 water reducer, and 100XR retarder were used as chemical admixtures.

- According to the workability factor & coarseness factor graph (Page 22) combined aggregate gradation for this project fell in the well-graded region. Similarly, the aggregate gradation (Page 23) indicated a well graded system.
- The weather conditions at the job site recorded by the PCC mobile lab is given in Table 1 below and graphically in Figures 3 to 5. The relative humidity ranged from 70% to 82%; the ambient temperature ranged from 69°F to 77.4 °F; the wind speed varied from 0 mph to 7 mph with; the concrete temperature ranged from 73 °F to 80.4 °F at during the recorded period.
- The fresh concrete tests include slump cone, unit weight, and water/cementitious materials ratio by microwave. CP Tech Center crew carried out tests for two sets of specimens PennDOT crew ran tests for six. Slump result was varied from 3.0 inches to 6.5 inches (performed by PennDOT). CP Tech Center crew performed unit weight tests in duplicate: the values are 147.3 lb/ft³ and 147.1 lb/ft³. The water-cementitious materials ratios obtained from microwave water-cementitious ratio tests were 0.50 and 0.46. The design value was 0.41. The data is provided on Page 16.
- The air content was varied from 5.0% to 7.1% with an average value of 6.0% based on eight sets of testing. The specified minimum was 6%.
- Setting time of the mix was determined as a single measurement: initial set occurred at 3.63 hours and the final set was achieved at 10.96 hours (Page 25).
- The feedback from PA department of Transportation on workability and durability was positive. Only some minor cracking over the pier at four months after bridge deck being constructed (Figure 14 and 15).
- The rapid chloride permeability test measures the electrical conductance of a concrete sample as its resistance to chloride ion penetration. The test results shown in Table 2 indicate a classification of “very low” chloride permeability according to ASTM C1202.

- The compressive strengths at 7 and 28 days and the 28/7 days strength development ratio is reported in Table 2.
- Two i-buttons were attached to reinforcing steel before the concrete placement: one was placed on top layer of reinforcement steel and the other was placed on bottom layer of reinforcement steel. The rate of cement hydration is dependent on the temperature and the time (Mindess, Young and Darwin, 2003). Maturity is used to monitor the cement hydration progress as a function of time and temperature. The temperature of concrete was recorded up to 28 hours. The concrete temperature over time is plotted in Figure 16 (a) and concrete maturity curve based on Nurse – Saul method (ASTM C 1074) is generated in Figure 16 (b).
- Compressive strength, splitting tensile strength and modulus of elasticity results (ASTM C 39, ASTM C 496, and ASTM C 469) are given in Table 3 and also plotted in Figures 17 to Figure 19.
- Free shrinkage test (ASTM C 157) was conducted in the laboratory. Three beams were wet cured for seven days and then moved to a dry room at 23°C and 50% relative humidity. The drying shrinkage results are given in Table 4 and also plotted in Figure 20.
- Restrained shrinkage test was conducted based on ASTM C 1581. Four rings were cast. The rings were demolded and the top surface was covered with paraffin wax 24 hours from casting. The rings were allowed to dry at 23°C and 50% relative humidity immediately after demolding. Strains in the steel rings were recorded every 10 minutes up to 28 days or until the concrete cracked. The configuration of restrained concrete rings is shown in Figure 21. The cracking potential is listed in Table 5 and shown graphically in Figure 22. The cracking potential is classified as “moderate high” based on the average stress rate.
- Salt scaling test (ASTM C 672) was performed: the specimens were subjected to 16 to 18 hours freezing and then allowed to thaw at $23 \pm 2.0^\circ\text{C}$ and a relative humidity of 45 to 55% for 6 to 8 hours. The solution of 4 % calcium chloride was replaced and the test was continued following visual examination. 50 freeze-thaw cycles were applied. The surface was rated on a scale of 0 to 5 with 0 having no scaling, 1 having

very slight scaling of 3 mm depth maximum without coarse aggregate visible, 2 having slight to moderate scaling, 3 having moderate scaling with some coarse aggregate visible, 4 having moderate to severe scaling, and 5 having severe scaling with coarse aggregate visible over entire surface. The photograph after 50th cycle was taken and shown in Figure 23. The visual ratings assigned to each specimen for cycles 0, 5, 10, 15, 20, 25, and 50 are given in Table 6.

Acknowledgements

The research team at the National Concrete Pavement Technology Center at Iowa State University sincerely thanks the Pennsylvania Department of Transportation for their cooperation, Plum Contracting Company and New Enterprise Stone & Lime Co., Inc for supplying the equipment and materials.

Project Data

The following test data is provided for information only, comments and conclusions will be reported in the comprehensive Phase III report of the pooled fund project *Development of Performance Properties of Ternary Mixtures*.

Mix Design & Misc. Info.

General Information

Project:	State Road 36 Section 20, Bridge Deck in Roaring Spring, Blair County, PA
Contractor:	Plum Contracting
Mix Description:	587 lb Cementitious
Mix ID:	ECMS#21899
Date(s) of Placement:	7/14/2010

Cementitious Materials	Source	Type	Spec. Gravity	lb/yd ³	Replacement by Mass %
Portland Cement:	Holcim-Hagerstown, MD.	Type I/II	3.150	323	
GGBFS:	GranCem-Camden, NJ (gr-100)	Grade 100	2.900	176	
Fly Ash:	Headwaters-Sammis Plant	Class F	2.400	88	14.99%
Silica Fume:					
Other Pozzolan:					
				587	lb/yd³
				6.2	sacks/yd³

Aggregate Information	Source	Type	Spec. Gravity SSD	Absorption (%)	% Passing #4
Coarse Aggregate:	NESL Roaring Spring	Dolomitic L.S.	2.840	0.32%	2.0%
Intermediate Aggregate #1:					
Intermediate Aggregate #2:					
Fine Aggregate #1:	NESL- lshman	Sandstone	2.610	0.94%	99.0%
Coarse Aggregate %:	59.4%				
Intermediate Aggregate #1%:					
Intermediate Aggregate #2%:					
Fine Aggregate #1 %:	40.6%				

Mix Proportion Calculations

Water/Cementitious Materials Ratio:	0.410
Air Content:	6.00%

	Volume (ft ³)	Batch Weights SSD (lb/yd ³)	Spec. Gravity	Absolute Volume (%)
Portland Cement:	1.643	323	3.150	6.088%
GGBFS:	0.973	176	2.900	3.603%
Fly Ash:	0.588	88	2.400	2.177%
Silica Fume:				
Other Pozzolan:				
Coarse Aggregate:	10.882	1,928	2.840	40.314%
Intermediate Aggregate #1:				
Intermediate Aggregate #2:				
Fine Aggregate #1:	7.430	1,210	2.610	27.528%
Water:	3.857	241	1.000	14.289%
Air:	1.620			6.002%
	26.993	3,966		100.000%
	Unit Weight (lb/ft³)	146.9	Paste	32.158%
			Mortar	60.217%

Admixture Information	Source/Description	oz/yd ³	oz/cwt
Air Entraining Admix:	MBVR AEA	7.04	1.20
Admix. #1:	Glenium 3030 WR	35.22	6.00
Admix. #2:	100XR RE	11.74	2.00
Admix. #3:			

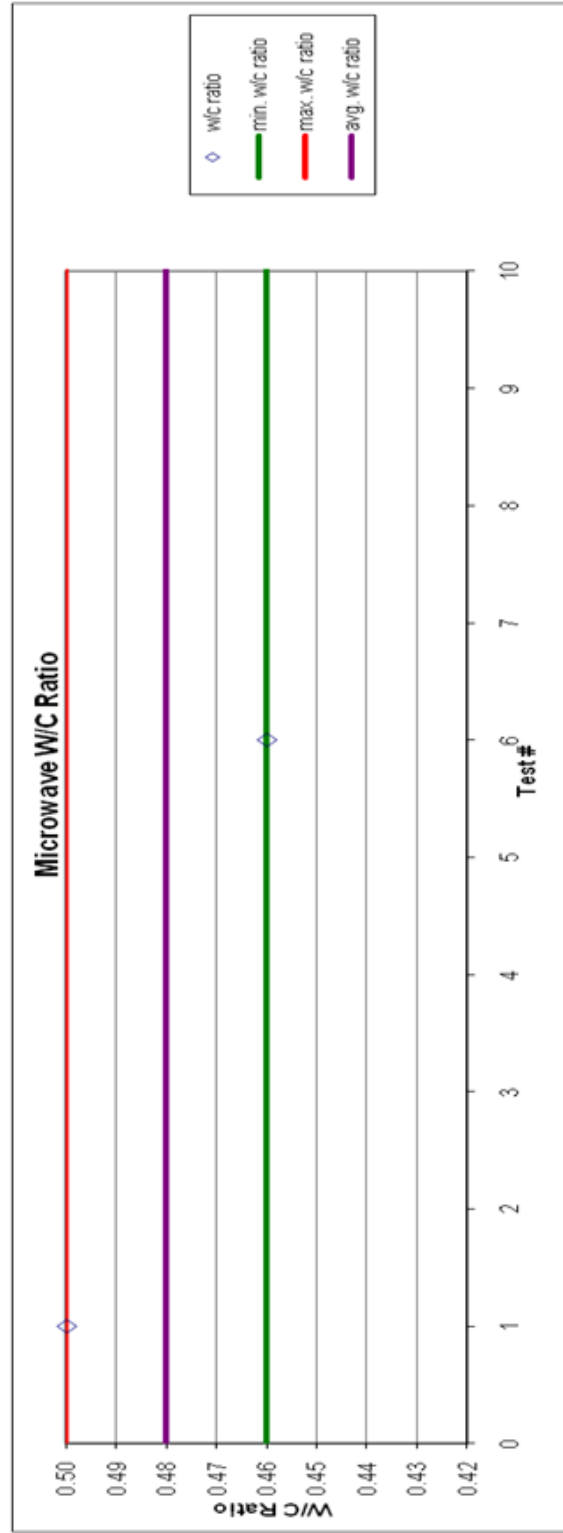
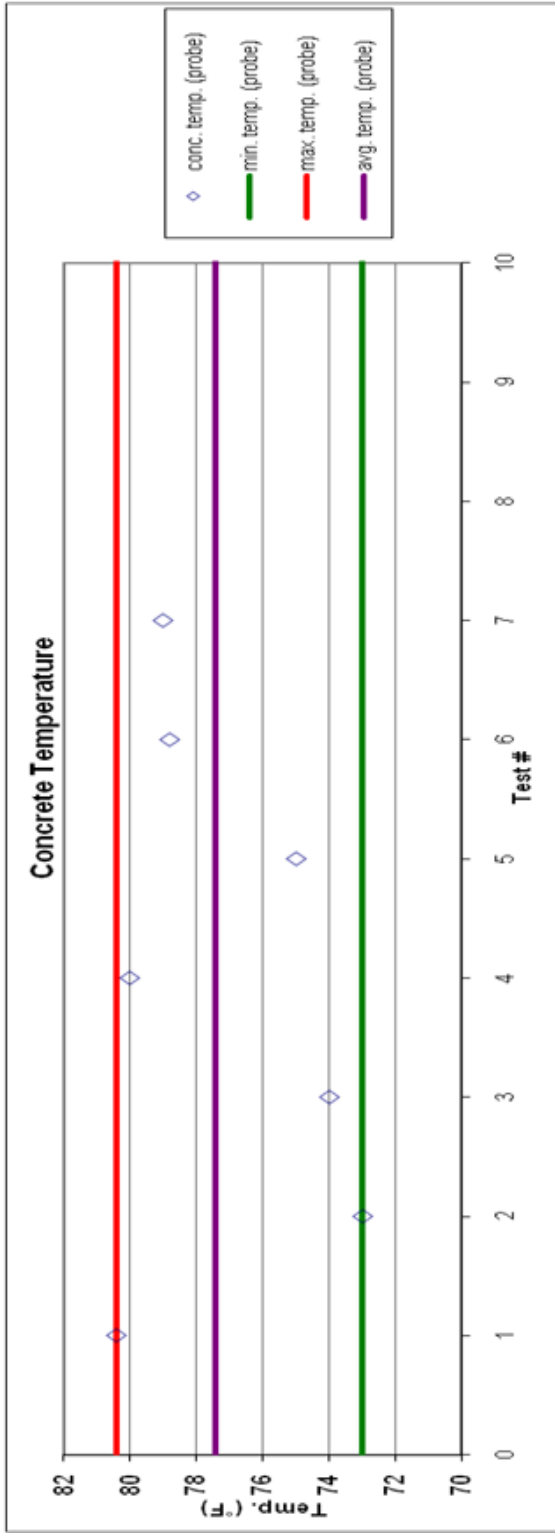
AVA Information	Absolute Volume (%)
Air Free Paste:	26.157%
Air Free Mortar:	54.215%

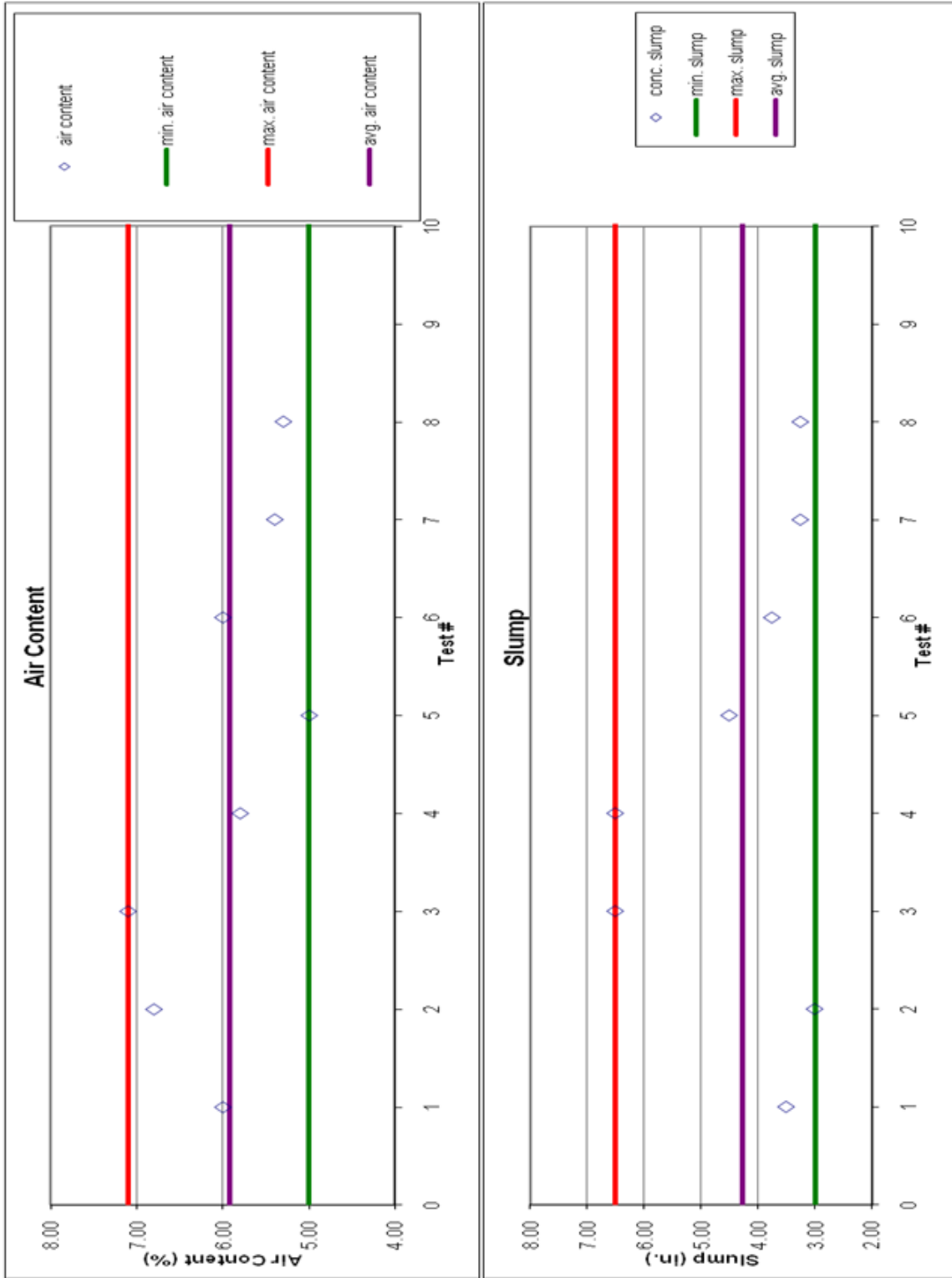


PA - Ternary Mixtures

S.R. 36 Section 20 Bridge Deck

Sample Information & Identification			Environmental Conditions				Fresh Concrete Workability Properties			Pressure Air
Sample Date	Sample Time	Sample Comments	Relative Humidity (%)	Ambient Temp. (°F)	Wind Speed (mph)	Conc. Temp. (probe) (°F)	Slump (in)	Unit Weight (lb/ft ³)	Microwave W/C Ratio (%)	% Air Content
14-Jul-10	7:20 AM	cp tech center sample taken at truck discharge	82.0	69.0	3.0	80.4	3.50	147.32	0.50	6.0
14-Jul-10	8:05 AM	PennDOT sample taken at pump discharge (quality control)	70.0	77.4	0.0	73.0	3.00	n/a	n/a	6.8
14-Jul-10	8:50 AM	PennDOT sample taken at pump discharge (acceptance test/quality control test)	75.0	75.4	0.0	74.0	6.50	n/a	n/a	7.1
14-Jul-10	8:50 AM	PennDOT sample taken at pump discharge (acceptance test/quality control test)	75.0	75.4	0.0	80.0	6.50	n/a	n/a	5.8
14-Jul-10	9:27 AM	PennDOT sample taken at pump discharge (quality assurance test)	77.0	74.6	0.0	75.0	4.50	n/a	n/a	5.0
14-Jul-10	9:30 AM	cp tech center sample taken at truck discharge	78.0	72.0	7.0	78.8	3.75	147.08	0.46	6.0
14-Jul-10	10:01 AM	PennDOT sample taken at pump discharge (quality control)	79.0	73.9	0.0	79.0	3.25	n/a	n/a	5.4
14-Jul-10	10:38 AM	PennDOT sample taken at pump discharge (quality control)	79.0	73.2	0.0	79.0	3.25	n/a	n/a	5.3







PA - Ternary Mixtures

Sample Information:

Project: SR 36 Section 20, Bridge Deck in Roaring Spring, Blair County, PA

Date: 14-Jul-10

Time: 7:20 AM

Type of Paving: Bridge Deck

Direction of Paving: n/a

Sta: n/a

Latitude: _____

Longitude: _____

Mix ID: _____

Truck IDs: _____

Sample Location Mark
& Comments: _____

Environmental Conditions:

Dew Point: 63.0

Relative Humidity: 82%

Wind Speed: 3.0

Ambient Temp.: 69.0

Concrete Properties:

Base/Soil Temp. (internal)(F): _____

Base Temp. (surface)(F): _____

Microwave Water Content Samples: _____

Calorimetry (ADIACAL Cylinders): 4 (7:53 am)

Set-Time (ASTMC403) Mortar Samples: _____

Cylinder for RCP & Perm. Voids Boil Test: use adiacal

Scaling Blocks: 3

Concrete Temp. (F): 80.4

Compressive, Tensile & MOR Cylinders: 30

Slump (in.): 3.50

Shrinkage Beams: 4

Air Content: 6.0%

Unit Weight (lb/ft³): 44.6



PA - Ternary Mixtures

Sample Information:

Project: SR 36 Section 20, Bridge Deck in Roaring Spring, Blair County, PA

Date: 14-Jul-10

Time: 9:30 AM

Type of Paving: Bridge Deck

Direction of Paving: n/a

Sta: n/a

Latitude: _____

Longitude: _____

Mix ID: _____

Truck IDs: _____

Sample Location Mark
& Comments: _____

Environmental Conditions:

Dew Point: 64.0

Relative Humidity: 78%

Wind Speed: 7.0

Ambient Temp.: 72.0

Concrete Properties:

Base/Soil Temp. (internal)(F): _____

Base Temp. (surface)(F): _____

Microwave Water Content Samples: _____

Calorimetry (ADIACAL Cylinders): 4 (10:00am)

Set-Time (ASTMC403) Mortar Samples: _____

Cylinder for RCP & Perm. Voids Boil Test: use adiacal

Scaling Blocks: n/a

Concrete Temp. (F): 78.8

Compressive, Tensile & MOR Cylinders: n/a

Slump (in.): 3.75

Shrinkage Beams: n/a

Air Content: 6.0%

Unit Weight (lb/ft³): 44.6

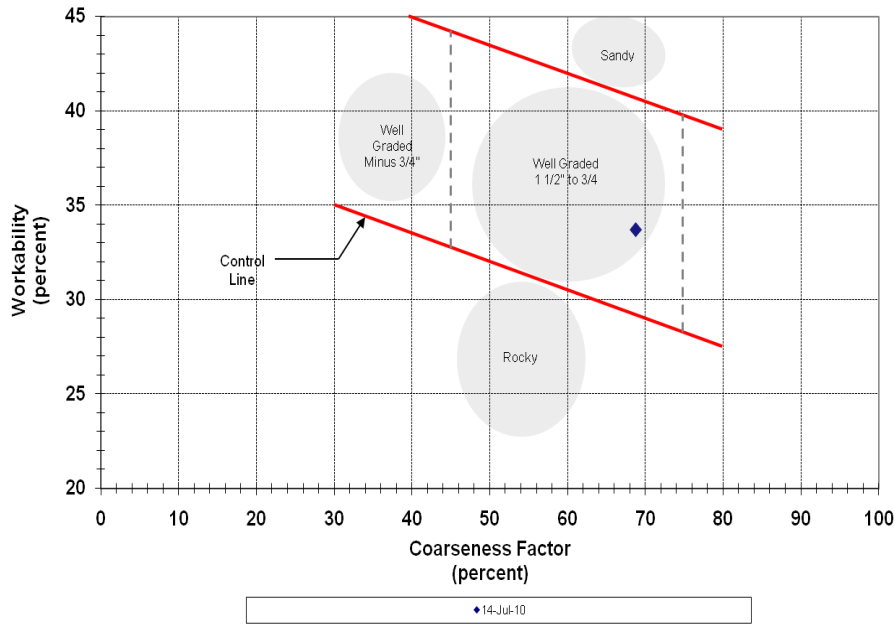
Project: Bridge Deck Paving in Roaring Spring, PA
 Mix ID: ECMS#21899
 Sample Comments:
 Test Date: 14-Jul-10

Total Cementitious Material: 587 lb/yd³
 Agg. Ratios: 59.00% 0.00% 41.00% 100.00%

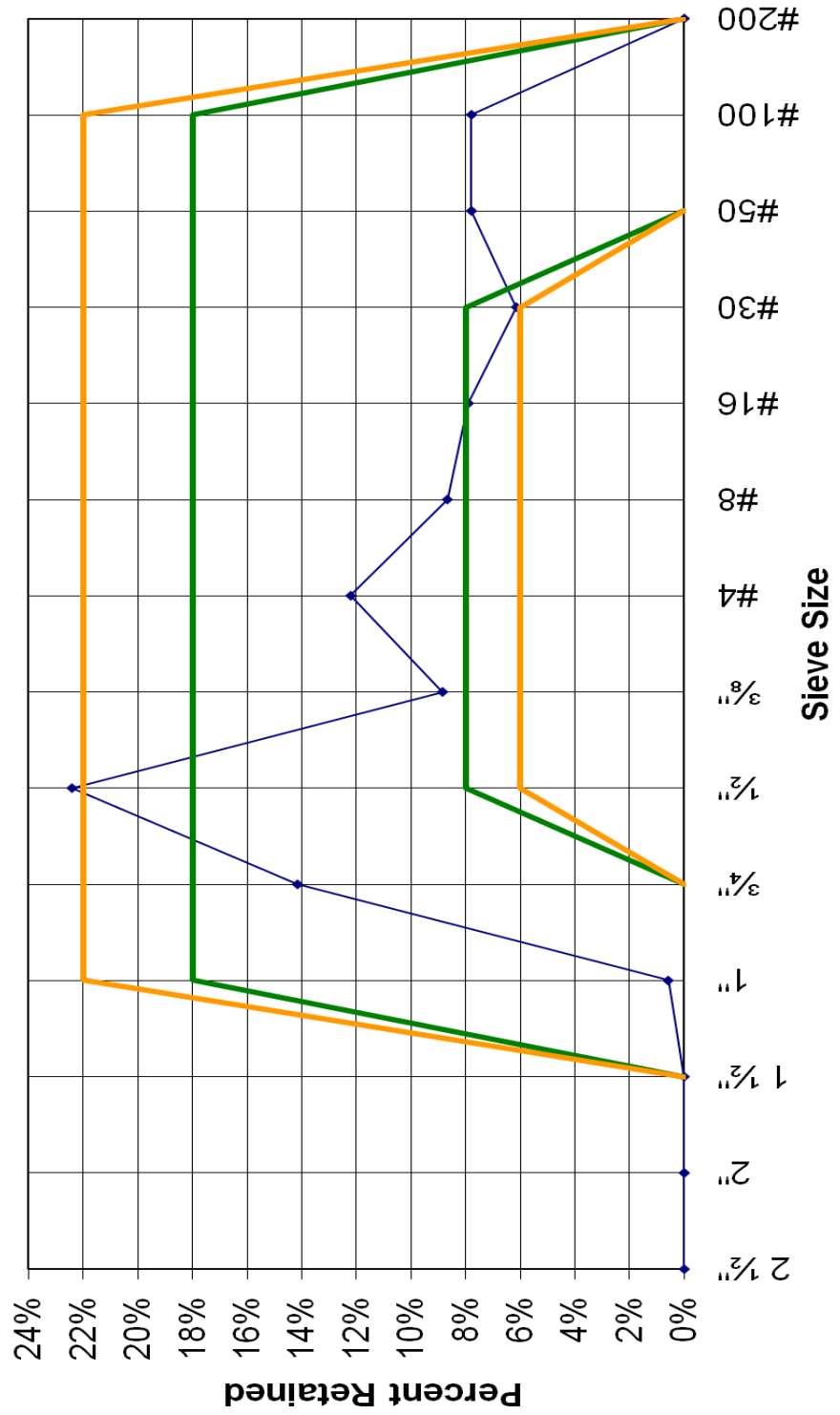
Sieve	Coarse	Intermediate	Fine #1	Fine #2	Combined % Retained	Combined % Retained On Each Sieve	Combined % Passing
2 1/2"	100%	0%	100%		0%	0%	100%
2"	100%	0%	100%		0%	0%	100%
1 1/2"	100%	0%	100%		0%	0%	100%
1"	99%	0%	100%		1%	1%	99%
3/4"	75%	0%	100%		15%	14%	85%
1/2"	37%	0%	100%		37%	22%	63%
3/8"	22%	0%	100%		46%	9%	54%
#4	2%	0%	99%		58%	12%	42%
#8	1%	0%	80%		67%	9%	33%
#16	1%	0%	60%		75%	8%	25%
#30	1%	0%	45%		81%	6%	19%
#50	1%	0%	26%		89%	8%	11%
#100	1%	0%	7%		97%	8%	3%
#200					100.0%		0.0%

Workability Factor: 33.7
 Coarseness Factor: 68.8

PA Ternary Mixtures
 Workability Factor & Coarseness Factor

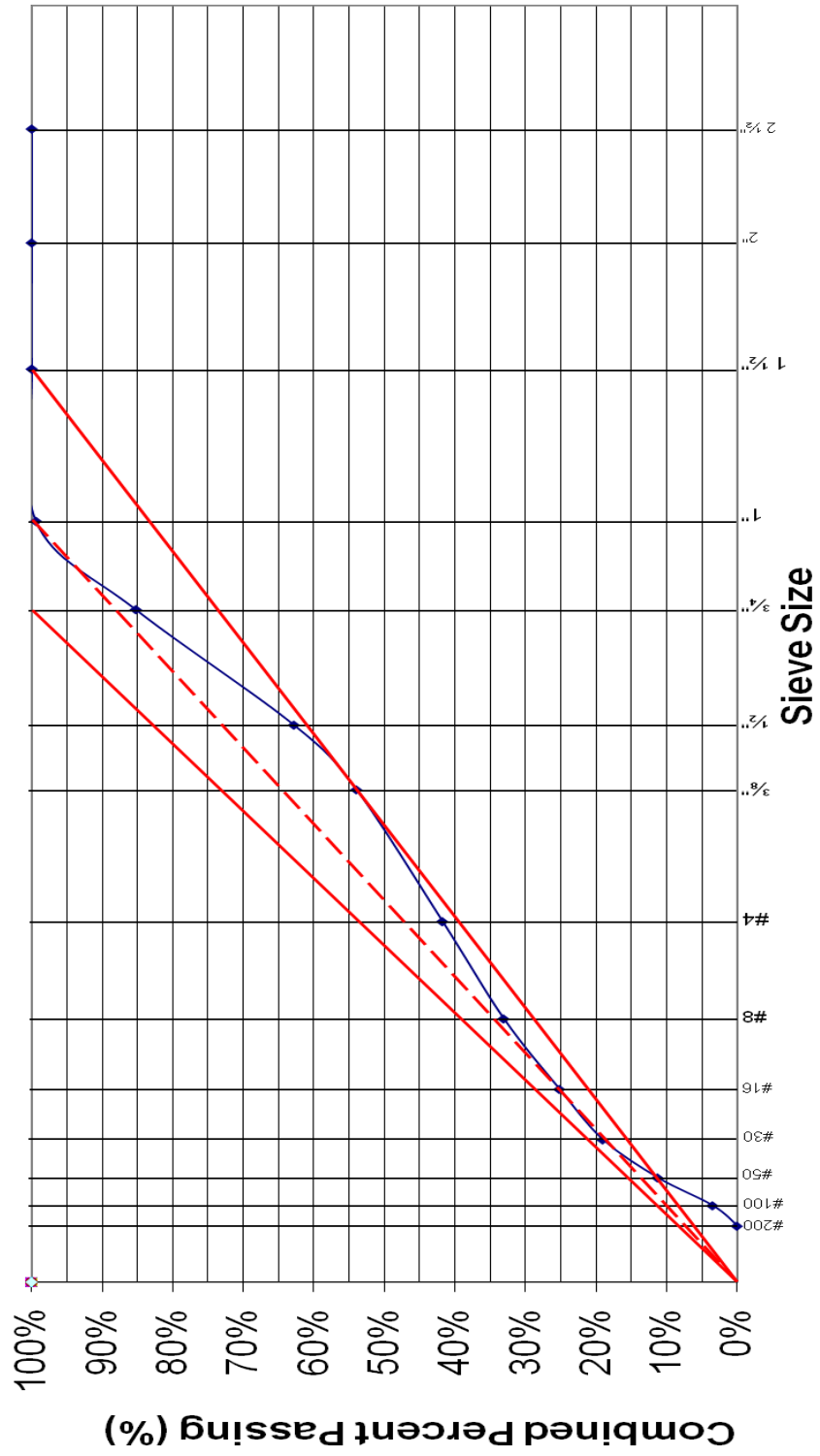


PA Ternary Mixtures
 Combined Percent Retained "8-18" & "6-22"



14-Jul-10

**PA Ternary Mixtures
0.45 Power Curve**



14-Jul-10



Pennsylvania - Ternary Mixtures

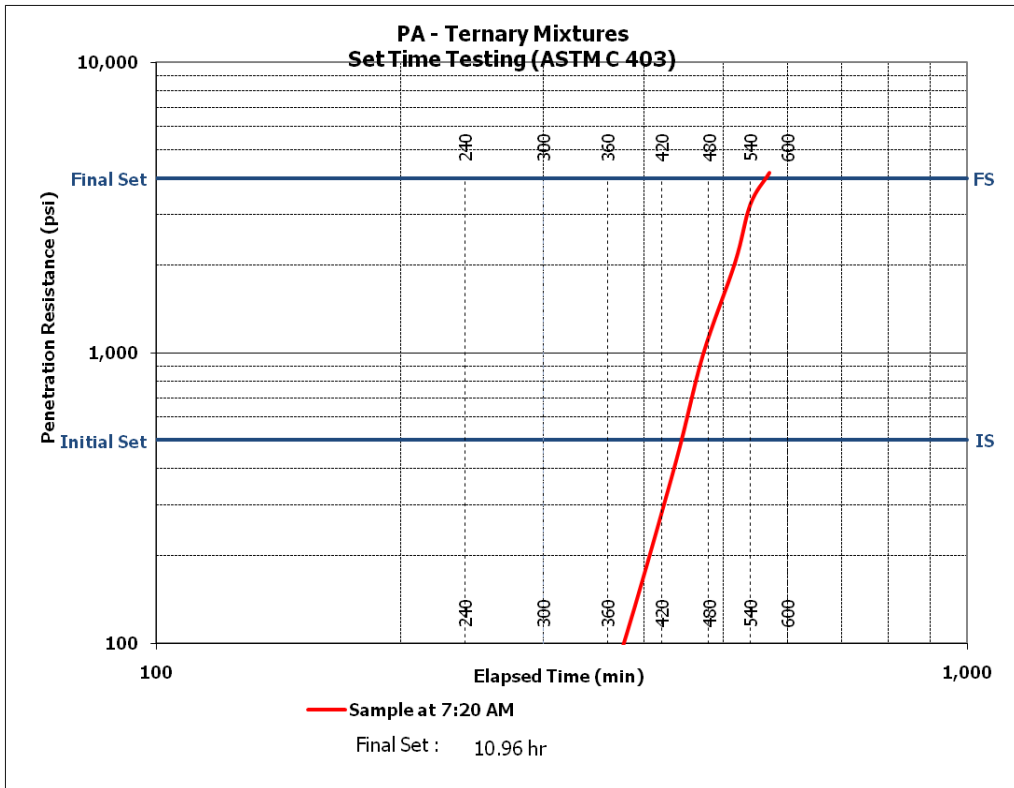
Set Time ASTM C 403

Project: SR 36 Section 20, Bridge Deck in Roaring Spring, Blair County, PA
 Date: 14-Jul-10 Start Time: 7:20 AM
 Sta: n/a

Test Data

Penetration Time (xx:xx-24 hr format)	Time (min)	Needle # (1,2,4,10,20 or 40)	Force (lb)	Penetration Resistance (psi)	Sample Temp. (°F)
12:50 PM	330.00	1	36	36.00	73.2
1:30 PM	370.00	2	42	84.00	74.7
2:35 PM	435.00	4	100	400.00	76.3
3:12 PM	472.00	10	98	980.00	78.1
3:57 PM	517.00	20	102	2040.00	77.9
4:20 PM	540.00	40	81	3240.00	77.9
4:50 PM	570.00	40	104	4160.00	77.4

Initial Set (at 500 psi PR)	estimated times using forecast function	218 minutes	3.63 hours
Final Set (at 4,000 psi PR)	using forecast function	658 minutes	10.96 hours





PA - Ternary Mixtures

Microwave Water Content Worksheet

Project: SR 36 Section 20, Bridge Deck in Roaring Spring, Blair County, PA
 Date: 14-Jul-10 Time: 7:20 AM
 Sta: n/a

Test Data

Mass of tray+cloth+block+fresh test sample, W_F (g)	3,722.3
Mass of tray+cloth+block, W_S (g)	2,198.3
Mass of tray+cloth+dry sample, W_D (g) (5mins)	3,686.7
Mass of tray+cloth+dry sample, W_D (g) (7 mins)	3,645.6
Mass of tray+cloth+dry sample, W_D (g) (9 mins)*	3,620.8
Mass of tray+cloth+dry sample, W_D (g) (11 mins)*	3,606.9
Mass of tray+cloth+dry sample, W_D (g) (13 mins)*	3,603.6
Mass of tray+cloth+dry sample, W_D (g) (15 mins)*	3,602.3
Mass of tray+cloth+dry sample, W_D (g) (17 mins)*	3,601.6
Mass of tray+cloth+dry sample, W_D (g) (Final)**	3,601.6
Water content percentage, W_C (%)	7.9%
Unit weight of fresh concrete, UW (lb/ft ³)* **	146.6
Total water content, W_T, (lb/yd³)	313.5
Total cementitious weight (lb/yd ³)	587
Fine aggregate weight (lb/yd ³)	1210
Coarse Aggregate weight (lb/yd ³)	1928
Intermediate Aggregate weight (lb/yd ³)	0
Fine aggregate absorption (%)	0.94%
Coarse aggregate absorption (%)	0.32%
Intermediate aggregate absorption (%)	0.00%
w/c	0.504

* If necessary (stop if the weight loss is less than 1g)

** Mass at test termination

***From unit weight test



Pennsylvania - Ternary Mixtures

Microwave Water Content Worksheet

Project: SR 36 Section 20, Bridge Deck in Roaring Spring, Blair County, PA
 Date: 14-Jul-10 Time: 9:30 AM
 Sta: n/a

Test Data

Mass of tray+cloth+block+fresh test sample, W_F (g)	3,786.1
Mass of tray+cloth+block, W_S (g)	2,198.0
Mass of tray+cloth+dry sample, W_D (g) (5mins)	3,753.3
Mass of tray+cloth+dry sample, W_D (g) (7 mins)	3,715.5
Mass of tray+cloth+dry sample, W_D (g) (9 mins)*	3,685.4
Mass of tray+cloth+dry sample, W_D (g) (11 mins)*	3,674.6
Mass of tray+cloth+dry sample, W_D (g) (13 mins)*	3,672.2
Mass of tray+cloth+dry sample, W_D (g) (15 mins)*	3,671.1
Mass of tray+cloth+dry sample, W_D (g) (17 mins)*	3,670.6
Mass of tray+cloth+dry sample, W_D (g) (Final)**	3,670.6
Water content percentage, W_C (%)	7.3%
Unit weight of fresh concrete, UW (lb/ft ³)* **	146.6
Total water content, W_T, (lb/yd³)	287.9
Total cementitious weight (lb/yd ³)	587
Fine aggregate weight (lb/yd ³)	1210
Coarse Aggregate weight (lb/yd ³)	1928
Intermediate Aggregate weight (lb/yd ³)	0
Fine aggregate absorption (%)	0.94%
Coarse aggregate absorption (%)	0.32%
Intermediate aggregate absorption (%)	0.00%
w/c	0.461

* If necessary (stop if the weight loss is less than 1g)

** Mass at test termination

***From unit weight test



ASTM C 1202-97



Test-compagny
Testing street 45
CompagnyCity
Some Country

Your own logo,
size=20x80mm



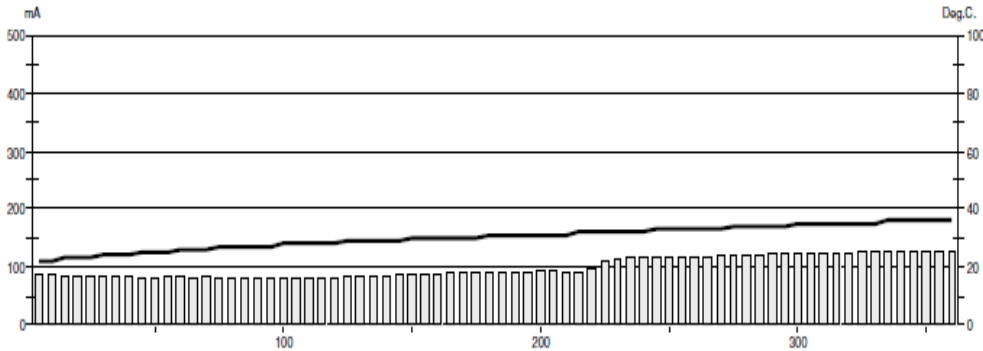
GERMANN INSTRUMENTS

DENMARK
Phone: +45 3907 7117
Fax: +45 3907 3107

USA
Phone: (547)329-8999
Fax: (547)329-8988

Test report

Voltage Used: 60
Testing time: 06:00 hour
Charge passed: 2144
Adjusted Charge passed: 1860
Permeability class: Low
Instrument number: 023907
Channel number: 1
Report date: 8/27/2010
Testing by:
Reference: PA TERN #1
Sample diameter: 102
Comment: ---



Time	°C	mA	Time	°C	mA	Time	°C	mA	Time	°C	mA
00:05	22	86.6	01:35	27	80.5	03:05	31	90.3	04:35	34	120.0
00:10	22	86.5	01:40	28	80.3	03:10	31	91.3	04:40	34	120.7
00:15	23	85.4	01:45	28	79.7	03:15	31	91.2	04:45	34	121.1
00:20	23	84.3	01:50	28	80.6	03:20	31	93.2	04:50	34	122.0
00:25	23	84.6	01:55	28	79.7	03:25	31	94.1	04:55	34	122.1
00:30	24	84.4	02:00	28	79.6	03:30	31	91.7	05:00	35	123.0
00:35	24	84.5	02:05	29	81.5	03:35	32	92.4	05:05	35	123.1
00:40	24	85.2	02:10	29	84.3	03:40	32	97.8	05:10	35	123.3
00:45	25	81.0	02:15	29	84.9	03:45	32	112.2	05:15	35	123.8
00:50	25	80.8	02:20	29	85.8	03:50	32	114.3	05:20	35	123.7
00:55	25	81.5	02:25	29	87.2	03:55	32	115.4	05:25	35	123.9
01:00	26	81.5	02:30	30	86.6	04:00	32	115.9	05:30	35	124.8
01:05	26	80.7	02:35	30	87.5	04:05	33	117.0	05:35	36	125.4
01:10	26	81.5	02:40	30	87.7	04:10	33	117.4	05:40	36	125.9
01:15	27	80.3	02:45	30	89.8	04:15	33	118.0	05:45	36	125.4
01:20	27	80.5	02:50	30	89.1	04:20	33	118.8	05:50	36	125.1
01:25	27	80.7	02:55	30	89.6	04:25	33	119.0	05:55	36	125.4
01:30	27	79.6	03:00	31	88.8	04:30	33	119.5	06:00	36	126.9



ASTM C 1202-97



Test-compagny
Testing street 45
CompagnyCity
Some Country

Your own logo.
size=20x80mm



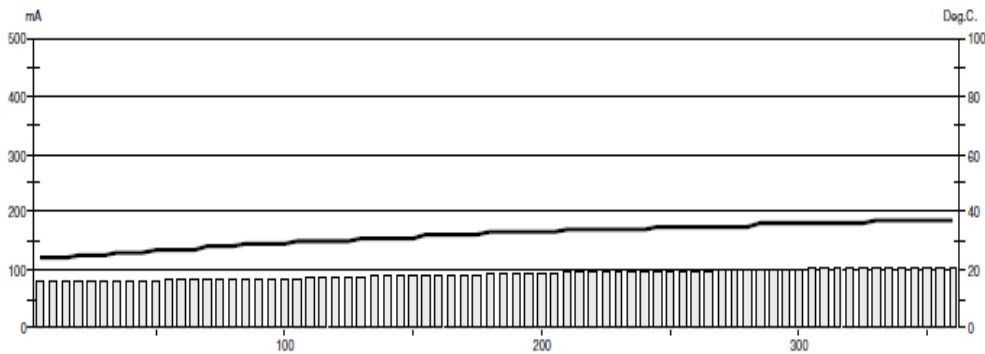
GERMANN INSTRUMENTS

DENMARK
Phone: +45 3967 7117
Fax: +45 3967 3167

USA
Phone: (847)329-9999
Fax: (847)329-8888

Test report

Voltage Used: 60
Testing time: 06:00 hour
Charge passed: 1995
Adjusted Charge passed: 1731
Permeability class: Low
Instrument number: 023907
Channel number: 2
Report date: 8/27/2010
Testing by:
Reference: PA TERN #2
Sample diameter: 102
Comment: ---



Time	°C	mA	Time	°C	mA	Time	°C	mA	Time	°C	mA
00:05	24	80.0	01:35	29	85.2	03:05	33	93.4	04:35	35	100.0
00:10	24	80.3	01:40	29	85.7	03:10	33	94.0	04:40	35	100.2
00:15	24	79.7	01:45	30	85.9	03:15	33	94.4	04:45	36	100.4
00:20	25	79.4	01:50	30	86.3	03:20	33	94.4	04:50	36	100.8
00:25	25	80.0	01:55	30	86.7	03:25	33	94.7	04:55	36	101.2
00:30	25	80.3	02:00	30	87.2	03:30	34	95.1	05:00	36	101.5
00:35	26	80.3	02:05	30	87.5	03:35	34	95.4	05:05	36	101.6
00:40	26	80.2	02:10	31	88.0	03:40	34	95.9	05:10	36	102.0
00:45	26	80.1	02:15	31	88.5	03:45	34	96.8	05:15	36	102.4
00:50	27	81.0	02:20	31	89.0	03:50	34	97.2	05:20	36	102.5
00:55	27	81.7	02:25	31	89.8	03:55	34	97.3	05:25	36	102.9
01:00	27	82.4	02:30	31	90.0	04:00	34	97.3	05:30	37	103.0
01:05	27	82.9	02:35	32	90.3	04:05	35	97.5	05:35	37	103.3
01:10	28	83.4	02:40	32	90.8	04:10	35	97.8	05:40	37	103.8
01:15	28	83.8	02:45	32	91.2	04:15	35	98.3	05:45	37	104.0
01:20	28	84.3	02:50	32	91.6	04:20	35	98.9	05:50	37	104.2
01:25	29	84.6	02:55	32	92.3	04:25	35	99.1	05:55	37	104.5
01:30	29	85.0	03:00	33	92.9	04:30	35	99.7	06:00	37	104.4



Figure 1 State Route 36 Section 20 bridge deck.

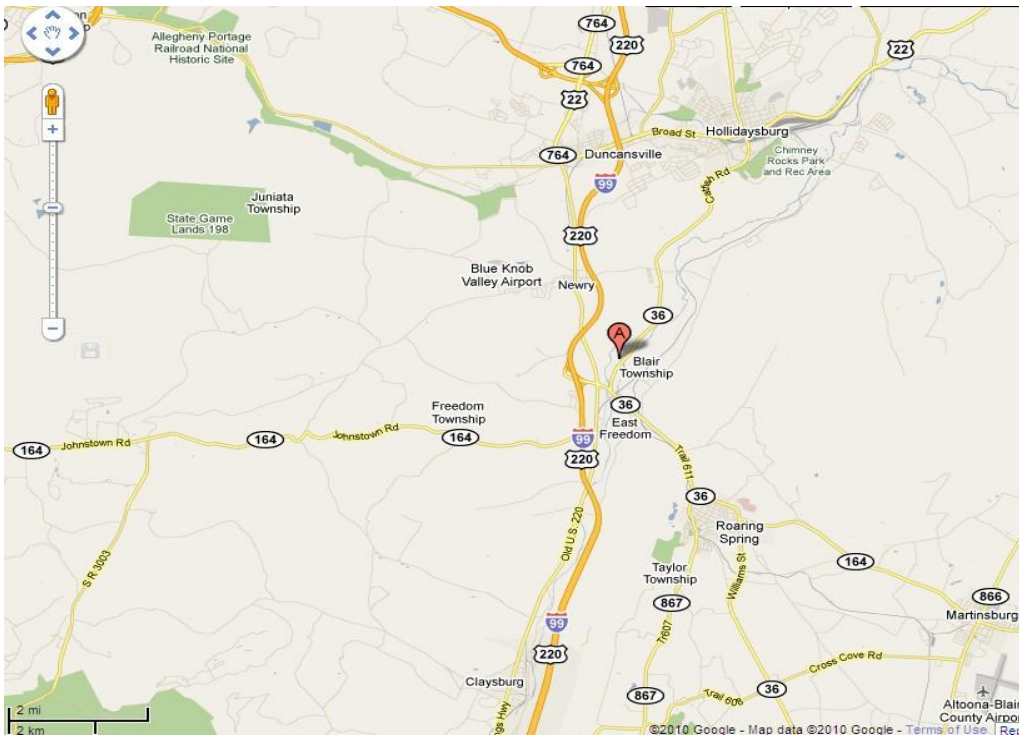


Figure 2 Project and mobile lab location.

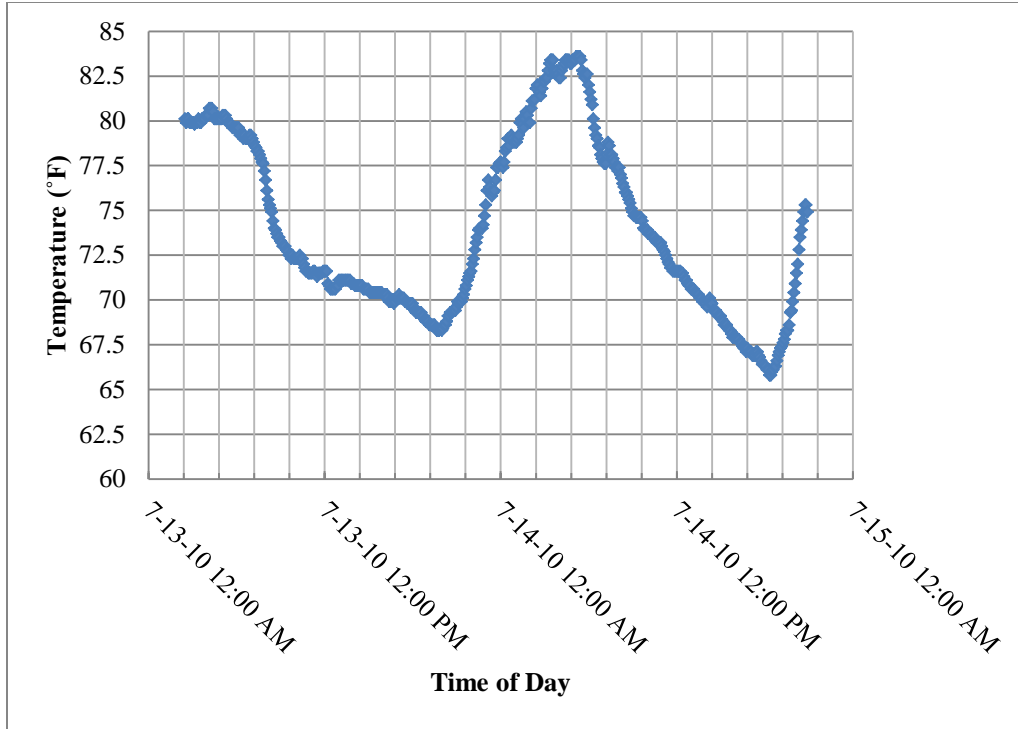


Figure 3 Ambient temperature versus time of day.

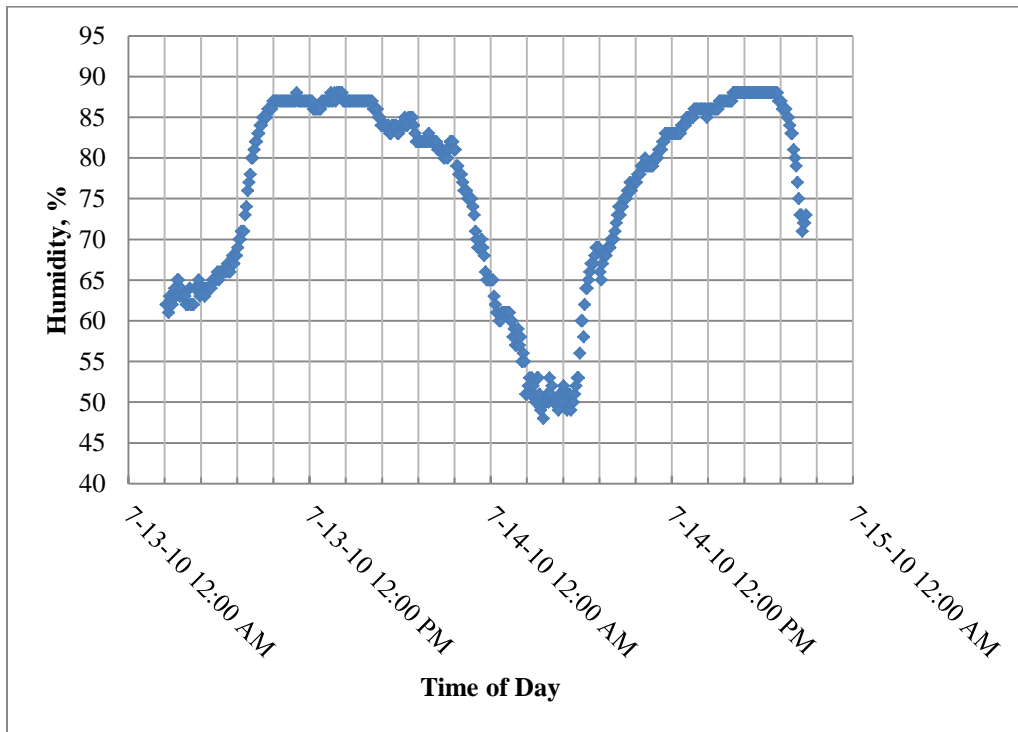


Figure 4 Relative humidity versus time of day.

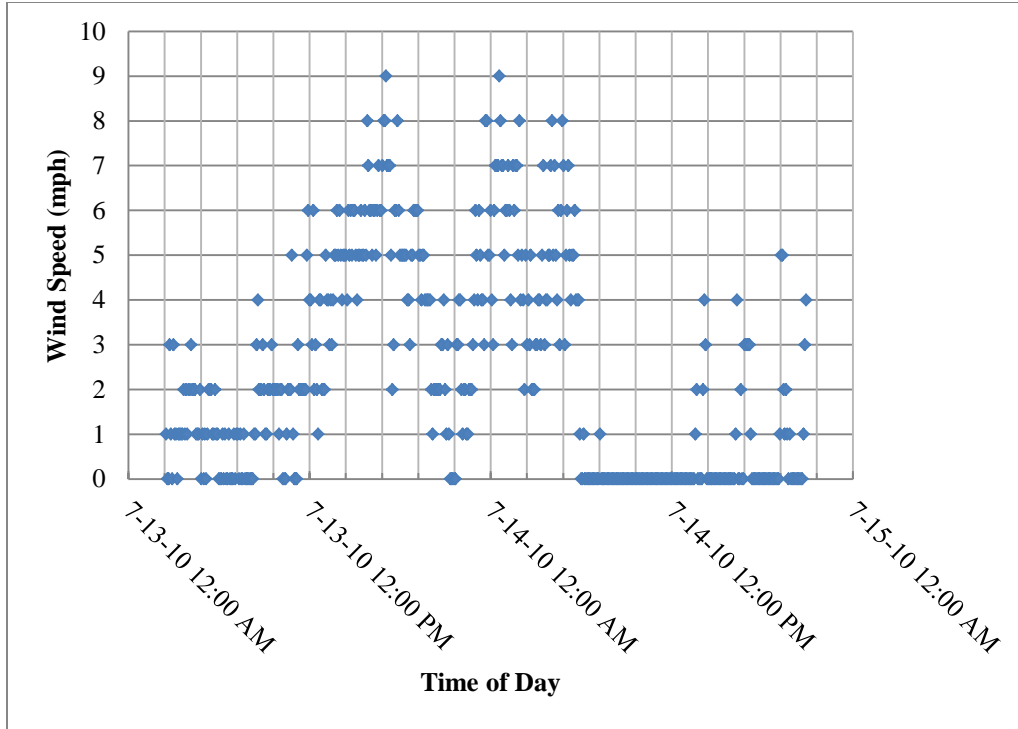


Figure 5 Wind speed versus time of day.



Figure 6 Concrete being tested by Penn DOT technicians .



Figure 7 Concrete being spread by construction crews.



Figure 8 Concrete being tested by CP Tech Center technician PCC mobile lab.



Figure 9 PCC mobile lab.



Figure 10 Concrete being finished.



Figure 11 Two i-buttons being embeded on site.



Figure 12 Concrete being vibrated.



Figure 13 Concrete temperature being tested by sensor.



Figure 14 Bridge deck surface at four months after being constructed.



Figure 15 Bridge deck surface at four months after being constructed.

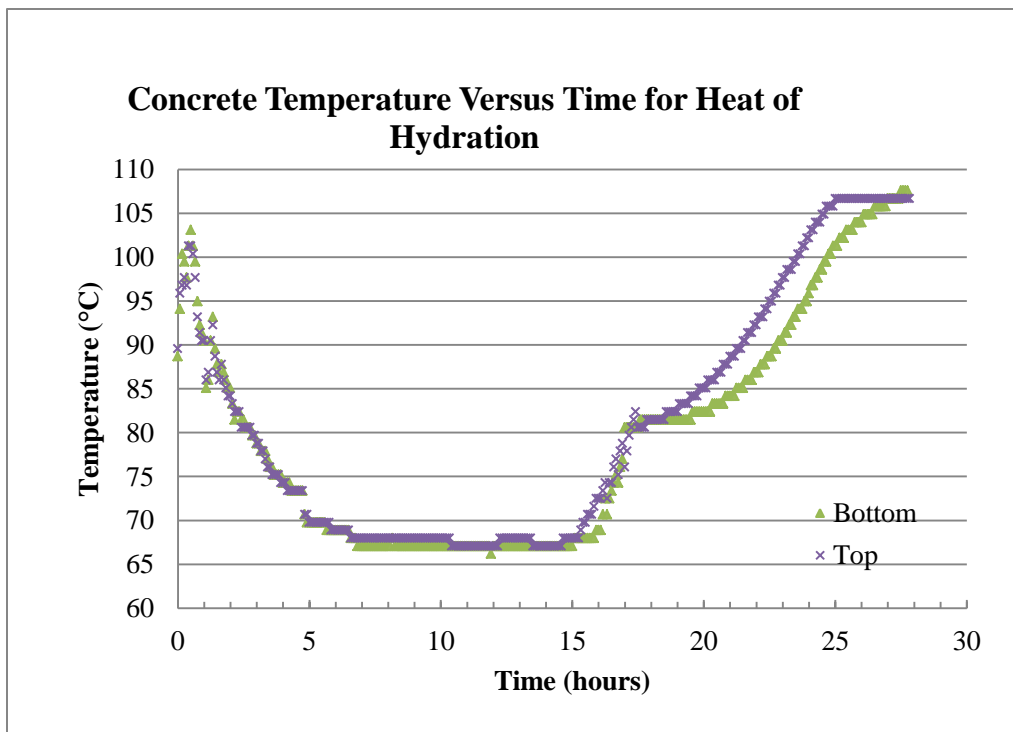


Figure 16 (a) Concrete temperatures versus time for heat of hydration.

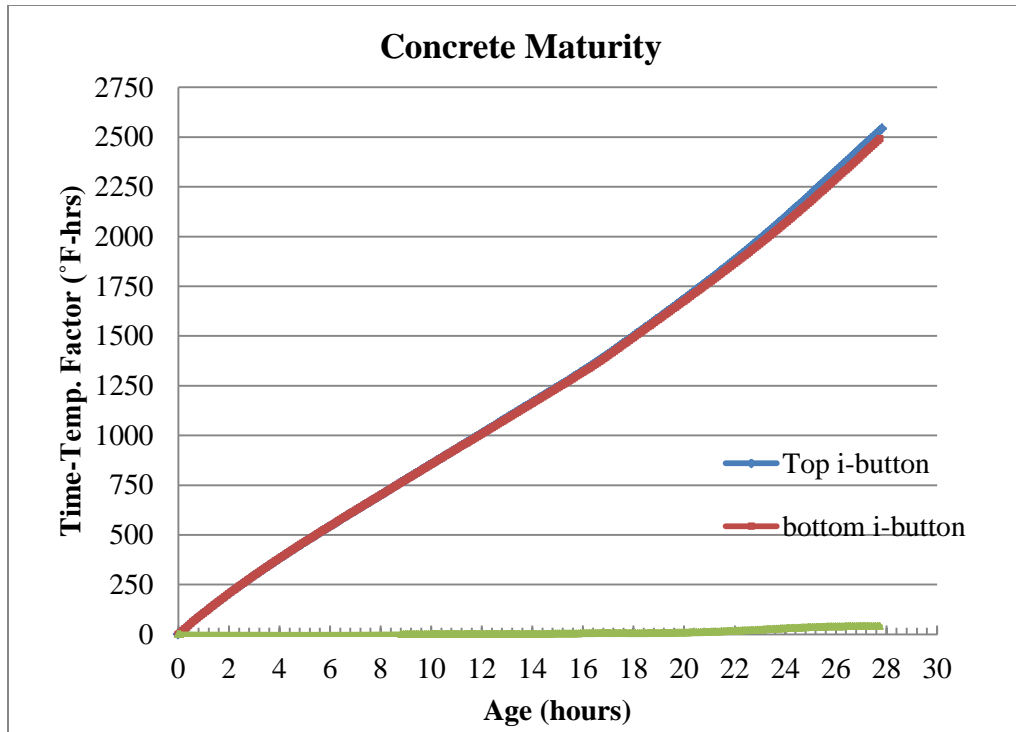


Figure 16 (b) Concrete maturity.

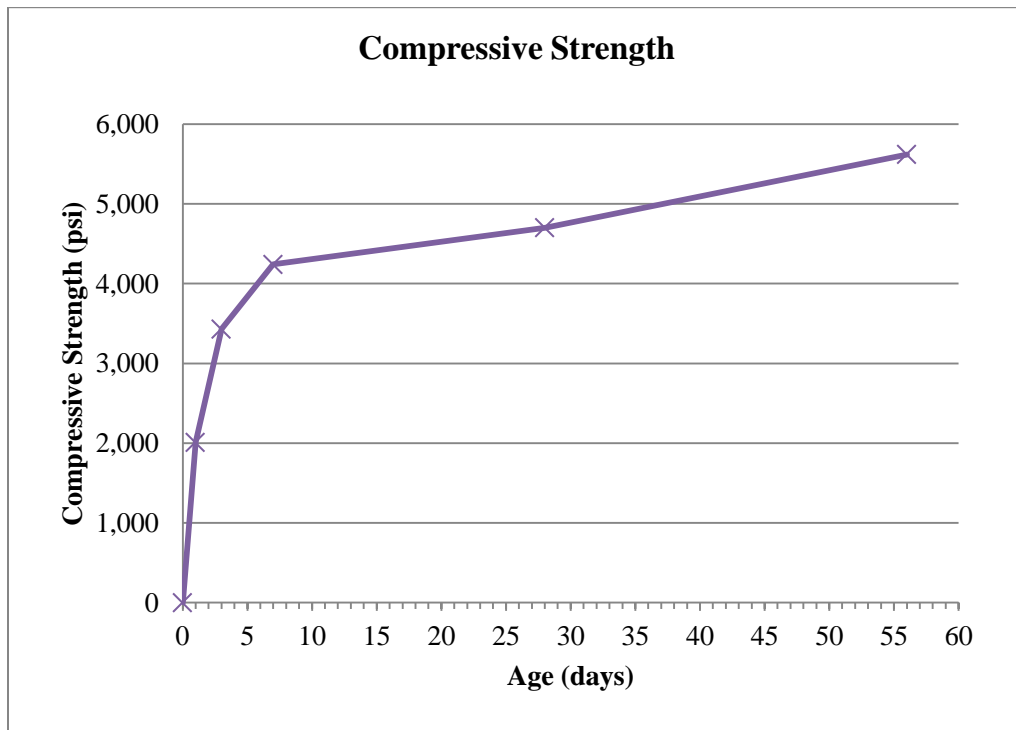


Figure 17 Compressive strength development with time.

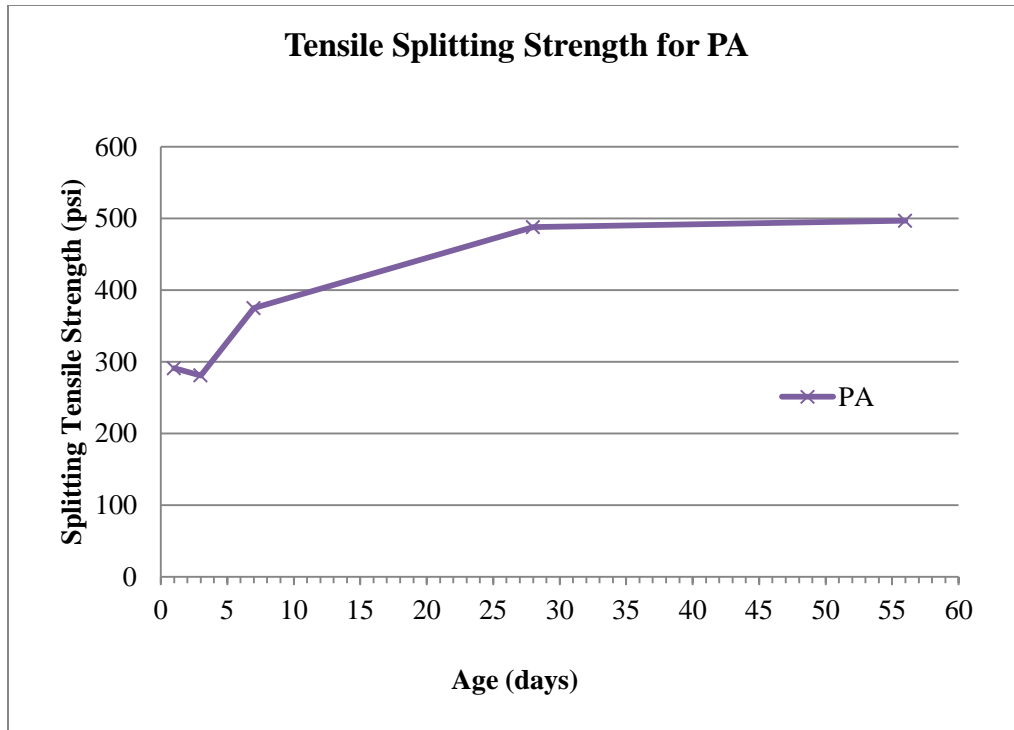


Figure 18 Tensile splitting strength development with time.

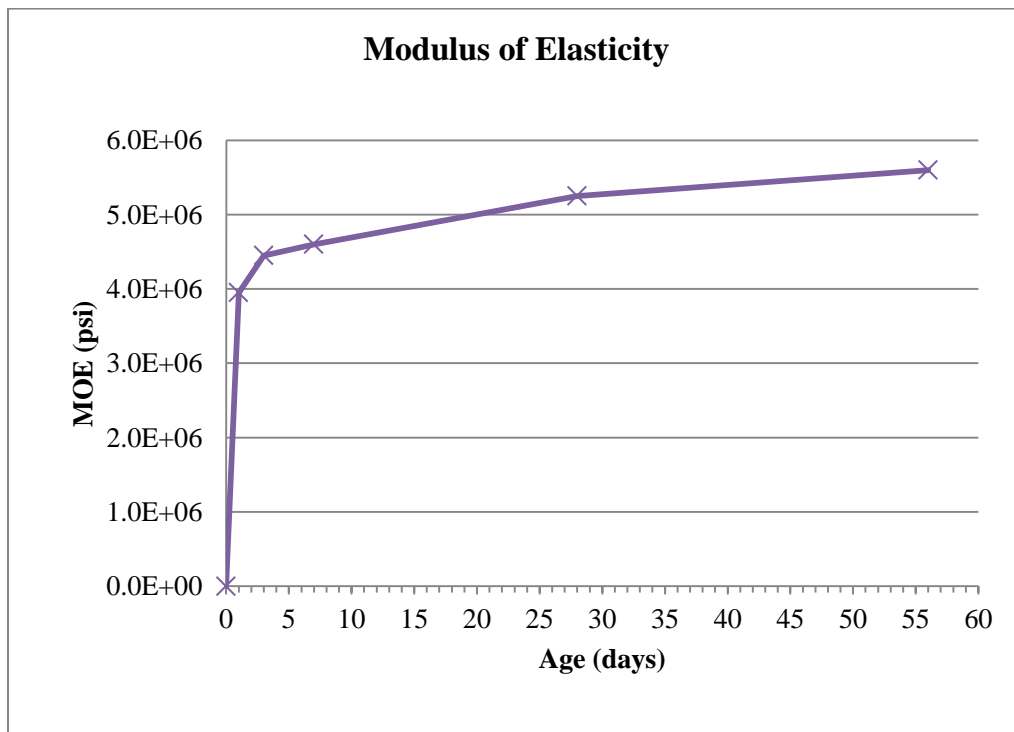


Figure 19 Modulus of elasticity development with time.

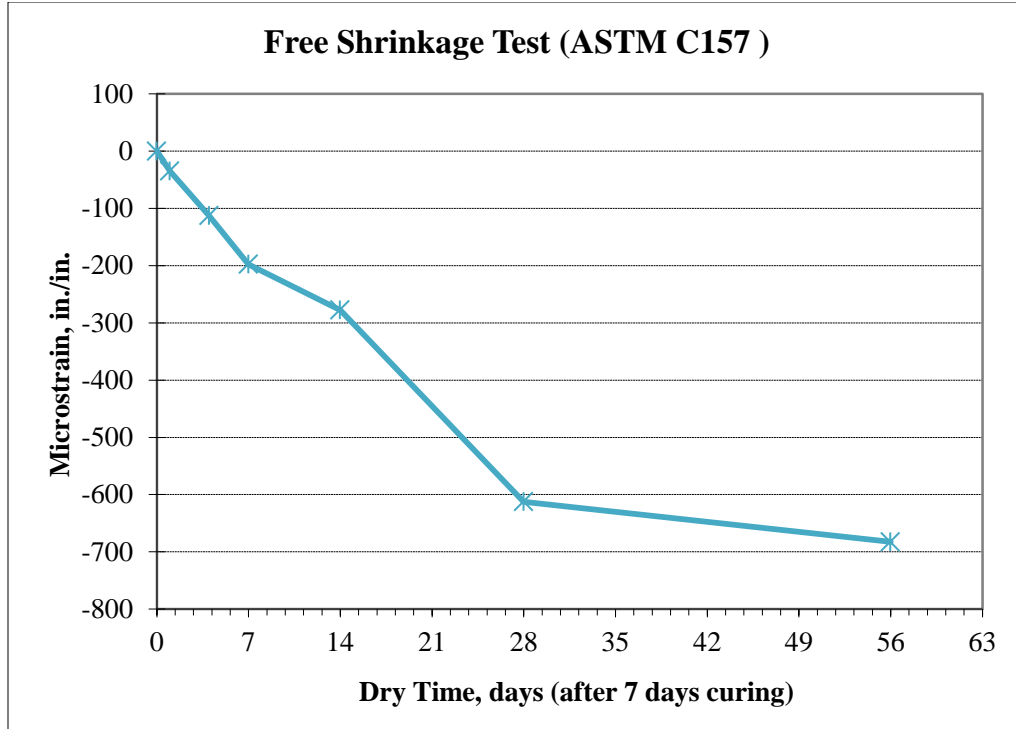


Figure 20 Free shrinkage of prisms (ASTM C 157).

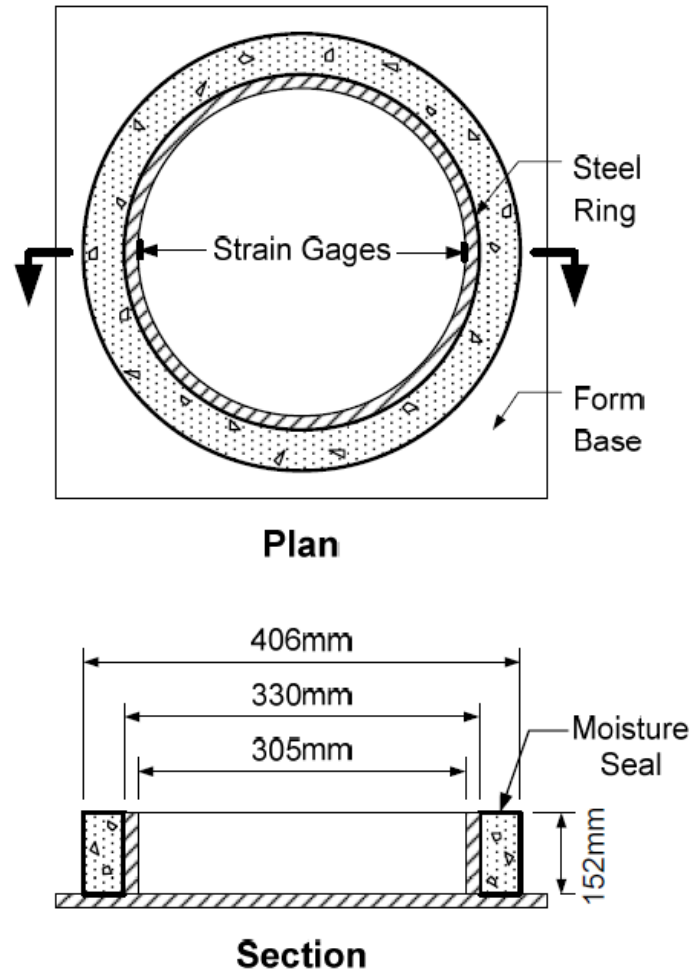


Figure 21 Configuration of restrained concrete ring samples.

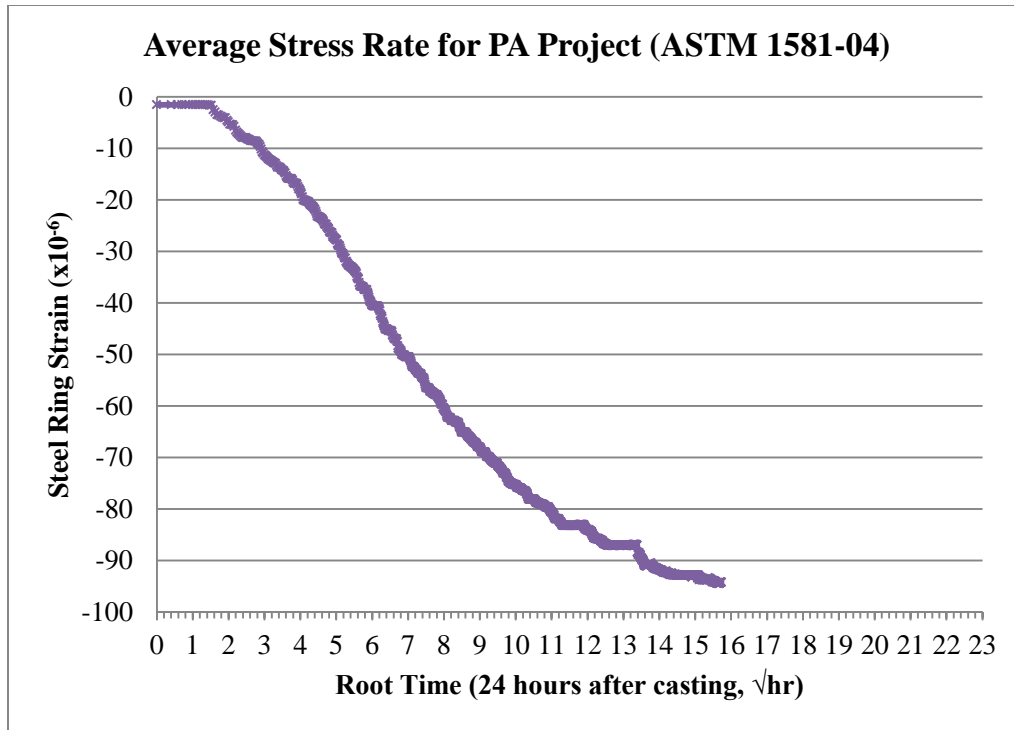


Figure 22 Strains of steel rings resulting from concrete shrinkage.



Figure 23 PA salt scaling sample after 50th freeze-thaw cycle.

Table 1 Ambient conditions of S.R. 36 Section 20 Bridge Deck Project

PA - Ternary Mixtures
S.R. 36 Section 20 Bridge Deck

Sample Information & Identification			Environmental Conditions			
Sample Date	Sample Time	Sample Comments	Relative Humidity (%)	Ambient Temp. (°F)	Wind Speed (mph)	Conc. Temp. (probe) (°F)
14-Jul-10	7:20 AM	cp tech center sample taken at truck discharge	82.0	69.0	3.0	80.4
14-Jul-10	8:05 AM	PennDOT sample taken at pump discharge (quality control)	70.0	77.4	0.0	73.0
14-Jul-10	8:50 AM	PennDOT sample taken at pump discharge (acceptance test/quality control test)	75.0	75.4	0.0	74.0
14-Jul-10	8:50 AM	PennDOT sample taken at pump discharge (acceptance test/quality control test)	75.0	75.4	0.0	80.0
14-Jul-10	9:27 AM	PennDOT sample taken at pump discharge (quality assurance test)	77.0	74.6	0.0	75.0
14-Jul-10	9:30 AM	cp tech center sample taken at truck discharge	78.0	72.0	7.0	78.8
14-Jul-10	10:01 AM	PennDOT sample taken at pump discharge (quality control)	79.0	73.9	0.0	79.0
14-Jul-10	10:38 AM	PennDOT sample taken at pump discharge (quality control)	79.0	73.2	0.0	79.0

Table 2 Properties of hardened concrete

Tests	Results		
7-day Compressive Strength, psi	4240		
28-day Compressive Strength, psi	4700		
Rapid Chloride Permeability, Coulombs	Sample 1 1860	Sample 2 1731	Average 1796
Strength Development 28/7 day fc Ratio	1.11		
Shrinkage Microstrain @ 28 days, in/in	612.5		
Average Stress Rate by Restrained Ring Test, psi/day	55.35		

Table 3 Summation of strength and modulus of elasticity

Location	Age, days	Compressive Strength, psi	Splitting Tensile Strength, psi	Modulus Of Elasticity, psi
PA	1	2,010	291	3.95E+06
	3	3,430	281	4.45E+06
	7	4,240	375	4.60E+06
	28	4,700	488	5.25E+06
	56	5,620	497	5.60E+06

Table 4 Free shrinkage test results

PA Project Free Shrinkage Test (ASTM C 157)						
Dry Time	Beam 1 change%	Beam 2 change %	Beam 3 change %	Beam 4 change %	Average	Microstrain
1	-0.002	-0.005	-0.004	-0.003	-0.003	-35
4	-0.010	-0.012	-0.010	-0.013	-0.011	-112.5
7	-0.019	-0.020	-0.019	-0.021	-0.020	-197.5
14	-0.026	-0.025	-0.031	-0.029	-0.028	-277.5
28	-0.061	-0.062	-0.064	-0.058	-0.061	-612.5
56	-0.070	-0.068	-0.065	-0.070	-0.068	-682.5

Table 5 Cracking potential and average stress rate (ASTM C 1581)

Cracking Potential for PA Project (ASTM C 1581)			
	Ring 1	Ring 2	Ring 3
Strain Rate Factor (in./in.x10 ⁻⁶)/hours ^{1/2}	-7.86	-5.56	-7.37
G (psi)	10.47x106	10.47x106	10.47x106
Absolute Value of α_{avg} (in./in.10 ⁻⁶)/day ^{1/2}	33.95		
Elapsed Time, tr (hours)	270.0	270.0	210.0
Elapsed Time, tr (days)	11.3	11.3	8.8
Stress Rate, q (psi/day) $q=GI\alpha_{avg}I/2\sqrt{t_r}$	53.0	53.0	60.1
Average Stress Rate, q (psi/day) $q=GI\alpha_{avg}I/2\sqrt{t_r}$	55.35		
Potential for cracking classification (ASTM 1581)	High (50 ≤ q)		

Table 6 Salt scaling test visual condition of specimen

PA Salt Scaling Samples	Condition of Surface					
	Cycle 5	Cycle 10	Cycle 15	Cycle 20	Cycle 25	Cycle 50
No. 1	1	1	1	2	2	2
No. 2	1	1	1	2	2	2
No. 3	1	1	1	2	2	2

POOLED FUND STUDY
UNITED STATES DEPARTMENT OF TRANSPORTATION
FEDERAL HIGHWAY ADMINISTRATION



DEVELOPMENT OF PERFORMANCE PROPERTIES OF TERNARY MIXTURES

**A Field Application of Ternary Mixtures
-An experience in construction of a bridge
deck project in Epsom, NH**

August 2010

U OF UTAH IOWA STATE UNIVERSITY


THE UNIVERSITY OF UTAH

National Concrete Pavement
Technology Center

Tech Center

Introduction

This document is a report of the activities and observations of a research team that performed on-site testing of a ternary mixture placed on a small bridge in Epsom, New Hampshire. The cementitious system comprised a Type II cement, Grade 120 slag cement, and Class F fly ash. The purpose of this research project is a comprehensive study of how supplementary cementitious materials (SCMs) can be used to improve the performance of concrete mixtures when used in ternary blends. This is the third phase of a project which intends to provide consulting to states and contractors on the use and field management of ternary mixtures. A state-of-the-art 44-foot long PCC mobile laboratory equipped for on-site cement and concrete testing was provided by the CP Tech Center to collect data and field observations.

Project Information

- The project was advertised in September 2009 for construction during 2010.
- Project No. Epsom 15266
- Located on NH Route 107, approximately thirteen miles east of Concord and one mile south of US Route 4.
- Contractor: Southern NH Poured Concrete Const., Inc.
- Bridge is situated on a low volume, two-lane rural road with 20 feet long by 30 feet wide.
- Bridge deck placement (the slab on the right with form using ternary mixture while left one using conventional binary mix for comparison purpose) (Figure 1)

Site Location

An area at the bridge site was prepared by the contractor for the PCC mobile lab. The location of the project site and the mobile lab is shown Figure 2.

Sampling and Testing Activities

The mobile lab arrived on site on August 9, 2010. Concrete placement, sampling and testing took place on August 10, 2010. Hardened samples were transported to Iowa State

University on August 14, 2010, for further testing. The following tests were conducted either in the field or in the laboratory:

- Calorimetry test (ASTM C 1679)
- Slump, unit weight, temperature and air content of fresh concrete – 1 test (ASTM C 143, ASTM C 138, ASTM C 231)
- Microwave w/c ratio – 1 test (AASHTO T 318)
- Initial set and final set of concrete – 1 test (ASTM C 403)
- Compressive strength, splitting tensile strength, static modulus of elasticity - 4” x 8” cylinders at 1-day, 3-days, 7-days, 28-days, and 56-days (ASTM C 39, ASTM C 496, ASTM C 469)
- Rapid chloride permeability - 4” x 8” cylinders at 56 days (ASTM C 1202)
- Salt scaling – 3 samples (ASTM C 672)
- Free shrinkage test – 3 beams (ASTM C 157)
- Restrained rings – 4 samples (ASTM C 1581)
- Two i-buttons are buried on top and bottom layer of reinforcement to investigate maturity of concrete. (ASTM C 1074)

Observations of the Research Team

The following observations were made in this field testing:

- The structure was originally designed to have a bituminous concrete wearing course, but the designer had revised it to have a bare deck for long-term observation purposes.
- The deck thickness was 23 inches. The cover for top mat of epoxy coated steel was approximately 5 1/8 inches and cover for bottom mat of steel is 1 ½ inches.
- Removable wood formwork was used in the deck construction.
- All concrete was delivered in three concrete ready-mix trucks. During construction process, ready-mix trucks dumped concrete into bridge deck. Concrete was manually spread out and vibrated by the construction crew.

- The mix design was prepared by Southern NH Poured Concrete Co, and approved by New Hampshire Department of Transportation. The mix proportions are given in the project data section.
- The State of New Hampshire has alkali reactive aggregate, therefore the specifications require mixes to contain 50% slag or fly ash unless the aggregate has been tested to determine the required percentage to mitigate ASR. Most of suppliers presently use fly ash from Brayton Point, MA. 50% replacement of combined Grade 120 slag cement and Class F fly ash were used as supplementary cementitious material. Strux 90/40 polymer fibers were also used at a dosage of 7 lb/cubic yard.
- According to the workability factor & coarseness factor graph (Page 21) combined aggregate gradation for this project falls in the well-graded region. Similarly, the combined percent retained curve (Page 22) indicates a well graded system.
- The weather conditions recorded by the PCC mobile lab are given in Table 1 and in Figures 3 to 5. The relative humidity ranged from 72% to 79%; the ambient temperature ranged from 71.8°F to 74.4 °F; the wind speed varied from 1 mph to 3 mph; the concrete temperature ranged from 80 °F to 83 °F during the recorded period.
- The fresh concrete tests include slump cone, unit weight, and water-cementitious materials ratio by microwave. During the construction, one set of samples was tested by CP Tech Center crew and four sets of testing were performed by NHDOT crew. Slump result was varied from 3.0 inches to 5.5 inches. Five sets of unit weight of concrete were available and ranged from 136 lb/ft³ (performed by NHDOT) to 141.18 lb/ft³ (performed by CP Tech Center). The microwave water-cementitious ratio was found to be 0.43; the design value is 0.44. The data are provided in Page 16.
- The air content ranged from 6.6% to 8.8% with an average of 7.4% over the five tests conducted. The specified minimum was 5%. It was noticed that the air content were reduced by adding 9 oz defoamer admixture during mixing. The data are provided on Page 17.
- Setting time of the mix was determined as a single measurement: initial set occurred at 5.24 hours and the final set was achieved at 8.12 hours (Page 24).

- The rapid chloride permeability test measures the electrical conductance of a concrete sample as its resistance to chloride ion penetration. The test results shown in Table 2 indicate a classification of “very low” permeability of chloride according to ASTM C1202.
- The strength development 28/7 f_c ratio is reported in Table 2.
- Two i-buttons were attached to reinforcing steel before the concrete placement: one was placed on top layer of reinforcement steel and the other was placed on bottom layer of reinforcement steel. The rate of cement hydration is dependent on the temperature and the time (Mindess, Young and Darwin, 2003). Maturity is used to monitor the cement hydration progress as a function of time and temperature. The temperature of concrete was recorded up to 28 hours. The concrete temperature over time is plotted in Figure 14 (a) and concrete maturity curve based on Nurse – Saul method (ASTM C 1074) is generated in Figure 14 (b).
- Compressive strength, splitting tensile strength and modulus of elasticity results (ASTM C 39, ASTM C 496, and ASTM C 469) are given in Table 3 and also plotted in Figures 15 to Figure 17.
- Free shrinkage test (ASTM C 157) was conducted in the laboratory. Three concrete beams were wet cured for seven days and then moved to a dry room at 23°C and 50% relative humidity. The drying shrinkage results are given in Table 5 and also plotted in Figure 18.
- Restrained shrinkage test was conducted based on ASTM C 1581. Four rings were cast. The rings were demolded and the top surface was covered with paraffin wax 24 hours from casting. The rings were allowed to dry at 23°C and 50% relative humidity immediately after demolding. Strains in the steel rings were recorded every 10 minutes up to 28 days or until the concrete cracked. The configuration of restrained concrete rings is shown in Figure 19. The cracking potential is listed in Table 5 and shown graphically in Figure 20. The cracking potential is classified as “moderate high” based on the average stress rate.
- Salt scaling test (ASTM C 672) was performed: the specimens were subjected to 16 to 18 hours freezing and then allowed to thaw at $23 \pm 2.0^\circ\text{C}$ and a relative humidity of

45 to 55% for 6 to 8 hours. The solution of 4 % calcium chloride was replaced and the test was continued following visual examination. 50 freeze-thaw cycles were applied. The surface was rated on a scale of 0 to 5 with 0 having no scaling, 1 having very slight scaling of 3 mm depth maximum without coarse aggregate visible, 2 having slight to moderate scaling, 3 having moderate scaling with some coarse aggregate visible, 4 having moderate to severe scaling, and 5 having severe scaling with coarse aggregate visible over entire surface. The photograph after 50th cycle was taken and shown in Figure 21. The visual ratings assigned to each specimen for cycles 0, 5, 10, 15, 20, 25, and 50 are given in Table 6.

Acknowledgements

The research team at the National Concrete Pavement Technology Center at Iowa State University sincerely thanks the New Hampshire Department of Transportation for their cooperation, Readimix Companies, Inc and Contractor Southern NH Poured Concrete Co. for supplying the materials and equipment.

Project Data

The following test data is provided for information only, comments and conclusions will be reported in the comprehensive Phase III report of the pooled fund project *Development of Performance Properties of Ternary Mixtures*.

Mix Design & Misc. Info.

General Information

Project:	RT-107, Epsom 15266, NH
Contractor:	Southern NH Poured Concrete Const., Inc.
Mix Description:	611 lb Cementitious
Mix ID:	
Date(s) of Placement:	8/10/2010

Cementitious Materials	Source	Type	Spec. Gravity	lb/yd ³	%
					Replacement by Mass
Portland Cement:	Ciment Quebec Type II	Type II	3.150	306	
GGBFS:	Lafarge North America	Grade 120	2.910	213	34.86%
Fly Ash:	Headwaters Resources	Class F	2.370	92	15.06%
Silica Fume:					
Other Pozzolan:					
				611	lb/yd³
				6.5	sacks/yd³

Aggregate Information	Source	Type	Spec. Gravity	Absorption	%
					SSD
Coarse Aggregate:	Pike-Hooksett	3/4 Blended Stone	2.670	0.65%	3.6%
Intermediate Aggregate #1:					
Intermediate Aggregate #2:					
Fine Aggregate #1:	Fillmore S&G	Sandstone	2.670	0.78%	99.2%
Coarse Aggregate %:	60.9%				
Intermediate Aggregate #1%:					
Intermediate Aggregate #2%:					
Fine Aggregate #1 %:	39.1%				

Mix Proportion Calculations

Water/Cementitious Materials Ratio:	0.443
Air Content:	5.00%

	Volume	(ft ³)	Batch Weights SSD		Absolute
			(lb/yd ³)	Spec. Gravity	Volume
					(%)
Portland Cement:	1.557		306	3.150	5.766%
GGBFS:	1.173		213	2.910	4.344%
Fly Ash:	0.622		92	2.370	2.304%
Silica Fume:					
Other Pozzolan:					
Coarse Aggregate:	10.938		1,800	2.670	40.511%
Intermediate Aggregate #1:					
Intermediate Aggregate #2:					
Fine Aggregate #1:	7.023		1,160	2.670	26.009%
Water:	4.338		271	1.000	16.066%
Air:	1.350				5.000%
	27.000		3,842		100.000%
		Unit Weight (lb/ft³)	142.3	Paste	33.480%
				Mortar	60.740%

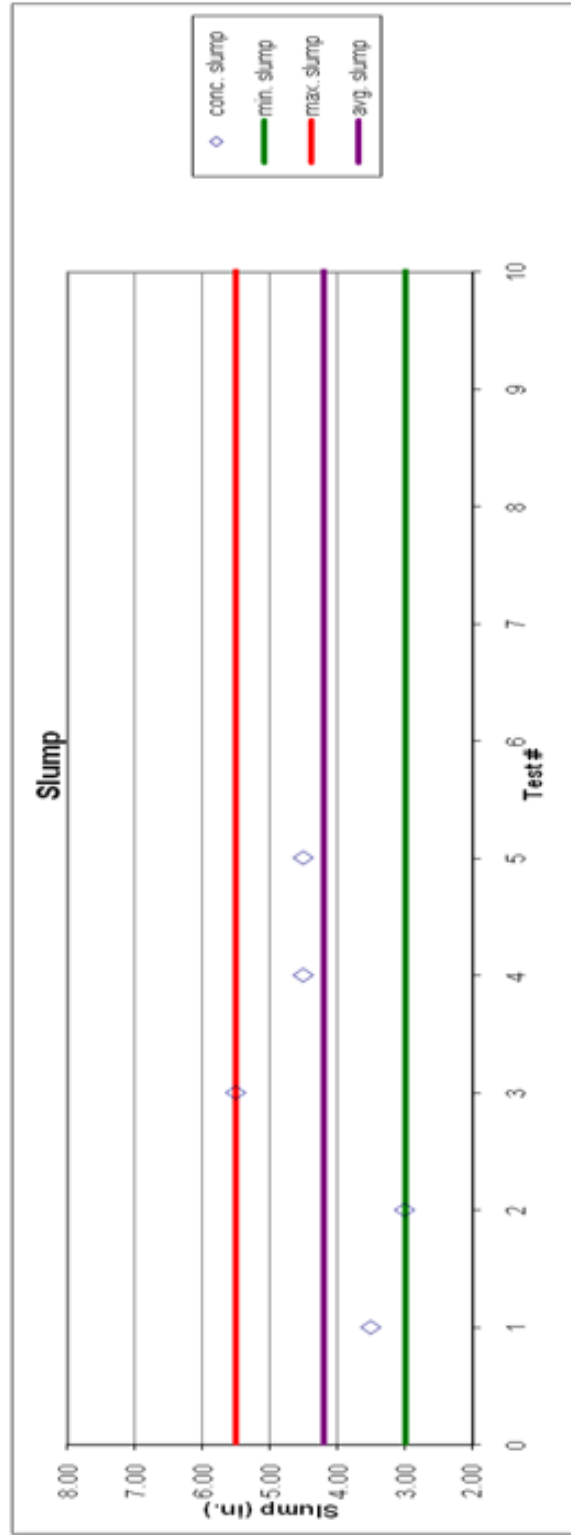
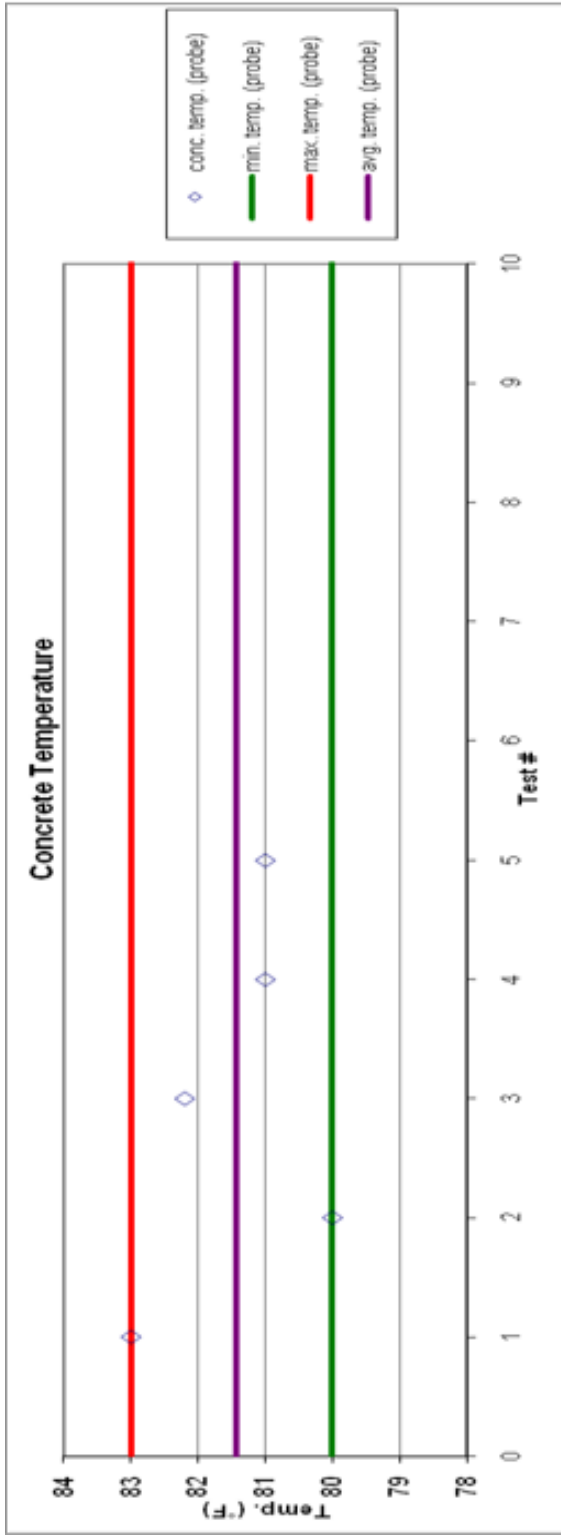
Admixture Information	Source/Description	oz/yd ³	oz/cwt
Air Entraining Admix:	W.R. Grace Daxex II AEA	3.80	0.62
Admix #1:	Glenium 7500-HRWR (BASF Admixtures)	27.50	4.50
Admix #2:	Strux 90/40 fibers (7 lb/cubic yard)		
Admix #3:			

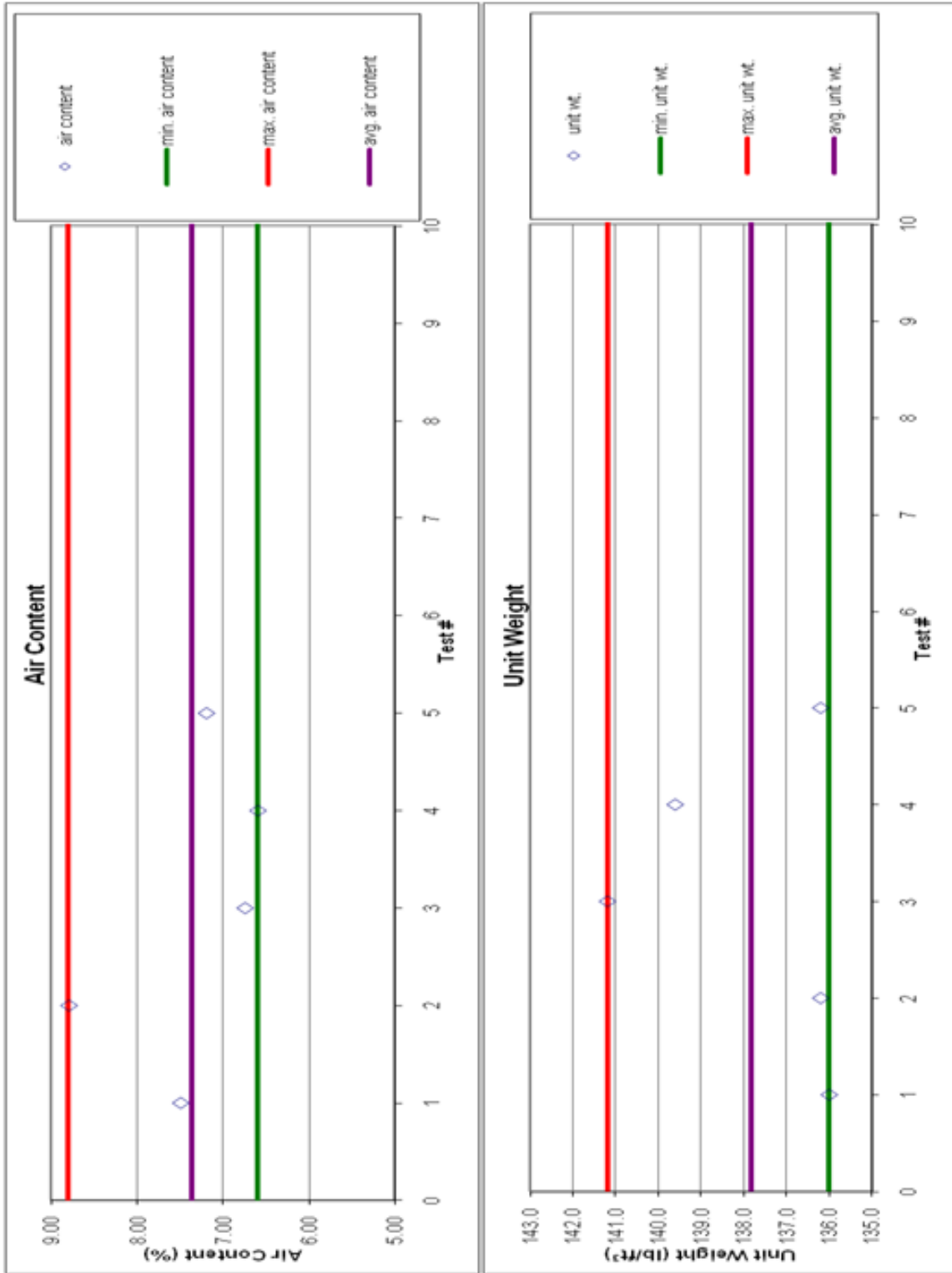
AVA Information	Absolute Volume	(%)
Air Free Paste:	28.480%	
Air Free Mortar:	55.740%	



New Hampshire - Ternary Mixtures
RT-107 Bridge Deck

Sample Information & Identification			Environmental Conditions				Fresh Concrete Workability Properties			Pressure Air
Sample Date	Sample Time	Sample Comments	Relative Humidity (%)	Ambient Temp. (°F)	Wind Speed (mph)	Conc. Temp. (probe) (°F)	Slump (in)	Unit Weight (lb/ft ³)	Microwave W/C Ratio (%)	% Air Content
10-Aug-10	8:22 AM	NHDOT sample taken at pump discharge (quality control)	79.0	71.8	3.0	83.0	3.50	136.00	n/a	7.5
10-Aug-10	9:00 AM	NHDOT sample taken at pump discharge (quality control)	75.0	73.1	1.0	80.0	3.00	136.20	n/a	8.8
10-Aug-10	9:15 AM	cp tech center sample taken at truck discharge	72.0	74.0	2.0	82.2	5.50	141.18	0.43	6.8
10-Aug-10	9:17 AM	NHDOT sample taken at pump discharge (quality control)	72.0	74.4	3.0	81.0	4.50	139.60	n/a	6.6
10-Aug-10	9:28 AM	NHDOT sample taken at pump discharge (quality control)	72.0	74.4	1.0	81.0	4.50	136.20	n/a	7.2





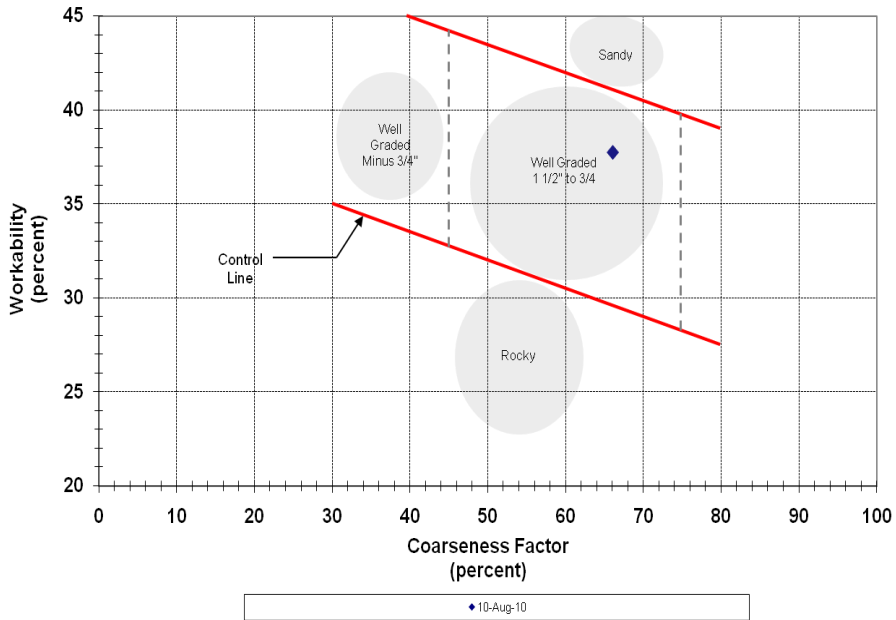
Project: RT-107 Epsom, NH
 Mix ID: 13266 Epsom, NH
 Sample Comments:
 Test Date: 10-Aug-10

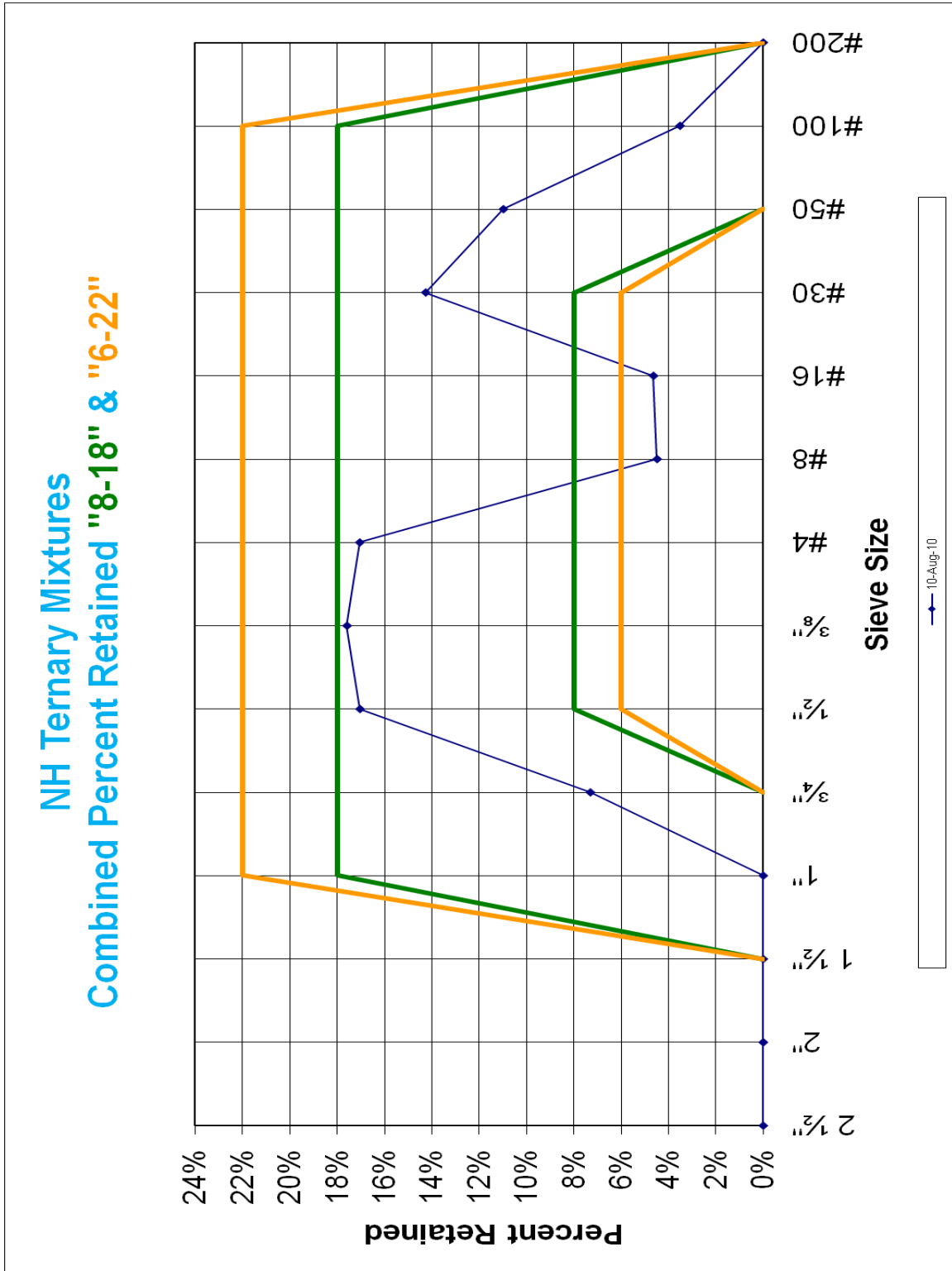
Total Cementitious Material: 611 lb/yd³
 Agg. Ratios: 60.90% 0.00% 39.10% 100.00%

Sieve	Coarse	Intermediate	Fine #1	Fine #2	Combined % Retained	Combined % Retained On Each Sieve	Combined % Passing
2 1/2"	100%	0%	100%		0%	0%	100%
2"	100%	0%	100%		0%	0%	100%
1 1/2"	100%	0%	100%		0%	0%	100%
1"	100%	0%	100%		0%	0%	100%
3/4"	88%	0%	100%		7%	7%	93%
1/2"	60%	0%	100%		24%	17%	76%
3/8"	31%	0%	100%		42%	18%	58%
#4	4%	0%	99%		59%	17%	41%
#8	1%	0%	91%		64%	4%	36%
#16	1%	0%	80%		68%	5%	32%
#30	1%	0%	43%		82%	14%	18%
#50	1%	0%	15%		93%	11%	7%
#100	1%	0%	6%		97%	4%	3%
#200			0.7%		99.7%		0.3%

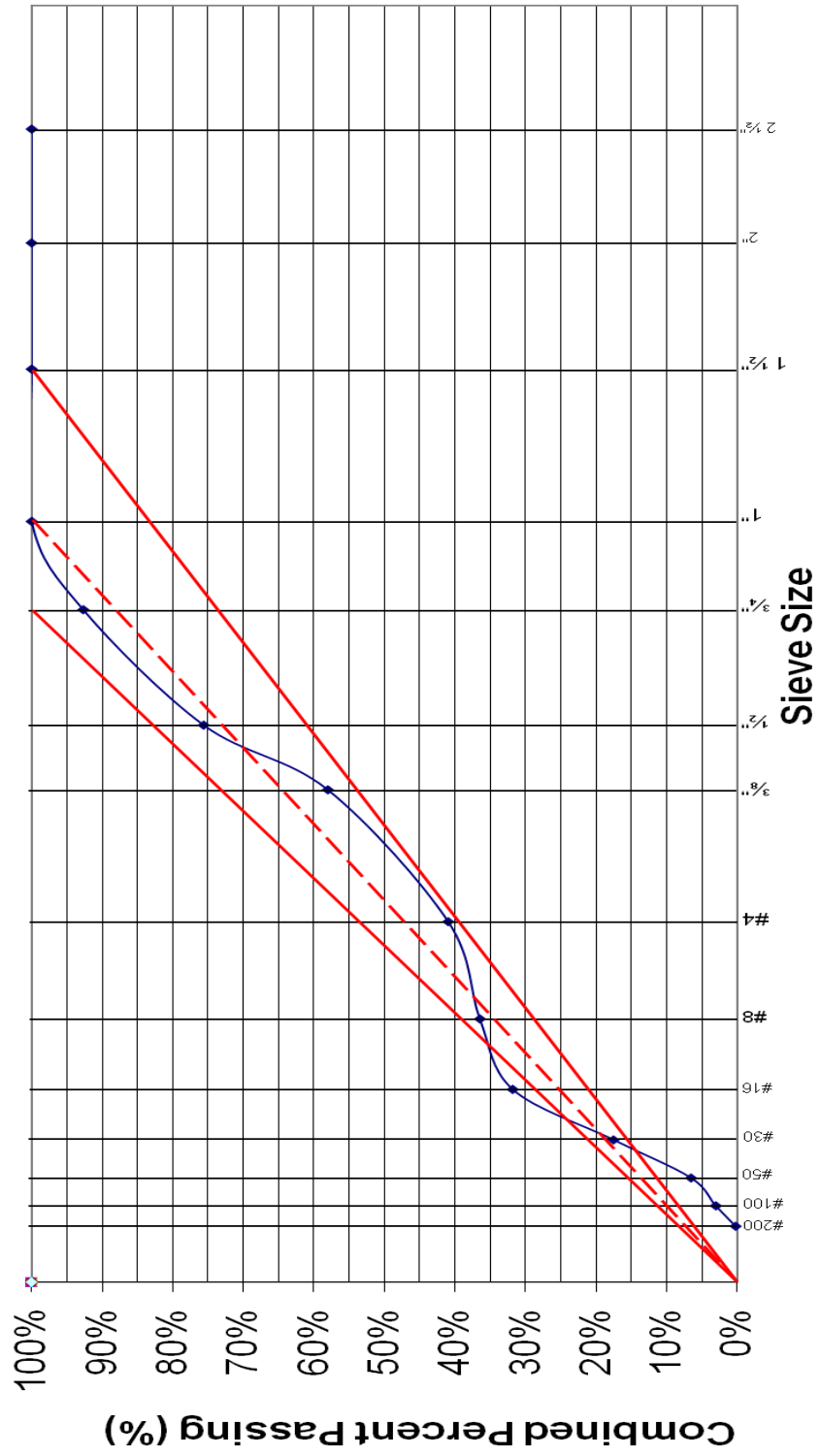
Workability Factor: 37.7
 Coarseness Factor: 66.1

NH Ternary Mixtures Workability Factor & Coarseness Factor





**NH Ternary Mixtures
0.45 Power Curve**





New Hampshire - Ternary Mixtures

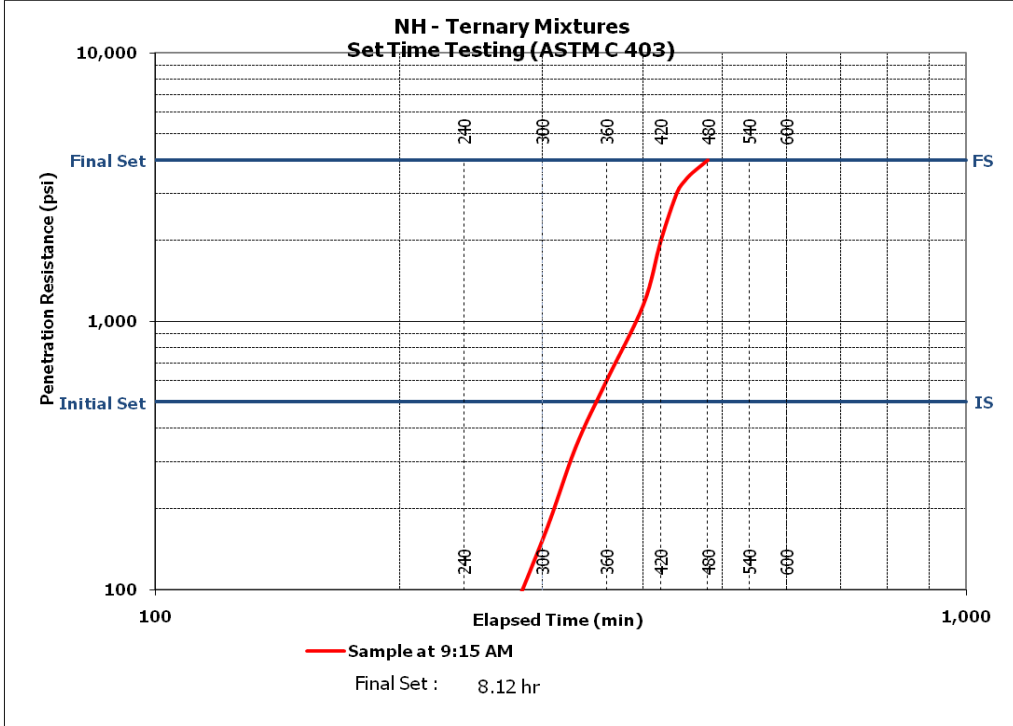
Set Time ASTM C 403

Project: RT-107, Epsom 15266, NH
 Date: 10-Aug-10 Start Time: 9:15 AM
 Sta: n/a

Test Data

Penetration Time (xx:xx-24 hr format)	Time (min)	Needle # (1,2,4,10,20 or 40)	Force (lb)	Penetration Resistance (psi)	Sample Temp. (°F)
12:50 PM	215.00	1	20	20.00	76.6
1:30 PM	255.00	2	24	48.00	76.6
2:15 PM	300.00	4	38	152.00	77.7
2:45 PM	330.00	10	34	340.00	78.8
3:15 PM	360.00	20	30	600.00	79.9
3:55 PM	400.00	20	58	1160.00	84.2
4:15 PM	420.00	20	100	2000.00	83.3
4:35 PM	440.00	40	76	3040.00	83.1
4:45 PM	450.00	40	84	3360.00	83.1
4:55 PM	460.00	40	90	3600.00	83.1
5:15 PM	480.00	40	100	4000.00	82.9

Initial Set (at 500 psi PR)	estimated times using forecast function	314 minutes	5.24 hours
Final Set (at 4,000 psi PR)	estimated times using forecast function	487 minutes	8.12 hours





New Hampshire - Ternary Mixtures

Microwave Water Content Worksheet

Project: RT-107, Epsom 15266, NH
 Date: 10-Aug-10 Time: 9:15 AM
 Sta: n/a

Test Data

Mass of tray+cloth+block+fresh test sample, W_F (g)	3,778.0
Mass of tray+cloth+block, W_S (g)	2,198.5
Mass of tray+cloth+dry sample, W_D (g) (5mins)	3,735.8
Mass of tray+cloth+dry sample, W_D (g) (7 mins)	3,698.4
Mass of tray+cloth+dry sample, W_D (g) (9 mins)*	3,670.2
Mass of tray+cloth+dry sample, W_D (g) (11 mins)*	3,662.1
Mass of tray+cloth+dry sample, W_D (g) (13 mins)*	3,660.1
Mass of tray+cloth+dry sample, W_D (g) (15 mins)*	3,659.8
Mass of tray+cloth+dry sample, W_D (g) (17 mins)*	
Mass of tray+cloth+dry sample, W_D (g) (Final)**	3,659.8
Water content percentage, W_C (%)	7.5%
Unit weight of fresh concrete, UW (lb/ft ³ ***)	141.2
Total water content, W_T, (lb/yd³)	285.3
Total cementitious weight (lb/yd ³)	611
Fine aggregate weight (lb/yd ³)	1160
Coarse Aggregate weight (lb/yd ³)	1800
Intermediate Aggregate weight (lb/yd ³)	0
Fine aggregate absorption (%)	0.78%
Coarse aggregate absorption (%)	0.65%
Intermediate aggregate absorption (%)	0.00%
w/c	0.433

* If necessary (stop if the weight loss is less than 1g)

** Mass at test termination

***From unit weight test



ASTM C 1202-97



Test-compagny
Testing street 45
CompagnyCity
Some Country

Your own logo.
size=20x80mm



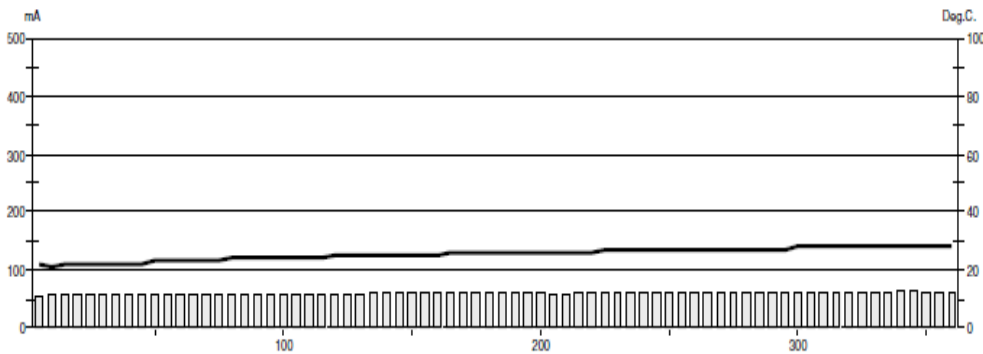
GERMANN INSTRUMENTS

DENMARK
Phone: +45 3907 7117
Fax: +45 3907 3107

USA
Phone: (547)329-8999
Fax: (547)329-8988

Test report

Voltage Used: 60
Testing time: 06:00 hour
Charge passed: 1279
Adjusted Charge passed: 1109
Permeability class: Low
Instrument number: 023907
Channel number: 1
Report date: 10/5/2010
Testing by: pjm
Reference: NH ternary
Sample diameter: 102
Comment: ---



Time	°C	mA	Time	°C	mA	Time	°C	mA	Time	°C	mA
00:05	22	54.3	01:35	24	58.3	03:05	26	60.1	04:35	27	60.4
00:10	21	55.5	01:40	24	58.5	03:10	26	60.2	04:40	27	59.9
00:15	22	55.1	01:45	24	58.5	03:15	26	60.1	04:45	27	60.6
00:20	22	55.6	01:50	24	57.7	03:20	26	59.4	04:50	27	61.1
00:25	22	56.0	01:55	24	56.6	03:25	26	59.0	04:55	27	61.0
00:30	22	55.9	02:00	25	57.8	03:30	26	58.8	05:00	28	61.3
00:35	22	56.1	02:05	25	57.6	03:35	26	59.6	05:05	28	61.0
00:40	22	57.9	02:10	25	59.1	03:40	26	59.9	05:10	28	60.8
00:45	22	58.0	02:15	25	59.3	03:45	27	60.1	05:15	28	60.8
00:50	23	58.1	02:20	25	59.4	03:50	27	60.1	05:20	28	60.8
00:55	23	58.1	02:25	25	59.5	03:55	27	60.1	05:25	28	60.9
01:00	23	58.1	02:30	25	59.6	04:00	27	60.1	05:30	28	60.9
01:05	23	58.0	02:35	25	59.7	04:05	27	60.1	05:35	28	61.3
01:10	23	58.0	02:40	25	59.7	04:10	27	60.1	05:40	28	61.4
01:15	23	57.8	02:45	26	59.8	04:15	27	60.0	05:45	28	61.4
01:20	24	57.8	02:50	26	60.0	04:20	27	60.2	05:50	28	61.2
01:25	24	58.0	02:55	26	60.0	04:25	27	60.3	05:55	28	61.2
01:30	24	58.2	03:00	26	60.1	04:30	27	60.3	06:00	28	60.5



ASTM C 1202-97



Test-compagny
Testing street 45
CompagnyCity
Some Country

Your own logo,
size=20x80mm



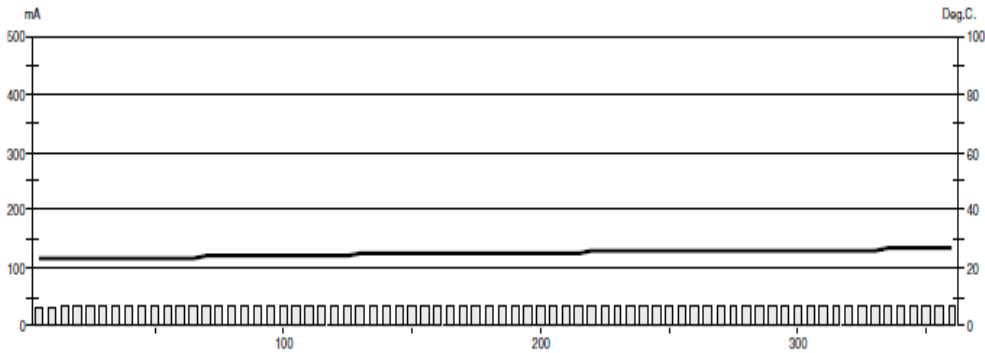
GERMANN INSTRUMENTS

DENMARK
Phone: +45 3907 7117
Fax: +45 3907 3107

USA
Phone: (847)329-8999
Fax: (847)329-8988

Test report

Voltage Used: 60
Testing time: 06:00 hour
Charge passed: 732
Adjusted Charge passed: 635
Permeability class: Very Low
Instrument number: 023907
Channel number: 2
Report date: 10/5/2010
Testing by: PJM
Reference: NH ternary
Sample diameter: 102
Comment: ---



Time	°C	mA	Time	°C	mA	Time	°C	mA	Time	°C	mA
00:05	23	31.6	01:35	24	33.1	03:05	25	33.9	04:35	26	34.5
00:10	23	32.2	01:40	24	33.2	03:10	25	34.0	04:40	26	34.4
00:15	23	32.7	01:45	24	33.3	03:15	25	34.0	04:45	26	34.4
00:20	23	33.1	01:50	24	33.4	03:20	25	34.1	04:50	26	34.5
00:25	23	33.2	01:55	24	33.4	03:25	25	34.1	04:55	26	34.8
00:30	23	33.3	02:00	24	33.4	03:30	25	34.2	05:00	26	34.7
00:35	23	33.4	02:05	24	33.5	03:35	25	34.2	05:05	26	34.7
00:40	23	33.3	02:10	25	33.6	03:40	26	34.3	05:10	26	34.6
00:45	23	33.3	02:15	25	33.6	03:45	26	34.2	05:15	26	34.7
00:50	23	33.3	02:20	25	33.6	03:50	26	34.1	05:20	26	34.7
00:55	23	33.1	02:25	25	33.6	03:55	26	34.3	05:25	26	34.7
01:00	23	33.1	02:30	25	33.6	04:00	26	34.3	05:30	26	34.8
01:05	23	33.0	02:35	25	33.7	04:05	26	34.4	05:35	27	34.9
01:10	24	32.9	02:40	25	33.8	04:10	26	34.4	05:40	27	34.9
01:15	24	32.9	02:45	25	33.8	04:15	26	34.4	05:45	27	35.1
01:20	24	33.0	02:50	25	33.8	04:20	26	34.4	05:50	27	35.2
01:25	24	33.0	02:55	25	33.9	04:25	26	34.3	05:55	27	35.2
01:30	24	33.1	03:00	25	33.9	04:30	26	34.5	06:00	27	35.2



Figure 1 Route 107 bridge deck in Epsom, NH.

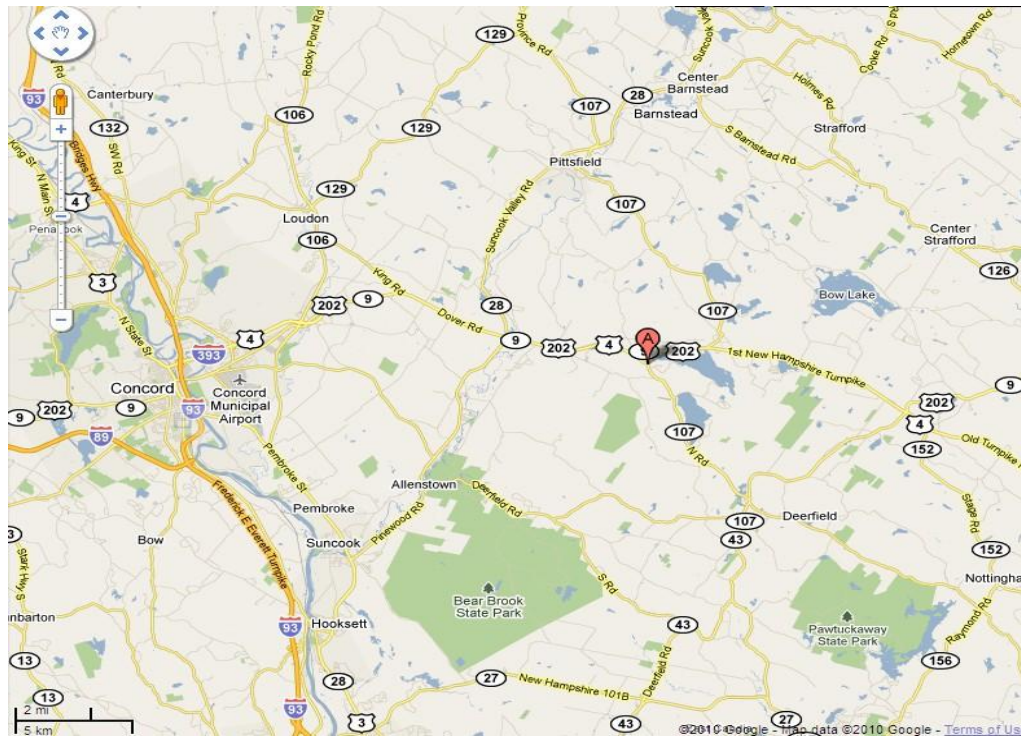


Figure 2 Project and mobile lab location.

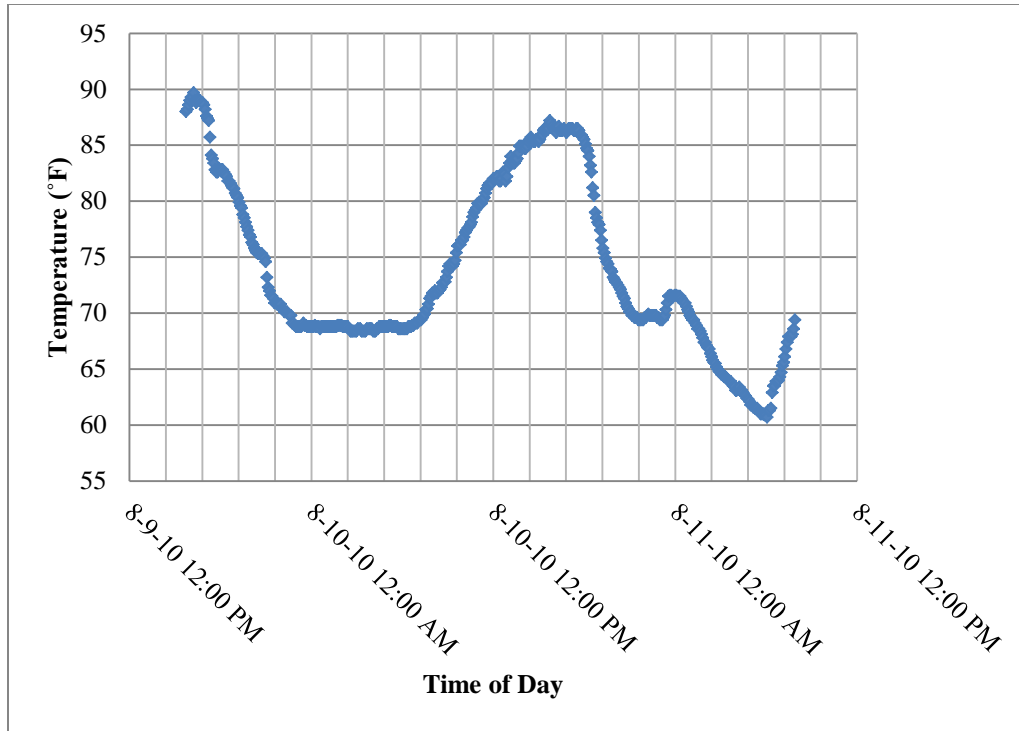


Figure 3 Ambient temperature versus time of day.

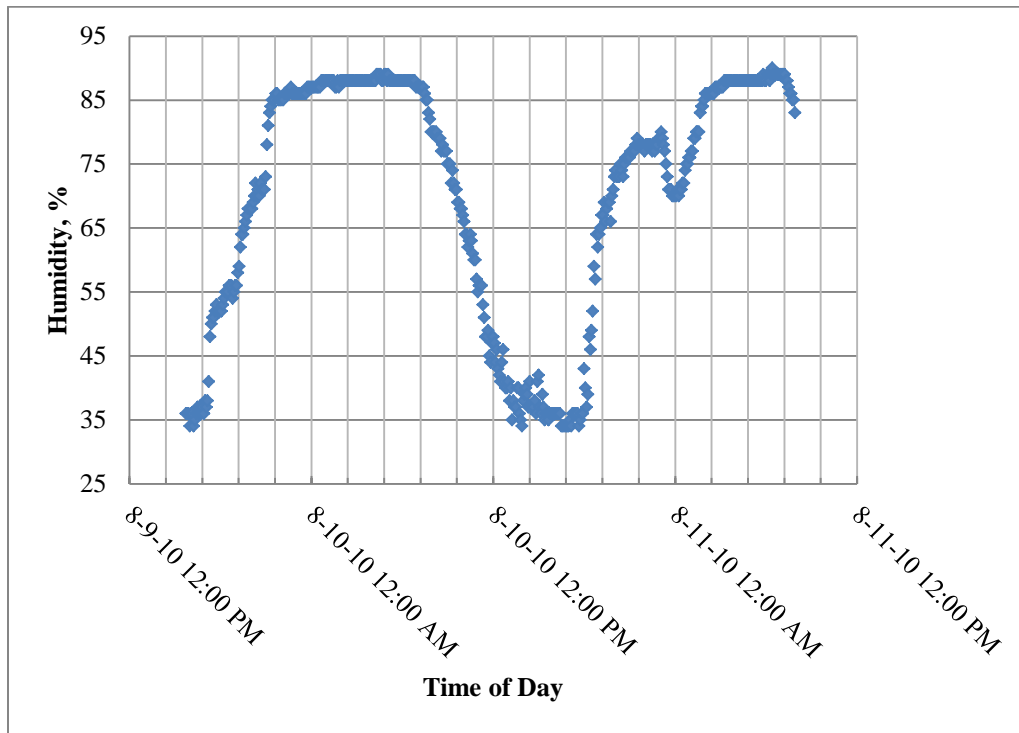


Figure 4 Relative humidity versus time of day.

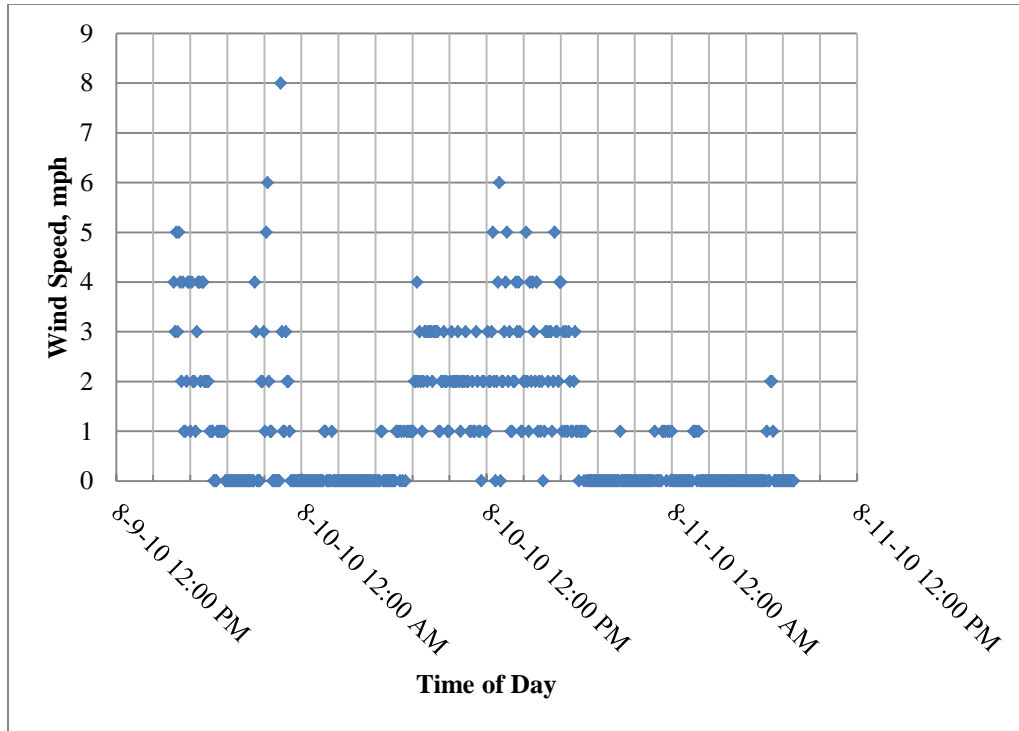


Figure 5 Wind speed versus time of day.



Figure 6 Bridge deck with removable wood form.



Figure 7 Concrete being placed.



Figure 8 Concrete being vibrated.



Figure 9 PCC mobile lab.



Figure 10 Two i-buttons being placed.



Figure 11 Fresh concrete.



Figure 12 Concrete being finished.



Figure 13 Concrete being cured with burlap.

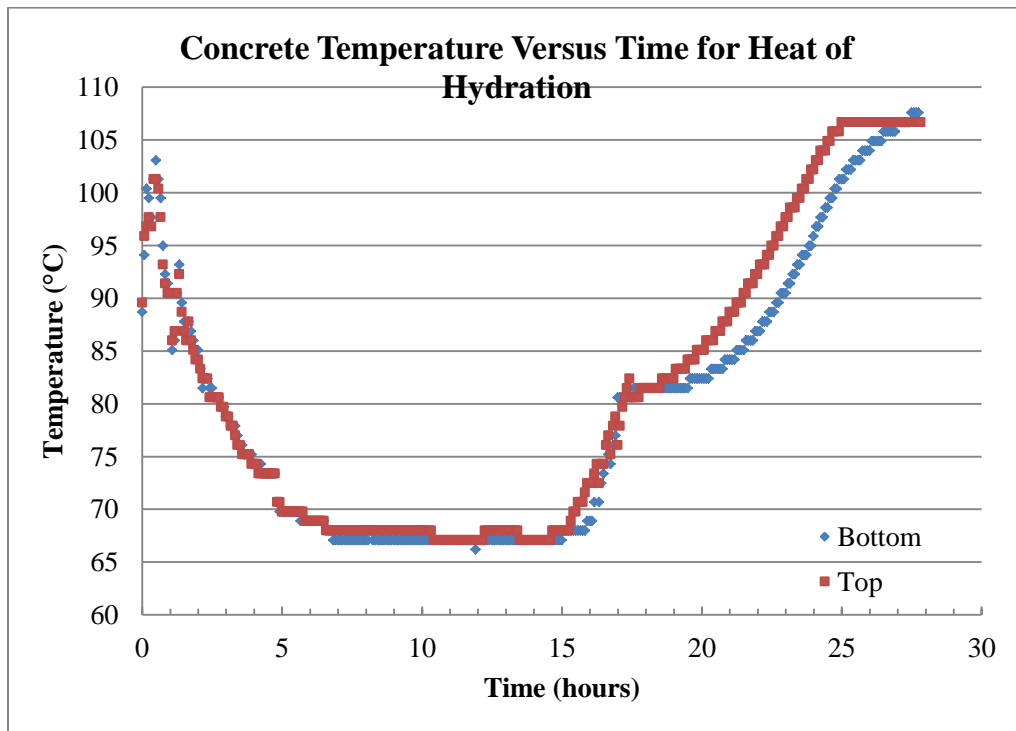


Figure 14 (a) Concrete temperatures versus time for heat of hydration.

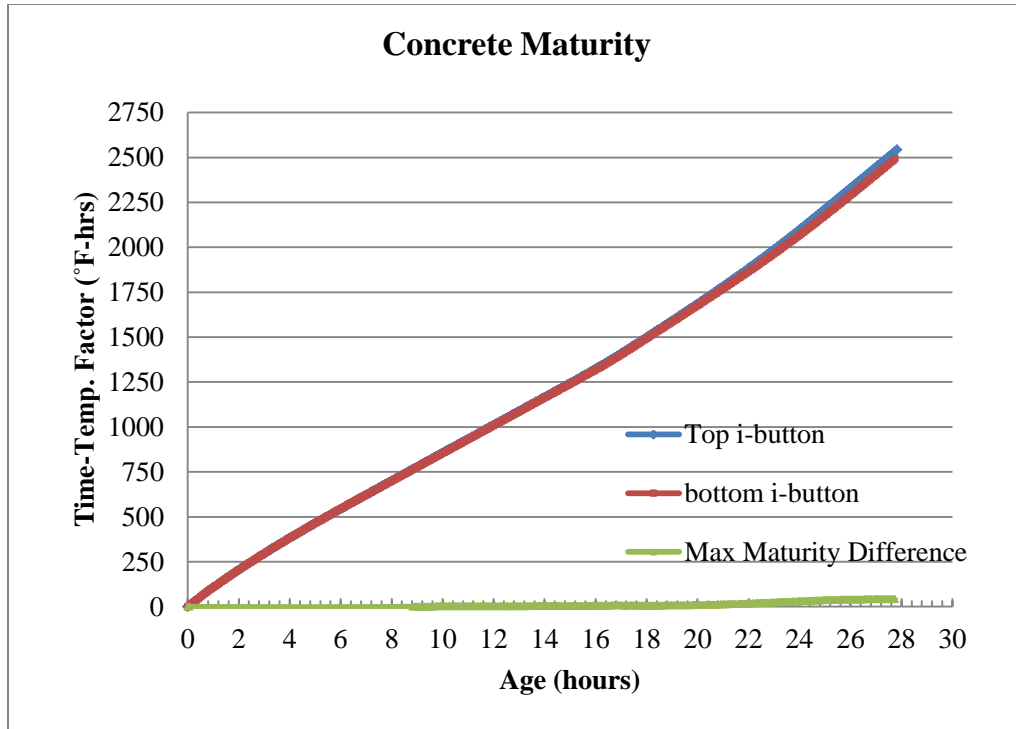


Figure 14 (b) Concrete maturity.

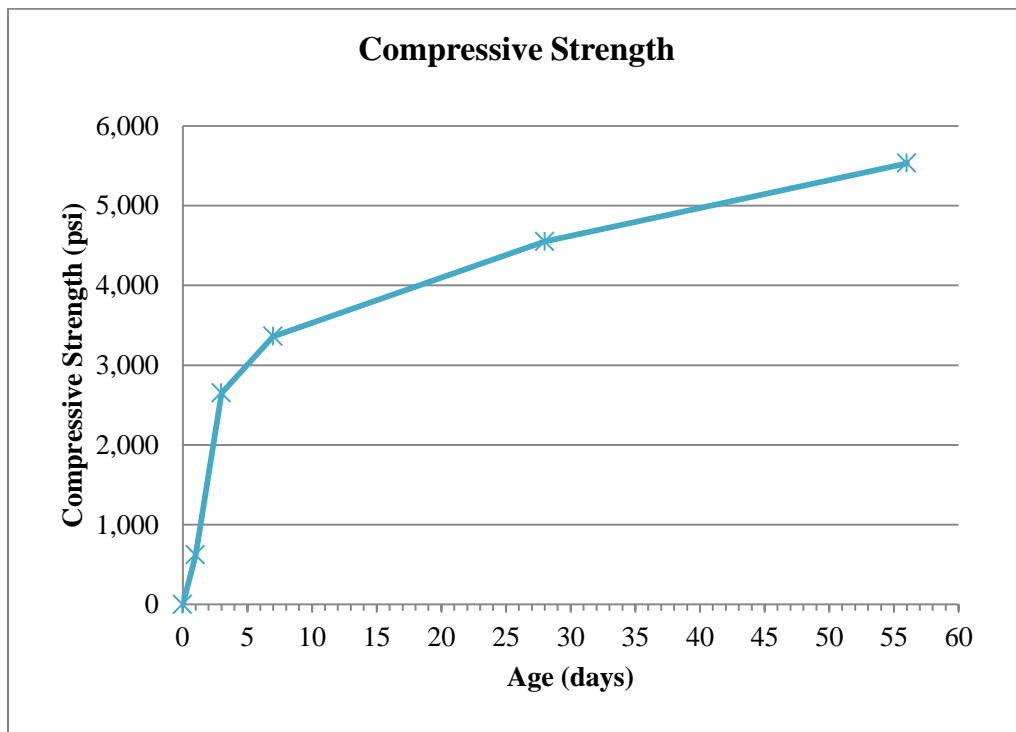


Figure 15 Compressive strength development with time.

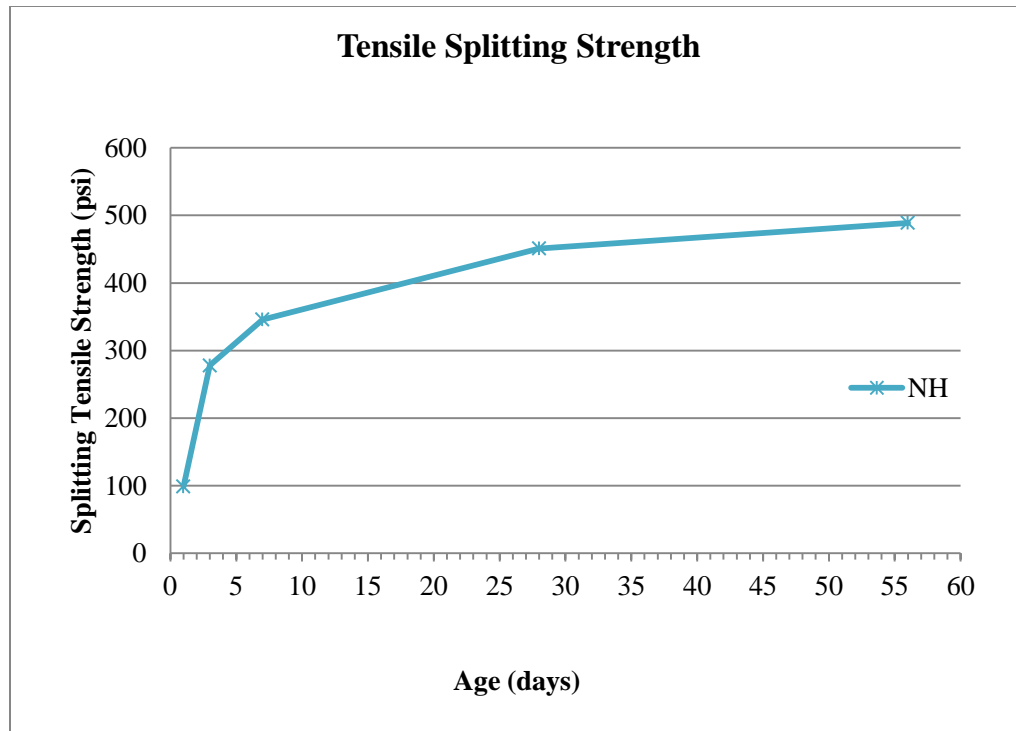


Figure 16 Tensile splitting strength development with time.

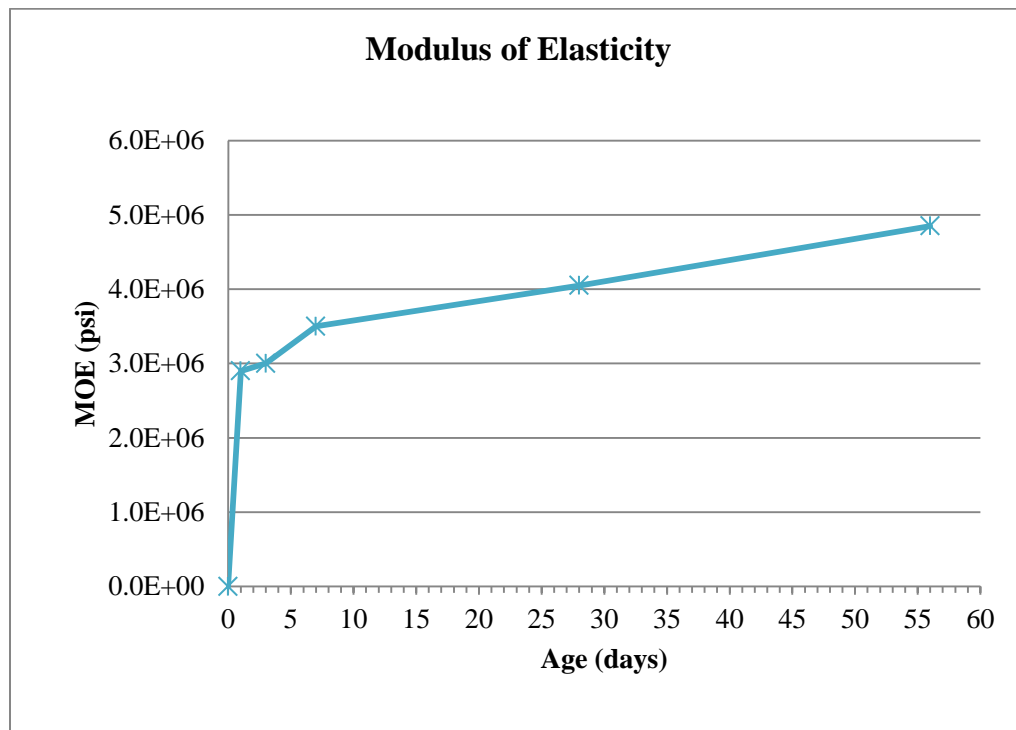


Figure 17 Modulus of elasticity development with time.

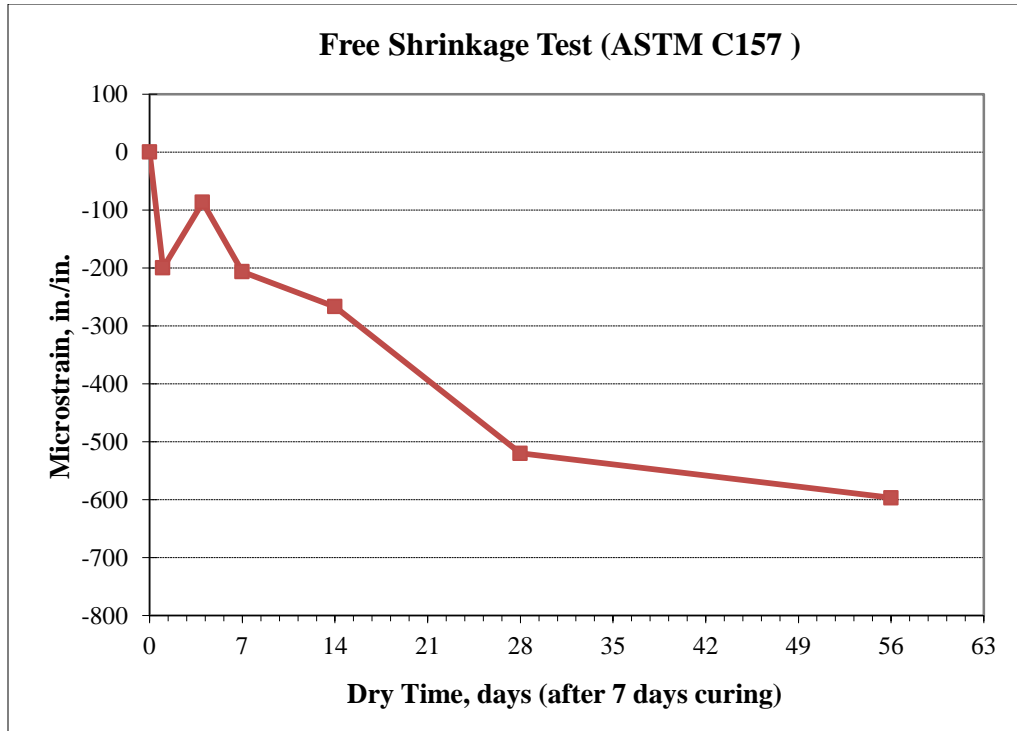


Figure 18 Free shrinkage of prisms (ASTM C 157).

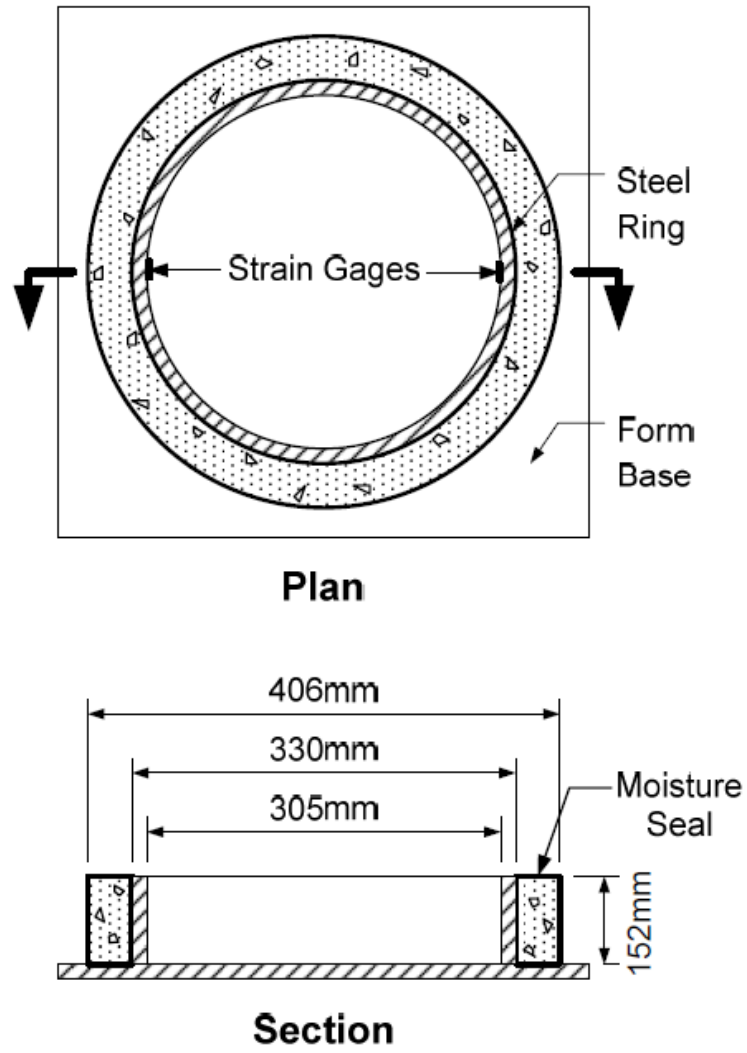


Figure 19 Configuration of restrained concrete ring samples.

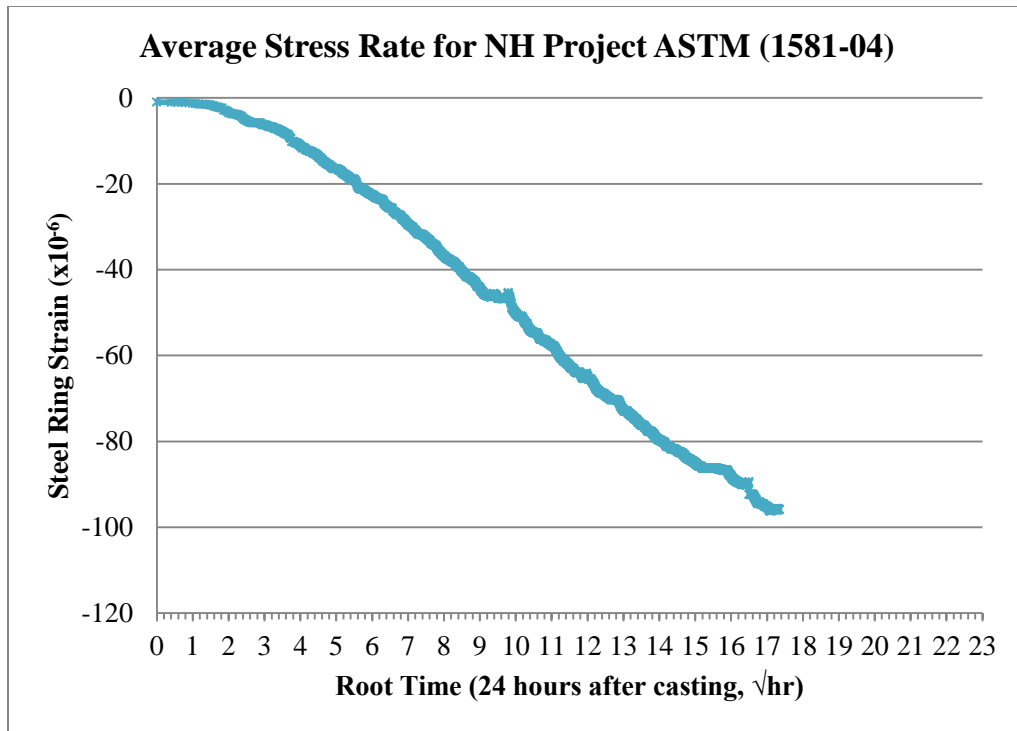


Figure 20 Strains of steel rings resulting from concrete shrinkage.



Figure 21 NH salt scaling sample after 50th freeze-thaw cycle.

Table 1 Ambient conditions of Route 107 Bridge Deck Project in NH

New Hampshire - Ternary Mixtures
RT-107 Bridge Deck

Sample Information & Identification			Environmental Conditions			
Sample Date	Sample Time	Sample Comments	Relative Humidity (%)	Ambient Temp. (°F)	Wind Speed (mph)	Conc. Temp. (probe) (°F)
10-Aug-10	8:22 AM	NHDOT sample taken at pump discharge (quality control)	79.0	71.8	3.0	83.0
10-Aug-10	9:00 AM	NHDOT sample taken at pump discharge (quality control)	75.0	73.1	1.0	80.0
10-Aug-10	9:15 AM	cp tech center sample taken at truck discharge	72.0	74.0	2.0	82.2
10-Aug-10	9:17 AM	NHDOT sample taken at pump discharge (quality control)	72.0	74.4	3.0	81.0
10-Aug-10	9:28 AM	NHDOT sample taken at pump discharge (quality control)	72.0	74.4	1.0	81.0

Table 2 Properties of hardened concrete

Tests	Results		
7-day Compressive Strength, psi	3360		
28-day Compressive Strength, psi	4550		
Rapid Chloride Permeability, Coulombs	Sample 1 1279	Sample 2 732	Average 1006
Strength Development 28/7 day fc Ratio	1.35		
Shrinkage Microstrain @ 28 days, in/in	520		
Average Stress Rate by Restrained Ring Test, psi/day	50.34		

Table 3 Summation of strength and modulus of elasticity

Location	Age, days	Compressive Strength, psi	Splitting Tensile Strength, psi	Modulus Of Elasticity, psi
NH	1	620	99	2.90E+06
	3	2,650	278	3.00E+06
	7	3,360	346	3.50E+06
	28	4,550	451	4.05E+06
	56	5,530	489	4.85E+06

Table 4 Free shrinkage test results

NH Project Free Shrinkage Test (ASTM C 157)					
Dry					
Time	Beam 1 change%	Beam 2 change %	Beam 3 change %	Average	Microstrain
1	-0.024	-0.021	-0.015	-0.020	-200.0
4	-0.015	-0.006	-0.005	-0.009	-86.7
7	-0.024	-0.016	-0.022	-0.021	-206.7
14	-0.029	-0.025	-0.026	-0.027	-266.7
28	-0.055	-0.048	-0.053	-0.052	-520.0
56	-0.064	-0.057	-0.058	-0.060	-596.7

Table 5 Cracking potential and average stress rate (ASTM C 1581)

Cracking Potential for NH Project (ASTM C 1581)				
	Ring 1	Ring 2	Ring 3	Ring 4
Strain Rate Factor (in./in.x10 ⁻⁶)/hours ^{1/2}	-7.06	-6.80	-6.35	-9.00
G (psi)	10.47x10 ⁶	10.47x10 ⁶	10.47x10 ⁶	10.47x10 ⁶
Absolute Value of α_{avg} (in./in.10 ⁻⁶)/day ^{1/2}	35.77			
Elapsed Time, tr (hours)	294.8	367.1	323.3	350.4
Elapsed Time, tr (days)	12.3	15.3	13.5	14.6
Stress Rate, q (psi/day) $q=GI\alpha_{avg}I/2\sqrt{t_r}$	53.4	47.9	51.0	49.0
Average Stress Rate, q (psi/day) $q=GI\alpha_{avg}I/2\sqrt{t_r}$	50.34			
Potential for cracking classification (ASTM 1581)	High (50 ≤ q)			

Table 6 Salt scaling test visual condition of specimen

NH Salt Scaling Samples	Condition of Surface					
	Cycle 5	Cycle 10	Cycle 15	Cycle 20	Cycle 25	Cycle 50
No. 1	1	1	1	1	2	3
No. 2	1	1	1	1	2	3
No. 3	1	1	1	1	2	3